# INVESTIGATING THE MECHANISMS OF INFECTION INDUCED THROMBOINFLAMMATION

by

Rachel Emma Lamerton

A thesis submitted to the University of Birmingham for the degree of DOCTOR OF PHILOSOPHY

UNIVERSITY OF BIRMINGHAM

Institute of Immunology and Immunotherapy
and Institute of Cardiovascular Sciences
College of Medical and Dental Sciences
University of Birmingham
March 2024

## Abstract

Dysregulated host responses to infection can turn the immune system from being the hero that wins the battle against harmful invading pathogens, to the enemy within that has the capacity to kill the host it was supposed to be protecting. This is the case in sepsis, which contributed to approximately 20% of worldwide deaths in 2017, and also in severe COVID-19, which killed over 5 million people up to December 2021. This thesis aimed to study the inflammatory responses involved in host immune system dysregulation.

One of the major problems in this dysregulation is the formation of thrombi by platelets and other blood components, which can lead to blockage of blood vessels, starving organs of oxygen. Invasive non-typhoidal *Salmonella* is a bloodstream infection estimated to cause >75,000 deaths per year, predominantly in sub-Saharan Africa. Whilst many different bacterial strains have been shown to interact with human platelets leading to their aggregation, whether *Salmonella* Typhimurium can do this was unknown. In this thesis I studied the interactions between *Salmonella* Typhimurium and platelets using platelet aggregometry, revealing *Salmonella* Typhimurium can indirectly activate platelets in a donor dependent manner, linked to the level of antibodies recognising *Salmonella* in the donor plasma. Platelet aggregates also form under physiological flow conditions over *Salmonella.*

Investigating the broader environment of the blood vessel by bringing endothelial cells into the study revealed binding interactions between these cells and *Salmonella* Typhimurium, which was strengthened upon the addition of IgG. Platelet adhesion occurred on *Salmonella* primed endothelial cells under both venous and arterial flow conditions, at sites distal to the *Salmonella.*

This thesis also investigated inflammatory responses to SARS-CoV-2, the pandemic of which was still severely disrupting the world at the start of this PhD. We found that SARS-CoV-2 protein-antibody complexes activate the classical complement pathway, with levels of complement activation differing

between convalescent COVID-19 patients who did not require hospital treatment versus those that did.

Overall, this thesis investigates and argues that three major components in blood vessels: platelets, endothelial cells, and complement, are all capable of contributing to the dysregulated host immune responses leading to severe damage.

## Acknowledgements

This PhD was funded by the Wellcome Trust Doctoral Training Programme 'Mechanisms of Inflammatory Diseases', with additional grants from Boehringer-Ingelheim and the University of Birmingham.

The first thanks go to Steve W, Robin and Graham for accepting me onto the MIDAS programme and giving me the opportunity to undertake this PhD – I'm so glad you got the funding to do MIDAS, and I'm so glad you picked me!

Double thanks to Steve W for being my go-to MIDAS person, and then my PhD supervisor. I have come such a long way since the first time I nervously sat in your office, and I couldn't have done this PhD without all your support, encouragement and advice (not to mention the posh Kleenex in the tricky tear-stained early stages of the PhD…!). Adam, thank you for giving me the opportunity to work in your lab, learn about why we should care about *Salmonella*, and figure out what I do and don't like in the world of science. First year helped me grow immeasurably, in the words of The Script 'Now she's stronger than you know, a heart of steel starts to grow'.

To my 4th floor colleagues and friends, my first PhD home, thank you for all your socially-distanced help! Edith – thank you for all your help when I joined, and for making those long Saturdays in the CIS as fun and enjoyable as possible! Ruby, thank you for all your help in the lab, and especially for your emotional support and understanding. Thanks also to Marisol, Sian J, Sian F, Areej, Gabby and Charlie for being great office and lab mates. Jamie, you started off as a great office and lab mate, and turned into a best friend, and I'm so glad our paths crossed. I can't thank you enough for all the good times (and shared bad times…) we've had together, for all your support and friendship, you're the best. Alba – I'm so glad you joined the group. Your understanding and advice has been invaluable, and I can't thank you enough for your kindness and messages while I was on my LoA.

To my 1st floor colleagues and friends, thank you for welcoming the strange *Salmonella* girl into the lab, and for allowing the platelet group to quickly become my new home! Sam, thank you for your supervision (and help with supervisors!) and being my general lab/PhD/life guru, and for knowing everything I could ever want to know about platelet assays. Eleyna, thank you for making the lab and office such a positive place to be, for all your help and friendship, and along with Alex, Luna and Teddy, thanks for the dog walks! Thanks to Rich for being my lab big brother, doing big brother things like eating/drinking all the things I didn't want to in Maastricht, listening in good times and bad and being another unfailing source of positivity in the lab! I really appreciate all the times you bled people for me, then encouraging me to learn myself. Who knew I'd be able to do that, and be totally cool with it?! Although I haven't the space to write a sentence about all of you (I wish I did!), you guys make/made the platelet group a truly great place to work, so thank you: Alex, Luis, Gina, Jo, Steve T, Neil, Natalie, Pip, Hrush, Gayle, Oriana, Beata, Ying, Julie, Tash, Martina and Caroline.

Thank you to the staff in the CIS for providing COVID samples, especially Sian F, Alex R, Tim and Chloe.

Thanks to the MIDAS students who I've been fortunate enough to share this journey with: David, Abbey, Poppy, Lisa and Sofia. Thank you for accepting me just as I am!

Thank you to Steve K for allowing me to come and have the most wonderful 3.5 months in Dublin. I learnt so much, and the whole experience gave me so much confidence. Dani and German, you two were the best, thank you for making me so welcome, and for making my time in Dublin so full of laughter and smiles. Thank you for teaching me so much in such a short space of time, and for being so patient! Thank you to the rest of the York House office, and to John, for being such a cheerful presence every morning.

I've been fortunate to have some great mentors throughout my PhD. Sara, Steve W paired us up because 'we're both so smiley', and I'm so glad he did. Thank you for all your help and support, I think you're amazing. Laura, thank you for listening to anything and everything I had to say. Christian, thank

you for being there throughout my journey when I needed you, and for your wonderful own brand of Aussie life advice.

Thank you to The People's Orchestra for all the musical nourishment throughout my PhD, and for providing me with a truly lovely friendship group in the Night Owls: Sarah, Lucy, Kevin, Rosie, Hannah Katherine and Liz. Sarah, thank you for being the best clarinet buddy, for all your support during/after my LoA and through the rocky clarinet times!

Last but not least, thank you to my family. To Grandad for always believing in me and encouraging me, Steven and Sarah for your love and support (and of course the free holidays in Amsterdam!) and to Mum and Dad, for always being there for me. You've picked me up (metaphorically and literally!) when things have been bad, been patient with me taking the long way round, and always provided support, love, encouragement and a listening ear (even if you don't understand what I'm on about when it comes to the science!). I couldn't have done this without you <3

Table of contents

## Publications and presentations

### Publications

**Lamerton RE**, Montague SJ, Perez-Toledo M, Watson SP and Cunningham AF (2024) Platelet aggregation responses to Salmonella Typhimurium are determined by host anti-*Salmonella* antibody levels [submitted]

Akbalut C, Arisz R…**Lamerton RE**…van Zonneveld A (2023) Blood coagulation and beyond: Position paper from Fourth Maastricht Consensus Conference on Thrombosis. Thromb Haemost. PMID 36913975

Marical-Juarez E, Perez-Toledo M, Nayar S, Pipi E, Alshayea A, Persaud R, Jossi SE, **Lamerton RE**, Barone F, Henderson IR, Cunningham AF (2023) Salmonella infection induces the reorganization of follicular dendritic cell networks concomitant with the failure to generate germinal centres. iScience. PMID: 36950118

Jossi SE, Arcuri M, Alshayea A, Persaud RR, Marcial-Juárez E, Palmieri E, Di Benedetto R, Pérez-Toledo M, Pillaye J, Channell WM, Schager AE, **Lamerton RE**, Cook CN, Goodall M, Haneda T, Bäumler AJ, Jackson-Jones LH, Toellner KM, MacLennan CA, Henderson IR, Micoli F, Cunningham AF (2023) Vi polysaccharide and conjugated vaccines afford similar early, IgM or IgG-independent control of infection but boosting with conjugated Vi vaccines sustains the efficacy of immune responses. Front Immunol. PMID: 37033932

**Lamerton RE***, Marical-Juarez E*, Faustini SE, Perez-Toledo M, Goodall M, Jossi SE, Newby ML, Chapple I, Dietrich T, Veenith T, Shields AM, Harper L, Henderson IR, Rayes J, Wraith DC, Watson SP, Crispin M, Drayson MT, Richter AG, Cunningham AF (2022). SARS-CoV-2 spike- and nucleoprotein- specific antibodies induced after vaccination or infection promote classical complement activation. Front Immunol. PMID: 35860286

Chawla H, Jossi SE, Faustini SE, Samsudin F, Allen JD, Watanabe Y, Newby ML, Marcial-Juarez E, **Lamerton RE**, McLellan JS, Bond PJ, Richter AG, Cunningham AF, Crispin M (2022) Glycosylation and serological reactivity of an expression-enhanced SARS-CoV-2 viral spike mimetic. J M Biol. PMID: 34717971

**Lamerton RE***, Lightfoot A*, Nieves DJ, Owen DM (2021). The role of protein and lipid clustering in lymphocyte activation. Front Immunol. PMID: 33767692

* joint first author

### Presentations

BSI West Midlands Symposium, 2024 [Oral presentation]

11th Symposium on Haemostasis, North Carolina, 2024 [Poster presentation]

Institute of Cardiovascular Science Away Day, Birmingham, 2023 [Oral presentation – Best flash talk prize]

6th EuPLAN conference, Bristol, 2023 [Poster presentation]

British Society for Haemostasis and Thrombosis, Birmingham, 2023 [Oral presentation – Scientist in Training award]

4th Mechanisms of Inflammatory Disease Symposium, Birmingham, 2022 [Oral presentation]

BHF site visit, Birmingham, 2022 [Poster presentation]

28th International Complement Workshop (virtual), 2021 [Oral presentation – ECR prize]

British Society of Immunology Congress, Edinburgh, 2021 [Poster presentation]

Institute of Immunology and Immunotherapy Away Day, Birmingham, 2021 [Poster presentation]

3rd Mechanisms of Inflammatory Disease Symposium, Birmingham, 2021 [Poster presentation]

## List of Figures

## List of tables

## List of Abbreviations

| | |
|---|---|
| ACD | Acid citrate dextrose |
| BSA | Bovine serum albumin |
| BHI | Brain heart infusion |
| CFU | Colony forming unit |
| COVID-19 | Coronavirus disease 2019 |
| COX | Cyclooxygenase |
| CRP | Collagen related peptide |
| DIC | Disseminated intravascular dissemination |
| DIC (imaging) | Differential interference contrast |
| DOUBLE VACC | >28 days post 2$^{nd}$ Pfizer vaccine samples |
| dPPP | Anti-STm SL1344 antibody depleted platelet poor plasma |
| ECs | Endothelial cells |
| ELISA | Enzyme linked immunosorbent assay |
| FB | Factor B (complement) |
| GBD | Global burden of disease study |
| HAoECs | Human aortic endothelial cells |
| hIgG | Human IgG (pooled) |
| HIPPP | Heat inactivated platelet poor plasma |
| HIT | Heparin induced thrombocytopenia |
| HMVLECs | Human lung microvascular endothelial cells |
| iNTS | Invasive non-typhoidal *Salmonella* |
| IQR | Inter quartile range |
| ITAM | Immunoreceptor tyrosine-based activation motif |

| | |
|---|---|
| ITU-CONV | 4 months post-COVID ITU treatment |
| KO | Knock-out |
| KRG | Krebs-Ringer Glucose |
| LB | Luria-Bertani broth |
| LPS | Lipopolysaccharide |
| mAb | Monoclonal antibody |
| MAC | Membrane attack complex |
| MBL | Mannose binding lectin |
| MERS | Middle eastern respiratory virus |
| MFI | Median fluorescence intensity |
| N | Nucleoprotein (from SARS-CoV-2) |
| NEG | COVID negative samples |
| NETs | Neutrophil extracelluar traps |
| NHC | Non-hospitalised convalescent samples |
| NHS | Normal human serum |
| NIR-AZA | Near Infrared BF2-azadipyrromethene |
| NSAIDs | Non-steroidal anti-inflammatory drugs |
| OD | Optical density |
| OMP | Outer membrane protein |
| OMVs | Outer membrane vesicles |
| PAMPs | Pathogen associated molecular patterns |
| PBMCs | Peripheral blood mononucleocytes |
| PBS | Phosphate buffered saline |
| PF4 | Platelet factor 4 |
| pNPP | Para-nitrophenyl phosphate |

| | |
|---|---|
| PPP | Platelet poor plasma |
| PRP | Platelet rich plasma |
| RCT | Randomised controlled trial |
| RT | Room temperature |
| S | Spike protein (from SARS-CoV-2) |
| SARS(-CoV) | Severe acute respiratory syndrome coronavirus |
| SARS-CoV-2 | Severe acute respiratory syndrome coronavirus 2 |
| SNP | Single nucleotide polymorphism |
| ST | Sequence type |
| STm | *Salmonella* Typhimurium |
| STm IgG | Anti-*Salmonella* antibody |
| TLRs | Toll-like receptors |
| $TxA_2$ | Thromboxane $A_2$ |
| VACC | 28 days post 1$^{st}$ Pfizer vaccine samples |
| VWF | Von Willibrand factor |
| WP | Washed platelet |
| WP/PPP | Washed platelets resuspended in PPP |
| WP/T | Washed platelets resuspended in Tyrode's buffer |
| WT | Wildtype |

# CHAPTER 1: INTRODUCTION

As long as humans have been on earth, they have been co-existing with, and fighting against pathogens. Whilst the adaptive immune system is thought to have evolved approximately 500 million years ago in jawed fish (Flajnik and Kasahara, 2010), one of the earliest recorded human interactions with pathogens are the smallpox lesions found on a preserved mummy from 1145 BCE (Morens et al., 2020). The earliest recorded pandemic, the "Plague of Athens", took place in 430 BCE and killed 25% of the population of Athens (Littman, 2009). Whilst it is debated which pathogen caused this plague, smallpox, plague, and *Salmonella* Typhi have all been proposed (Littman, 2009).

Fast-forward to the present day, and we are still at war with pathogens. With the ability to cause both acute and chronic illness, there is still an incredible amount of research to be done in order to understand host-pathogen interactions and how best to treat the myriad of conditions pathogens can cause. For example, the COVID-19 pandemic caused severe disruption worldwide, with 287 million confirmed cases reported up to 31 December 2021, and an estimated global excess of deaths of 14.83 million (Msemburi et al., 2023). Furthermore, sepsis, whereby host responses to infection become dysregulated and lead to life-threatening organ dysfunction, contributed to 20% of worldwide deaths in 2017, with a total of 48.9 million cases (Rudd et al., 2020).

Both sepsis and COVID-19 are associated with thrombosis. Disseminated intravascular coagulation (DIC) takes place in approximately 35% of sepsis patients, and most septic patients will develop thrombocytopenia (Levi and van der Poll, 2017). Approximately one third of patients with severe COVID-19 (receiving intensive care treatment) experienced thrombotic complications during the initial outbreak (Klok et al., 2020). The coagulopathy associated with COVID-19 shares some features with DIC, but is distinct, with a higher frequency of venous thromboembolism and arterial thrombosis, and higher D-dimer and fibrinogen levels in severe COVID-19 (Iba et al., 2020, Knight et al., 2022).

With clear morbidity and mortality arising from infections, but also being worsened by dysregulated host responses, such as in sepsis, the work in this thesis focusses on unravelling aspects of host thromboinflammatory responses in one bacterial example, *Salmonella*, and one viral example, SARS-CoV-2, which are introduced in the following sections.

## 1.1 *Salmonella enterica*

*Salmonella* are Gram-negative, rod-shaped, flagellated bacteria. There are just two species (see Figure 1.1), with *S. bongori* and *S. enterica* subspecies II, IIIa, IIIb, IV and VI tending to be found in cold-blooded vertebrates and the environment rather than clinical isolates (Fabrega and Vila, 2013). Nearly all clinical isolates therefore belong to *S. enterica* subspecies I, which contains more than 1000 serovars (Brenner et al., 2000). Typhoidal *Salmonella* serovars, such as *S. enterica* Typhi and Paratyphi are largely human-restricted, and are the causative agents of typhoid fever – a life-threatening invasive disease (Gal-Mor et al., 2014). These serovars are endemic in the developing world where clean water

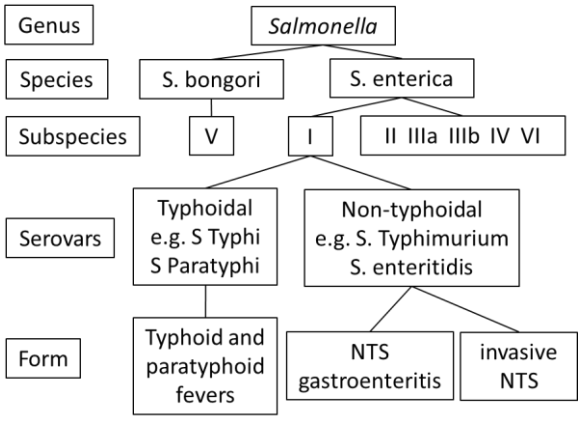


**Figure 1.1: Classification of *Salmonella* species.**

and sanitation facilities are lacking. In contrast, serovars causing non-typhoidal *Salmonella* are present worldwide, and generally cause self-limiting gastroenteritis in the developed world. However, some non-typhoidal *Salmonella* serovars, for example *S.* Typhimurium sequence type (ST) 313, are able to cause invasive disease, and have become a leading cause of bacteraemia in sub-Saharan Africa (Morpeth et al., 2009). This invasive non-typhoidal *Salmonella* is discussed further in section 1.1.2.

### 1.1.1 *Salmonella* outer membrane structure

As a Gram-negative bacterium, the *Salmonella* cell wall contains an inner membrane, periplasm, and an outer membrane (Figure 1.2). Lipopolysaccharide (LPS) forms the outer leaflet of the outer membrane, and each molecule is made up of lipid A, core oligosaccharide, and repeating O-antigen units. Lack of O-antigen renders *Salmonella* strains avirulent (Fierer and Guiney, 2001). *Salmonella* O-antigens are synthesised by the Wzx/Wzy pathway, with mutant strains lacking wzy only able to express a single O-antigen unit, and mutant strains lacking wbaP unable to synthesise any O-antigen units at all (Wright and Kanegasaki, 1971).

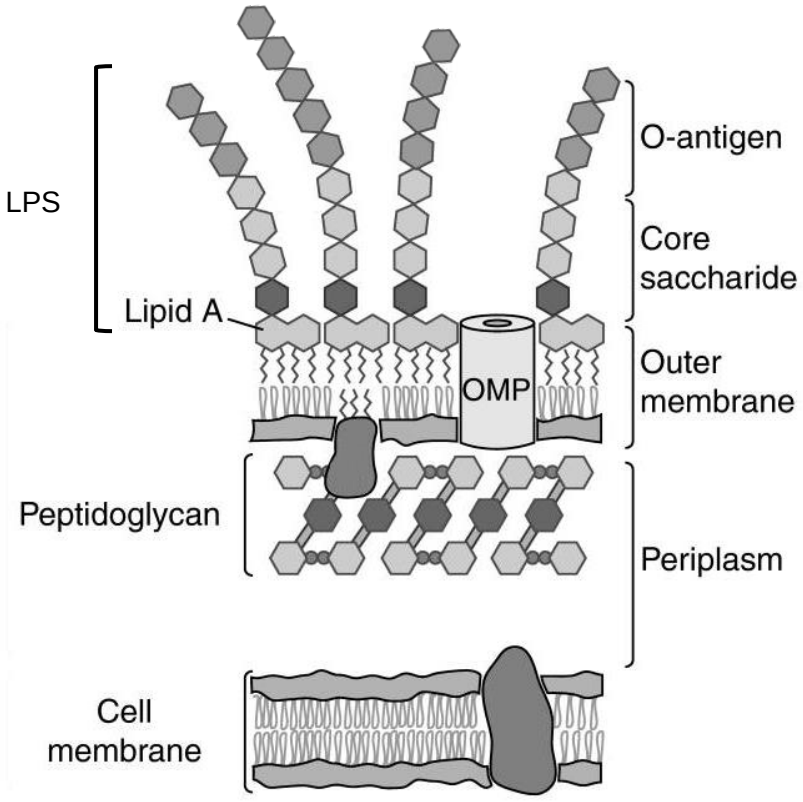


**Figure 1.2: Structure of *Salmonella* outer membrane**. Lipopolysaccharide is made up of lipid A in the outer membrane, to which core saccharide and repeating O-antigen chain lengths are attached. O-antigen chain lengths vary from 0 - >100 repeats. OMP = outer membrane protein. Adapted from (Silhavy et al., 2010).

### 1.1.2 Invasive non-typhoidal *Salmonella*

Whilst for immunocompetent individuals in developed settings non-typhoidal *Salmonella* typically manifests as self-limiting gastroenteritis, the picture is different in sub-Saharan Africa. Here, highly invasive forms of *S.* Typhimurium have emerged, labelled as clade ST313 (Figure 1.3). These strains are able to cross the gut barrier and enter the bloodstream, causing invasive non-typhoidal *Salmonella* (iNTS), and are now the dominant isolates in many sub-Saharan regions (Feasey et al., 2012). Strains are becoming increasingly multi-drug resistant (Van Puyvelde et al., 2023), with the representative epidemic strain D23580 resistant to streptomycin, sulphonamide, chloramphenicol, ampicillin and trimethoprim (Yang et al., 2015).

In adults, the main risk factor for iNTS is HIV, followed by old age. Children have more risk factors, with malnutrition, current or recent malaria (especially severe malarial anaemia), and sickle-cell anaemia increasing risk, as well as HIV (Feasey et al., 2012).

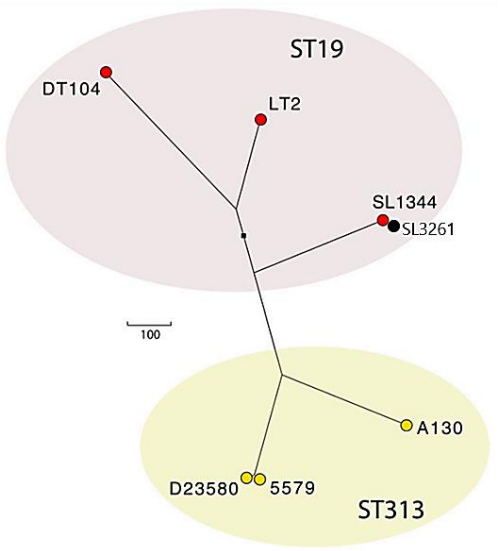


**Figure 1.3: Radial phylogram showing the relationship of S. Typhimurium isolates.** Branch lengths show the number of single nucleotide polymorphisms. Black square shows ancestral root. Yellow circles are clade ST313, red circles are clade ST19. Adapted from (Kingsley et al., 2009).

### 1.1.3 Clinical aspects of invasive non-typhoidal *Salmonella*

Patients experiencing an iNTS infection typically present with fever, with diarrhoea being uncommon. Diagnosis is difficult due to the lack of pathognomonic presentation – there are many other diverse symptoms, ranging from splenomegaly, severe anaemia and pneumonia, often due to co-infections. Therefore, blood cultures are the only way to know someone has iNTS.

Unfortunately, diagnosis is difficult, with a lack of blood culture facilities throughout Africa. Even when these facilities are present, the length of time blood cultures take to provide results (>48 hours), means iNTS causes significant morbidity and mortality. The lack of facilities also means obtaining accurate statistics on the impact of iNTS is difficult. Estimates from the Global Burden of Disease Study (GBD) suggest globally 535,000 cases of iNTS occurred in 2017, leading to over 77,500 deaths (Stanaway et al., 2019). The highest incidence of cases was in sub-Saharan Africa, at 34.5 cases per 100,000 person years. A meta-analysis carried out since the GBD study suggests a slightly higher incidence in Africa at 51 cases per 100,000 person years (Marchello et al., 2021). A further study focussing on mortality suggested a fatality rate of 15%, with septicaemia being the most prevalent complication, occurring in 57.2% of participants studied (Marchello et al., 2022). Those with HIV are at significantly higher risk of mortality due to iNTS, with the odds of death increasing by 2.4 (Marchello et al., 2022).

## 1.2 COVID-19

The SARS-CoV-2 virus was first reported in China in late December 2019. By March 2020 the virus had spread across the world, leading to its declaration by the World Health Organisation as a global pandemic (WHO, 2020). Up to the end of 2021, more than 287 million confirmed cases had been reported, along with over 5 million confirmed deaths (Msemburi et al., 2023).

The illness caused by SARS-CoV-2 virus infection is named COVID-19, and people are very variably affected, from asymptomatic infections, through to those requiring mechanical ventilation in hospital through to fatality. It is now well appreciated that certain factors lead to higher risk of severe COVID-

19 and mortality, including increasing age, the male gender, smoking and obesity (Dessie and Zewotir, 2021) as well as chronic kidney disease, heart failure and diabetes (Wingert et al., 2021, Kaeuffer et al., 2020).

### 1.2.1 Severe COVID-19

Although extremely difficult to quantify due to limited testing at the start of the pandemic, and a lack of appreciation of the level of asymptomatic cases, estimates from meta-analyses suggest the initial Wuhan SARS-CoV-2 outbreak led to severe COVID-19 disease in approximately 23% of people, and mortality in 6% of those infected (Li et al., 2021a).

Although many viruses that enter the body via the respiratory tract are restricted to infecting this area of the body (White and Brown, 1999), other viruses are capable of disseminating more widely throughout the body (e.g. measles and rubella) (White and Brown, 1999). SARS-CoV-2 falls into the latter category in severe disease, with wide ranging affects from kidney injury to myocarditis to skin infection, with the effect of SARS-CoV-2 on organs reviewed here in Lopes-Pacheco et al. (2021) and Gavriatopoulou et al. (2020). In terms of the bloodstream, although infective SARS-CoV-2 has not been able to be cultured from the blood of those with COVID-19 (Andersson et al., 2020, Saa et al., 2022), many studies have shown SARS-CoV-2 RNA (Jacobs et al., 2022, Stein et al., 2022, Hagman et al., 2022, Giacomelli et al., 2023, Jarhult et al., 2021, Andersson et al., 2020, Wang et al., 2020, Li et al., 2021b, Myhre et al., 2021, Saa et al., 2022) and spike and nucleoprotein antigens are present in the bloodstream (Ogata et al., 2020, Hingrat et al., 2020) . High levels of RNAemia and N antigenemia are associated with worse outcomes (Jacobs et al., 2022, Hagman et al., 2022, Jarhult et al., 2021, Li et al., 2021b, Costa et al., 2022, Verkerke et al., 2022, Wick et al., 2022, Zhang et al., 2022).

## 1.3 The immune system

In order to fight off the innumerate number of pathogens humans will encounter across the course of their lifetime, the immune system has evolved over thousands of years (Buchmann, 2014). The body

needs layers of defence in place to protect itself from unwanted invaders, and these can be generally split into the two branches of the immune system: the innate immune system and the adaptive immune system.

### 1.3.1 The innate immune system

The innate immune system is the non-specific, first line of defence against pathogens. The different types of barriers that make up innate immunity can be split into anatomical/physiological barriers, cellular barriers and humoral barriers. Examples of anatomical and physiological barriers include intact skin, mucous membranes for trapping microbes, the low pH of the stomach to kill pathogens and enzymes such as lysozyme that can cleave bacterial cell walls (Marshall et al., 2018, Turvey and Broide, 2010). Humoral immunity comprises anti-microbial peptides, and the complement pathway (see section 1.4) and cellular innate immunity includes the non-specific actions of macrophages, dendritic cells, natural killer cells, platelets and neutrophils. These cells are able to recognise pathogens via pathogen associated molecular patterns (PAMPs), such as double-stranded RNA, LPS and flagellin. Whilst the innate immune system provides a fast response to pathogens, and can recognise PAMPS, it is unable to recognise pathogen-specific antigens, which is where the adaptive immune system comes in.

### 1.3.2 The adaptive immune system

The hallmark of the adaptive immune system is immunological memory to specific antigens, whereby antigen-specific responses to repeat infections of the same pathogen can be induced much more quickly upon reinfection. Antigen-presenting cells, such as dendritic cells and macrophages, phagocytose pathogens and present fragments of the microbe on their cell surface. This allows activation of T cells into either cytotoxic T cells, which express CD8 and release enzymes to destroy the pathogen, or helper T cells, which express CD4 and can activate B cells. B cells then proliferate and

differentiate into memory B cells, which allow a quick response upon reinfection, or plasma B cells, which produce large amounts of antibody.

### 1.3.3 Antibodies

Antibodies have multiple functions. Firstly, antibodies can neutralise pathogens by binding to them and blocking their attachment to cells, thereby stopping cell entry or damage (Forthal, 2014). Antibodies can also act as opsonins, where the antibody coating the pathogen labels it as ready for phagocytosis (Murphy et al., 2008). An additional function of antibodies is to activate the classical complement system (see section 1.4), which leads to destruction of the pathogen by cell lysis.

There are five antibody subclasses: IgA, IgD, IgE, IgG and IgM. IgG is the most abundant isotype in serum, followed by IgA, IgM, IgD and IgE (Janeway et al., 2001b). Each have specialist functions and tissue distribution, for example, IgA is primarily found at mucosal sites, whereas IgE is predominantly located in tissues, bound to mast cells and basophils. Most relevant to this thesis are IgG and IgM, described further below.

### 1.3.4 IgM

IgM is the first antibody isotype to be produced by B cells, but in a primary response they tend to be of low affinity. However, in the blood, IgM is typically in the form of pentamers or hexamers (Brewer et al., 1994), whose 10 or 12 antigen binding sites combined allow high affinity binding (Murphy et al., 2008). This ability to bind multiple repeated antigens makes IgM particularly effective at binding bacterial capsules for example. Due to the large nature of these IgM complexes (>900 kDa), their location is mainly restricted to the bloodstream (Sathe and Cusick, 2022), although they can be directly trafficked across the mucosal epithelium by the polymeric immunoglobulin receptor (Matsumoto, 2022). The main function of IgM antibodies is to activate the classical complement pathway, and their oligomeric nature makes them the most efficient isotype at doing so (Sorman et al., 2014).

### 1.3.5 IgG

IgG makes up the largest proportion of antibody in the blood, and unlike IgM, is mostly monomeric, allowing it to leave the bloodstream and enter tissues. In a similar manner to IgM however, it can form hexamers, the higher affinity of which can enhance complement activation (Diebolder et al., 2014). It is further split into subclasses 1-4, each having slightly different functions. On the whole, IgG antibodies are effective at neutralising and opsonising pathogens (Murphy et al., 2008). IgG3 is the most efficient IgG subclass at activating the complement system, followed by IgG1 (Sorman et al., 2014). IgG1 subclass antibodies are often induced to proteins, along with lower levels of IgG3 and IgG4 (Vidarsson et al., 2014). IgG2 antibodies tend to be induced to bacterial capsular polysaccharides, and IgG4 is often induced by allergens (Vidarsson et al., 2014).

## 1.4 The complement system

The complement system is often described as being the bridge between the innate and adaptive immune system. Made up of over 40 different proteins found in blood plasma and cell surfaces, the proteolytic complement cascades begin with the identification of a pathogen, leading to the cleavage of complement proteins into anaphylatoxin and opsonin fragments, ending with the assembly of the membrane attack complex on the pathogen surface. Three different pathways make up the complement system, the classical, lectin and alternative pathways. Despite their different initiation steps, they all lead down the cascade to the same end point: pathogen opsonisation, lysis, and recruitment of inflammatory mediators (Figure 1.4).

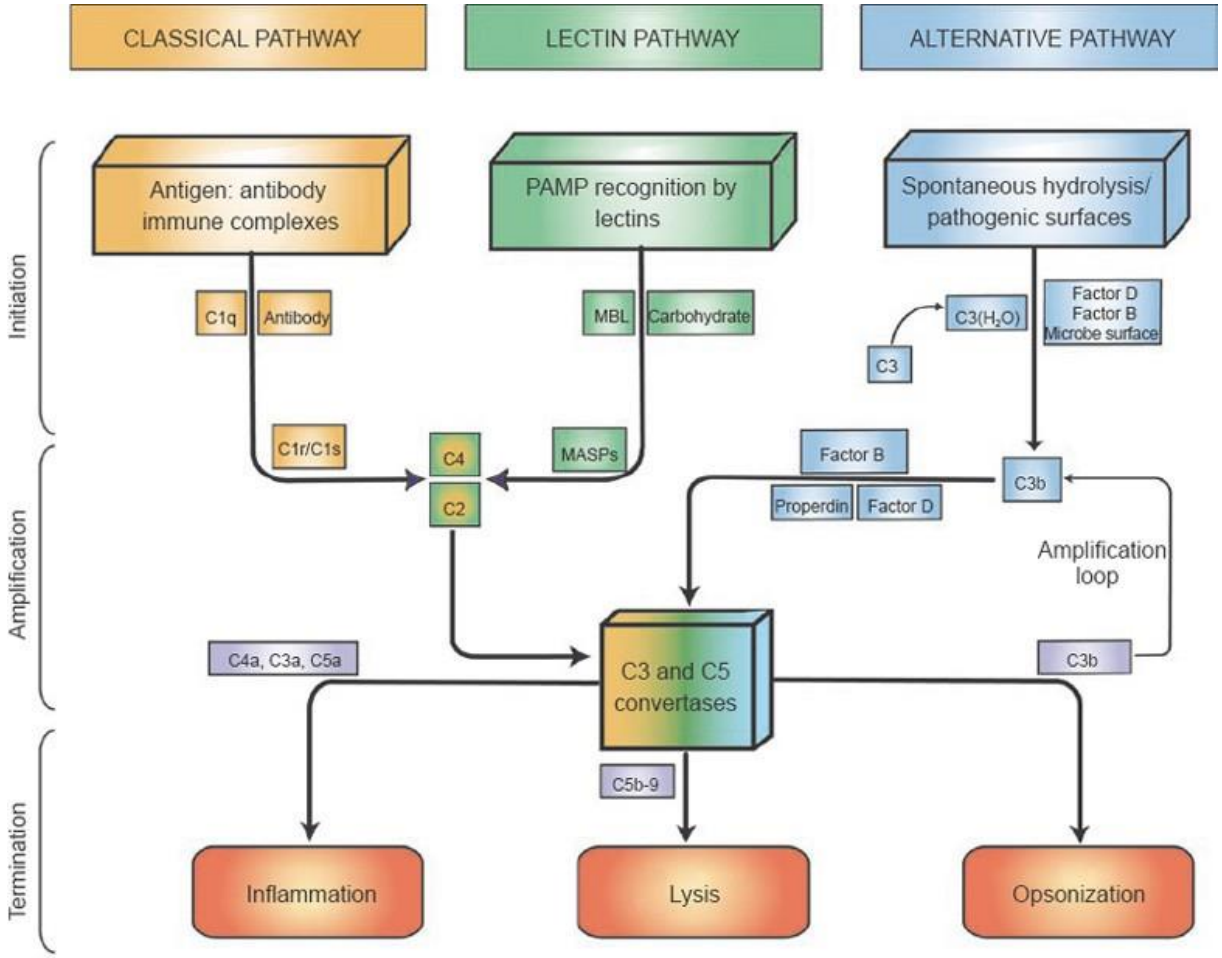


**Figure 1.4: Summary of the three different complement pathways**, all converging to have the same outcomes, taken from (Dunkelberger and Song, 2010). The three complement pathways all have different triggers, but converge at the terminal pathway (C5 convertase) to give the same outcomes, of inflammation, lysis and opsonisation.

### 1.4.1 The classical complement pathway

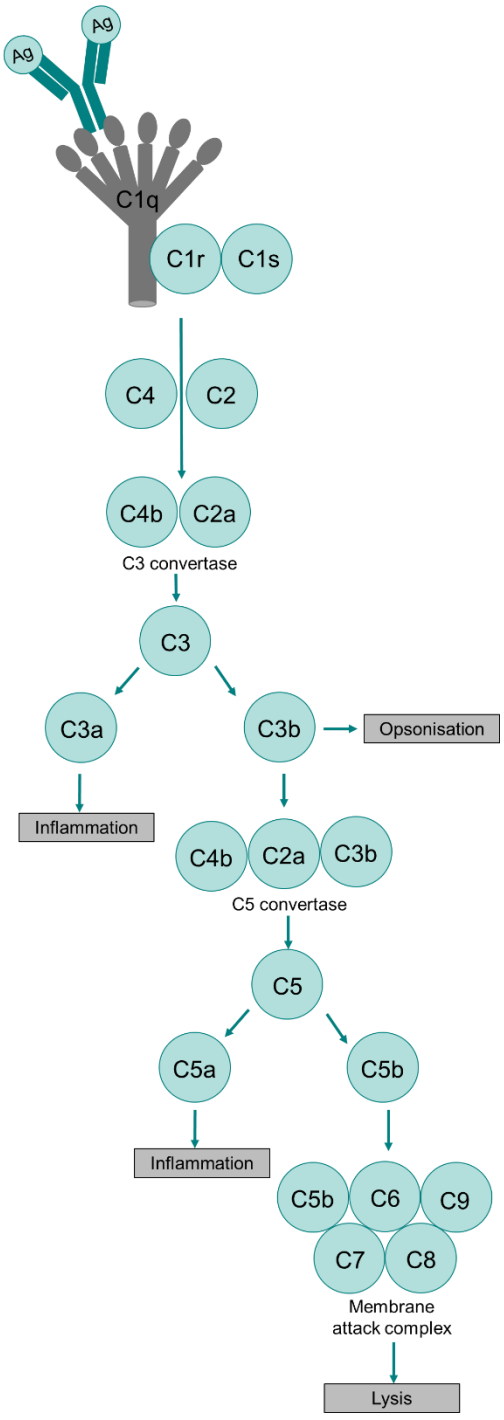


**Figure 1.5: Summary of the classical complement pathway cascade.** Binding of C1q to an antibody-antigen complex starts the classical complement cascade, leading to inflammation, opsonisation and lysis. Ag = antigen.

The first component of the classical pathway is C1q. A hexameric molecule, with six globular heads and triple-helical collagen-like tails, arranged in a so-called "bunch-of-tulips" fashion, it has further components C1r and C1s bound to the tails. Activation of the pathway via C1q can occur in three different ways: binding to the antigen-antibody complex; binding to antigen-C-reactive protein complex; or direct binding to the bacterial surface (Murphy et al., 2008). Upon this binding of the globular heads, a conformation change occurs in C1r, which can then cleave and activate the C1s zymogen. The C1s can now cleave C4 into C4a and C4b, with C4b binding to the adjacent pathogen or cell surface. This cleavage leaves C4b with a highly reactive thioester bond, which is quickly hydrolysed by water if the C4b is unable to bind the pathogen surface, thereby being an inbuilt safety mechanism. C2 binds this C4b, and is cleaved into two parts by C1s, with the C2a component remaining bound to the C4b. The C4b2a complex makes up the C3 convertase, with serine protease C2a cleaving C3 molecules into C3a, an anaphylatoxin promoting inflammation, and C3b, an opsonin. C3b can either coat the pathogen surface, labelling for phagocytosis or it can stay bound to C4b2a, making the C4b2a3b C5 convertase. C5 binds to the C3b

part of the convertase, whereby is it cleaved into C5a and C5b, again by the C2a serine protease. This is the last proteolytic step of the cascade (Figure 1.5), leading on to the formation of the membrane attack complex (MAC). In brief, C6 and C7 bind to the C5b, with C7 inserting itself into the pathogen lipid bilayer. Further binding of C8 and C9 allows the formation of the MAC pore structure. This hydrophilic ~100Å diameter pore leads to osmotic cell lysis and destruction of the pathogen – importantly nucleated, metabolically active mammalian cells are resistant to lysis by the MAC (Morgan, 1989).

### 1.4.2 Complement opsonisation

When C3b is formed, up to 1000 molecules can bind in the vicinity of a single active C3 convertase (Murphy et al., 2008). These C3b molecules act as opsonins, labelling the pathogen, and are recognised by complement receptor 1 (CR1), expressed on neutrophils and macrophages. This recognition alone does not lead to stimulation of phagocytosis, with a further signal needed. For example, C5a co-stimulation is needed to activate macrophages to phagocytose pathogens bound to the CR1 receptor. Extracellular matrix proteins such as fibronectin are also capable of providing this further signal to allow phagocytosis (Janeway et al., 2001a).

### 1.4.3 Complement anaphylatoxins

As well as MAC formation and C3b opsonisation, the anaphylatoxin fragments produced in the complement cascade play equally important role. Able to increase vascular permeability and smooth muscle contraction, along with phagocytic cell recruitment, the anaphylatoxins provide initiation of the adaptive immune system. Table 1.1 details the functions of the three anaphylatoxins.

**Table 1.1: The effects of complement anaphylatoxins**

| Anaphylatoxin | Effect |
|---|---|
| C5a | • Increase of neutrophil and monocyte: vessel wall adherence, phagocytic activity and migration to antigenic site<br>• Increases CR1 and CR3 expression on neutrophils and macrophages |
| C5a and C3a | • Induce endothelial cell adhesion molecules<br>• Activate mast cells |
| C5a, C4a and C3a | • Increase vascular permeability<br>• Increase smooth muscle contraction |

### 1.4.4 Complement neutralisation of viruses

There are four main mechanisms by which complement can affect the viral lifecycle (Morgan, 1990). Antibodies and complement binding to the virus surface can cause virus particles to aggregate, therefore lowering the number of infective particles available (Johnson et al., 2008). The binding of antibody and complement can also mask the antigens on the virus surface, mostly through the deposition of C3b, therefore preventing viral adhesion to host cells (Beebe et al., 1983). This is thought to be the major mechanism of neutralisation, but needs activation of the classical pathway to work effectively (Morgan, 1990, Ross, 1986). This coating of the viral particle also allows effective interaction with Fc and complement receptors on phagocytic cells, leading to destruction of the virus (Van Strijp et al., 1989). Finally, as mentioned in section 1.4.1, the formation of the MAC could lead to viral lysis. However, it is worth noting that for lysis to occur *in vitro*, large amounts of antibody/complement are required, likely making it unlikely to be the most effective method of the four detailed here (Morgan, 1990, Ross, 1986).

## 1.5 Platelets

Platelets are anucleate cell fragments of 1-3 μm in size, derived from megakaryocytes. They are present in humans at 150-400 x $10^9$/L and have a lifespan of just 7-10 days. Platelets contain three types of granules, which are released upon platelet activation: alpha granules, dense granules, and lysosomal granules. Alpha granules are the largest and most abundant of the three, with 50-60 per platelet (Ali et al., 2015). They contain a multitude of proteins that aid platelet adhesion and stable clot formation, as well as promoting inflammation and wound repair. These include fibrinogen, von Willebrand factor (VWF), platelet factor 4 (PF4), growth factors and microbicidal proteins (Ali et al., 2015). Dense granules contain small molecules that act as positive feedback signals, recruiting further platelets (Heijnen and van der Sluijs, 2015). These include ADP, ATP, GTP, serotonin, polyphosphate, $Ca^{2+}$ and histamine (Chen et al., 2018). The third type of granule, lysosomes, contain proteases and glycosidases, thought to be involved in thrombus remodelling (Meng et al., 2015).

### 1.5.1 The role of platelets in haemostasis

Classically, the main role of the platelet is haemostasis – the stopping of bleeding caused by damage to a vessel via clot formation. At the site of vascular injury, platelets adhere to the exposed collagen, leading to activation, granule release and formation of aggregates, allowing the formation of the platelet plug. Key platelet receptors involved in this process include GPVI, which binds collagen allowing platelet adhesion to the vessel wall, PAR-1 and $P2Y_1$/$P2Y_{12}$ which bind thrombin and ADP respectively leading to platelet activation, and αIIbβ3, which causes platelet aggregation upon binding to its multiple ligands including fibrinogen and VWF (Scridon, 2022).

### 1.5.2 The role of platelets in arterial and venous thrombosis

Whilst haemostasis is essential to allow for wound recovery, dysregulation in this process can cause thrombosis. Thrombosis is the pathological formation of a clot which limits the flow of blood through the vessel, and Virchow's triad describes three factors contributing to thrombus formation: vascular

injury, blood stasis and hypercoagulability (Kushner et al., 2022). Thrombi contain various components, including platelets, fibrin and red blood cells, and the proportion of these components typically varies depending on whether the thrombus is arterial or venous.

Arterial thrombi are generally thought of as 'white' platelet rich thrombi, with small amounts of fibrin and red blood cells. They usually develop due to the rupture of an atherosclerotic plaque in areas of high shear stress. In contrast, venous thrombi are typically 'red', with high red blood cell and fibrin content, and lower amounts of platelets, and occur in vessels with low shear stress (Scridon, 2022). Therefore, arterial thrombi tend to be treated with antiplatelet agents, and venous thrombi with anticoagulation agents. However, the 'arterial = white' and 'venous = red' dogma is starting to be challenged. A study of clots removed from the arteries of 177 patients with ischemic stroke showed a continuous variation in the composition of platelet and red blood cell rich regions, with some clots highly platelet rich, some highly red blood cell rich, and the majority with a combination of the two (Staessens et al., 2020). In addition, the location of clot formation can influence the composition of the clot. In contrast to the mixture of platelet and red blood cell rich areas seen in arterial ischaemic stroke, clots in the arteries of patients with myocardial infarction tend to be rich in fibrin (Alkarithi et al., 2021).

### 1.5.3 The role of platelets in immunity

As well as their role in haemostasis and thrombosis, platelets also play an important role in immunity. Platelet alpha granules contain kinocidins (classical chemokines with direct microbial activity (Yeaman, 2010)), thrombocidins and defensins, all of which are microbicidal proteins (Ali et al., 2015). These have been shown to kill or inhibit growth of pathogens such as *Escherichia coli, Staphylococcus aureus, Candida albicans* and *Cryptococcus neoformans* (Tang et al., 2002, Yeaman et al., 2007). Furthermore, PF4 is able to kill S. Typhimurium (Yeaman et al., 2007). Interestingly, platelets (and/or their secretome) are reported to be able to kill *S. aureus,* but not *Streptococcus. pneumoniae* (Wolff et al., 2020).

The receptors on the platelet surface also contribute to the role of platelets as immune cells. FcγRIIA can recognise immune complexes, and the complement receptors gC1q and CR3 (reported to be upregulated on activated platelets) can recognise C1q and C3a/C5a respectively (Martel et al., 2011, Peerschke et al., 2003, Burkhart et al., 2012). FcγRIIA is further discussed in section 1.5.7, and complement-platelet interactions in section 1.5.6.

The toll-like receptors (TLRs) are another key family in the platelet's role as an immune cell. They are able to recognise a wide variety of pathogen associated molecular patterns, for example, TLR-2 in complex with TLR-6 can recognise porins and lipotechoic acid amongst others, flagellin is a TLR-5 ligand, and LPS a TLR-4 ligand (Sameer and Nissar, 2021).

Platelets can also exert effects on other immune cells. The addition of platelets to plasma and neutrophils was shown to increase the effectiveness of neutrophil phagocytosis of periodontopathogens *Aggregatibacter actinomycetemcomitans* and *Porphyromonas gingivalis,* with the bacteria able to induce platelet-leukocyte aggregates in whole blood via TLR2. Interestingly, the combination of complement opsonisation of the bacteria and platelets led to the most effective neutrophil phagocytosis of the bacteria (compared to these components alone) (Assinger et al., 2011).

As well as exerting effects on neutrophils, activated platelets can also modulate the function of monocytes and CD4+ T cells. The addition of activated platelets to PMBC cultures stimulated with tetanus toxin or *P. gingivalis* led to the promotion of an anti-inflammatory phenotype, with a reduction in TNF-α production and an increase in IL-10 production, which was linked to platelet CD40L production. Furthermore, this inhibition of TNF-α was suggested to be responsible for the reduction in CD4+ T cell proliferation induced by the two pathogens when activated platelets were present (Gudbrandsdottir et al., 2013).

Platelets can also act as 'transporters' of bacteria, with *Listeria monocytogenes* binding to platelets which delivered the bacteria to a particular subset of highly immunogenic dendritic cells (Verschoor et

al., 2011). The initial adherence of bacteria to platelets was shown to be mediated by C3, and also occurred in *S. aureus, Enterococcus fecalis, Bacillus subtilis*, and nonencapsulated *S. pneumoniae,* but not in encapsulated *S. pneumoniae* (Verschoor et al., 2011).

As well as their interactions with other immune cells, platelets are also capable of internalizing bacteria. *S. aureus* and *P. gingivalis* can be taken up by platelets into vacuoles (Li et al., 2008), and IgG complexes can be internalised (Antczak et al., 2011). This internalisation of IgG complexes was shown to occur via FcyRIIA in transgenic mouse platelets (Worth et al., 2006). However, it is unknown whether this is helpful to the host or not. There is ongoing debate as to whether this internalisation kills the platelets, or simply protects them from being killed by other immune cells (White, 2006, Jahn et al., 2022).

As shown, platelets can directly influence immunity themselves, by the release of antimicrobial peptides and other cytokines they produce, as well as interacting with other immune cells and modulating their responses. When it comes to bacterial infections, there are multiple ways platelets can interact with bacteria. Platelet-bacterial interactions can lead to thrombus formation, and whether this is of help or hinderance to the host is discussed below.

### 1.5.4 Mechanisms of platelet activation by bacteria

Bacteria can activate platelets in three ways: directly, indirectly, or via toxins (Kerrigan, 2015). Examples of direct interactions include that of the *Streptococcus sanguinis* SrpA protein and platelet GPIbα; *Staphylococcus epidermis* SdrG protein and αIIbβ3; and *S. aureus* SpA and gC1q-R (Kerrigan, 2015). Indirect action takes place via a bridging protein, such as IgG, fibrinogen or VWF, for example *S. aureus* ClfA binds IgG which binds platelet FcγRIIA. Finally, bacterial toxins can interact with platelets – *E. coli* verotoxin can bind to glycosphingolipids (Kerrigan, 2015). In this manner, bacteria can interact with platelets and potentially lead to activation and aggregation. Unlike responses to traditional platelet agonists, bacterial-induced platelet aggregations have a variable lag time, and give all-or-

nothing responses (Cox et al., 2011). There are two possible consequences from platelet aggregation in response to bacteria: a helpful limit to bacterial dissemination by trapping the pathogen in the thrombus, or an unhelpful thrombotic response that leads to host damage.

### 1.5.5 Immunothrombosis and thromboinflammation

Immunothrombosis is the concept first put forward by Engelmann and Massberg in 2013. The goal of this innate immune response is to protect the host by recognising the pathogen and inhibiting its dissemination by trapping it in a blood clot. This response forms both a protective barrier around the bacteria, minimising its movement, and allows a focal point for the gathering of the immune cells needed to destroy the pathogen (Palankar and Greinacher, 2019). This includes the recruitment of neutrophils and the formation of neutrophil extracellular traps (NETs), which are particularly effective at killing bacteria (Brinkmann et al., 2004).

The dysregulation of this immunothrombosis process, or unregulated thrombus formation due to vessel injury or other inflammatory triggers, can lead to pathological thrombus formation. This damaging response is termed thromboinflammation (Guo and Rondina, 2019), an example of which is DIC, the uncontrolled thrombotic response seen in approximately 35% of patients with severe sepsis (Okamoto et al., 2016, Levi and van der Poll, 2015, Levi and Ten Cate, 1999). The uncontrolled thrombosis can reduce and block blood flow, leading to organ damage. Paradoxically, this clotting consumes platelets and clotting factors in places where they are not needed, leaving patients prone to bleeding.

In the context of *Salmonella* Typhimurium infection, there is a paucity of data on the thrombotic responses in humans. Many case reports have been published describing thrombotic events concurrent with *Salmonella* infections of various serovars (Carey et al., 2001, Saini et al., 2021, Lin et al., 2022, García-Fernández-Bravo et al., 2019, Taneda et al., 2019, Strutynskaya et al., 2020, Ghosh and Samanta, 1994, Suppamutharwyam and Radhakrishnan, 2022, Prakash et al., 2016), but there is a

lack of larger scale studies assessing the frequency of these events. *Salmonella* Typhimurium has however been well studied in mice. Whilst thrombi kinetics were different between the liver and the spleen, thrombi in both organs contained minimal numbers of bacteria (Beristain-Covarrubias et al., 2019a), suggesting more of a thromboinflammatory response than an immunothrombotic response.

### 1.5.6 Interactions between platelets and complement

With platelets and complement both present in the blood, and both involved in the immune response, the question arises as to whether there is interaction between the two.

Platelets express multiple complement receptors, which are upregulated upon platelet activation: C1q receptors cC1qR (binds the collagen-like portion of C1q) and gC1qR/p33 (binds the globular C1q head domain); C3aR, and C5aR1 (Speth et al., 2015, Martel et al., 2011). They also express complement regulatory proteins on their surface, including Factor H, C4 binding protein, and C1-inhibitor. Factor D, Factor H, C1-inhibitor and C3 are amongst those shown to be contained in alpha granules (Devine and Rosse, 1987, Speth et al., 2015, Maynard et al., 2007). Activated platelets can bind complement components – C5b-9 is not detected on resting platelets in platelet rich plasma, but is found on the surface of platelets after stimulation with traditional agonists (Martel et al., 2011).

Complement is able to induce platelet activation in multiple ways. C1q has been shown to upregulate P-selectin (Skoglund et al., 2010, Peerschke and Ghebrehiwet, 1997), and also to enhance platelet aggregation in response to immune complexes (Peerschke and Ghebrehiwet, 1997). The majority of work looking at C1q and platelets was carried out in the 1990s by Peerschke and Ghebrehiwet, with few recent developments aside from the Skoglund study. With some aspects of Peerschke's work unable to be replicated (S. P. Watson 2023, personal communication, 14 November), further work needs to be carried out to assess the role of C1q in platelet activation. Aside from C1q, C3a is able to induce platelet aggregation (Polley and Nachman, 1983). C5b-9 formation, which occurs upon platelet

aggregation to common agonists (Martel et al., 2011), can trigger the release of alpha granules (Sims and Wiedmer, 1995).

On the flip side, platelets can also activate the complement system. Examples of this include C3b and properdin binding to P-selectin on platelets, triggering activation of the alternative pathway (Del Conde et al., 2005, Saggu et al., 2013), and the release of chondroitin sulfate from activated platelets leading to complement activation via C1q (Hamad et al., 2008).

The interplay between complement and platelets/thrombus formation is elegantly demonstrated in multiple mouse studies. Mice deficient in C3 have abnormal platelet responses, with prolonged bleeding times, decreased platelet aggregation and decreased thrombus stability (Gushiken et al., 2009). In a model of venous thrombus formation, mice lacking either C3 or C5 had impaired venous thrombus formation (Subramaniam et al., 2017). This effect is seen even more strongly in the *Salmonella* Typhimurium mouse model, where the thrombi seen in the spleen and liver are completely absent in mice lacking C3 or C5 (Persaud and Cunningham, 2022, personal communication, 3 February), suggesting an important role in thrombus formation for the complement system.

Finally, complement has also been shown to be involved in platelet aggregation responses to bacteria, with the removal of complement from the system abolishing aggregation responses to *S. sanguinis* (Ford et al., 1996). Platelet gC1qR/p33 has also been shown to bind to a variety of different pathogens including *S aureus* protein A (Nguyen et al., 2000)*, Listeria monocytogenes* internalin B (Peerschke et al., 2003), and viral proteins from HIV, Epstein-Barr and herpes simplex (Peerschke et al., 2003).

### 1.5.7 FcγRIIA receptor

The platelet FcγRIIA receptor is a single chain receptor consisting of two extracellular immunoglobulin-like domains, a transmembrane domain and an immunoreceptor tyrosine-based activation motif (ITAM) on the cytoplasmic tail (Qiao et al., 2015). The receptor has a low affinity for IgG but binds with high avidity to multiple IgGs when part of an immune complex. It is the only Fc receptor present on

human platelets, and is not found on mouse platelets, meaning they do not have the capacity to bind IgG complexes (Worth et al., 2006). The FcγRIIA copy number differs between donors, with estimates ranging from 400-4500 copies (Tomiyama et al., 1992, Karas et al., 1982, Burkhart et al., 2012).

FcγRIIA can be activated in multiple ways, all of which involve cross-linking of the receptor, for example IgG-opsonised pathogens, cross-linked IV.3 mAb, or immune complexes such as antibodies bound to heparin/PF4 as seen in heparin induced thrombocytopenia (HIT) (Arman and Krauel, 2015). Signalling via FcγRIIA can lead to many different effector functions, including platelet aggregation, pathogen killing and microvesicle release (Arman and Krauel, 2015).

### 1.5.8 The link between heparin-induced thrombocytopenia, PF4 and bacteria

PF4 is a positively charged chemokine, primarily stored in platelet alpha granules. As mentioned above, FcγRIIA can be activated by immune complexes including antibodies bound to heparin-PF4 complexes, the cause of HIT. HIT is a serious complication arising from heparin treatment, whereby instead of the intended anticoagulant effects, heparin-PF4 complexes lead to thrombosis. When the negatively charged heparin binds to the positively charged PF4, a conformational change in the PF4 creates neoepitopes (Kreimann et al., 2014) to which, in HIT patients, anti-PF4 antibodies bind. It is thought that HIT is a mis-directed anti-bacterial response, originally evolved to allow the immune system to recognise the strong negative charge of bacteria (Greinacher and Warkentin, 2023). The adaptive immune system recognises antigens, and the interactions are purely structural/shape related. One theory is that the use of anti-PF4 antibodies has evolved as a way for the immune system to allow recognition of bacteria via their strong negative charge (Krauel et al., 2011). In a similar manner to HIT, negatively charged bacteria will bind to positively charged PF4, opening up the neoepitopes to which anti-PF4 antibodies can bind (Krauel et al., 2012). Once one response has been carried out in this manner, this then allows the adaptive immune system to respond with anti-PF4 antibodies upon further infections. Usually, in the case of a new pathogen, the adaptive immune system would take 1

-2 weeks to recognise and make sufficient levels of antibody in order for an effective response to begin. The theory behind PF4-bacterial interactions however, is that the PF4 is able to act as a short-cut to antibody response, by effectively turning the generic strong negative charge of bacteria into a single antigen, allowing the adaptive immune response to be activated.

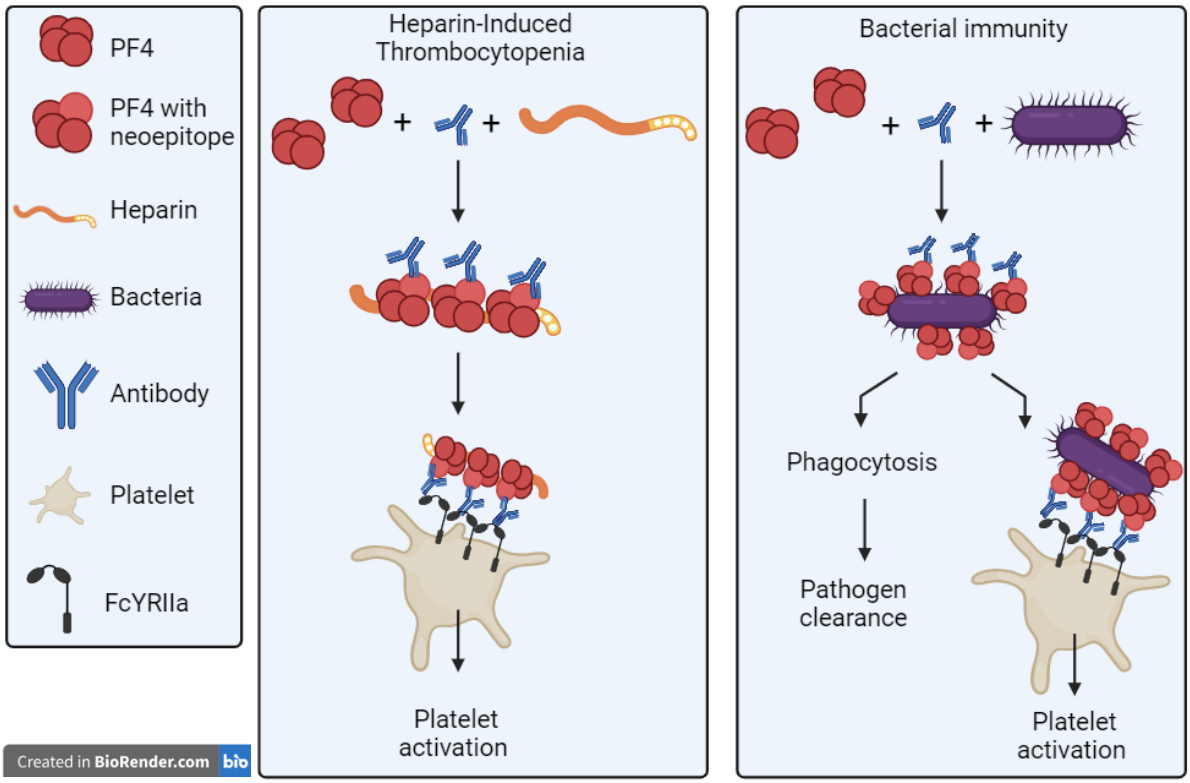


**Figure 1.6: The similarities between heparin-induced thrombocytopenia (HIT) and bacterial immunity.** In HIT, antibodies to the PF4-heparin complex lead to platelet activation and thrombosis. This is thought to be a mis-directed response evolved to provide a quicker adaptive immune response to bacteria via their charge attraction to PF4, which can then be recognised by antibodies leading to pathogen clearance.

**Table 1.2: Pathogens able to induce human platelet aggregation in vitro.** * = pathogens for which platelet aggregation occurred in a strain/isolate specific manner.

| Pathogen | | Interacts with these host factors | References |
|---|---|---|---|
| **Bacteria** | Gram +/- | | |
| *Aerococcus urinae** | + | IgG/ FcγRIIA, fibrinogen, complement | Shannon et al. (2010) |
| *Cutibacterium acnes** | + | IgG/ FcγRIIA, fibrinogen, complement | Petersson et al. (2018) |
| *Escherichia coli* | - | IgG/ FcγRIIA, αIIbβ3, complement | Moriarty et al. (2016), Watson et al. (2016); Landsem et al. (2022) |
| *Fusobacterium necrophorum** | - | | Forrester et al. (1985) |
| *Helicobacter pylori* | - | IgG/ FcγRIIA, GPIb | Byrne et al. (2003) |
| *Lactobacillus salivarius* | + | IgG/ FcγRIIA, fibrinogen | Collins et al. (2012) |
| *Porphyromonas gingivalis* | - | IgG/FcγRIIA, GPIb | Naito et al. (2006) |
| *Staphylococcus aureus* | + | IgG/FcγRIIA, fibronectin, fibrinogen, αIIbβ3, complement, VWF | Fitzgerald et al. (2006), Miajlovic et al. (2007), Kerrigan et al. (2008), Loughman et al. (2005); Arman et al. (2014), Vanassche et al. (2012); (O'Brien et al., 2002) |
| *Staphylococcus epidermidis* | + | IgG/ FcγRIIA, Fibrinogen | Brennan et al. (2009) |
| *Streptococcus agalactiae* | + | IgG/ FcγRIIA, Fibrinogen | Pietrocola et al. (2005) |
| *Streptococcus gordonii* | + | IgG/ FcγRIIA, αIIbβ3, GPIbα | Arman et al. (2014), Keane et al. (2010a); Takamatsu et al. (2005) |
| *Streptococcus oralis* | + | IgG/ FcγRIIA, GPIbα, | Tilley et al. (2013); Arman et al (2014) |
| *Streptococcus pneumoniae* | + | IgG/ FcγRIIA, TLR2 | Keane et al. (2010b); Arman et al. (2014) |
| *Streptococcus pyogenes* | + | IgG/ FcγRIIA, Fibrinogen | Shannon et al. (2007), Svensson et al. (2014) |
| *Streptococcus salivarius* | + | IgG/ FcγRIIA | Sullam et al. (1988) |
| *Streptococcus sanguinis* | + | IgG/ FcγRIIA, fibrinogen, complement, GPIbα | Arman et al. (2014) Pampolina and McNicol (2005), Sullam et al. (1988), Ford et al. (1997); Ford et al. (1996); Ford et al. (1997); Kerrigan et al. (2002), Plummer et al. (2005) |

| | | |
|---|---|---|
| **Viruses** | | |
| Influenza* H1N1, H5N1 | | Jansen et al. (2020) |
| **Fungi** | | |
| *Candida* species*, excluding *C. albicans* | | Willcox et al. (1998) |
| *Histoplasma capsulatum* | IgG/ FcγRIIA, fibrinogen, ADP | Des Prez et al. (1980) |
| *Mucor circinelloides* | IgG/ FcγRIIA, αIIbβ3 | Ghuman et al. (2019) |

### 1.5.9 *In vitro* studies of pathogen-induced platelet aggregation

Bacteria are by far the most well characterized pathogen type in terms of their effects on platelet aggregation, as demonstrated in Table 1.2. Whilst there are many described interactions between viruses and platelets, both direct and indirect, (reviewed in Assinger, 2014 and Schrottmaier et al, 2022) evidence of viral-induced platelet aggregation is rare, with many viruses such as Hantavirus, Junin virus and Lassa virus associated with inhibition of platelet aggregation (Cummins et al., 1990, Laine et al., 2015, Cummins et al., 1989). Similarly, few studies have taken place investigating fungal induced platelet aggregation.

Multiple different platelet receptors have been implicated in bacterial-induced platelet aggregation responses. As summarised in Table 1.2, FcγRIIA (and/or its ligand, IgG) is the most widely studied, with the receptor shown to be required for aggregation to all bacterial species listed. Other plasma components that can bridge the gap between bacteria and platelet, leading to aggregation via αIIbβ3, are fibrinogen and VWF, which bind *S. aureus* clumping factors A and B, and protein A respectively (O'Brien et al., 2002). Some bacterial species can bind directly to platelet receptors – oral streptococcal bacteria contain highly glycosylated serine-rich proteins which bind to GPIbα inducing aggregation (Kerrigan et al., 2002, Kerrigan et al., 2007, Tilley et al., 2013).

A role for complement has also been suggested in multiple different bacteria by multiple different groups to varying levels of specificity. Ford et al (1996) specify the alternative complement system as being involved in *S. sanguinis* platelet aggregation, whereas other studies paint a broader picture of complement involvement via heat-inactivation of plasma/serum or the use of zymosan to consume complement components (Loughman et al., 2005, Miajlovic et al., 2007). An important consideration in experimental design when looking at complement involvement in platelet aggregation is the requirement of the complement system for positive divalent ions – the classical and lectin pathways require $Ca^{2+}$ and $Mg^{2+}$, whilst the alternative pathway requires $Mg^{2+}$ only (Snyderman and Pike, 1975).

This becomes a problem when using common anti-coagulants to stop platelet activation upon taking blood. Sodium citrate is a divalent metal ion chelator, meaning it can inhibit complement activity in PRP. Addition of the required complement ions can be added to PRP along with PPACK to inhibit thrombin activation, however Martel et al (2011) found PPACK inhibited the alternative pathway. Other anticoagulants are also unsuitable, with heparin inhibiting the classical pathway by potentiating C1 inhibitor (Caughman et al., 1982), as well as impairing the alternative pathway, and hirudin inhibiting C5b-9 formation on platelets activated by collagen (Martel et al., 2011). Interestingly however, multiple papers have used PRP obtained in sodium citrate without adding back in the required ions, and found inhibition, or increase in lag time of aggregation when heat inactivating to remove complement activity (Ford et al., 1996, Petersson et al., 2018). These differences occur compared to their controls, despite the probable lack of $Ca^{2+}$ and $Mg^{2+}$ ions, perhaps suggesting there is enough free $Ca^{2+}$ still in the samples to allow complement functionality. To avoid possible problems with lack of $Ca^{2+}$ and $Mg^{2+}$ ions, Eriksson et al recommend the use of lepirudin, a recombinant hirudin, for whole blood platelet impedance measurements, as it is a highly specific thrombin inhibitor with no known effects on complement function (Eriksson et al., 2019).

The seminal paper describing the mechanisms behind bacterial induced platelet aggregations came from Arman et al in 2014. The paper brings together the requirement for FcγRIIA and the link between HIT and bacterial immune responses. They studied Gram positive bacterial strains frequently involved in infectious endocarditis (*S. sanguinis, Streptococcus gordonii, Streptococcus oralis* and *S. aureus*) and sepsis (*S. pneumoniae*). As per other bacterial strains, in PRP, all-or-nothing aggregation was observed, with lag times varying from 120-900 seconds depending on the strain. FcγRIIA engagement was required, with signalling being reinforced by integrin αIIbβ3, leading to the release of alpha and dense granules. ADP and thromboxane $A_2$ were also needed to reinforce platelet activation signals, with dual inhibition of these blocking platelet aggregation. When trying to induce platelet activation in washed platelets, a source of pooled human IgG was required for aggregation, and the further addition of

fibrinogen reduced the lag time. The exception to this was *S. pneumoniae,* which was unable to cause aggregation under these conditions in 3/5 of the donors tested. PF4 was able to bind to all the bacterial strains, reducing the lag time when used in the washed platelet/IgG/fibrinogen system. Taking into account the likely mechanism of this as anti-PF4 antibodies opsonising the bacteria as described above in section 1.5.8, it could be argued that this is an unusual finding – estimates of anti-PF4 antibodies in the population are approximately 6 % for IgG (Hursting et al., 2010, Krauel et al., 2011) and 19% for IgM (Krauel et al., 2011), so the ability for PF4 to reduce lag time in the donors tested perhaps suggests an alternative mechanism of action as it's unlikely all the donors used had anti-PF4 antibodies present. Arman et al theorise that IgG-coated bacteria binding to FcγRIIA is likely to be the central pathway involved in all bacterial-induced platelet aggregation, leading to αIIbβ3 signalling either by inside-out signalling, or by the direct binding of other bacterial proteins. This combined signalling leads to granule release, where ADP, thromboxane $A_2$ and PF4 are released, which then amplify the signal further via positive feedback mechanisms.

## 1.6 The vasculature

### 1.6.1 Endothelial cells

Endothelial cells (ECs) line all blood vessels, with an estimated 6 x $10^{11}$ ECs in the average human body (Sender et al., 2016). They are attached to the basal lamina, which is synthesised and secreted by the ECs, and comprises mainly of collagen, laminin, entactin and heparan sulfate proteoglycans (Simionescu and Antohe, 2006). EC characteristics differ between the arterial and venous systems, with arterial ECs tending to be more elongated and narrower than venous ECs (Simionescu and Antohe, 2006), and ECs present in the aorta are up to 10 x thicker than those found in capillaries and veins (Kruger-Genge et al., 2019). Most adhesion molecules are preferentially expressed on venous ECs over arterial ECs, meaning leukocyte-EC interactions tend to only be found in the venous system (Simionescu and Antohe, 2006). Furthermore, the organ in which the ECs are found has an influence on the EC phenotype, with Weibel-Palade bodies (where VWF is stored) abundant in the pulmonary vasculature, but lacking in the thoracic aorta (Kruger-Genge et al., 2019).

### 1.6.2 Endothelial cell functions

ECs do not simply provide a tube for blood to flow through, they have many functions and are able to dynamically influence the vascular environment (Michiels, 2003). They play a vital role in vascular homeostasis, with the release of prostacyclin and nitric oxide by healthy ECs important in limiting platelet aggregation for example. They are able to control blood flow via vasoconstriction and vasodilation, which are induced by the production of factors such as nitric oxide, adenosine, and metabolites of arachidonic acid such as prostaglandins (Feletou, 2011). However, whilst healthy ECs have an antithrombotic, anti-inflammatory phenotype, this can change upon infection or injury. The pro-thrombotic EC phenotype allows interactions with platelets, causing them to roll, adhere and form stable thrombi (reviewed in Coenen et al. 2017) . Upon activation, ECs release VWF, which interacts with platelet GP1b, causing platelet rolling along the EC surface. Rolling can also be facilitated by

interactions between platelet P-selectin and EC P-selectin glycoprotein ligand-1 (PSGL-1). Platelets then adhere to ECs via interactions between platelet αIIbβ3 and EC αVβ3 and ICAM-1, whose expression is upregulated in activated ECs (Feletou, 2011). Activation of surrounding platelets is stimulated by thrombin, ADP and thromboxane, leading to stable thrombus formation. Upregulation of other adhesion molecules on activated ECs such as E-selectin, VACM-1 and P-selectin allow not only platelet interactions, but white blood cell adherence, leading to their transmigration to infected tissues for example.

### 1.6.3 Endothelial cell junctions

ECs form a selective barrier for the transport of molecules, proteins and cells between blood and tissues. In order to form this barrier and maintain the required levels of permeability that vary between vascular beds, there are three different types of cell-cell junctions: tight junctions, adherens junctions and gap junctions. These junctions do not just function as sites of contact between adjacent ECs, but play a role in signalling to regulate vascular homeostasis and vessel growth (Dejana, 2004). Tight junctions provide a barrier, restricting permeability of the vessel and maintaining cell polarity. They tend to be well developed and organised in arteries, but less so in veins (Bazzoni and Dejana, 2004). Claudins, occludins, junctional adhesion molecules and zona occludens proteins make up the main adhesive proteins found in tight junctions. Adherens junctions provide paracellular permeability to leukocytes and solutes, and play a role in signalling to regulate vessel growth. The main adhesive protein in adherens junctions is vascular endothelial cadherin (VE-cadherin). Gap junctions function as communication structures where small molecular weight solutes can pass through to neighbouring ECs, and are formed by connexins. VE-cadherin and claudin-5 (adherens and tight junctions respectively) work together to control the overall tightness of the EC barrier (Razakandrainibe et al., 2013).

The variation in expression of these junctions, and how they are organised varies between the type of blood vessel and how much permeability the organ served by the blood vessel requires. For example, the endothelium of large arteries has a larger proportion of tight junctions to allow high levels of control over permeability, whereas junctions in postcapillary venules are lax in their organisation to allow high levels of trafficking (Bazzoni and Dejana, 2004).

## 1.7 Aims of thesis

Whilst it is clear that iNTS causes significant morbidity and mortality in sub-Saharan Africa (Stanaway et al., 2019), and is able to induce a well-defined thrombotic response in mice (Hitchcock et al., 2015), research into how *Salmonella* interacts with components of the bloodstream in humans is very limited. Whilst mechanisms of bacterial-induced platelet aggregation have been described for pathogens such as multiple *Streptococci* strains, *E. coli* and *S. aureus* as described in section 1.5.9, no research has been done into the effects of *Salmonella* Typhimurium strains on platelets. The overall aim of this thesis was to investigate host-pathogen interactions taking place in the bloodstream, specifically:

A) To investigate the mechanisms of platelet activation by *Salmonella* Typhimurium strains

B) To investigate how *Salmonella* Typhimurium strains interact with platelets and endothelial cells under static and flow conditions

Furthermore, as the work for this thesis started during the COVID-19 pandemic, the host-pathogen interactions of SARS-CoV-2 were also investigated, with a focus on the classical complement system to fill in the knowledge gaps at that time, specifically:

C) To establish whether SARS-CoV-2 can activate the complement system and investigate the role of antibodies from different patient groups in complement activation.

# CHAPTER 2: MATERIALS AND METHODS

## 2.1 Materials

**Table 2.1: Reagents used**

| Product name | Company | Catalogue number |
|---|---|---|
| Agar | VWR | 84609.0500 |
| Anti-*Salmonella* IgG antibody (STmIgG) | Abcam | ab35156 |
| Brain Heart Infusion | Sigma<br>VWR | 53286<br>84626.0500 |
| BSA (Bovine serum albumin) | Sigma-Aldrich | A4697 |
| Calcium chloride | Sigma-Aldrich | 21115 |
| Endothelial cell growth medium MV | Promo Cell | C-22020, supplementary mix C-39225 |
| Endothelial cells (Human aortic endothelial cells - HAoECs) | Promo Cell | C-12271 |
| Fibrinogen | Millipore | 341576<br>Lot number: 2893826 |
| Fluoroshield™ mount with DAPI | Sigma-Aldrich | F6057 |
| Human pooled IgG (hIgG) | Sigma-Aldrich | 14506 |
| LB agar | Sigma-Aldrich | L2897 |
| LB broth | Sigma-Aldrich | L3022 |
| Magnesium chloride | Sigma-Aldrich | M1028 |
| NIR-AZA | RCSI chemistry department | NA |
| PBS (phosphate buffered saline) tablets | Thermo Fisher Scientific | 18912014 |
| Para-nitrophenyl phosphate (pNPP) | Thermo Fisher Scientific | 34045 |
| PF4 ELISA kit | ImmuCor | HAT45G |
| Pierce BCA protein assay kit | Thermo Fisher Scientific | 23225 |
| Platelet factor 4 | Chromatec GmbH | |
| Pooled human plasma (PPP, chapter 4) | Innovative Research | IPLALIH-50ml 30837 |
| Sodium citrate | Sigma-Aldrich | S-4641 |
| TMB Core | Bio-Rad | BUF056B |
| TNF-alpha | Gibco | PHC3016 |
| Triton X-100 | Sigma-Aldrich | X100 |
| Trypsin-EDTA | Sigma-Aldrich | T3924-500ml |
| Tween-20/polysorbate 20 | Acros organics | 23362500 |

**Table 2.2: Agonists, antagonists and inhibitors**

| Agonists, antagonists and inhibitors | Use | Source |
|---|---|---|
| Apyrase (Grade VII) | ATP/ADP hydrolysis for ADP sensitive platelets | Sigma-Aldrich A6535 |
| Cangrelor | $P2Y_{12}$ antagonist | The Medicines Company |
| Collagen related activating peptide (CRP) | GPVI agonist | CambCol Ltd |
| Compstatin | C3 inhibitor | MedChemExpress HY-P10361CS-7604 |
| Eptifibitide | αIIbβ3 inhibitor | GSK |
| Fab IV.3 | FcγRIIA inhibitor | Ying Di, University of Birmingham |
| FUT-175 | Broad spectrum complement inhibitor | Apexbio A2586 |
| Heparin sodium | Negatively charged polysaccharide | Wockhardt UK Ltd |
| Indomethacin | Cyclooxygenase inhibitor | Sigma, I7378 |
| MRS 2179 | $P2Y_1$ receptor antagonist | Sigma |
| TRAP-6 peptide (SFLLRN) | PAR-1 receptor agonist | AltaBioscience |
| PPACK | Thrombin inhibitor | Cambridge biosciences, FPRCK-01 |
| Prostacyclin | Platelet inhibitor | Cayman Chemicals 18220 |

**Table 2.3: Composition of buffers used**

| Buffer | Components |
|---|---|
| Acid citrate dextrose (ACD) | 120 mM sodium citrate<br>110 mM glucose<br>80 mM citrate dextrose<br>In distilled water, final pH ~4.4 |
| Krebs Ringer Glucose (KRG) | 120 mM NaCl<br>4.9 mM KCl<br>1.2 mM $MgSO_4$<br>1.7 mM $KH_2PO_4$,<br>8.3 mM $Na_2HPO_4$<br>10 mM glucose<br>In distilled water, final pH 7.4 |
| Lysis buffer | 0.1 M NaOAc<br>0.1% Triton X-100<br>In distilled water, final pH 5.5 |

| | |
|---|---|
| Modified Tyrode's | 134 mM NaCl<br>2.9 mM KCl<br>0.34 mM $Na_2HPO_4.12H_2O$<br>12 mM $NaHCO_3$<br>20 mM HEPES<br>1 mM $MgCl_2$<br>5 mM glucose<br>In distilled water, final pH 7.4 |

## 2.2 Preparation of bacteria

### 2.2.1 *Salmonella* strains

10 ml Luria-Bertani (LB) broth was inoculated with one colony of the relevant bacteria and incubated statically at 37°C overnight. The following morning, to obtain log phase bacteria, cultures were diluted 1:5 or 1:10 in pre-warmed LB broth to a total volume of 10 ml and incubated for 2 hours at 37°C, 200 rpm (25 mm throw). $OD_{600}$ was measured and bacteria were spun at 10,000 g for 5 minutes. Pellets were resuspended in phosphate buffered saline (PBS), then centrifuged and resuspended a further two times to wash bacteria. At the final resuspension, pellets were resuspended in PBS to give a final $OD_{600}$ of 1, relating to the approximate colony forming unit (CFU)/ml shown in Table 2.4. *Salmonella enterica* serovar Typhimurium is shortened to STm from hereon in.

**Table 2.4: *Salmonella* strains used in this thesis.**

| Strains | Characteristics | ~ CFU/ml in 1 $OD_{600}$ |
|---|---|---|
| STm SL3261 *aroA*$^-$ | Attenuated STm strain, deficient in *aroA* gene (rendering strain auxotrophic for aromatic amino acids). Parent strain: SL1346; Grandparent strain: SL1344. (Hoiseth and Stocker, 1981) Source: Dr Robert A Kingsley | $5 \times 10^8$ |
| STm SL1344 | Virulent *aroA+* STm strain. Parent strain: S2337, isolated from calves. (Hoiseth and Stocker, 1981) Source: Dr Robert A Kingsley | $1 \times 10^9$ |
| STm SL1344 mCherry | Above strain labelled with mCherry<br>Source: Dr Robert A Kingsley | $1 \times 10^9$ |
| STm D23580 | Virulent invasive multi-drug resistant STm ST313 pathovar, isolated from a child in Malawi (Kingsley et al., 2009) Source: Dr Robert A Kingsley | $1 \times 10^9$ |

| | | |
|---|---|---|
| SW515 STm SL1344 OmpA$^-$ | As SL1344 above, with deletion of OmpA gene. Source: Dr Robert A Kingsley | 1 x $10^9$ |
| RAK82 STm SL1344 OmpR$^-$ | As SL1344 above, with deletion of OmpR gene. (Gil-Cruz et al., 2009) Source: Dr Robert A Kingsley | 1 x $10^9$ |
| STm 14028 OmpD$^-$ | As 14028 below, with deletion of OmpD gene. Source: Dr Anna Schager, University of Birmingham | 1 x $10^9$ |
| *Salmonella enterica* serovar Enteritidis D24954 | Virulent strain of S. Enteritidis isolated from a child in Malawi. (MacLennan et al., 2010). Source: Prof Calman MacLennan | 1 x $10^9$ |
| STm 14028 | Descendant of CDC 60-6516, isolated from chickens. (Jarvik et al., 2010) Source: Thermo Fisher | 2 x $10^9$ |
| STm 14028 wzy$^-$ | *wzy* gene deletion leading to a single O-antigen on LPS. Source: Areej Alshayea, University of Birmingham | 2 x $10^9$ |
| STm 14028 wbap$^-$ | *wbap* gene deletion, causing no O-antigen on LPS. Source: Areej Alshayea, University of Birmingham. | 1 x $10^9$ |
| STm 14028 tolR$^-$ | Deletion of *tolR* gene leading to vesicle hyperblebbing from outer membrane. Source: Prof Ian Henderson | 1 x $10^9$ |
| STm 14028 tolR$^-$ wzy$^-$ | As *tolR* mutant above with additional deletion of *wzy* gene, leading to a single O-antigen on LPS. with Source: Areej Alshayea, University of Birmingham | 1 x $10^9$ |
| STm 14028 tolR$^-$ wbap$^-$ | As *tolR* mutant above with additional deletion of *wbap* gene, causing no O-antigen on LPS. Source: Areej Alshayea, University of Birmingham | 5 x $10^8$ |

### 2.2.2 Other bacterial strains

*Staphylococcus aureus* Newman and *Streptococcus oralis* CR834 were both grown in brain heart infusion (BHI) media to stationary phase. 10ml BHI broth was inoculated with one colony and incubated statically at 37°C overnight. The following morning cultures were washed as per *Salmonella* above, and normalised to either $OD_{600}$ = 1.6 or $OD_{600}$ = 1.0, relating to the approximate CFU/ml shown in Table 2.5.

**Table 2.5: Other bacterial strains used in this thesis.**

| Strains | Characteristics | ~ CFU/ml in 1.6 $OD_{600}$ |
|---|---|---|
| *Staphylococcus aureus* Newman | Human clinical isolate (Duthie and Lorenz, 1952), reference strain for *S. aureus* Source: Professor Timothy Foster, Trinity College Dublin, Ireland, via Professor Steve Kerrigan, RCSI, Dublin, Ireland. | $1 \times 10^9$ ($OD_{600}$ = 1.0 approx $1 \times 10^8$) |
| *Streptococcus oralis* CR834 | Isolated from the human mouth Source: Professor Ian Douglas, University of Sheffield, UK, via Professor Steve Kerrigan, RCSI, Dublin, Ireland. | $4 \times 10^9$ |

## 2.3 Preparation of human platelets

### 2.3.1 Blood collection and ethics – for platelet project

Ethics for the collection of blood from healthy donors was granted by the University of Birmingham Internal Ethical Review (ERN_11-0175).

Venous blood was collected from consenting donors (who had not taken aspirin or non-steroidal anti-inflammatory drugs (NSAIDs) in the previous 10 days) into 3.2% or 3.8% sodium citrate vacuette blood containers (Greiner Bio-One) tubes using a 21 gauge needle.

### 2.3.2 Preparation of platelet rich plasma and platelet poor plasma

Blood anti-coagulated in 3.2% citrate was centrifuged at 200 g for 20 minutes at room temperature (RT). The supernatant of platelet rich plasma (PRP) was removed before centrifugation of the remaining buffy coat layer and red cells at 1000 g for 10 minutes at RT. This yielded a supernatant of platelet poor plasma (PPP) for use as a blank in aggregometry. Platelet counts were measured in PRP using either a Coulter Counter or XP-300 (Sysmex).

### 2.3.3 Preparation of washed platelets

Blood was taken into tubes containing 1:9 3.8% citrate. A further 10% acid citrate dextrose (ACD) was added for anticoagulation, before centrifugation at 200 g for 20 minutes at RT. PRP supernatant was removed and 0.2 µg/ml prostacyclin was added before centrifugation at 1000 g for 10 minutes. Supernatant was discarded and pellet resuspended in modified Tyrode's plus 0.2 µg/ml prostacyclin and 3 ml ACD. This mixture was centrifuged for 10 minutes at 1000 g. Supernatant was discarded and platelet pellet resuspended to a concentration of 2 x $10^8$ platelets/ml. Washed platelets were rested for 30 minutes prior to experiments.

### 2.3.4 Preparation of ADP sensitive platelets

22% ACD was added to blood taken in 3.2% citrate blood tubes before centrifugation at 200 g for 20 minutes at RT. Supernatant PRP was transferred into fresh tubes, where a further 10% ACD was added, before centrifugation at 500 g for 15 minutes at RT. PPP was removed, and platelet pellet surface was washed gently 3 times with Krebs-Ringer Glucose buffer (KRG) plus 0.01 U/ml grade 7 apyrase. For washed platelet assays, pellets were resuspended in KRG buffer with 0.01 U/ml grade 7 apyrase, counted and adjusted to 2 x $10^8$ platelets/ml, before addition of 1mM $Ca^{2+}$ (calcium chloride). For donor swap assays, pellets were resuspended in PPP (obtained from separate 3.2% blood tubes to be ACD-free, spun at 1000 g for 10 minutes) with 0.01 U/ml grade 7 apyrase, counted, and adjusted to 2-3 x $10^8$ platelets/ml.

### 2.3.5 Antibody depletion of PPP

PPP was obtained as per section 2.3.2, aliquoted and frozen at -20 °C for up to two weeks. STm SL1344 bacteria was grown overnight as detailed in section 2.2.1. The pellet from 3 ml of culture (normalised to $OD_{600}$ = 1) was resuspended in 3 ml thawed PPP and rotated gently at 4°C for 2 hours. This was then centrifuged for 5 minutes at 10,000 g to pellet bacteria, with the resulting STm SL1344-specific antibody-depleted PPP (dPPP) supernatant obtained and stored overnight at 4°C before use the

following day in aggregation experiments. ADP sensitive platelet method (section 2.3.4) was used to wash platelets, which were then resuspended in either thawed PPP or dPPP.

## 2.4 Platelet aggregometry

Platelet aggregation experiments were carried out on a PAP-8 aggregometer (Bio-data Corp). Total volume per aggregation was 300 µl. Cuvettes with PRP or washed platelets were pre-warmed at 37°C for 2 minutes and stirred at 1200 rpm for 1 minute before addition of agonist. 1200 rpm stirring and 37°C incubation was maintained throughout. Traces were recorded for at least 30 minutes. Donor specific PPP, or Tyrode's buffer was used as blank measurement for PRP and washed platelet assays respectively. For inhibition studies, platelets were incubated with inhibitor for at least 3 minutes prior to start of recording. For complement inhibition assays, PRP was incubated with 40 µM PPACK for 5 minutes before addition of 1-2 mM calcium chloride and magnesium chloride.

## 2.5 Flow cytometry (for FcγRIIA)

3 µl of either FITC conjugated mouse anti-human CD32 (BD pharmingen), FITC mouse IgG2b κ isotype control (BD pharmingen) or PBS was added to 100 µl PRP. Samples were incubated in the dark for 30 minutes, before further dilution with 250 µl PBS. Samples were analysed using either a C6 Accuri (BD Biosciences) or a cytoFLEX (Beckman Coulter) flow cytometer.

## 2.6 Antibody ELISAs

### 2.6.1 COVID-19 antibody ELISA

SARS-CoV-2 HexaPro spike protein (stabilised version of the Wuhan strain) was a kind donation from Prof Max Crispin, made by Maddy Newby as described in Lamerton et al, 2022 (see chapter 5). Nucleoprotein was made by the University of Birmingham Protein Expression Facility. 96 well high-binding plates (Corning) were coated with 0.1 µg S or N protein (total 50 µl per well) in PBS and incubated overnight at 4°C. Plates were washed with PBS-0.1 % (v/v) Tween 20, 3 times. These washes

were carried out between all subsequent steps. Plates were blocked with 2% (w/v) bovine serum albumin (BSA) in PBS-0.1% Tween 20 for 1 hour at RT. Serum was diluted 1 in 40 in 2% (w/v) BSA in PBS-0.1% Tween 20 and incubated for 1 hour at RT. For combined IgG, IgA and IgM measurements, 100 µl pre-diluted IgGAM HRP-conjugated antibody from The Binding Site (EACONJ654) was used, and incubated at RT for 1 hour. For individual IgG isotypes the following HRP-conjugated monoclonal antibodies were used:

**Table 2.6: Details of antibodies used for COVID antibody ELISAs**

| Antibody target | Clone | Dilution | Source |
|---|---|---|---|
| IgG total | R-10 | 1:8000 | Dr Margaret Goodall, University of Birmingham |
| IgG total | 2040-05 | 1:8000 | Southern Biotech |
| IgG1 | MG6.41 | 1:3000 | Dr Margaret Goodall, University of Birmingham |
| IgG2 | MG180.02 | 1:3000 | Dr Margaret Goodall, University of Birmingham |
| IgG3 | MG5.161 | 1:1000 | Dr Margaret Goodall, University of Birmingham |
| IgG4 | RJ4 | 1:1000 | Dr Margaret Goodall, University of Birmingham |
| IgA | MG156 | 1:4000 | Dr Margaret Goodall, University of Birmingham |
| IgM | AF6 | 1:2000 | Dr Margaret Goodall, University of Birmingham |

Plates were developed for up to 20 minutes using 100 µl TMB Core (Bio-Rad) and the reaction stopped with 50 µl 0.2 $H_2SO_4$. Optical density (OD) at 450nm was read using a SpectraMax ABS Plus plate reader.

### 2.6.2 *Salmonella* antibody ELISA

*Salmonella* was grown as detailed in section 2.2.1, and protein levels/concentration quantified using a Pierce™ BCA protein assay kit (Thermo Fisher) as per manufacturer's instructions. Nunc maxisorp 96 well plates (Thermo Fisher Scientific) were coated with 1 µg of the appropriate *Salmonella* strain in PBS and incubated overnight at 4°C. Plates were washed with PBS three times. Plates were blocked with 2% (w/v) BSA in PBS-0.1% Tween 20 for 1 hour at RT. Plates were washed three times with PBS-0.1% Tween 20. This wash step was carried out between all consequent steps. Serum was initially diluted 1 in 20 in 2% (w/v) BSA in PBS-0.1% Tween 20, before serially diluting down 1 in 2 or 1 in 3, and incubated for 1 hour at RT. 100 µl of antibody was incubated at RT for 1 hour, antibodies used are

detailed in Table 2.7. Plates were developed for up to 10 minutes using 100 µl TMB-Core (Bio-Rad) and the reaction was stopped with 50 µl 0.2M $H_2SO_4$. $OD_{450}$ was read using a SpectraMax ABS Plus plate reader.

**Table 2.7: Details of antibodies used for *Salmonella* antibody ELISAs**

| Antibody target | Clone | Dilution | Supplier |
|---|---|---|---|
| IgG total | 2040-05 | 1:8000 | Southern Biotech |
| IgG1-Fc | HP6001 | 1:4000 | Southern Biotech |
| IgG2-Fc | 31-7-4 | 1:4000 | Southern Biotech |
| IgG3-hinge | HP6050 | 1:4000 | Southern Biotech |
| IgG4-Fc | HP6025 | 1:4000 | Southern Biotech |

### 2.6.3 PF4 IgG ELISA

Assay was carried out using the ImmuCor PF4 IgG ELISA kit as per manufacturers instructions, and OD 405 read on a molecular devices VERSA max plate reader.

## 2.7 Complement ELISAs

### 2.7.1 Blood collection and ethics – for complement project

Ethical approval was granted by the London-Camden and Kings Cross Research Ethics Committee reference 20/HRA/1817 for obtaining samples from groups 1-4 (described below). For group 5 samples, ethical approval was granted by the North West ethics committee, Preston CIA UPH IRAS, reference REC 20\NW\0240.

Group 1: Non-vaccinated individuals without any reported COVID infection (NEG). These sera were taken from University Hospitals Birmingham NHS Foundation Trust healthcare workers in May 2020 as part of the COVID-19 seroconversion (CoCo) study (Shields et al., 2021b). To ensure these sera were truly COVID antibody negative for the purposes of our study, samples were screened using a clinically

validated, CE marked ELISA against IgG, IgA and IgM to the S glycoprotein (Cook et al., 2021, Faustini et al., 2021) (manufactured by The Binding Site, product MK654). This assay is described further in section 2.6.1 and chapter 5. As samples were taken prior to widespread PCR testing upon COVID symptoms, and before the introduction of SARS-CoV-2 vaccines (participation in SARS-CoV-2 vaccine trials was an exclusion criterion for this study, as well as current COVID-19 symptomology), the absence of anti-S antibodies is a reliable surrogate marker of no previous infection. Samples containing an anti-N response were excluded from this group as they were suggestive of previous infection.

Group 2: Individuals vaccinated 28-35 days previously with BNT162b2 (Pfizer) vaccine (VACC), with no evidence of previous SARS-CoV-2 infection (as determined by an absence of anti-N antibodies). These samples were taken as part of the COVDENT study (Shields et al., 2021a).

Group 3: Individuals vaccinated with their second dose of BNT162b2 vaccine at least 28 days previously (DOUBLE VACC), with no evidence of infection (as determined by absence of anti-N antibodies). These samples were taken as part of the COVDENT study (Shields et al., 2021a).

Group 4: Non-vaccinated individuals with suspected previous COVID-19 infection that did not require hospitalisation (non-hospitalised convalescent, NHC). These samples were taken as part of the CoCo study (Shields et al., 2021b), where healthcare workers had previously self-isolated due to suspected COVID-19. As per group 1, this was confirmed by anti-S IgGAM testing, the most reliable surrogate marker of previous COVID-19 infection available for samples taken in May 2020.

Group 5: Non-vaccinated individuals with prior COVID-19 infection that required intensive care treatment (ITU-CONV) during the first COVID wave. These patients had PCR confirmed SARS-CoV-2, and samples were taken a minimum of 4 months after discharge from intensive care.

### 2.7.2 Complement ELISA – C1q

96 well high-binding plates (Corning) were coated with 0.1 µg S or N protein (total 50 µl per well) in PBS. After incubation overnight at 4 °C, plates were washed with PBS-0.1% (v/v) Tween 20, 3 times. These washes were carried out between all subsequent steps. Plates were blocked for 1 hour at RT with 2% (w/v) BSA in PBS-0.1 % Tween 20. Patient serum was heat-inactivated by incubating in a water bath for 30 minutes at 56°C. They were then diluted 1 in 5 with 2% BSA supplemented with 5 mM magnesium chloride and 5 mM calcium chloride. 50 µl/well was added to the antigen-coated plate and incubated at 37°C for 1 hour. 50 µl/well COVID antibody negative (as measured by ELISA in section 2.6.1, same source used throughout) normal human serum (NHS) at a 1 in 40 dilution (in 2% BSA with 5 mM magnesium chloride and 5 mM calcium chloride) was added and incubated for 1 hour at RT. 100 µl rabbit anti-C1q FITC antibody (Invitrogen PA5-16601) at a 1 in 200 dilution (in 2% BSA) was incubated at 37°C for 1 hour. 100 µl HRP conjugated swine anti-rabbit (Dako P0399) at a 1 in 2000 dilution (in PBS-0.1% Tween 20) was incubated for 1 hour at RT. The assay was amplified using the Perkin Elmer ELAST amplification kit as per manufacturer's instructions, with an optimised dilution of streptavidin of 1 in 800, incubated for 20 minutes. 100 µl TMB Core (Bio-Rad) was used to develop plates for 10 minutes, before being stopped with 50 µl 0.2M $H_2SO_4$. $OD_{450}$ was read using a SpectraMax ABS Plus plate reader.

### 2.7.3 Complement ELISA – C3b, C4b, C5b

Plates were coated and washed as described above in the C1q ELISA. Plates were blocked using 100 µl/well Starting Block (Thermo Fisher) for 10 minutes. Patient serum was heat-inactivated as for C1q assay above, but instead diluted 1 in 5 with Starting Block supplemented with 5 mM magnesium chloride and 5 mM calcium chloride. 50 µl was added to antigen-coated plate and incubated at 37°C for 1 hr. NHS was added as described above, but instead diluted 1 in 40 with Starting Block supplemented with 5 mM magnesium chloride and 5mM calcium chloride. 100 µl (diluted in PBS-0.1 %

Tween 20) of the following anti-human monoclonal antibodies were incubated at 37°C for 1 hr: mouse anti-C4b at 1 in 22,500 (Invitrogen, LF-MA0198); mouse anti-C3b at 1 in 10,000 (Invitrogen MAI-70053) and mouse anti-C5b at 1 in 10,000 (Invitrogen DIA 011-01-02). 100 µl HRP conjugated goat anti-mouse (Southern Biotech 1010-05) at a 1 in 4000 dilution was incubated for 1 hour at RT. Plates were developed and read as described above.

## 2.8 Cell culture and shearing

Human aortic endothelial cells (HAoECs) (Promo Cell) were grown in endothelial cell growth media MV (Promo Cell) with supplement pack (containing 5% fetal calf serum 0.4% endothelial cell growth supplement, 10 ng/ml epidermal growth factor (recombinant human), 90 µg/ml heparin and 1 µg/ml hydrocortisone) and further supplements of 5% fetal calf serum, 200 U/ml penicillin and 200 µg/ml streptomycin at 37°C, 5 % $CO_2$. Cells were routinely used at passages 7-10.

To shear, cells were plated in 6 well plates at 2 x $10^5$ cells/well and grown to confluency. Cells were then washed with PBS, given fresh media, and sheared at 10 dynes/$cm^2$ on a rotator inside the incubator for 24 hours.

## 2.9 Para-nitrophenyl phosphate binding assay

Bacteria were grown overnight as in section 2.2 and normalised to $OD_{600}$ = 1. In a 96 well plate, wells were coated with approximately 1 x $10^8$ CFU bacteria and left to adhere for 2 hours at 37°C. After washing with PBS, wells were blocked with 1% BSA (in PBS) for 1 hour. Block was washed off with PBS, then 2.5 x $10^4$ HAoECs/well (in pen/strep free media) were added and incubated at 37°C, 5% $CO_2$ for 2 hours to adhere. Wells were gently washed with pen/strep free media to remove unbound HAoECs. 20mM pNPP (Thermo Fisher) was added to lysis buffer (see Table 2.3). 200 µl of this was added per well and incubated for 2 hours at 37°C, 5% $CO_2$. The plate was read at 405 nm using a VictorX plate reader (Perkin Elmer).

## 2.10 Immunofluorescence

Sterile coverslips were broken into segments to fit in a 6 well plate, sealed in well with clear nail varnish and left to dry in sterile conditions overnight. HAoECs were seeded at 2 x $10^5$ cells/well and left to attach for 2-4 days until confluent. Cells were then sheared as in section 2.8. Media was removed, cells washed gently with PBS, and incubated with 1ml PPP or media per well for 30 minutes. Cells were washed again prior to infection with STm SL1344 at MOI 10 or MOI 40 for 1 hour (in cell media without antibiotics). Bacteria was washed away 3 times with warm PBS, before fixing cells with 4% formaldehyde for 15 minutes at RT. Cells were permeabilised in 0.1% Triton X-100 (in PBS) for 5 minutes at RT. After 3 further PBS washes, cells were blocked in 5 % BSA in PBS for 30 minutes. BSA was washed off with 3x PBS washes and cells were stained with an AlexaFluor 488 conjugated VE-cadherin antibody (Santa Cruz) at 1:100 dilution (in 1% BSA in PBS) for 90 minutes in the dark. This was achieved by applying 100 µl drop of antibody to a fresh glass slide and inverting the cell-coated coverslip on it cell-side down. After incubation, cells were washed a further 3 times with PBS before mounting cell side down on a fresh glass slide containing a drop of DAPI-containing Fluorishield mounting media. Cells were then imaged using a Zeiss AxioObserver Z1 microscope.

## 2.11 Whole blood flow assays

### 2.11.1 Blood collection and ethics – Dublin project

Whole blood was obtained from healthy donors under approval from the Royal College of Surgeons Ethics Committee (REC 1121). Blood was taken into syringes with 10% volume of 3.2% sodium citrate.

### 2.11.2 Flowing whole blood over bacteria

Bacteria was grown up overnight and normalised to $OD_{600}$ = 1.0 as per section 2.2. 50 µl normalised culture per channel was added to an uncoated Ibidi µ-slide VI 0.4 (Ibidi) and incubated for 2 hours at 37°C to allow bacterial adherence. Excess liquid was removed from cylinders (without disturbing liquid in channel to avoid bubbles, see Figure 2.1) before channel and cylinders were filled with 1% BSA in PBS to block at 37°C for 1 hour.

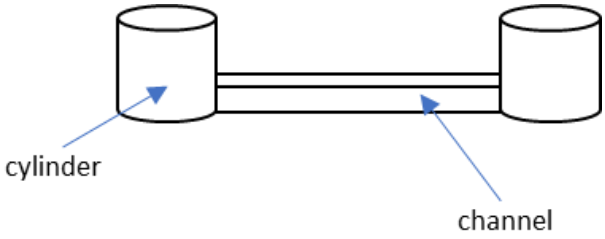


**Figure 2.1: Diagram of a single channel on a 6-channelled Ibidi µ-slide** to demonstrate what is meant by cylinder and channel.

Meanwhile, PRP was obtained from whole blood and incubated with Near Infrared BF2-azadipyrromethene (NIR-AZA) dye (made in house in the RCSI chemistry department (Wu et al., 2019)) at a 1 in 40 dilution (5µM) stain the platelets. This was incubated in the dark for 2 hours with gentle rocking. NIR-AZA dye is a fluorescent probe which binds non-specifically to plasma membrane and cytosol (Fitzpatrick et al., 2022), and once internalised is prevented from leaving the cytosol by addition of poly(ethylene-glycol) units covalently linked onto the fluorophore (Daly et al., 2017, Wu et al., 2019). Immediately prior to flow experiment, NIR-AZA incubated PRP was recombined with haematocrit.

Excess BSA was removed from chamber cylinders and replaced with PBS. Flow tubing was infused with PBS before attaching to channels. PBS was gently pushed through the system before attaching "out" flow tube to a Harvard PhD2000 syringe pump system set to 2 dynes/$cm^2$. Blood was flowed through the system for 3-5 minutes, before washing away of unbound cells by flowing PBS through the system at 1 dyne/$cm^2$. Images were taken using a Zeiss AxioObserver Z1 microscope.

### 2.11.3 Flowing whole blood over *Salmonella*-primed endothelial cells

HAoECs were sheared for 24 hours (as section 2.8) and seeded into ibiTreat Ibidi µ-slide VI 0.4 slides (Ibidi) at 80,000 cells in 60 µl/channel. Cells were incubated at 37°C/5% $CO_2$ for 2 hours to allow adherence. Blood was obtained and platelets stained as sections 2.11.1 and 2.11.2, but NIR-AZA was used at a dilution of 1 in 60 (3.3µM) to conserve supply. Bacteria were grown as section 2.2.1 and normalised to $OD_{600}$ = 1.

HAoECs were blocked with 1% BSA (in cell media) for 1 hour at 37°C/5% $CO_2$. Flow experiment was set up as described in section 2.11.2. PBS was flowed through system first to remove any unbound HAoECs. This was followed by flow of mCherry labelled STm SL1344 (at $OD_{600}$ = 1) at 2 dynes/cm$^2$ (1.56 ml/min; 275 s$^{-1}$) for 2 minutes. PBS was flowed through the system for 2 minutes to wash out unbound bacteria. Whole blood (with NIR-AZA stained platelets) was flowed through the system for 5 minutes at either venous (2 dynes/cm$^2$; 1.56 ml/min; 275 s$^{-1}$) or arterial (8 dynes/cm$^2$; 4.54 ml/min; 800 s$^{-1}$) flow rates. PBS was then washed through the system to remove unbound cells and allow imaged to be taken. A Zeiss AxioObserver Z1 microscope with 37°C incubator chamber/heat pad was used for imaging.

## 2.12 Statistical analysis

Statistical analysis was carried out using Graph Pad Prism 9.4.1. Results are presented as stated in figure legend, either with median ± IQR (where large donor variation occurred), mean ± SD, or mean ± SEM (in chapter 4, where 3 technical repeats per biological repeat were averaged). Significance was assumed at $p < 0.05$. Shapiro-Wilk, Anderson-Darling and D'Agostino and Pearson normality testing was carried out and normality assumed if at least 2 of the 3 tests assigned normality.

Paired t-tests were carried out for paired normally distributed data. Friedman test with Dunn's multiple comparison test was used for matched (3 groups) where data was not normally distributed. For unpaired, not normally distributed data, Kruskal-Wallis with Dunn's multiple comparison test was

used. To assess correlations, the Pearson correlation coefficient or the Spearman rank correlation was calculated for normal and not normally distributed data respectively.

# CHAPTER 3: MECHANISMS BEHIND DONOR VARIATION IN *SALMONELLA*-INDUCED PLATELET AGGREGATION

## 3.1 Introduction

Invasive non-typhoidal *Salmonella* (iNTS) is a leading cause of bacteraemia in sub-Saharan Africa (Marchello et al., 2021, Stanaway et al., 2019), and treatments are becoming increasingly limited due to the rise of antimicrobial resistant strains (Kingsley et al., 2009). Therefore, it is important to understand the underlying mechanisms behind the interactions of *Salmonella* in the bloodstream in order to open new possible avenues for treatment.

### 3.1.1 *Salmonella* mouse model

One way of gaining understanding of iNTS is through mouse models. Systemic *Salmonella* infections can be modelled in susceptible strains of mice using attenuated *Salmonella* Typhimurium (STm) strains such as STm SL3261, which mice are able to clear over a period of months (Beristain-Covarrubias et al., 2019b). Results from the mouse model have shown thrombosis occurs with differing kinetics in the spleen and liver. Whilst thrombi in the spleen occur within 24 hours of infection and resolve rapidly (Beristain-Covarrubias et al., 2019a), those in the liver do not develop until seven days post-infection, and are sustained through until at least day 21, before resolving around the 28 day mark (Hitchcock et al., 2015). Unusually, thrombi in both organs are venous 'white' platelet-rich thrombi, in contrast to that generally observed – typically venous thrombi are 'red' and made up of mostly erythrocytes, with arterial thrombi being 'white' platelet driven thrombi (Beristain-Covarrubias et al., 2019b, Jerjes-Sanchez, 2004). Furthermore, contrary to what would be expected of an immunothrombotic response, the thrombi found in the spleen and liver contained minimal numbers of STm, suggesting they are not efficient bacterial traps (Beristain-Covarrubias et al., 2019a). Of particular importance to the thrombi

formation in the liver is the CLEC-2-podoplanin axis, with depletion of CLEC-2 on platelets significantly inhibiting the thrombotic response (Hitchcock et al., 2015).

### 3.1.2 The effect of *Salmonella* on human platelets

Whilst clear thrombotic responses are seen in the mouse model, little is known about whether similar responses occur in humans. There are case reports detailing individuals who developed thrombosis most likely due to their invasive *Salmonella* infection (Taneda et al., 2019, García-Fernández-Bravo et al., 2019, Prakash et al., 2016, Suppamutharwyam and Radhakrishnan, 2022, Strutynskaya et al., 2020, Ghosh and Samanta, 1994), but larger scale studies do not exist. With numerous differences between mouse and human platelets, including mice expressing over 10 x the amount of CLEC-2 on their platelet surface compared to humans (Zeiler et al., 2014, Gitz et al., 2014), mouse platelets not expressing FcγRIIA, and mice having over twice the concentration of platelets as humans (Schmitt et al., 2001), it was unclear whether *Salmonella* would be able to activate human platelets in a similar manner to in the mouse model. Therefore, the Cunningham lab produced preliminary data looking at whether STm can activate platelets isolated from healthy donors (unpublished). This revealed surprising results – whilst STm was able to activate platelets in PRP in some donors, in other donors aggregation did not take place at all (Figure 3.1). Three different STm strains were tested: SL1344, a wild-type reference strain; SL3261, the attenuated version of SL1344, and D23580, an invasive isolate from sub-Saharan Africa. Interestingly, in the small number of samples tested, the invasive isolate STm D23580 was the strain the most donors responded to, with the attenuated STm SL3261 strain not able to induce aggregation in any of the donors tested.

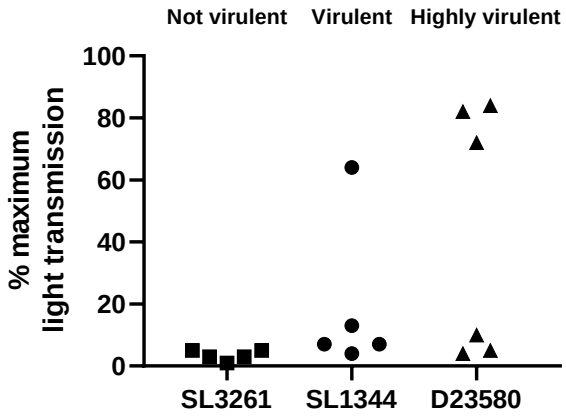


**Figure 3.1: Preliminary results of platelet aggregation responses to different strains of *Salmonella***. Platelet rich plasma was stimulated with ~ 5 x $10^8$ CFU/ml STm SL3261 or ~ 1 x $10^9$ STm SL1344 or D23580 at a 1:9 bacteria:platelet ratio. Platelets were kept at 37°C, stirring at 1200rpm, and light transmission monitored for 30 minutes. n ≥ 5.

### 3.1.3 Chapter aims

Based on these preliminary results, we wanted to further explore the mechanisms behind *Salmonella*-platelet interactions, and the basis of the donor and strain variation. Therefore, the aims of this chapter were to:

a) Assess the extent of platelet aggregation to STm SL3261, SL1344 and D23580 in a cohort of over 20 healthy donors
b) Investigate the mechanistic reasons behind differences in donor responses
c) Investigate mechanistic reasons behind strain differences in ability to cause platelet aggregation

## 3.2 Results

### 3.2.1 Investigating the induction of platelet aggregation by *Salmonella* in healthy donors

#### 3.2.1.1 *Salmonella* does not directly activate platelets *in vitro* in washed platelets

Whilst inflammation due to *Salmonella* Typhimurium (STm) infection has been shown to cause platelet-rich thrombi in mice, how STm affects human platelets is not known. Some bacteria, such as *S. sanguinis* and *S. gordonii* can activate platelets directly, by binding to the platelet von Willebrand factor receptor GPIbα (Cox et al., 2011).

To test whether STm can activate platelets directly, light transmission aggregometry was used as a measure of platelet aggregation. ~1 x $10^9$ CFU/ml STm was added to washed platelets from healthy donors at a 1:2 volume ratio, and levels of light transmission monitored for 30 min. Whilst the platelets were responsive to the PAR-1 receptor agonist peptide TRAP-6, none of the three STm strains tested, SL3261, SL1344 and D23580, caused any platelet aggregation (Figure 3.2) showing STm cannot directly activate platelets.

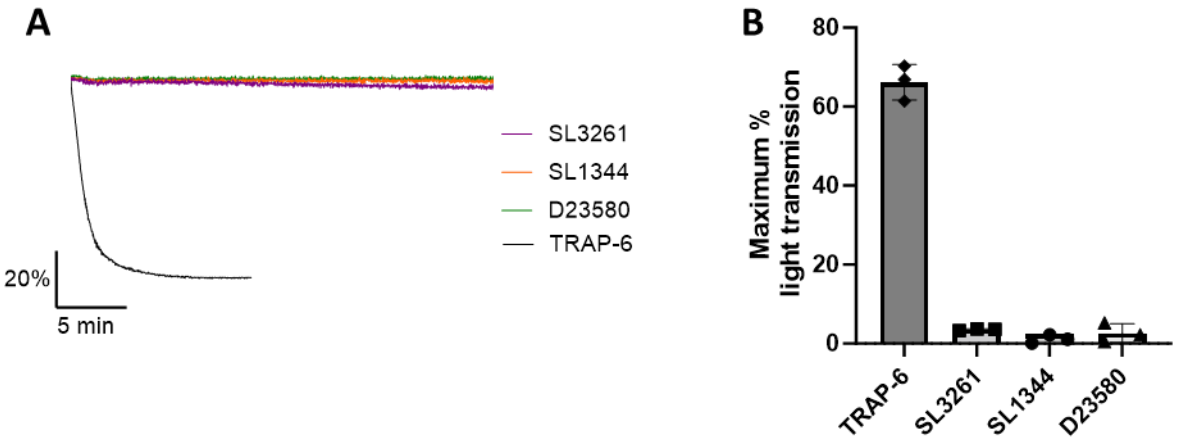


**Figure 3.2: *Salmonella* cannot directly activate platelets.** A) Washed platelets at 2 x $10^8$/ml were stimulated with either 100µM TRAP-6, ~5 x $10^8$ CFU/ml *Salmonella* Typhimurium (STm) strain SL3261, ~1 x $10^9$ CFU/ml STm SL1344 or STm D23580 at a 1:2 bacteria:platelet volume ratio. Platelets were kept at 37°C, stirring at 1200rpm, and light transmission monitored in a PAP-8 aggregometer for 30 minutes. Traces representative of n = 3. B) As A, n = 3. Bars represent mean ± SD.

#### 3.2.1.2 *Salmonella* can indirectly activate platelets in a donor and strain dependent manner

Other bacteria can indirectly activate platelets, with plasma proteins acting as a bridge between the two. For example, fibrinogen can bind to *S. aureus* via its Clumping Factor A protein, as well as binding to the platelet αIIbβ3 integrin (Kerrigan, 2015). To assess indirect activation, aggregometry was carried out in PRP. All three STm strains activated platelets indirectly, but in a donor and strain dependent manner (Figure 3.3). Donors were categorised into: strong responders, those whose maximum aggregation was >60%; mid responders, whose maximum aggregation was 20-60%; weak responders, whose aggregation was <20% but still had a clear aggregation-style curve; and non-responders, whose light transmission levels remained linear (Figure 3.3A,B). The median maximum light transmission % increase for STm SL1344 was 42% (IQR 17.5-85%), higher than those of STm SL3261 and STm D23580, at 11% (IQR 0-26%) and 22% (IQR 9-58%) respectively (Figure 3.3C). In donors who responded, as well as variation in maximum aggregation levels, the time taken for aggregation to occur (lag time) also varied. STm SL1344 gave the median quickest lag time at 8 min (IQR 6-9.5 min), significantly faster than STm D23580 with a median of 10 min (IQR 9-12 min), and STm SL3261 with a median of 10.5 min (IQR 9-12 min) (Figure 3.3D). Overall, STm SL1344 gave the largest and quickest aggregation responses, followed by STm D23580, with STm SL3261 giving the weakest platelet responses. As shown in Figure 3.3E, over 75% of donors were strong or mid responders to STm SL1344, reducing to ~50% for STm D23580, and less than 40% for STm SL3261.

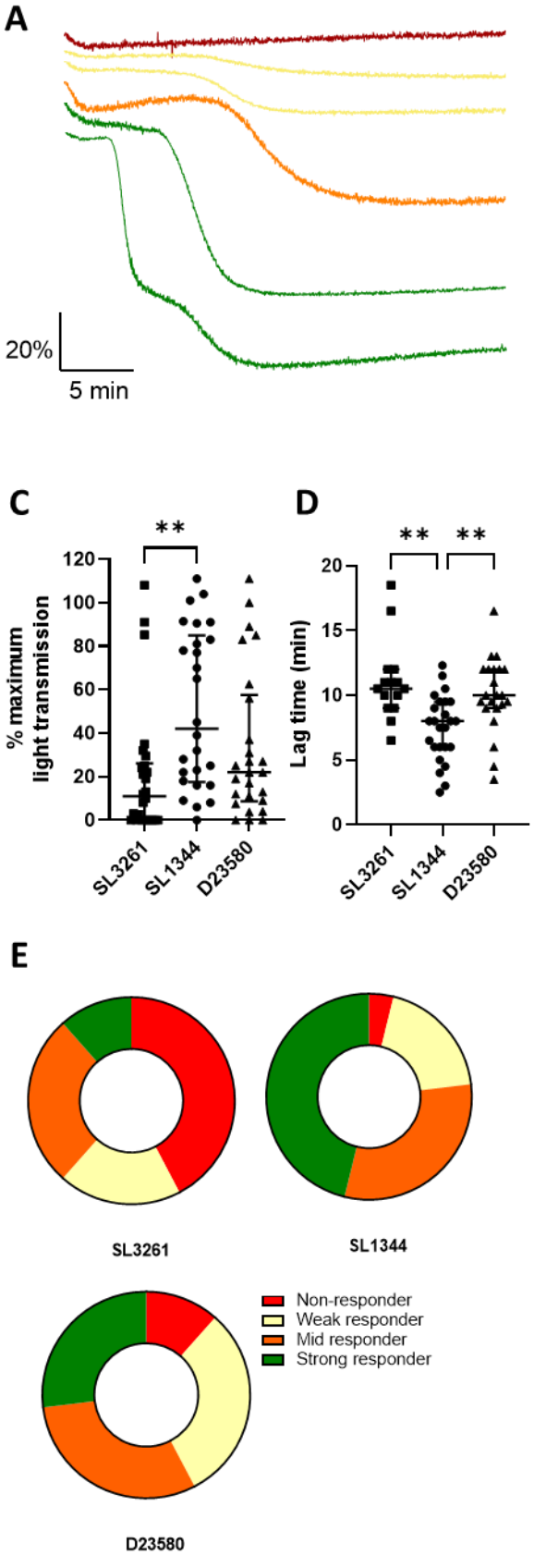


B

| Donor | SL3261 | SL1344 | D23580 |
|---|---|---|---|
| A | | | |
| B | | | |
| C | | | |
| D | | | |
| E | | | |
| F | | | |
| G | | | |
| H | | | |
| I | | | |
| J | | | |
| K | | | |
| L | | | |
| M | | | |
| N | | | |
| O | | | |
| P | | | |
| Q | | | |
| R | | | |
| S | | | |
| T | | | |
| U | | | |
| V | | | |
| W | | | |
| X | | | |
| Y | | | |
| Z | | | |
| Non responder | 11/26 42% | 1/26 4% | 3/26 11% |
| Weak responder | 5/26 19% | 5/26 19% | 8/26 31% |
| Mid responder | 7/26 27% | 8/26 31% | 8/26 31% |
| Strong responder | 3/26 12% | 12/26 46% | 7/26 27% |

**Figure 3.3: *Salmonella* can indirectly activate platelets in a donor and strain dependent manner.** PRP was stimulated with ~5 x $10^8$ CFU/ml STm strain SL3261, ~1 x $10^9$ CFU/ml STm SL1344 or STm D23580 at a 1:2 bacteria:platelet volume ratio. Platelets were kept at 37°C, stirring at 1200rpm, and light transmission monitored in a PAP-8 aggregometer for 30 minutes. Colour coding: strong responders (green; >60% maximum aggregation), mid responders (orange; 20-60% maximum aggregation), weak responders (cream, <20% maximum aggregation, but still with a curve), and non-responders (red, no aggregation). A) Representative traces from the different colour-

coded categories to STm SL1344. B) Table summarising responses to SL3261, SL1344 and D23580 from n = 26 healthy donors. C) Numerical maximum light transmission results for responses to SL3261, SL1344 and D23580. N =26. Bars represent median and inter-quartile range. D) Lag times taken for aggregation to occur to SL3261 (n = 15), SL1344 (n = 25) and D23580 (n = 22). Bars represent median and inter-quartile range. Kruskal-Wallis with Dunn's multiple comparisons test was performed, ** $p < 0.005$. E) Pie charts to demonstrate differences in platelet responses between strains (n = 26).

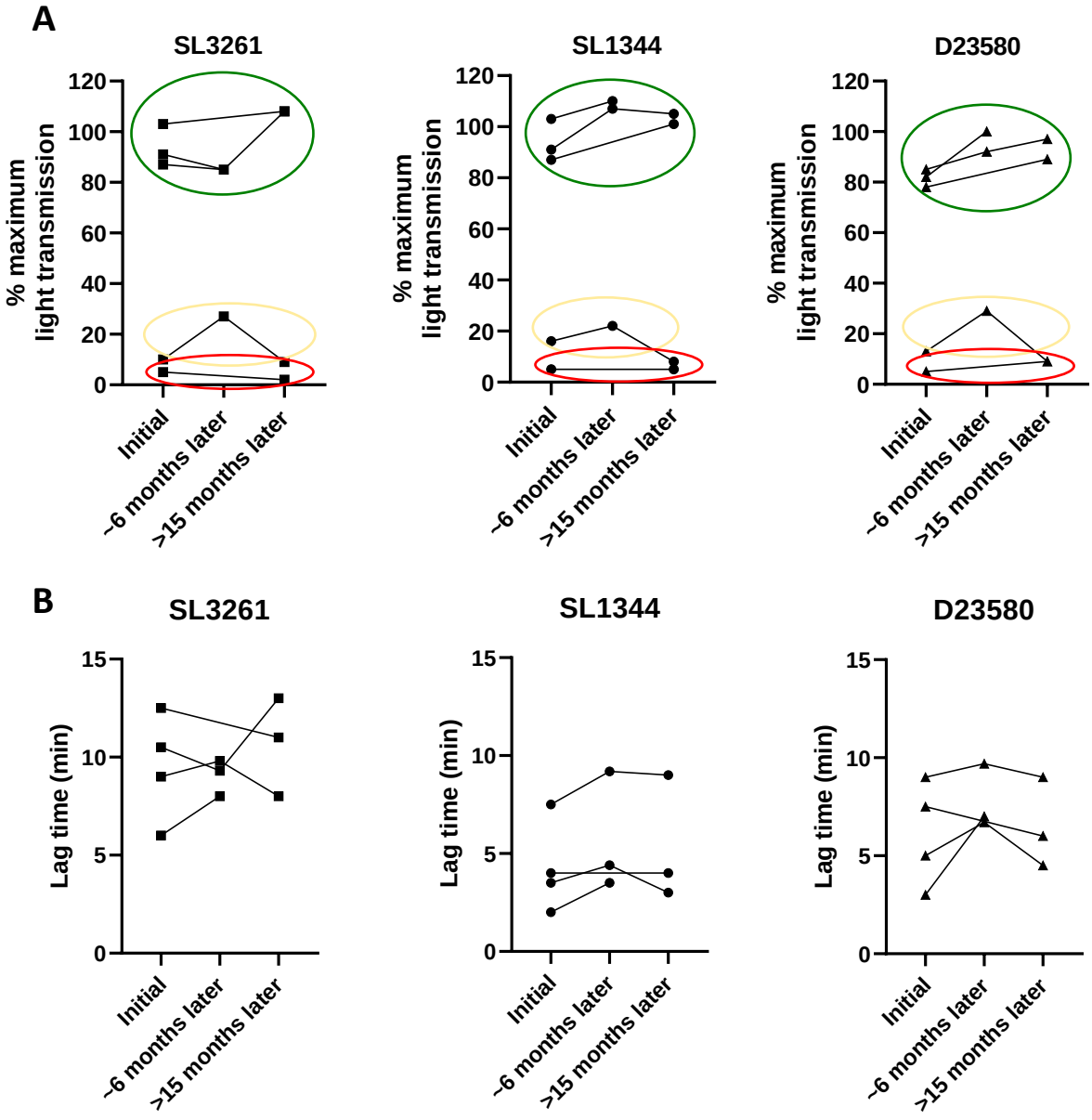


**Figure 3.4: Donor responses to *Salmonella* are consistent over time.** PRP was stimulated with ~5 x $10^8$ CFU/ml STm SL3261, ~1 x $10^9$ CFU/ml STm SL1344 or STm D23580 at a 1:2 bacteria:platelet volume ratio. Platelets were kept at 37°C, stirring at 1200rpm, and light transmission monitored in a PAP-8 aggregometer for 30 minutes. ~6 month time point runs from 182-196 days after initial measurement, >15 months covers tests >450 days after initial measurement. A) Maximum light transmission percentages of donors over time. Coloured circles: strong responders (green; >60% maximum aggregation), weak responders (cream, <20% maximum aggregation, but still with a curve), and non-responders (red, no aggregation). n = 5. B) Lag times of donors over time. n = 4.

#### 3.2.1.3 Donor responses to *Salmonella* are consistent over time

With such marked variation between donors, it was important to assess whether individual responses were stable or varying over time. Donor responses to all three strains were measured again approximately six months and ≥ 15 months after the initial measurement. As demonstrated in Figure 3.4A, responses within individuals remain relatively stable over time, with any variation remaining within the same strong, weak or non-responder category. Lag times also remained similar, with the majority of donor lag times only varying by a couple of minutes (Figure 3.4B).

#### 3.2.1.4 Platelet count in PRP does not affect aggregation responses to *Salmonella*

In washed platelets, platelet concentration is normalised when resuspending the pellet in buffer. However, in PRP using the native platelet count is recommended (Mani et al., 2005, Cattaneo et al., 2013), with one paper suggesting that addition of PPP to normalise platelet count can inhibit platelet aggregation (Cattaneo et al., 2007). Therefore, all aggregation experiments were carried out in un-adjusted PRP. To check that differing platelet counts were not causing the variation seen in response to STm, platelet count was measured and plotted against the maximum light transmission %. As shown in Figure 3.5, there is no correlation between platelet count and aggregation levels for any of the three strains tested.

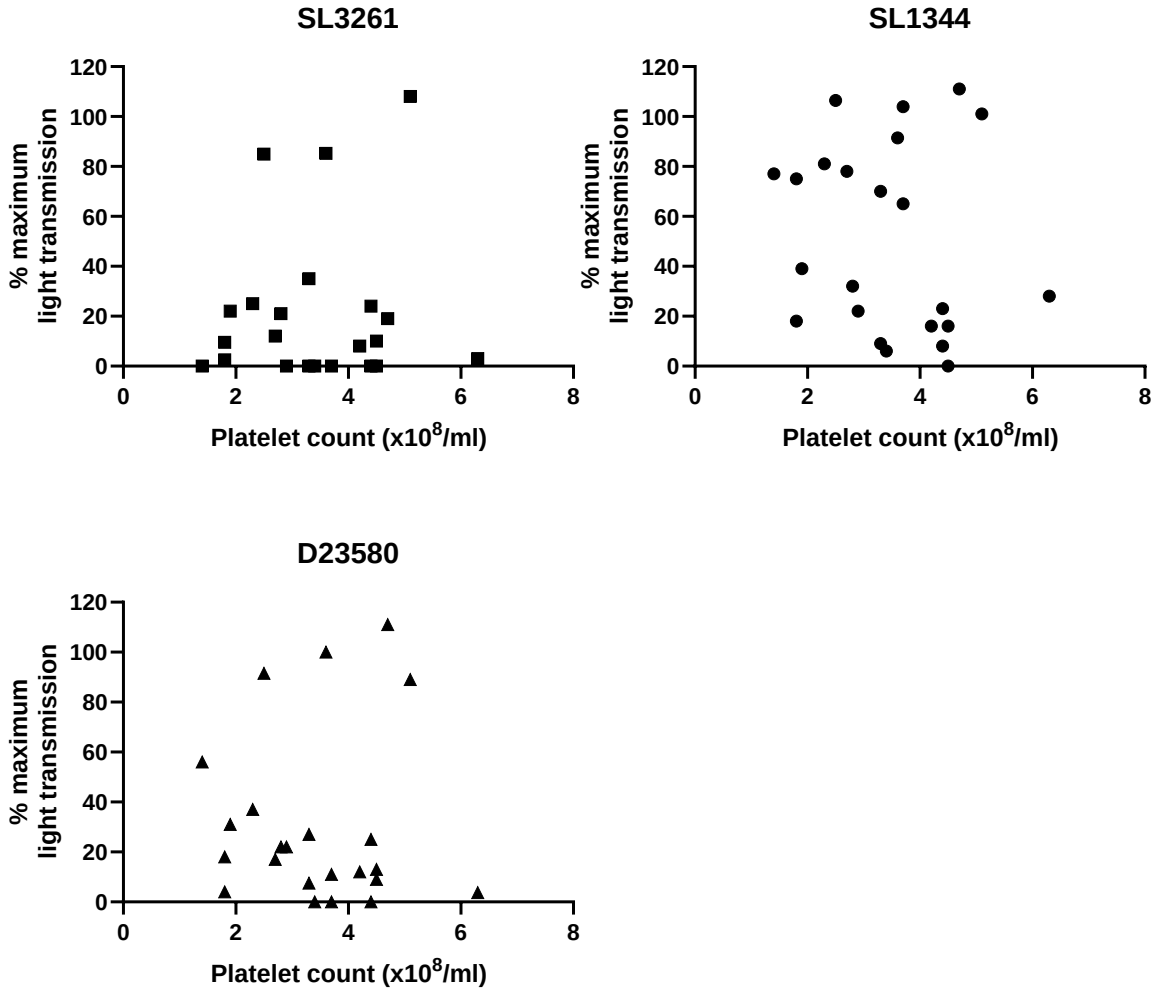


**Figure 3.5: Platelet count in PRP does not affect aggregation responses to *Salmonella*.** Maximum aggregation responses from Figure 3.3C were correlated against platelet count measured in PRP. Spearman rank correlation was calculated: SL3261 r = 0.01, p = 0.96; SL1344 r = -0.16, p =0.47; D23580 r = -0.18, p = 0.40. n =23.

### 3.2.2 Characterising platelet aggregation in response to *Salmonella*

#### 3.2.2.1 Platelet aggregation, not agglutination, occurs in response to *Salmonella*

Platelet aggregation is an active process whereby receptors on the platelet surface are engaged and lead to signalling pathway activation. This ultimately results in activation and adhesion of the platelets to one another, forming platelet aggregates. On the other hand, agglutination is a passive process, where platelet signalling pathways are not engaged, but proteins binding to the platelets causes platelets to clump together. One way to distinguish between the two is by using an inhibitor of the integrin αIIbβ3, a receptor vital for platelet aggregation (Bennett, 2005). If agglutination is taking place, addition of the inhibitor eptifibatide will not have an effect on the measured light transmission levels. As shown in Figure 3.6, addition of eptifibatide reduced maximum aggregation levels in all donors and strains tested. Larger decreases were seen in stronger responders, but weak responders still saw a small decrease in maximum light transmission. Eptifibatide significantly reduced maximum light transmission levels in SL1344 and D23580, but not in SL3261. This is likely due to the reduced number of samples able to be tested for SL3261 due to fewer strong responders, and the decreased scope for reduction in weakly responding samples.

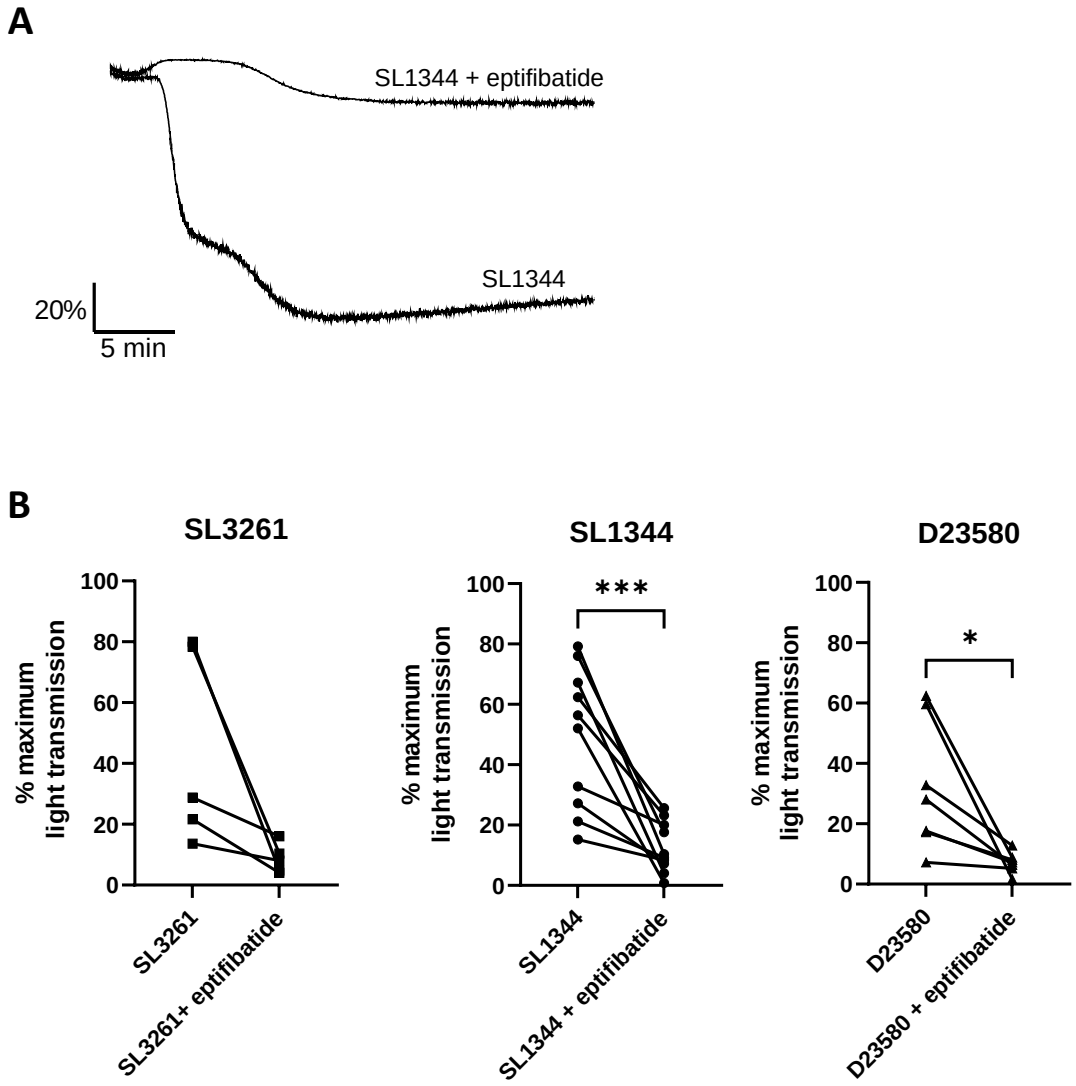


**Figure 3.6: Platelet aggregation, not agglutination, is taking place in response to *Salmonella*.** 9μM eptifibatide was pre-incubated with PRP for 3 minutes, before stimulation with ~5 x $10^8$ CFU/ml STm SL3261, ~1 x $10^9$ CFU/ml STm SL1344 or STm D23580 at a 1:2 bacteria:platelet volume ratio. Platelets were kept at 37°C, stirring at 1200rpm, and light transmission monitored in a PAP-8 aggregometer for 30 minutes. A) Representative trace from a strong responder to SL1344. B) Pooled data from a range of responders from strong through to weak. Data were normally distributed, so a paired t-test was carried out. *** $p < 0.001$, * $p < 0.05$. n = ≥ 5.

### 3.2.2.2 The secondary mediators ADP and thromboxane $A_2$ contribute to *Salmonella*-induced platelet aggregation

Upon activation, platelets release ADP from their dense granules which can amplify and stabilise the responses of platelets to other agonists. The two ADP receptors present on the platelet surface are $P2Y_1$ and $P2Y_{12}$. $P2Y_1$ is responsible for the 'early stage' platelet activation, whose signalling through Gq mediates a transient rise in cytoplasmic $Ca^{2+}$, enabling platelets to change shape. However, the aggregation caused via $P2Y_1$ signalling is rapidly reversible due to desensitisation of the ADP receptor. $P2Y_{12}$ is the ADP receptor that is responsible for providing stability and amplification to the aggregation response, where its signalling via Gi leads to inhibition of adenylyl cyclase and activation of PI3kinase. In response to ADP alone, both receptors are needed in order to result in full platelet aggregation.

In bacterial induced platelet aggregations, inhibiting the $P2Y_{12}$ receptor has shown the need for ADP in platelet aggregation to strains including *S. oralis, S. gordonii and S. aureus* (Arman et al., 2014, Hannachi et al., 2020, Yeaman, 2010). However, in order to see significant inhibition with *S. sanguinis* and *S. pneumoniae,* both $P2Y_{12}$ and thromboxane $A_2$ ($TxA_2$) synthesis needed to be inhibited (Arman et al., 2014). $TxA_2$ is synthesised *de novo* by activated platelets via cyclooxygenase (COX) enzymes, and stimulates further platelet aggregation in a positive feedback loop.

To assess the involvement of ADP and $TxA_2$ in STm induced platelet aggregation, multiple inhibitors were used (Figure 3.7). MRS2179, a $P2Y_1$ inhibitor, resulted in only minor reductions in aggregation in 2/3 donors. The $P2Y_{12}$ inhibitor cangrelor fully inhibited aggregation in 2/3 donors, with the COX inhibitor indomethacin fully inhibiting aggregation in 1/3. The combination of cangrelor and indomethacin together however led to complete inhibition in all 3 donors, suggesting STm induced platelet aggregation requires both ADP and $TxA_2$.

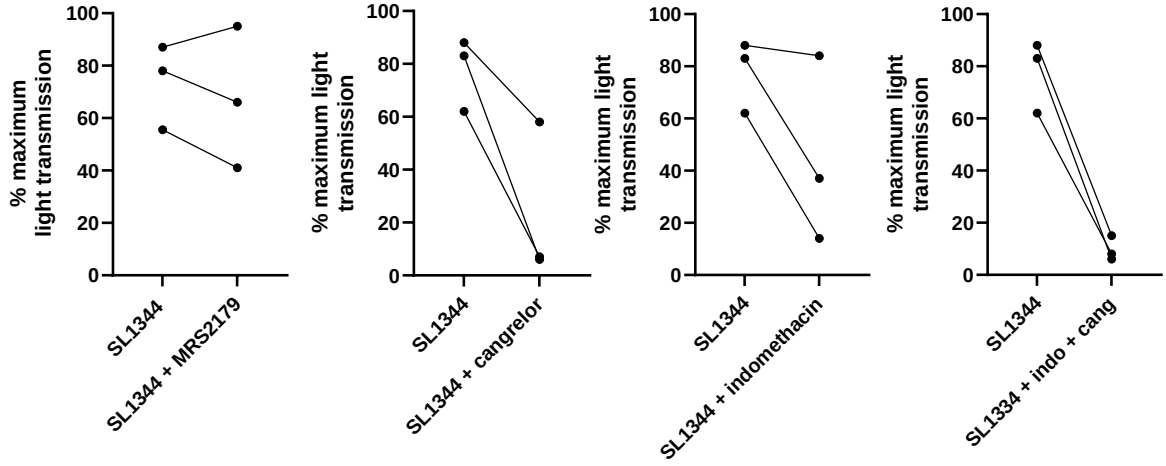


**Figure 3.7: Secondary mediators ADP and thromboxane A2 are involved in *Salmonella*-induced platelet aggregation.** PRP was incubated with the following for 3 minutes: either 20µM MRS2179, 1µM cangrelor, 10µM indomethacin, vehicle control, or both indomethacin and cangrelor. PRP was then stimulated with ~1 x $10^9$ CFU/ml STm SL1344 at a 1:2 bacteria:platelet volume ratio. Platelets were kept at 37°C, stirring at 1200rpm, and light transmission monitored in a PAP-8 aggregometer for 30 minutes. n = 3.

### 3.2.2.3 Complement is not involved in *Salmonella*-induced platelet aggregation

Complement proteins are known to be involved in the mechanisms of several different bacterial induced platelet aggregation responses including *S. sanguinis* (Ford et al., 1996), *E. coli* (Moriarty et al., 2016) and *Cutibacterium acnes* (Petersson et al., 2018). Two different complement inhibitors were used to investigate whether complement plays a role in STm platelet aggregation: compstatin, a C3 inhibitor (Morikis et al., 1998), and FUT-175, a broad-spectrum serine protease inhibitor, inhibiting C1r and C1s (Aoyama et al., 1984). PRP was treated with PPACK to allow addition of the $Ca^{2+}$ and $Mg^{2+}$ ions required to facilitate any complement pathway involvement. Neither inhibitor caused a decrease in platelet aggregation levels alone, (Figure 3.8) although a very small decrease in aggregation was observed when both inhibitors were used together.

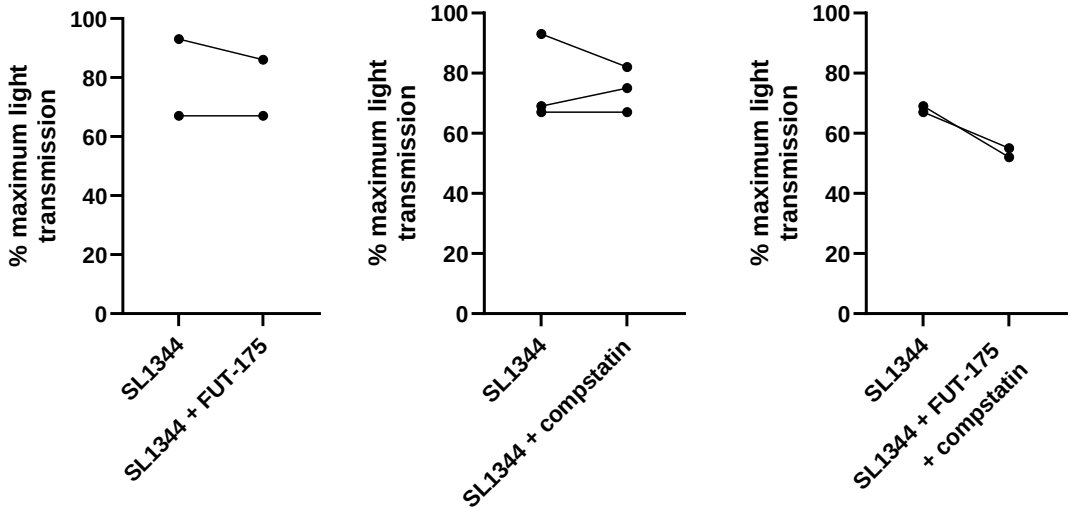


**Figure 3.8: Complement is not required for platelet aggregation by *Salmonella* to occur.** PRP was incubated with 40µM PPACK for 5 minutes before addition of 1 or 2mM calcium chloride and magnesium chloride. 10µM FUT-175, 28µM compstatin, vehicle, or both FUT-175 and compstatin were added for 3 minutes, before stimulation with ~1 x $10^9$ CFU/ml STm SL1344 at a 1:2 bacteria:platelet volume ratio. Platelets were kept at 37°C, stirring at 1200rpm, and light transmission monitored in a PAP-8 aggregometer for 30 minutes. n ≥ 2.

### 3.2.2.4 FcγRIIA engagement is required for aggregation responses to *Salmonella*

The platelet IgG receptor FcγRIIA has been implicated in the mechanisms of platelet aggregation to many bacterial strains, including Gram positive bacteria such as *S. aureus* and *S. pneumoniae* (Arman et al., 2014), and Gram negative bacteria such as *E. coli* (Moriarty et al., 2016, Watson et al., 2016). To see whether this receptor is important in STm-induced platelet aggregation, the F(ab) fragment of the FcγRIIA blocking monoclonal antibody IV.3 was used. The majority of platelet donor responses were reduced to basal levels with F(ab) IV.3 (Figure 3.9). For the donor whose aggregation level rose with addition of F(ab), addition of the higher avidity $F(ab)_2$ IV.3 resulted in inhibition of the aggregation response. In the remaining donors where aggregation levels were higher than basal with F(ab) IV.3, using the higher avidity $F(ab)_2$ IV.3 caused a further reduction in aggregation. This suggests that, like with many other bacterial strains, FcγRIIA is required in order for platelet aggregation to take place in response to STm.

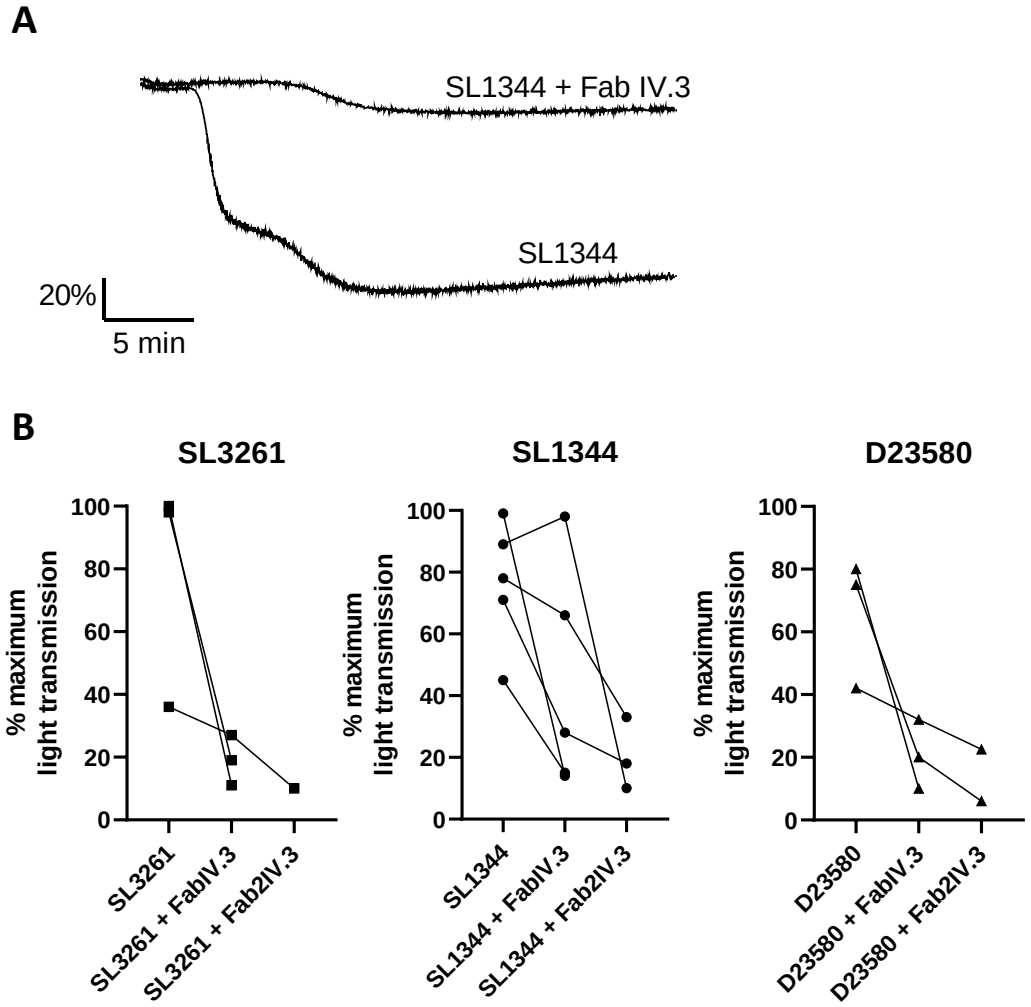


**Figure 3.9: FcγRIIA engagement is required for aggregation responses to *Salmonella.*** 20μM F(ab) IV.3, 10μM $F(ab)_2$ IV.3 or vehicle were preincubated with platelets before stimulation with ~5 x $10^8$ CFU/ml STm SL3261, ~1 x $10^9$ CFU/ml STm SL1344 or STm D23580 at a 1:2 bacteria:platelet volume ratio. Platelets were kept at 37°C, stirring at 1200rpm, and light transmission monitored in a PAP-8 aggregometer for 30 minutes. A) Representative aggregation trace of a strong responder to SL1344 with F(ab) IV.3 inhibition. B) Maximum light transmission data from n ≥ 3.

### 3.2.3 Investigating causes of donor variation in platelet aggregation responses to *Salmonella*

#### 3.2.3.1 Levels of FcγRIIA on the platelet surface do not affect magnitude of responses to *Salmonella*

FcγRIIA has previously been shown to be responsible for inter-donor variation to heat aggregated IgG (Rosenfeld et al., 1987). With FcγRIIA implicated in platelet aggregation responses to STm, surface levels of the receptor were measured to assess whether copy number were responsible for the donor variation observed (Figure 3.10). The Pearson r values show a very weak positive correlation, but no statistical significance, so FcγRIIA surface levels do not appear to be responsible for the variation in platelet responses to STm.

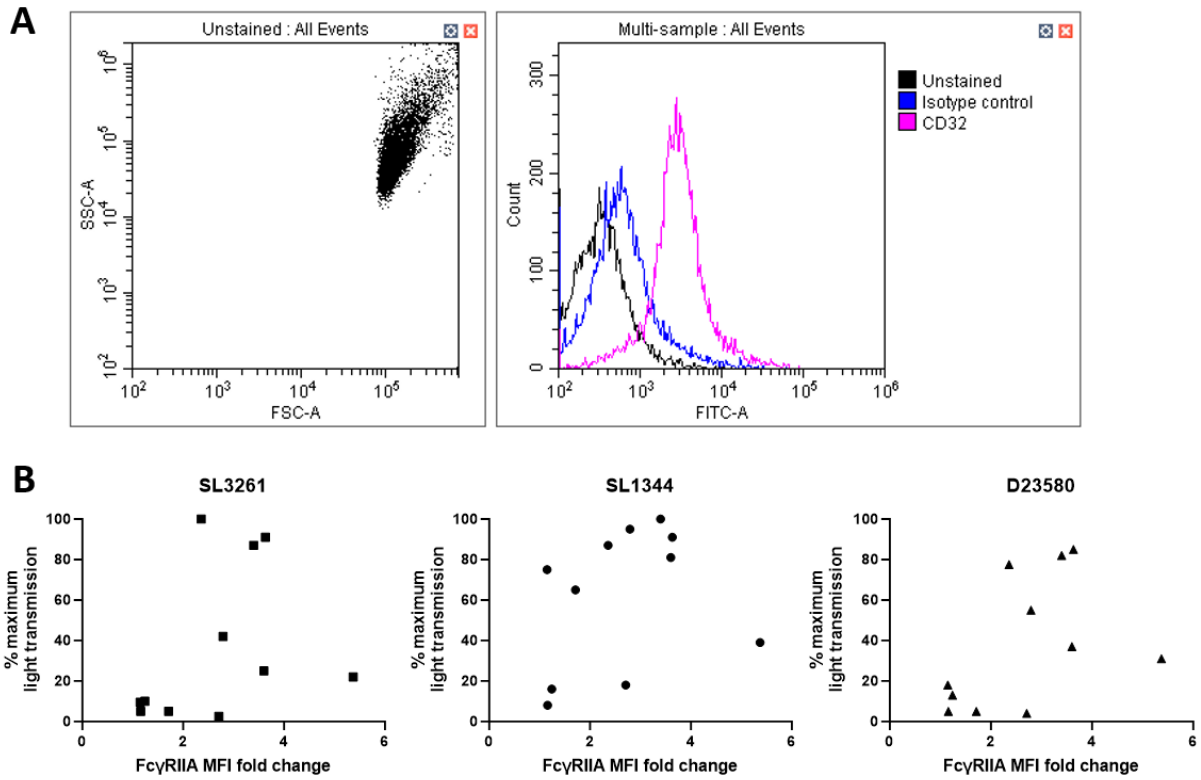


**Figure 3.10: Levels of FcγRIIA on the platelet surface do not affect magnitude of responses to *Salmonella*.** Flow cytometry was used to measure levels of FcγRIIA (CD32a) on the platelet surface. A) Flow cytometry was carried out on washed platelets. Fold change from isotype control median fluorescence intensity (MFI) to CD32 MFI was calculated to normalise data obtained on two different flow cytometers. B) Results were plotted against maximum light transmission results from Figure 3.3C. All data were normally distributed, so Pearson correlation coefficient was calculated: SL3261 r = 0.35, p = 0.29, $r^2$ = 0.12; SL1344 r = 0.29, p = 0.39, $r^2$ = 0.08; D23580 r = 0.46, p = 0.16, $r^2$ = 0.21. n = 11.

#### 3.2.3.2 A plasma component is responsible for donor variation in platelet aggregation responses to *Salmonella*

In order to provide further clues as to whether a platelet component, a plasma component, or a combination of both were responsible for the donor variation, a donor swap assay was devised. Blood was taken from both a strong responder and a weak responder. ACD-free PPP from both donors was obtained, as well as washed platelet pellets, using an ADP-sensitive platelet preparation (see section 3.2.3.3 for reasoning behind choice of platelet preparation). Four combinations of platelets and plasma were made: strong responder platelets resuspended in strong responder plasma (S/S), strong responder platelets resuspended in weak responder plasma (S/W), weak responder platelets resuspended in weak responder plasma (W/W), and weak responder platelets resuspended in strong responder plasma (W/S) (Figure 3.11A). S/S aggregation levels show the baseline strong response, with W/W showing the baseline weak response. Upon resuspending strong responder platelets in weak responder plasma, aggregation levels drop to the W/W level, implying a plasma component is vital. This is confirmed by the S/S level being reached when weak responder platelets are resuspended in strong responder platelets (Figure 3.11B,C).

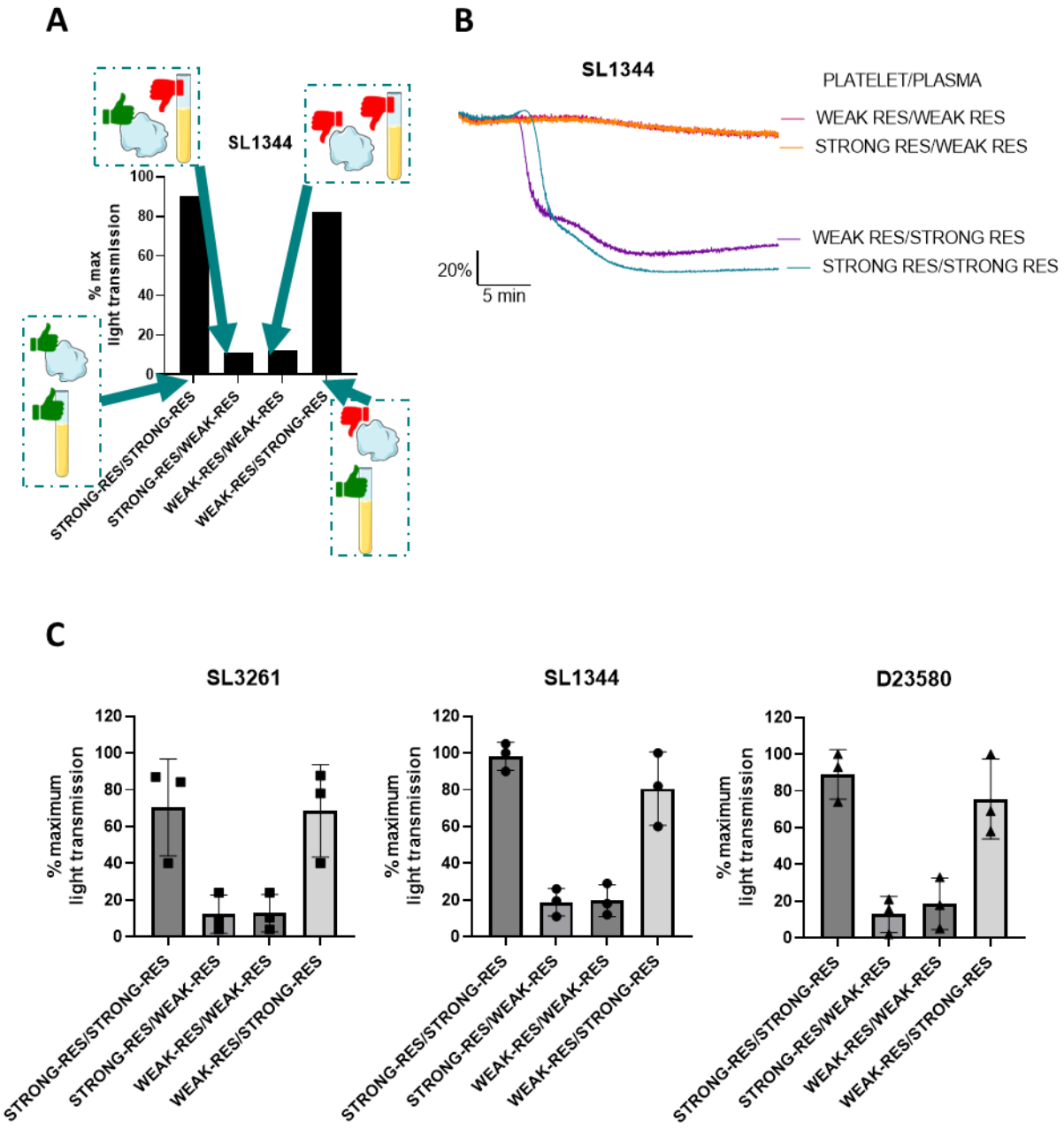


**Figure 3.11: A plasma component is responsible for donor variation in platelet aggregation responses to *Salmonella*.** Two washed platelet pellets from a strong and weak responder were obtained using an ADP-sensitive preparation and resuspended in ACD-free PPP from both donors. Platelet concentrations were 2.3-2.5 x $10^8$ /ml depending on PPP amounts obtained for dilution. These were then stimulated with ~1 x $10^9$ CFU/ml STm SL1344 at a 1:2 bacteria:platelet volume ratio. Platelets were kept at 37°C, stirring at 1200rpm, and light transmission monitored in a PAP-8 aggregometer for 30 minutes. A) Example schematic showing combinations of platelets and plasma – green thumbs up for the strong responder component, red thumbs down for the weak responder component. B) Representative traces of a donor swap experiment. C) Pooled n = 3 (two different strong responders and two different weak responders in three different combinations), bars are mean ± SD.

### 3.2.3.3 Washed platelets resuspended in PPP do not give similar responses to PRP

In the process of optimising the donor swap experiments above, it became apparent that resuspending washed platelets in plasma did not give optimal responses. Figure 3.12A,B shows the differences in responses to traditional platelet agonists TRAP-6 and CRP in PRP, along with washed platelets (WP) from a traditional preparation (methods section 2.3.3) resuspended in Tyrode's buffer (WP/T normal prep), or PPP (WP/PPP normal prep). Whilst WP/T normal prep gave reduced maximum aggregation levels compared to PRP, agonists still gave good responses. However, in the WP/PPP normal prep, no response was seen to high dose TRAP-6, and a minimal response to high dose CRP. Interestingly, if swapping the platelet washing protocol to an ADP sensitive one (methods section 2.3.4), TRAP-6 initiates a small, reversible aggregation, whilst CRP gives the same response as in PRP (Figure 3.12A,B). When investigating the difference platelet preparations make in response to STm, similar results are seen, with maximum aggregation reduced by over 4 times in the WP/PPP normal prep compared to PRP (Figure 3.12B, right hand graph). The reduction was just under 2 times when changing the prep to ADP sensitive, so this method was used for all assays where resuspension of platelets in PPP was needed.

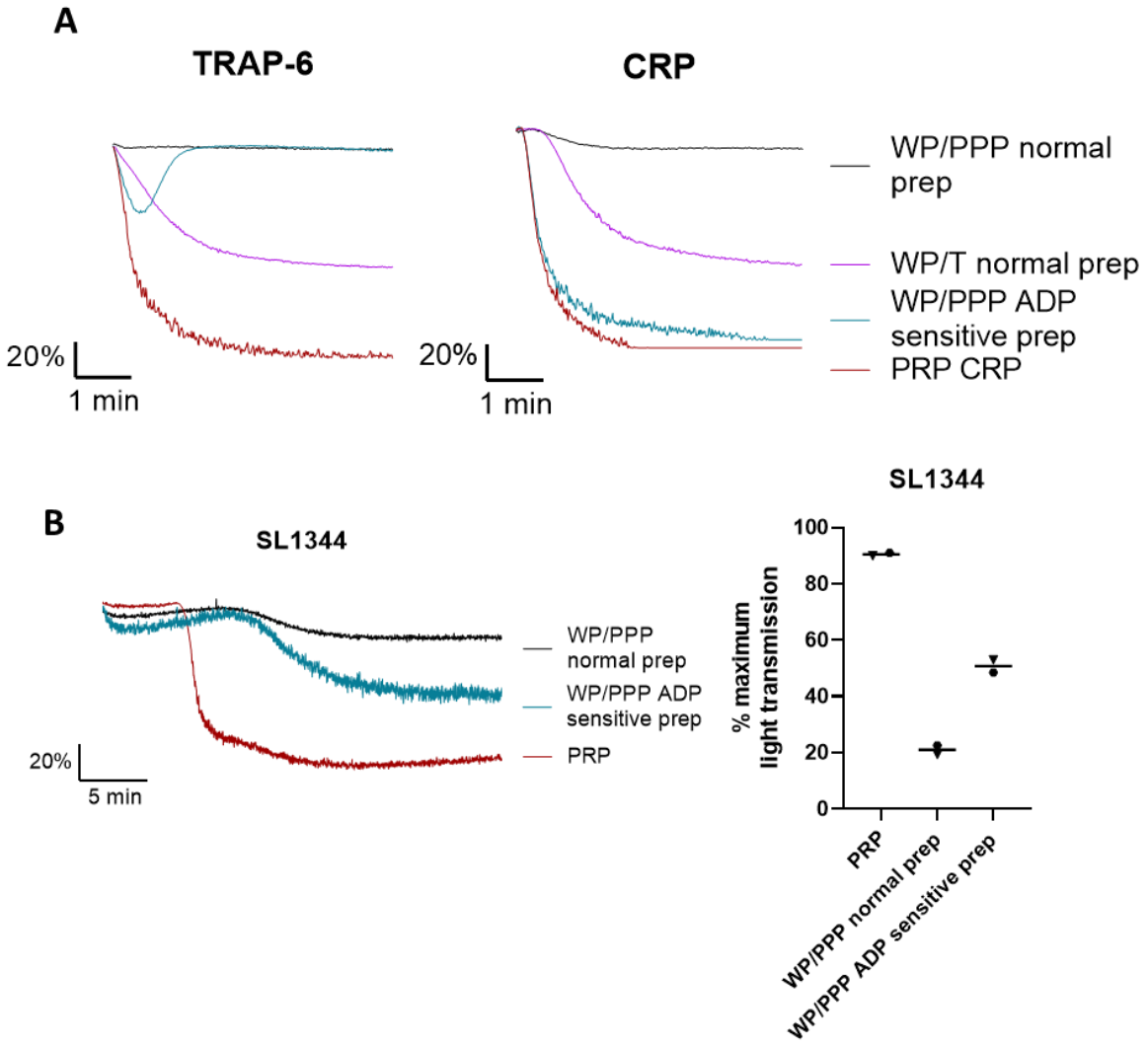


**Figure 3.12: Washed platelets resuspended in PPP do not give similar responses to PRP.** Washed platelets were either prepared using the standard method (section 2.3.3) or using an ADP sensitive method (section 2.3.4). Pellets were then resuspended into either PPP (WP/PPP) or Tyrode's buffer (WP/T). PRP was also prepared (section 2.3.2). 100µM TRAP-6 or 10µM collagen-related peptide (CRP) was added and responses measured for five minutes. n = 1. B) The same types of platelet preparations as in A were used, minus WP/T, as this does not permit aggregation to STm SL1344. Platelets were stimulated with ~1 x $10^9$ CFU/ml STm SL1344. Left hand side figure shows representative aggregation traces, right hand figure showed pooled data from n = 2.

### 3.2.3.4 Depletion of anti-*Salmonella* antibodies in plasma stops platelet aggregation induced by *Salmonella*

With confirmation of a plasma component being responsible for donor variation, and a known role for the FcγRIIA receptor, the next step was to confirm whether the ligand of FcγRIIA, IgG, was vital for platelet aggregation. Anti-STm antibodies were depleted from PPP by incubation with 1 x $10^9$ CFU/ml STm SL1344 for 2 hours at 4°C, before centrifugation to remove bacteria. In a similar manner to the donor swaps above, one ADP sensitive platelet preparation pellet was resuspended in this antibody depleted PPP (dPPP), with the other pellet resuspended in normal PPP (WP/PPP) as a control. As shown in Figure 3.13, the antibody depletion led to no or low aggregation to STm SL1344, demonstrating that anti-STm antibodies are required for STm induced platelet aggregation.

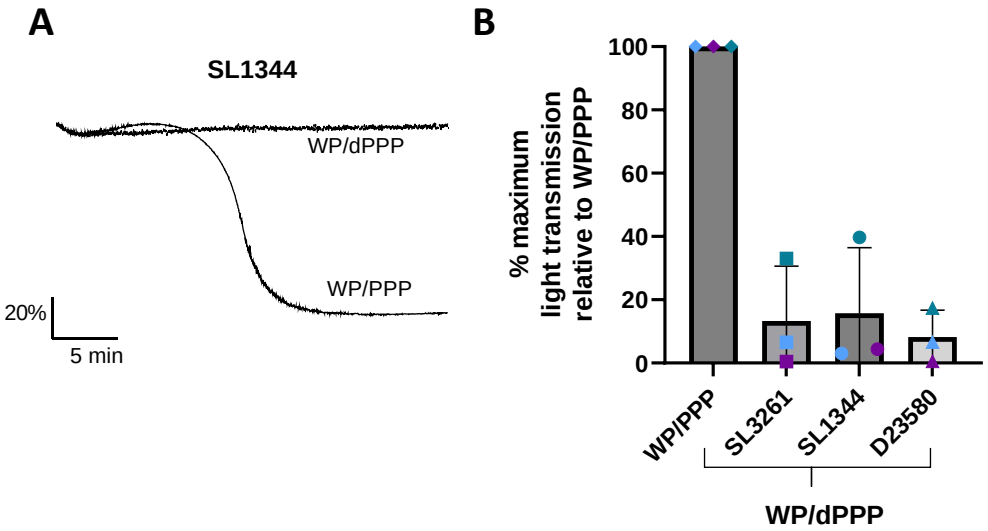


**Figure 3.13: Depletion of anti-*Salmonella* antibodies in plasma stops platelet aggregation induced by *Salmonella*.** PPP was obtained prior to day of experiment. Anti-*Salmonella* antibodies were depleted by incubating PPP with 1 x $10^9$ CFU/ml STm SL1344 for two hours at 4°C, before centrifuging to remove bacteria. The supernatant of antibody depleted PPP (dPPP) was frozen, along with control PPP. On day of aggregation, fresh blood was taken, platelet pellets made using the ADP sensitive platelet preparation and resuspended in either dPPP or PPP. These were then stimulated by either ~5 x $10^8$ CFU/ml STm SL3261, ~1 x $10^9$ CFU/ml STm SL1344 or STm D23580 at a 1:2 bacteria:platelet volume ratio. Platelets were kept at 37°C, stirring at 1200rpm, and light transmission monitored in a PAP-8 aggregometer for 30 minutes. A) Representative trace of a strong responder to SL1344 WP/PPP and their response in WP/dPPP. B) Pooled data from n = 3. Colours represent separate donors – blue and purple were strong responders, teal a weak responder. Data are presented as WP/dPPP responses to the three bacteria relative to the control WP/PPP level taken as 100% maximum aggregation.

### 3.2.3.5 Total anti-*Salmonella* IgG antibody levels correlate with platelet aggregation levels

Using a whole bacteria ELISA, levels of anti-STm antibodies against the three strains were measured. Although the total IgG results were normally distributed, the maximum aggregation levels for STm SL3261 and STm D23580 were not, so when carrying out statistical tests on the correlation graphs, the non-parametric Spearman rank correlation coefficient was calculated (Figure 3.14). All three strains gave moderately positive correlations of total IgG against maximum aggregation levels, with Spearman r values of 0.65, 0.52 and 0.61 for STm SL3261, SL1344 and D23580 respectively, significant for STm SL3261 and D23580 (Figure 3.14, left hand side). The lag times for all three strains were normally distributed, so the parametric Pearson correlation coefficient was able to be calculated. As 5/12 donors tested were non-responders to SL3261, only 7 samples had lag times able to be plotted, leading to a Pearson r value of -0.3141, and no significance. However, for SL1344 (n = 11) and D23580 (n = 10), the Pearson r values of -0.77 and- 0.74 were significant (Figure 3.14, right hand side). Taking the correlations for both maximum aggregation and lag time into account strongly suggests that the more anti-STm antibody a donor has, the stronger and faster their STm induced platelet aggregation.

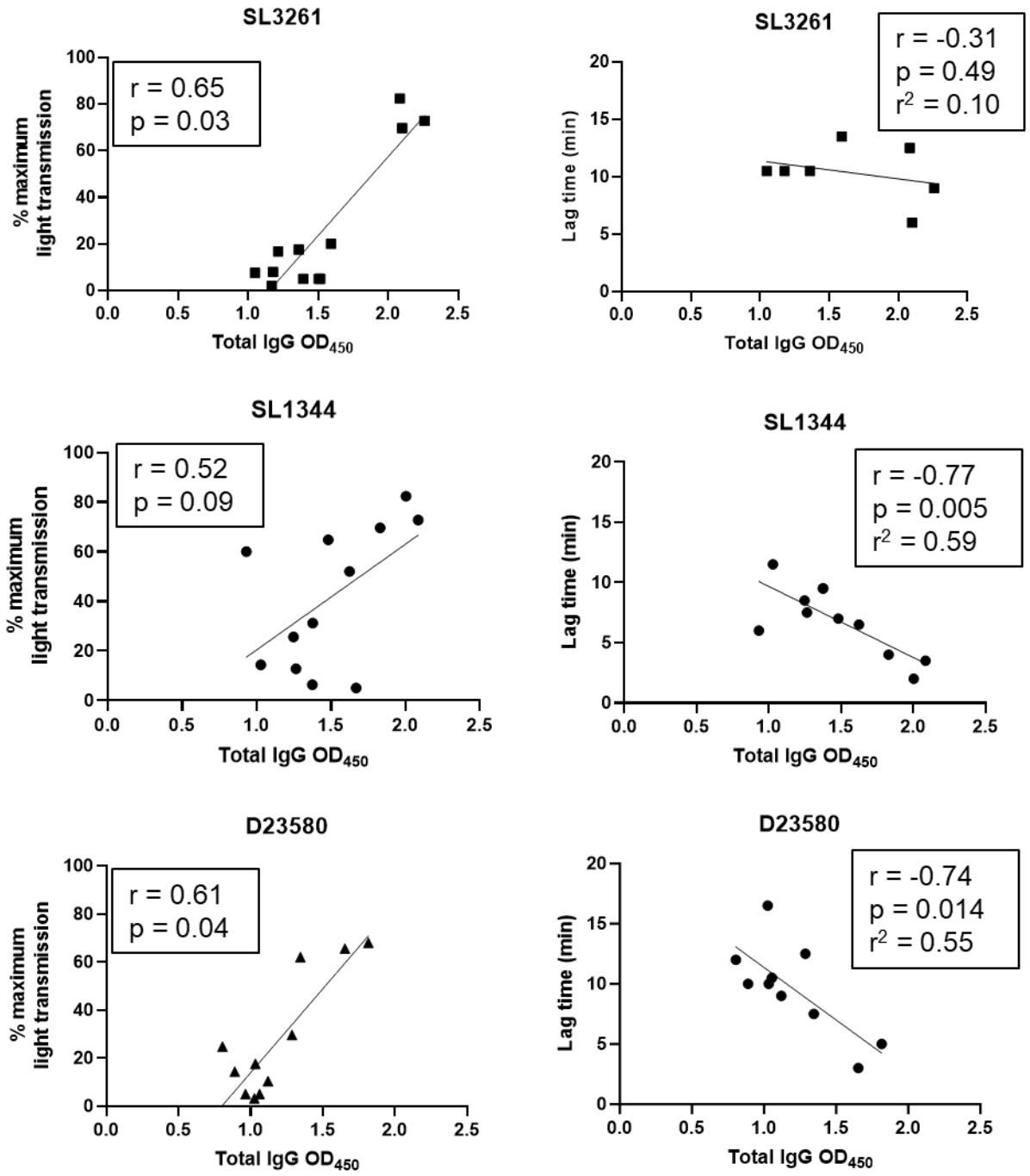


**Figure 3.14: Total anti-*Salmonella* IgG antibody levels correlate with platelet aggregation levels.** Total IgG levels to each three bacteria were measured using an in-house ELISA (section 2.6.2). Resulted presented are from the 1 in 20 serum dilution. These results were correlated against maximum light transmission levels (left hand figures) and lag time (right hand figures) from Fig 3.3. Maximum light transmission results were not all normally distributed, so Spearman rank correlation coefficient was calculated. Lag times were all normally distributed, so Pearsons correlation coefficient was calculated. Best fit lines added with simple linear regression. For left hand graphs, n = 12. For right hand graphs n ≥ 7.

### 3.2.3.6 No individual IgG subclass is responsible for variation in platelet aggregation responses to *Salmonella*

With variation in total IgG levels to STm reflecting in the platelet aggregation response, the levels of individual IgG subclasses were measured (Figure 3.15) to see whether a particular isotype was responsible for activating platelets. When correlating these against aggregation responses (Figure 3.16), Spearman r values were calculated as not all data sets were normally distributed. The only significant correlations were between maximum aggregation and IgG2 levels for STm SL1344, and lag time and IgG1 levels of STm D23580 (Figure 3.16B). Given the lack of consistency between strains, and no single isotype having a statistically significant correlation to both the maximum aggregation level and the lag time, it is not possible to conclude that a single IgG isotype is responsible for the aggregation response.

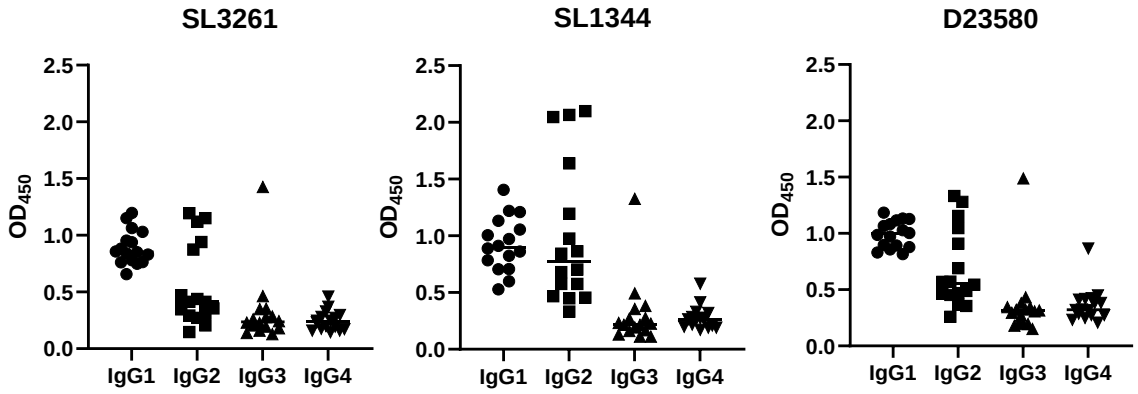


**Figure 3.15: Levels of IgG subclass antibodies against *Salmonella* strains.** In house ELISAs were carried out to measure levels of anti-*Salmonella* IgG subclass antibodies to each of the three strains. N = 16. Bars = median.

**A**

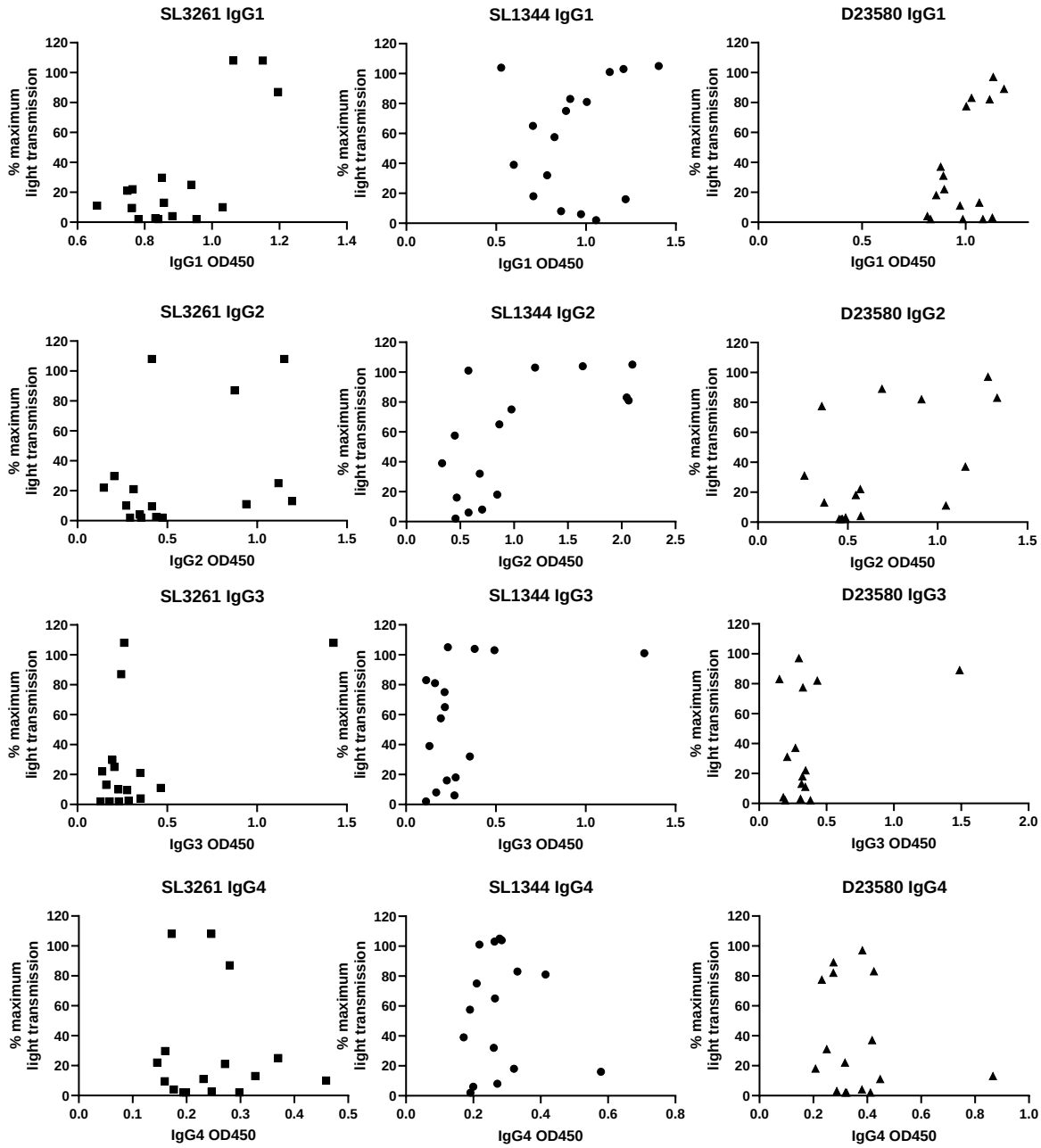
SL3261 IgG1
SL1344 IgG1
D23580 IgG1
SL3261 IgG2
SL1344 IgG2
D23580 IgG2
SL3261 IgG3
SL1344 IgG3
D23580 IgG3
SL3261 IgG4
SL1344 IgG4
D23580 IgG4
% maximum light transmission
IgG1 OD450
IgG2 OD450
IgG3 OD450
IgG4 OD450

**B**

**SL3261**

| | Spearman, r | | P value | |
|---|---|---|---|---|
| | % Max aggregation | Lag time | % Max aggregation | Lag time |
| IgG1 | 0.41 | -0.12 | 0.119 | 0.757 |
| IgG2 | 0.18 | -0.20 | 0.505 | 0.579 |
| IgG3 | 0.20 | -0.39 | 0.453 | 0.274 |
| IgG4 | -0.05 | -0.25 | 0.867 | 0.486 |

**SL1344**

| | Spearman, r | | P value | |
|---|---|---|---|---|
| | % Max aggregation | Lag time | % Max aggregation | Lag time |
| IgG1 | 0.12 | -0.51 | 0.656 | 0.053 |
| IgG2 | **0.66** | -0.50 | **0.006** | 0.059 |
| IgG3 | 0.36 | -0.48 | 0.169 | 0.073 |
| IgG4 | 0.26 | -0.06 | 0.326 | 0.835 |

**D23580**

| | Spearman, r | | P value | |
|---|---|---|---|---|
| | % Max aggregation | Lag time | % Max aggregation | Lag time |
| IgG1 | 0.40 | **-0.77** | 0.122 | **0.003** |
| IgG2 | 0.50 | -0.09 | 0.052 | 0.761 |
| IgG3 | 0.20 | -0.42 | 0.448 | 0.155 |
| IgG4 | -0.16 | 0.17 | 0.547 | 0.587 |

**Figure 3.16: No individual IgG subclass is responsible for variation in platelet responses to *Salmonella*.** In house ELISAs were carried out to measure levels of anti-*Salmonella* IgG subclass antibodies to each of the three strains. A) Results were correlated against maximum aggregation.B) Spearman r values and p values for graphs in A, plus correlations against lag time (graphs not shown). **Statistically significant results are bold**. n = 16 for maximum aggregations. n ≥ 7 for lag times.

To see whether combinations of isotypes provided stronger correlations, OD values from subclasses were combined and correlation calculations re-done. IgG4 was not included in combinations other than all 4 subclasses as this subclass makes up the smallest proportion of total IgG in blood (Rispens and Huijbers, 2023), and very little variation in IgG4 was seen in our donor cohort (Figure 3.15). For STm SL1344 all combinations of IgG subclass apart from IgG1 and 3 were strongly positively correlated to both maximum aggregation levels and lag time (Figure 3.17). For STm SL3261 and D23580, different combinations of isotypes gave significant moderate positive correlations (Figure 3.17). This suggests that the individual isotype is not important, rather the overall level of antibody able to coat the bacterium, regardless of subclass, relates to the level and speed of platelet aggregation seen.

**A**

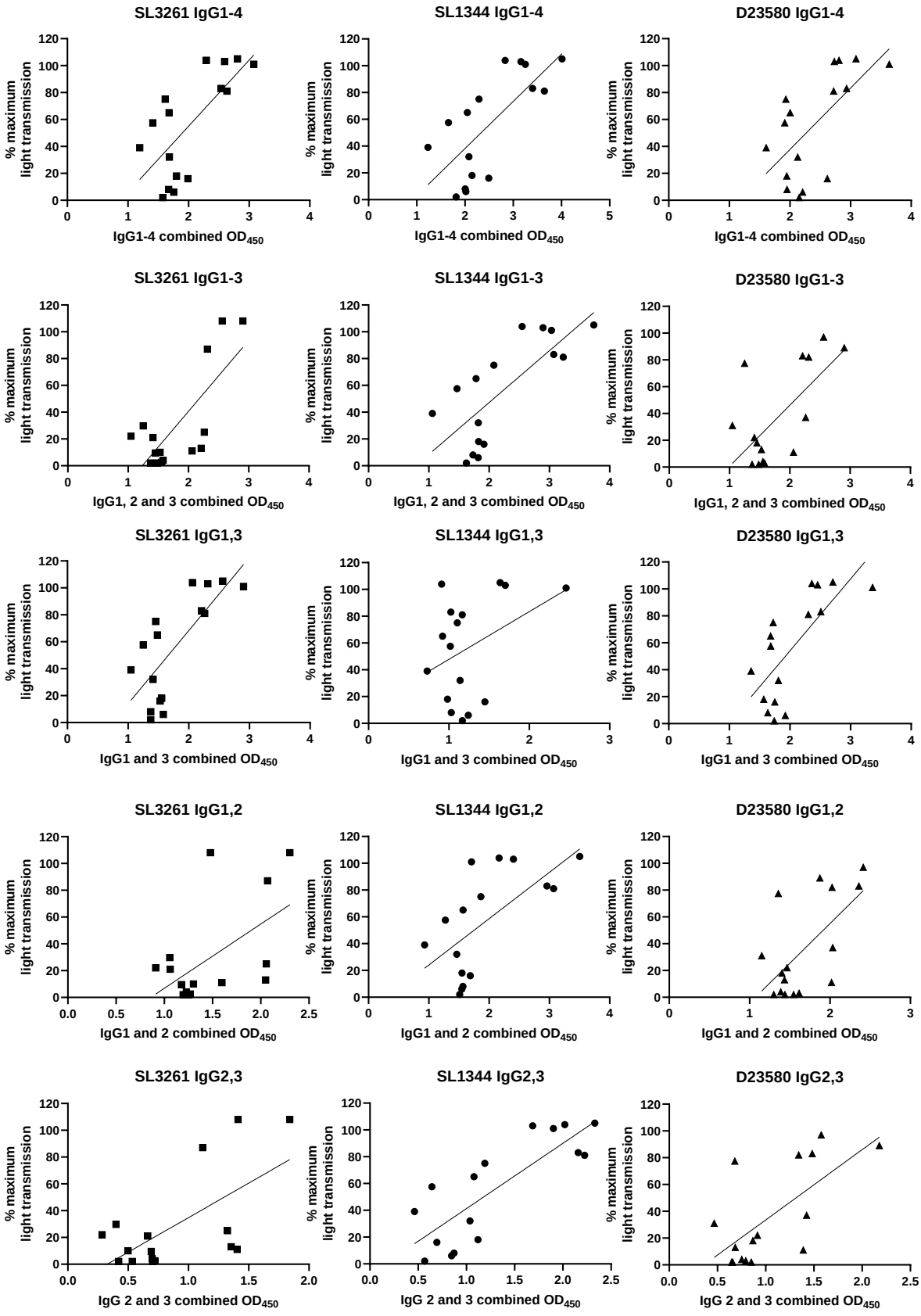
SL3261 IgG1-4
SL1344 IgG1-4
D23580 IgG1-4
SL3261 IgG1-3
SL1344 IgG1-3
D23580 IgG1-3
SL3261 IgG1,3
SL1344 IgG1,3
D23580 IgG1,3
SL3261 IgG1,2
SL1344 IgG1,2
D23580 IgG1,2
SL3261 IgG2,3
SL1344 IgG2,3
D23580 IgG2,3
% maximum light transmission
IgG1-4 combined OD450
IgG1, 2 and 3 combined OD450
IgG1 and 3 combined OD450
IgG1 and 2 combined OD450
IgG 2 and 3 combined OD450

**B**

**SL3261**

| | Spearman, r | | P value | |
|---|---|---|---|---|
| | % Max aggregation | Lag time | % Max aggregation | Lag time |
| IgG1,2,3,4 | **0.52** | -0.06 | **0.042** | 0.891 |
| IgG1,2,3 | 0.49 | -0.14 | 0.057 | 0.704 |
| IgG1,2 | 0.36 | -0.23 | 0.176 | 0.532 |
| IgG1,3 | **0.50** | -0.25 | **0.050** | 0.486 |
| IgG2,3 | 0.39 | -0.09 | 0.134 | 0.810 |

**SL1344**

| | Spearman, r | | P value | |
|---|---|---|---|---|
| | % Max aggregation | Lag time | % Max aggregation | Lag time |
| IgG1,2,3,4 | **0.73** | **-0.66** | **0.002** | **0.009** |
| IgG1,2,3 | **0.73** | **-0.67** | **0.002** | **0.008** |
| IgG1,2 | **0.73** | **-0.71** | **0.002** | **0.004** |
| IgG1,3 | 0.10 | **-0.57** | 0.713 | **0.028** |
| IgG2,3 | **0.81** | **-0.62** | **0.0003** | **0.016** |

**D23580**

| | Spearman, r | | P value | |
|---|---|---|---|---|
| | % Max aggregation | Lag time | % Max aggregation | Lag time |
| IgG1,2,3,4 | 0.47 | -0.44 | 0.067 | 0.133 |
| IgG1,2,3 | **0.63** | -0.55 | **0.010** | 0.055 |
| IgG1,2 | 0.49 | -0.39 | 0.056 | 0.189 |
| IgG1,3 | 0.26 | **-0.79** | 0.325 | **0.002** |
| IgG2,3 | **0.64** | -0.35 | **0.009** | 0.240 |

**Figure 3.17: Combinations of IgG subclass correlate with platelet aggregation responses.** In house ELISAs were carried out to measure levels of anti-*Salmonella* IgG subclass antibodies to each of the three strains. A) OD's were combined from multiple subclasses, and totals correlated against maximum aggregation. n = 16. Lines are simple linear regression. B) Spearman rank correlation values and p values for graphs shown in A, as well as for correlation graphs with lag time (graphs not shown). **Statistically significant results are bold**. n = 16 for maximum aggregations. n ≥ 7 for lag times.

### 3.2.3.7 Platelet aggregation to *Salmonella* cannot be reconstituted in washed platelets with the addition of pooled human IgG and fibrinogen

With the level of anti-STm antibody clearly related to the strength of platelet aggregation when carried out in PRP, it follows that adding IgG to the system in washed platelets should allow similar responses. Based on previous work, where for some bacterial strains addition of fibrinogen helped reduce lag time and increase maximum aggregation (Arman et al., 2014), fibrinogen was also added to give maximum chance of successful aggregation. Despite the platelets responding normally to the PAR-1 activating peptide TRAP-6, aggregation was not seen upon addition of STm SL1344, pooled human IgG (hIgG) and fibrinogen at physiological concentrations (Figure 3.18A). Increased concentrations of these reagents were also tested with no effect (data not shown). In lieu of hIgG, a polyclonal rabbit anti-*Salmonella* antibody was used (STmIgG), but this also made no difference in the outcome (Figure 3.18A). To ensure there were no problems with the hIgG and fibrinogen stocks, the same tests were done on *S. oralis*, for which aggregation in washed platelets with the addition of hIgG and fibrinogen has been previously published (Arman et al., 2014). For *S. oralis* under these conditions, full aggregation took place within 5 minutes (Figure 3.18B), confirming there were no issues with the reagents.

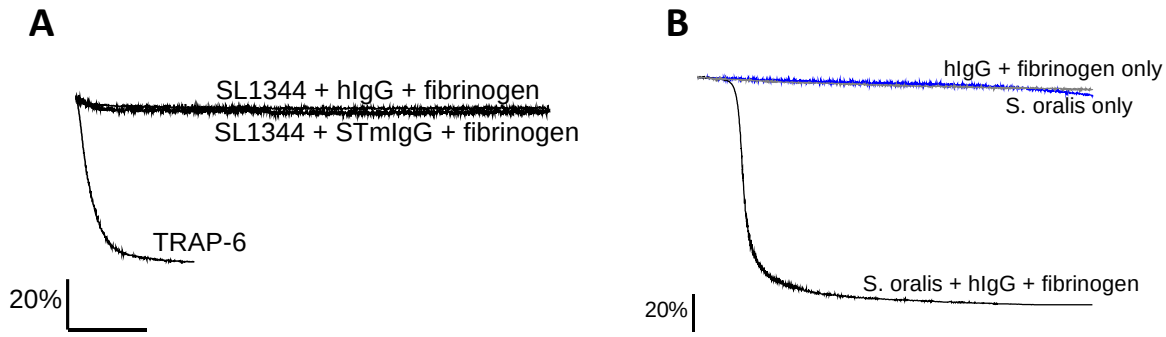


**Figure 3.18: Platelet aggregation to *Salmonella* cannot be reconstituted in washed platelets with the addition of pooled human IgG and fibrinogen.** Platelets were washed and resuspended in Tyrode's buffer. A) TRAP-6 at 100µM was used as a control. 0.1 mg/ml pooled human IgG (hIgG) or 0.1 mg/ml polyclonal rabbit anti-*Salmonella* antibody (STmIgG), plus 1 mg/ml fibrinogen and ~1 x $10^9$ CFU/ml STm SL1344 were added to washed platelets, in a 1:2 bacterial:platelet volume ratio. B) hIgG and fibrinogen added as in A. ~4 x $10^9$ CFU/ml *S. oralis* was added to platelets at a 1:10 bacterial:platelet ratio. n ≥ 1.

### 3.2.4 Investigating the role of PF4 in *Salmonella*-induced platelet aggregation

#### 3.2.4.1 High dose heparin inhibits *Salmonella*-induced platelet aggregation

As described in section 1.5.8, PF4 can bind to bacteria and induce binding of anti-PF4 antibodies (Krauel et al., 2011). Further to this, Arman et al (2014) have shown that PF4 was able to reduce the lag time of bacterial induced platelet aggregations in washed platelet preparations. This was not the case in PRP, likely due to the highly positively charged PF4 binding to other plasma proteins rather than the bacteria. Instead, to investigate a potential role of PF4 in PRP, heparin was used. With its strong negative charge, heparin is able to bind PF4, with the ratio of PF4/heparin causing different effects. At lower heparin doses, lag time was reduced for the five strains investigated in (Arman et al., 2014), whereas at higher doses effects were more variable, with both reduction and increase of lag time in different strains, and total inhibition of response in some cases.

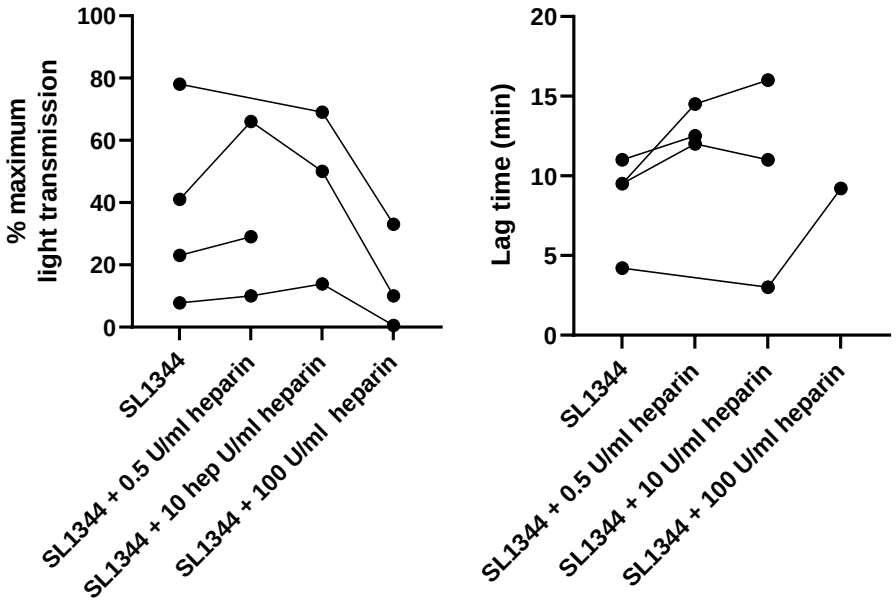


**Figure 3.19: High dose heparin inhibits *Salmonella*-induced platelet aggregation.** Differing doses of heparin (0.5, 10 and 100 U/ml) were pre-incubated with PRP for 3 minutes prior to addition of ~1 x $10^9$ CFU/ml STm SL1344 at a 1:2 bacteria:platelet volume ratio. Platelets were kept at 37°C, stirring at 1200rpm, and light transmission monitored in a PAP-8 aggregometer for 30 minutes. Each line is one different donor, n = 4.

When testing different heparin concentrations with STm platelet aggregations, lower doses caused a small increase in maximum aggregation, but the largest effect was at a high dose of heparin, which caused inhibition of the aggregation response (Figure 3.19, left hand side). Addition of any dose of heparin caused an increase in lag time in 6 out of the 7 tests (Figure 3.19, right hand side). This suggests that PF4 could be involved in STm induced platelet aggregations.

### 3.2.4.2 Platelet aggregation to *Salmonella* cannot be reconstituted in washed platelets with the addition of pooled human IgG, fibrinogen and PF4

With the possibility of PF4 involvement, the same experiments as in section 3.2.3.7 (washed platelets supplemented with hIgG and fibrinogen before stimulation with STm SL1344) were performed, with the addition of PF4, to see whether the presence of this molecule allowed aggregation. Addition of PF4, hIgG and fibrinogen alongside STm SL1344 did not cause any aggregation effect when added to washed platelets (Figure 3.20).

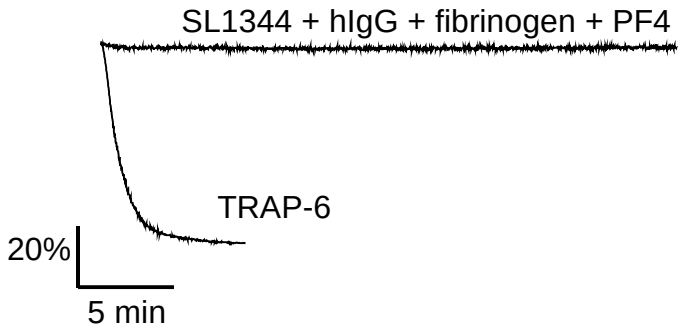


**Figure 3.20: Platelet aggregation to *Salmonella* cannot be reconstituted in washed platelets with the addition of pooled human IgG, fibrinogen and PF4**. Platelets were washed and resuspended in Tyrode's buffer. A) TRAP-6 at 100µM was used as a control. 0.1 mg/ml pooled human IgG (hIgG), 1 mg/ml fibrinogen, 10µg/ml PF4 and ~1 x $10^9$ CFU/ml STm SL1344 were added to washed platelets, in a 1:2 bacterial:platelet volume ratio. Representative trace from n = 2.

### 3.2.4.3 Donor samples are negative for anti-PF4 complex antibodies

With the high dose heparin inhibition suggesting a possible role for PF4, but the addition of PF4 to the system still not causing platelet aggregation in washed platelets, donor samples were tested for the presence of anti-PF4 antibodies. These antibodies would be needed for PF4 to be playing a role in the platelet aggregation as discussed in section 1.5.8 and Krauel et al (2011). To test for these antibodies, the Immucor PF4 IgG ELISA, a HIT screening assay was used. The Immucor ELISA uses polyvinyl sulfonate-PF4 complexes, which mimics heparin-PF4 (Visentin et al., 2001), and therefore also likely mimics bacteria-PF4 complexes.

12/13 samples gave a negative result (Figure 3.21), with just one sample giving an OD slightly above the positive cut-off line. The donor whose sample tested positive is a weak responder to all three strains, making the result unlikely to have any significance. Therefore, with the majority of samples not containing detectable IgG anti-PF4 antibodies, and the addition of PF4 still not allowing STm induced aggregation in a washed platelet system, it can be concluded that PF4 is unlikely to be playing a role in platelet aggregation to STm in this *in vitro* system.

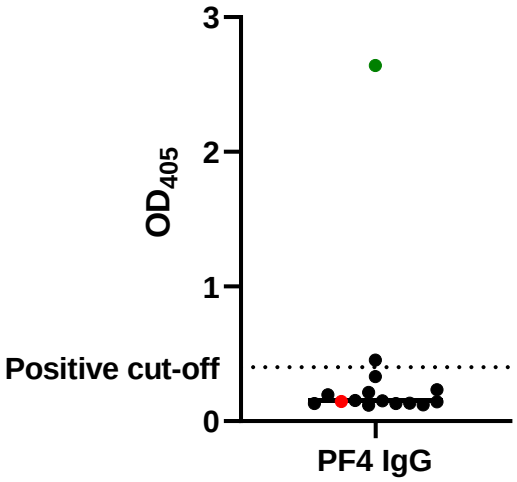


**Figure 3.21: Donor serum samples are negative for anti-PF4 complex antibodies.** The Immucor PF4 IgG ELISA was carried out as per manufacturers instructions. Red dot = negative control, green dot = positive control. As per instructions, samples with an OD equal or greater than 0.4 are classed as positive results. n = 13.

### 3.2.5 Investigating the role of antibody in platelet aggregation by *Salmonella*

#### 3.2.5.1 Platelet aggregation to *Salmonella* can be reconstituted in ADP sensitive platelets with the addition of anti-*Salmonella* antibody

With PF4 unlikely to be playing a role, it was important to assess why, with antibody already being identified as a key component in the donor variation, adding antibody to STm did not result in aggregation in washed platelets. Section 3.2.3.3 showed that when resuspending washed platelets in PPP, an ADP sensitive platelet preparation gave larger aggregation responses than a standard platelet preparation. However, for experiments in sections 3.2.3.7 and 3.2.4.2, a standard preparation was used, as platelets were being resuspended in buffer, rather than PPP, and a standard preparation had been used for these experiments in Arman et al. (2014). However, with the results using ADP-sensitive platelets in mind, the experiments from sections 3.2.3.7 and 3.2.4.2 were re-run using this prep.

Again, with the addition of hIgG and fibrinogen, *S. oralis* (and *S. aureus* as an additional positive control) caused full aggregation of platelets within a lag time of 5 minutes. STm SL1344 plus hIgG and fibrinogen still did not lead to platelet aggregation (Figure 3.22A). However, substituting the hIgG for polyclonal rabbit anti-*Salmonella* IgG (STmIgG) did allow for STm induced platelet aggregation (Figure 3.22B). This aggregation was possible with the addition of STmIgG alone, with the addition of fibrinogen increasing the maximum aggregation and speed of response by a minor amount. Addition of PF4 to the system made no difference to the level and rate of aggregation.

With the conditions for aggregation optimised, dose-response curves using the STmIgG were able to be performed (Figure 3.22C). In the donors tested, interestingly, STm SL13144 was able to aggregate at lower concentrations of STmIgG than D23580 and SL3261, mirroring the results seen in PRP. Furthermore, keeping the maximal concentration of STmIgG allowed responses to be seen with decreasing amounts of STm SL1344 (Figure 3.22D)

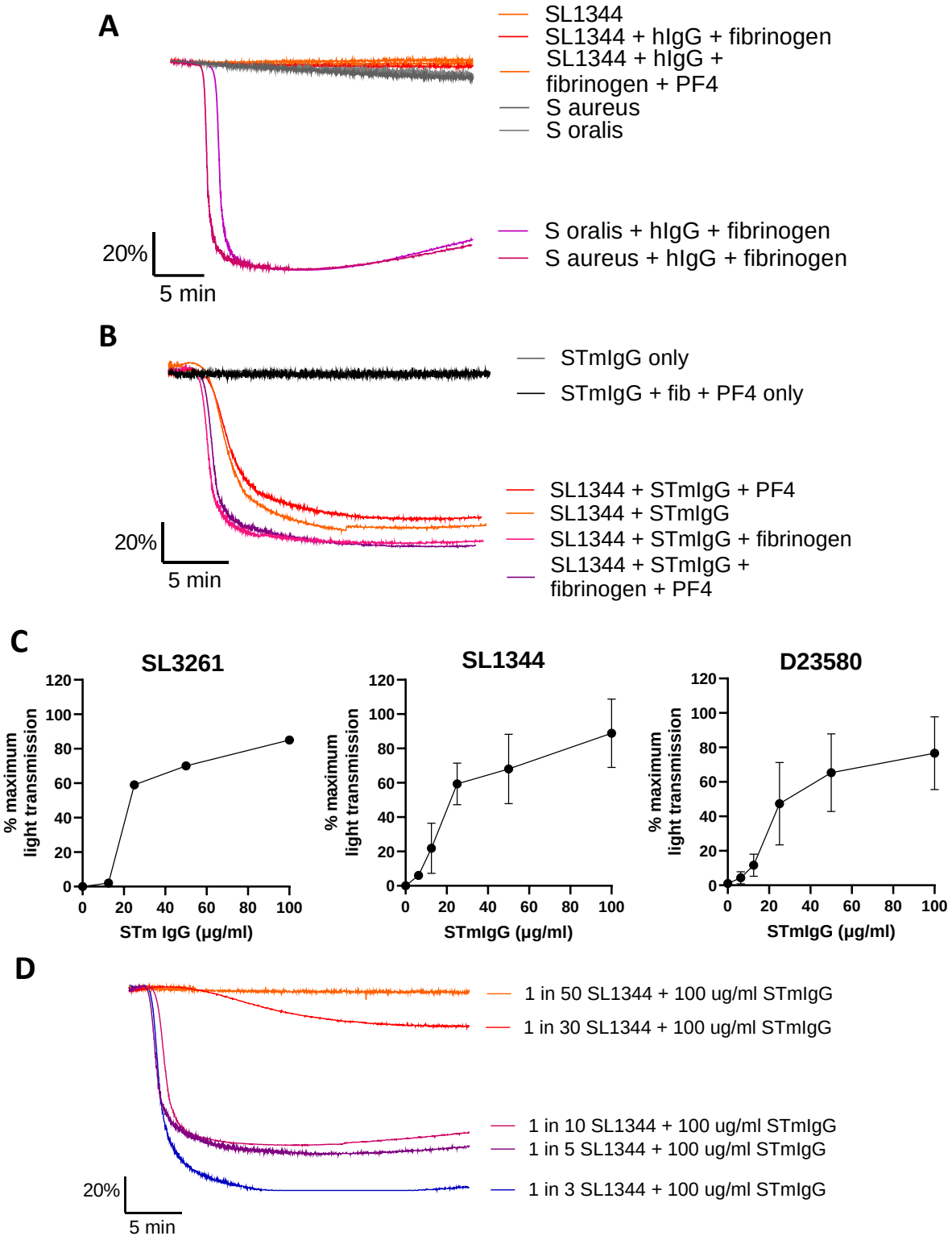


**Figure 3.22: Platelet aggregation to *Salmonella* can be reconstituted in ADP sensitive platelets with the addition of anti-*Salmonella* antibody.** Washed platelets were made using an ADP-sensitive method. A) Platelets were stimulated either with ~1 x $10^8$ CFU STm SL1344, ~1.2 x $10^8$ CFU *S. oralis*, or ~3 x $10^7$ CFU *S. aureus.* Pooled human IgG (hIgG), fibrinogen and PF4 were added as labelled at the following concentrations: 0.1 mg/ml, 1 mg/ml, 10 µg/ml. n = 1 B) As A, but using a polyclonal rabbit anti-*Salmonella* antibody (STmIgG) instead of hIgG. Representative traces of n = 2 C) Dose response curves to the three *Salmonella* strains using STmIgG. SL3261 n =1, SL1344 and D23580 n = 3. Bars are mean ± SD. D) Keeping the amount of platelets the same throughout, the final bacterial dilution was reduced. 0.1 mg/ml STmIgG was added to each. n = 1.

To conclude this section, platelet aggregation responses to STm are donor dependent, with the amount of anti-*Salmonella* IgG antibody in the plasma correlating with the level of platelet aggregation and the speed at which it occurs. This finding is mirrored in washed platelets with the addition of STm specific IgG antibody being the only supplement required to cause STm induced platelet activation, with higher antibody levels causing higher aggregation levels.

## 3.2.6 Investigating why *Salmonella* strains differ in their capacity to induce platelet aggregation

### 3.2.6.1 *Salmonella* O-antigen chain length affects platelet aggregation responses

The three *Salmonella* strains used thus far are all variants of *Salmonella* Typhimurium. STm SL1344 is the grandparent strain of STm SL3261, which has an additional *AroA* gene knockout leading to its attenuation (Hoiseth and Stocker, 1981). Aside from this, the two strains should be genetically the same. STm D23580 however, has diverged (see Figure 1.3 in introduction), and has single nucleotide polymorphisms, insertions and in particular, many deletions in its genome in comparison to STm SL1344 (Kingsley et al., 2009). Two of the genes degraded in comparison to SL1344 are putative outer or integral membrane proteins, with a further deletion of a secreted protein implicated in long-term intestinal persistence in mice (Kingsley et al., 2009). With STm SL3261 and STm SL1344 being so closely related, but STm D23580 having many genetic differences, assessing why these strains have different phenotypes when it comes to activating platelets is difficult.

Therefore, specific mutants of a different STm reference strain, wildtype (WT) 14028, were used as a starting point to identify whether variation in O-antigen chain length could be one component that causes different platelet aggregation responses. The 14028 Δ*wzy* strain expresses LPS with only one O-antigen repeat, whilst the 14028 Δ*wbap* strain expresses LPS with no O-antigen repeats (Figure 3.23A). 10428 Δ*tolR* mutants have an unstable outer membrane, causing vesicles to bleb from the membrane (Figure 3.23B). The double mutants bleb outer membrane vesicles (OMVs) with either wild-

type LPS, one or no antigen repeats for 14028 Δ*tolR,* 14028 Δ*tolR*Δ*wzy* and 14028 Δ*tolR*Δ*wbap* respectively.

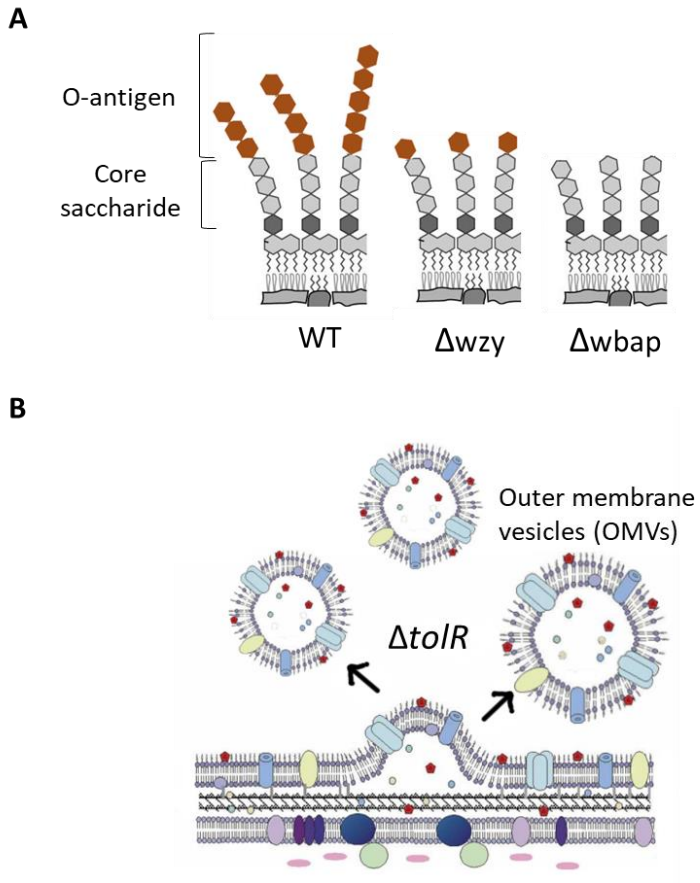


**Figure 3.23: Diagrams demonstrating the effects of different knock-out strains used.** A) Adapted from (Silhavy et al., 2010). Brown hexagons represent one O-antigen repeat: WT LPS has a mixture of O-antigen lengths from 0-100. Δwzy has one O-antigen per LPS, whilst Δwbap does not contain any O-antigen. B) Adapted from (Kuehn and Kesty, 2005). ΔtolR mutants have an unstable cell membrane leading to blebbing and formation of outer membrane vesicles.

Figure 3.24 shows the variation in responses to the different strains. As with the three original STm strains tested, there is both strain and donor variation. The same colour coding system has been used, with donors split into strong, mid, weak and non-responders (Figure 3.24A,B). Taking the strong and mid responders only for further analysis shows that in both the WT 14028 and the 14028 Δ*tolR*, the removal of most or all of the O-antigen chain causes a reduction in platelet aggregation (Figure 3.24C,D). In the majority of donors, aggregation levels are reduced to a minimum, although there are

some donors whose platelets were still able to aggregate strongly, although still mostly at a lower level compared to the WT. Despite the maximum aggregation levels being lower for the O-antigen mutants, the median lag times between the 14028 mutants remained static at 6 minutes, albeit with much less donor variation in the Δ*wzy* and Δ*wbap* mutants (Figure 3.24E). For the Δ*tolR* strains, the median lag times were 4, 2 and 2.5 minute for the single Δ*tolR* mutant, Δ*tolR*Δ*wzy* and Δ*tolR*Δ*wbap* respectively (Figure 3.24E). Together, these data suggest that O-antigen plays a key role in STm induced platelet aggregation, and that having a larger available surface area of outer membrane allows for quicker platelet aggregation.

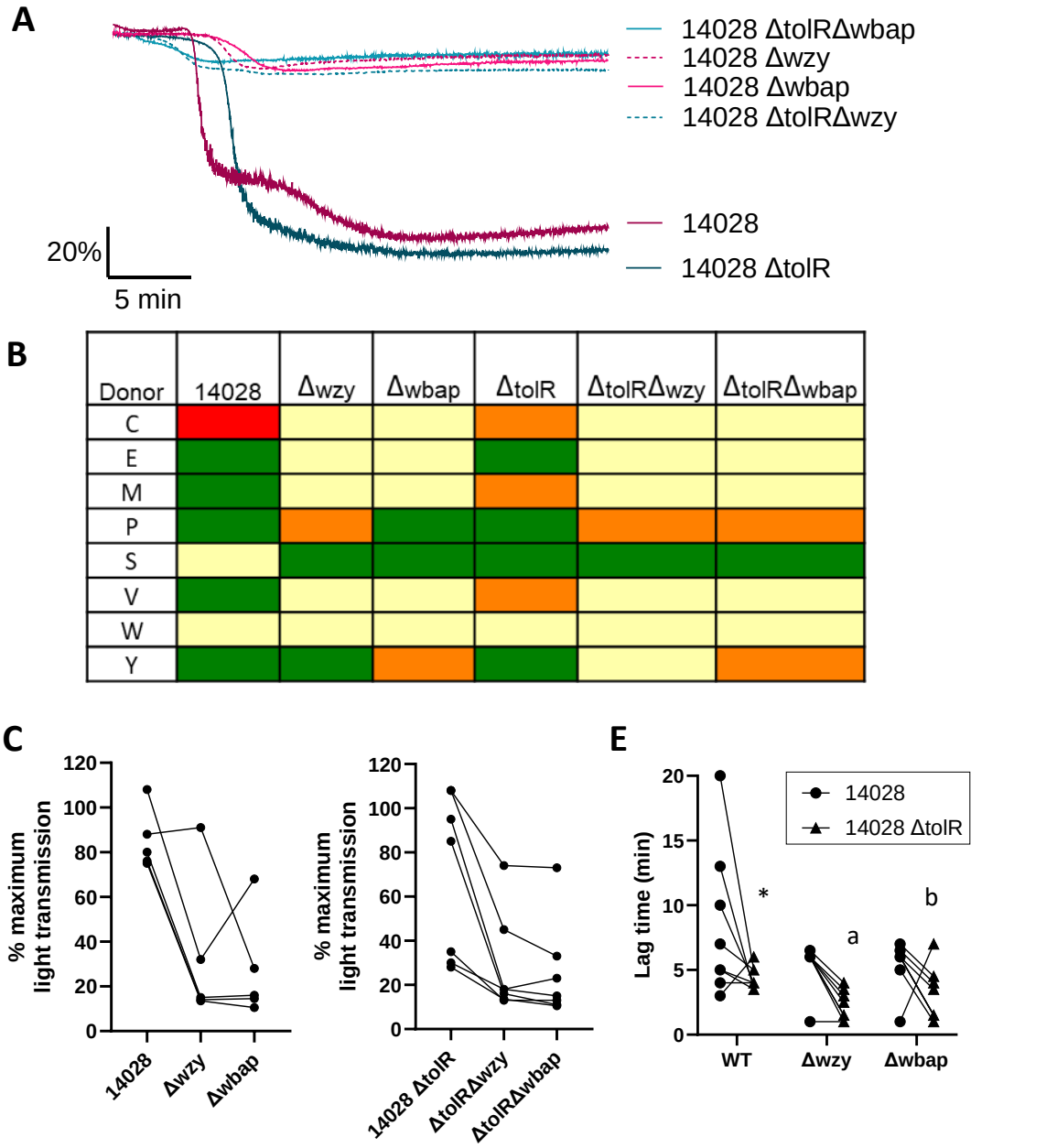


**Figure 3.24: *Salmonella* O-antigen chain length affects platelet aggregation responses.** Strains were added to platelets at a 1:2 volume ratio. The final concentrations of bacteria were: ~ 6.7 x $10^8$ CFU/ml 14028 and 14028 Δ*wzy,* ~3.3 x $10^8$ CFU/ml 14028 Δ*wbap*, 14028 Δ*tolR*, 14028 Δ*tolR*Δ*wzy* and ~ 1.7 x $10^7$ CFU/ml 14028 Δ*tolR*Δ*wbap*. A) Aggregation traces from donor E, which can be seen in comparison to others in B. B) Table showing donor variation in responses to 14028 mutants. Colour coding: strong responders (green; >60% maximum aggregation), mid responders (orange; 20-60% maximum aggregation), weak responders (cream, <20% maximum aggregation, but still with a curve), and non-responders (red, no aggregation). C) Only donors who responded strongly to 14028 are plotted. Maximum aggregation % to 14028, and its O-antigen mutants. n = 5 D) Only strong and mid responders to 14028 Δ*tolR* are plotted. Maximum % aggregation to 14028 Δ*tolR* and its O-antigen mutants. n = 7. E) Comparison of lag times between 14028 and 14028 Δ*tolR* mutants, and their O-antigen mutants. n = 8. Friedman test for paired samples (non-parametric) with Dunn's multiple comparisons test revealed significance between the WT ΔtolR (*) and ΔwzyΔtolR (a) with an adjusted P value of 0.0054, and between WT ΔtolR (*) and ΔwbapΔtolR (b) with an adjusted P value of 0.0489.

## 3.3 Discussion

This chapter shows that *Salmonella* Typhimurium can activate platelets, but in a donor and strain dependant manner. Platelets are activated indirectly, with STm SL3261 least able to cause strong activation, and STm SL1344 most able. The levels of anti-STm IgG antibody in the donor serum are strongly linked to the variation in platelet responses, with higher antibody levels resulting in stronger and faster platelet activation. It appears that one factor involved in the variation of responses between strains could be variation in the LPS O-antigen chain, with knock-out strains showing markedly reduced platelet activation when O-antigen is absent.

The first aim of this chapter was to assess the responses of a larger cohort of healthy donors to three STm strains: the attenuated lab strain STm SL3261, wild-type strain STm SL1344 and invasive clinical isolate STm D23580. Preliminary results from the Cunningham lab showed STm D23580 was capable of activating platelets in the most number of donors, with STm SL3261 not able to activate any of the donors tested. However, upon testing a larger cohort of donors, STm SL1344 was the strain able to induce aggregation in most donors. STm SL3261 remained the strain with the weakest responses. One reason behind the difference seen between these results and the preliminary data could be the dilution of bacteria used. In the preliminary studies, a 1 in 10 bacterial dilution was added to the platelets. However, when optimising the dilutions for this thesis, it was found that those donors who had minimal aggregation responses at 1 in 10 showed stronger responses using a 1 in 3 bacterial dilution. Therefore, this dilution was used moving forward. It is also interesting to think about the possible impact of the COVID-19 pandemic on the donor responses. The preliminary data was obtained prior to the pandemic, whereas the donors used in this thesis started being tested at the beginning of 2022. Due to the pandemic, in the two years prior to this, people's travel had been severely restricted, which could perhaps have reduced the general exposure to bacteria such as *Salmonella*, impacting on the IgG levels in donors and therefore platelet aggregation responses seen.

Testing STm responses in both washed platelets and PRP, showed that STm indirectly activates platelets. Some bacteria are able to directly interact with platelets, for example the *S. pneumoniae* lipopeptide can activate platelets by binding toll-like receptor 2 (Keane et al., 2010b), but many bacteria need a plasma component for in order for platelet aggregation to occur. Bacterial induced platelet aggregation where IgG has been shown to be involved include *S. epidermis* (Brennan et al., 2009), *Helicobacter pylori* (Byrne et al., 2003) and *S. sanguinis* (Arman et al., 2014, Ford et al., 1997), so it fits that the addition of anti-*Salmonella* IgG to STm and platelets leads to aggregation.

What is more unusual is the extent of the donor variation observed. Previous studies have shown variation in lag time to *S. sanguinis* (Ford et al., 1997, Ford et al., 1996), *S. oralis* CR834 (Tilley, 2013) and *Cutibacterium acnes* (Petersson et al., 2018), but variation in maximum aggregation has not been shown, with bacterial induced aggregation commonly referred to as an all-or-nothing response (Kerrigan, 2015). Therefore, to see this kind of variation in maximum aggregation to STm is surprising. However, it is a consistent result, observed throughout many different donors PRP, and within donors when using washed platelets with differing amounts of either STmIgG or dilutions of SL1344 itself. In agreement with this result, one paper has reported variation in the responses of 23 donor aggregation levels when using 500µg/ml heat aggregated human IgG (Rosenfeld et al., 1987). Interestingly, using seven of their donors, they managed to show a positive correlation between levels of FcγRIIA on the platelet surface and aggregation levels, in contrast to that found here with STm. This difference could be due to the difference in the activating ligand used, and the difference in platelet preparation – Rosenfeld et al used washed platelets, whereas PRP was used here. It would be interesting to test more donors using the ADP sensitive washed platelet preparation and a sub-optimal amount of STmIgG (around 12.5µg/ml for SL1344) to see whether this invoked donor variation in washed platelets, and whether this more standardised approach, lacking what could be interference by plasma proteins, would show a correlation between responses and FcγRIIA levels.

In terms of variation between strains, this is more commonly observed, with 7/11 strains of *S. oralis* tested in Tilley (2013) able to cause platelet aggregation, with the remaining four strains unable to. Variation has also been shown with four *C. acnes* strains (Petersson et al., 2018) and 21 different *H. pylori* strains (Corcoran et al., 2007). What is less well understood are the reasons behind these strain differences, a question that remains with *Salmonella*, especially given the similarities between STm SL1344 and STm SL3261.

Clear correlations between the amount of anti-STm antibody present and the degree and speed of platelet aggregation to STm were shown (Figure 3.14). A study analysing the same in *S. sanguinis* did not find a correlation between bacterial specific IgG and lag time (Ford et al., 1997), showing just how variable the mechanisms between different bacteria can be. This difference could be due to the nature of the cell membranes, with STm being Gram negative, but *S. sanguinis* being Gram positive. The results in this thesis suggest a role for the LPS O-antigen in STm induced platelet aggregation, but with Gram positive strains lacking LPS, this could account for the mechanistic differences between the strains. Another factor to take into account is that *S. sanguinis* is a commensal oral microbe, making it a bacteria that the majority of people live with, in contrast to *Salmonella* which is pathogenic, which could also effect the links between IgG levels and platelet aggregation. I would hypothesise that the donor variation seen in this cohort is heavily influenced by the nature of the healthy donors tested. If this study was carried out in sub-Saharan Africa for example, I would expect higher levels of strong responders, due to the high prevalence levels of anti-*Salmonella* antibodies in the population (Stockdale et al., 2019).

Although my results showed correlations between total anti-STm IgG, no role for individual subclasses was revealed. Instead, it is likely that the particular IgG subclass is unimportant, rather any combination of antibodies can come together to bind STm allowing aggregation proportional to the amount of antibody bound. Having said that, FcγRIIA has different affinities for the different

subclasses, in the order IgG3>IgG1>IgG4>IgG2 (Vidarsson et al., 2014). Furthermore, these affinities differ depending on the single nucleotide polymorphism (SNP) at position 131 (sometimes labelled as position 166 if the signal peptide is included in the counting (Nagelkerke et al., 2019)). A histidine (H) at this position has increased affinity for IgG1 and IgG2, compared to the arginine (R) haplotype (Anania et al., 2019, Bruhns et al., 2009). This has functional consequences, with clear variation in platelet aggregation responses shown to anti-CD9 antibody, which activates platelets via the FcγRIIA receptor (Worthington et al., 1990). Results showed HH homozygotes had the lowest average aggregation response, RR homozygotes the highest average response, and R/H heterozygote sitting on average between the two homozygotes, albeit with much higher variation in responses (Worthington et al., 1990). With HIT proposed to be a mis-directed bacterial response (Krauel et al., 2011), a role for this SNP in HIT could provide clues to the donor variation seen to STm. However, although many studies on this subject area have been carried out, the results remain controversial, with some studies suggesting increased frequency of 131H in HIT, but others suggesting the opposite (Denomme, 2012). Furthermore, there are other SNPs in FcγRIIA which have yet to be studied so intensely (Nagelkerke et al., 2019), including a leucine insertion that increases binding affinity to IgG (present in ~17% of those in a cohort from Ghana (Omar et al., 2012)) and Q27W, which causes reduced $Ca^{2+}$ mobilisation therefore altering down-stream signalling (frequency of 0.5% in a healthy Dutch control population, but 4% in a common variable immunodeficiency cohort (Flinsenberg et al., 2014)). Whilst consensus has not been made in terms of the role of genetic variation in FcγRIIA in HIT, these mutations could be having an effect on platelet responses to bacteria. With my results showing that reducing the concentration of STmIgG added to SL1344 in ADP-sensitive washed platelets from 25µg/ml to 12.5µg/ml takes you from a strong response to a weak response, the amount of antibody in the system is clearly very important. Therefore, the affinity different antibody subtypes have for platelets could alter responses. For example, antibodies to polysaccharides such as *Salmonella* LPS are largely of the IgG1 and IgG2 subclasses (Vidarsson et al., 2014, Ferrante et al., 1990). With the HH homozygote

known to have higher affinity for IgG2 antibodies than the RR homozygote, this affinity difference could potentially be enough to alter the amount of antibody bound to the platelet at any one time, triggering the difference between a strong response and a weak response.

A further consideration around IgG is the length of time the anti-STm antibodies circulate in the body. Figure 3.4 shows donor platelet responses are stable for over a year, which taken in conjunction with Figure 3.13 showing aggregation is dependent on anti-STm specific antibody, suggest that antibody is still present. Generally antibody levels wane over time without repeat exposure, but *in vivo* would quickly be produced again upon re-infection. Therefore, it might not necessarily be expected that enough anti-STm antibody would remain over a period of > 1 year as is implied in the stability of donor responses here. In a study looking at antibodies to STm O-antigen in >1000 individuals, 82% were deemed seropositive, with most of the seronegative responses occurring in those under 18 months of age (Stockdale et al., 2019). However, this study was in Uganda, a population who would be exposed STm at very different levels to the healthy population tested in this thesis, and only covers one point in time. There is little data on the decay profiles of *Salmonella* antibodies in humans. One study has shown that in confirmed STm patients, an STm LPS ELISA (specificity 98% and sensitivity superior than that of the Widal assay, a commonly used test for *Salmonella* in developing countries) showed IgG antibodies present in 57% of individuals after 1 month, reducing to 44%, 31%, and 11% after 3, 6 and 12 months respectively (Strid et al., 2007). To check for cross-reactivity with other antigens, samples from patients with other gastrointestinal illnesses (excluding STm) were tested in the assay. 24% of those with *H. pylori* tested positive for IgG, A or M using the STm LPS assay, as well as 21% of those with *Yersinia enterocolitica,* and 12% of those with *E. coli or Campylobacter* species infections (Strid et al., 2007). Interestingly, in similar tests looking at the STm flagellar H antigen, IgG positivity levels were 61%, 27% and 25% at 1 month, 3 months and 6 months respectively (Dalby et al., 2005). However, this antigen gave much greater cross-reactivity, with samples from those with diagnosed *E. coli, Y. enterocolitica, Campylobacter* species, and *H. pylori* giving IgG positivity values of 50%, 95%, 45% and

80% respectively (Dalby et al., 2005). These results suggest that whilst in some people antibody responses are maintained for over a year after infection, there could be significant cross-reactivity between *Salmonella* H and O antigens and other gut infections. It would be worthwhile carrying out the ELISA used in Figure 3.14 on the samples used in this thesis to look at aggregation over time, to see whether the antibody levels of those particular samples remained stable. Furthermore, delving into the ELISA assay further to begin to establish which parts of the bacteria the antibodies are binding to could help provide information on whether the antibodies are truly *Salmonella* specific, or cross reactive. One way of investigating this could be to use serum pre-absorbed with other bacteria, for example *E. coli,* and see whether this then reduces the level of antibodies measured in the *Salmonella* ELISA assay. This is important to establish, as it has implications for whether the higher levels of antibody required to cause platelet aggregation are only seen in those who have had previous *Salmonella* infection, or are present in people who have had other bacterial gut infections.

One result that caused challenges whilst working on this thesis was the differences in platelet responses depending on the type of preparation used, especially when resuspending platelets in PPP. Figure 3.12 shows that traditional agonists TRAP-6 and CRP cause higher levels of platelet aggregation in PRP than in washed platelets resuspended in Tyrode's buffer. This makes sense due to the additional plasma proteins in PRP, such as fibrinogen, which will enhance the platelet aggregation process. However, upon resuspending platelet pellets in PPP, difficulties begin to emerge, with no or strongly reduced responses seen to TRAP-6, CRP and STm SL1344. Current guidelines state that tests using PRP should not be adjusted to a standard platelet concentration (Cattaneo et al., 2013), as diluting with PPP can artifactually inhibit the platelet aggregation (Cattaneo et al., 2007). The reason for this is not well studied, but has been suggested to have some involvement of ADP, which quickly desensitises the $P2Y_1$ ADP receptor. Normally contained within platelets and red blood cells, ADP is thought to be released during the high speed centrifugation used to obtain PPP, like it can be during shear stress (Alkhamis et al., 1988) . Indeed, a study that looked at the activation of platelets harvested from

different levels of the centrifuge tube found that those closest to the red cell layer were less able to aggregate than those furthest away (Aursnes and Vikholm, 1984). Removal of ADP from the system stopped any inhibition based on proximity to the red cells, suggesting the mechanical stress placed upon the red blood cells was causing release of ADP, leading to desensitisation of the platelets (Aursnes and Vikholm, 1984). Interestingly, the Cattaneo (2007) study that diluted PRP with PPP utilised apyrase to see whether breaking down the ADP helped stop the PPP-induced inhibition, but this only prevented a minor amount of inhibition, suggesting other factors are involved. One of these could be nitric oxide, which is typically released by endothelial cells to prevent unwanted platelet aggregation (Vallance and Chan, 2001). However, it can also be produced by red blood cells upon increased levels of shear and/or mechanical stress (Ulker et al., 2009, Ulker et al., 2011), so could potentially be released by red blood cells during the 1000 g centrifugation to obtain PPP. However, with an *in vivo* half life of just seconds (Thomas et al., 2001), increasing up to ~500 seconds *in vitro* (Hakim et al., 1996), it is debatable whether this would last long enough in PPP to have any effect on the platelets. Regardless of the mechanism, Figure 3.12 clearly shows that resuspending washed platelets made with the normal washed platelet prep in PPP does not allow any significant platelet aggregation to occur upon stimulation with the agonists tested. However, upon isolating the platelets using an ADP-sensitive preparation and then resuspending in PPP, a better aggregation response is seen, especially with stimulation by CRP, which gave results analogous to those in PRP. There are multiple reasons why this could be. Firstly, after the spin to obtain PRP, the ADP-sensitive preparation has only one more centrifugation step compared to two in the normal preparation, and this step is at 50% lower speed compared to the normal preparation. This gentler preparation will naturally help the platelets desensitise less. The wash step/s are also different – in the ADP sensitive preparation the pellet is not resuspended, rather the surface is gently washed instead. Again, this more gentle protocol exerts less force on the platelets, reducing chances of desensitisation. Finally, both the wash and resuspension buffer, or PPP, if that is being used to resuspend, have the addition of 0.01 U/ml grade VII apyrase. If

any of the centrifugation steps are causing the release of extra ADP from red blood cells, then this apyrase can break down the ADP, stopping the desensitisation of the platelets. When optimising the ADP-sensitive protocol preparation, two different grades of apyrase were used – grade III, at 0.05 U/ml, and grade VII, at 0.01 U/ml. Platelet aggregation was only observed when using the grade VII apyrase, likely because the grade III apyrase has a 10x larger ATPase to ADPase ratio than the grade VII, making grade III more potent in ATPase activity, and grade VII more potent in ADPase activity (Vigne et al., 1998). Unfortunately, the Cattaneo paper (2007) does not state which grade of apyrase was used, but it would perhaps explain the lack of rescue observed using apyrase if it was grade III.

In comparison to the results of Arman et al (2014), who tested the ability of Gram positive bacteria *S. sanguinis, S. aureus, S. gordonii, S. oralis* and *S. pneumoniae* to aggregate platelets, the findings in this thesis for STm aggregation have multiple differences. Firstly, in Arman et al. (2014), aggregation occurred upon addition of 100µg/ml hIgG in 4/5 strains tested in washed platelets, which I was unable to carry out successfully with STm. Interestingly, for the fifth strain tested, *S. pneumonia,* aggregation was unsuccessful in 3/5 donors upon addition of hIgG and fibrinogen, either suggesting another plasma component is involved, or perhaps that the level of antibody against *S. pneumoniae* in the hIgG was on the borderline for causing aggregation. I hypothesise that with *S. oralis, S. gordonii, S. aureus* and *S. sanguinis* being commensal microbes, sufficient levels of antibodies against them were found in the pooled hIgG. For *S. pneumoniae*, whilst it can be commensal, one paper estimated nasal carriage prevalence at just 2.9% in a study throughout nine european countries (Yahiaoui et al., 2016), meaning it is likely that there were significantly fewer anti-*S. pneumoniae* antibodies in the hIgG than for the other bacteria. It follows that with *Salmonella* not being commensal, and not routinely frequently encountered in western countries, that levels of anti-*Salmonella* antibody in the hIgG could be minimal, meaning the antibody levels in the pooled hIgG were insufficient to allow aggregation.

Furthermore, in the Arman paper, for 3/4 bacteria that activated washed platelets, addition of fibrinogen as well as hIgG was able to reduce the lag time and increase maximum aggregation levels compared to using hIgG alone. For STm, fibrinogen addition did not have as large an affect as for *S. aureus, S. gordonii* and *S. oralis*, but this is likely because the dose of 100µg/ml STmIgG used already caused swift, maximal aggregation, not leaving enough room for fibrinogen to enhance the response. I propose that by adding fibrinogen when lower doses of STmIgG are used, such as <25µg/ml, fibrinogen would be more likely to have an enhancing effect. Alternatively, it could be that the fundamental structural differences in cell structures of Gram positive and Gram negative bacteria are causing these differences.

Finally, Arman et al showed that addition of PF4 to the washed platelet assay reduced the lag time observed, along with the addition of low dose heparin to PRP, showing PF4 was able to modulate the bacterial-induced platelet aggregation, something I did not observe with STm. Again, it could be due to the structural differences between Gram positive and negative cell walls, or that if using the STmIgG at lower doses, perhaps PF4 would be able to enhance the non-maximal responses seen. This would fit with the data in Figure 3.19 that shows inhibition of responses with high dose heparin, which could be binding the PF4 and scavenging it away from the bacteria, reducing aggregation responses. However, the results of the PF4-IgG ELISA in Figure 3.21 appear to contradict this. With 12/13 donors not having detectable IgG antibodies to the neoepitopes produced when PF4 binds polyanions, how could PF4 be enhancing the aggregation? The 7.7% positivity rate for anti-PF4 IgG antibodies in my donor population mirrors that seen in larger studies, with 6.6% positivity for total IgGAM in a study of 3795 healthy donors (Hursting et al., 2010) and 6.1% IgG positivity in a study of 4029 healthy donors (Krauel et al., 2011). The proposition by Greinacher is that PF4 binding to bacteria allows antibodies to recognise the negative charge, allowing activation of the adaptive immune system before specific anti-bacterial antibodies have been made. Therefore, if 95% of the general population do not have these when measured in the anti-PF4 ELISA, it is difficult to understand how PF4 could be reducing platelet

lag times *in vitro* as seen in Arman et al. Interestingly, Buka et al (2024) showed PF4 alone can activate platelets in a donor dependent manner at doses of 10 μg/ml and above. Arman et al used 20 μg/ml PF4, so the decreased lag time observed could be due to the effects of PF4 directly. There could also be other mechanisms, or other changes that happen to the bacteria upon binding to PF4 that enhance the aggregation which have not yet been discovered.

The use of STm 14028 O-antigen mutants showed that aggregation responses generally change from strong to weak upon deletion of most or all of the O-antigen repeats. However, all donors were still able to respond weakly to the strains with no O-antigen. Research into the role of LPS in platelet aggregation assays has shown that whilst LPS is unable to cause platelet aggregation on its own (in both PRP and washed platelets), it can enhance aggregation responses to subthreshold levels of common agonists such as thrombin, CRP and U46619 (Koessler et al., 2019, Zhang et al., 2009, Lopes Pires et al., 2017). This appears to fit with the 14028 mutant results – in the majority of donors, without the O-antigen, STm could induce a small amount of aggregation. This could be caused by other surface proteins on the STm membrane, where perhaps the copy number is not high enough to trigger full aggregation. With the aid of the O-antigen however, this initial small amount of aggregation could be being enhanced to give the strong aggregation seen to the WT 14028 in most donors. Interestingly, using the Δ*tolR* mutant, which causes membrane instability leading to the release of many outer membrane vesicles (OMVs), caused the aggregation lag times to reduce. The OMVs could potentially be providing more opportunities or surface-area for antibody-antigen complexes to cross-link FcγRIIA.

To conclude, this chapter has shown that STm can induce platelet aggregation in a donor dependent manner, related to the amount of anti-STm antibody an individual has. However, there are limitations in the methods carried out here. Firstly, aggregation assays are inherently non-physiological. Only involving platelets and (sometimes) plasma removes the important contributions of other blood cells. For example, neutrophil extracellular traps (NETs) are known to affect platelet aggregation and

thrombus formation (Zhou et al., 2022). In the STm mouse model, NET markers are seen in thrombi, (Beristain-Covarrubias et al., 2019a), and *in vitro,* mouse neutrophils form NETs upon the addition of STm (M. Perez-Toledo, 2023, personal communication, 23 November), but the impact of neutrophils are excluded during aggregation experiments. Whilst stirring is carried out, aggregations do not accurately mirror the effects of shear stress in the blood vessel, and any interactions with endothelial cells are missed. Furthermore, in order to see aggregation, a standard dose of $1 \times 10^8$ CFU was used, and whilst this was able to be reduced to $3.3 \times 10^7$ CFU in Figure 3.22, and is in line with the magnitude of doses used in other bacterial aggregation studies, this is still a very high dose compared to what would be seen *in vivo.*

Therefore, in order to more physiologically model the effects of STm on platelets, I carried out blood flow experiments over endothelial cells whilst on placement at the Royal College of Surgeons in Ireland. This work is detailed in the next chapter.

# CHAPTER 4: *SALMONELLA* IN THE VASCULATURE: INTERACTIONS BETWEEN LIVE BACTERIA, ENDOTHELIAL CELLS AND PLATELETS

## 4.1 Introduction

While the last chapter focussed on the interactions between STm and platelets alone under the stirring conditions of an aggregometer, in the blood stream STm will come into contact with white and red blood cells, as well as the endothelial cells (ECs) lining the blood vessel. Furthermore, all of these take place in the context of the shear stress exerted by the blood flow through the vessels.

### 4.1.1 Pathogen-endothelial cell interactions

The barrier formed by ECs is vital in regulating homeostasis, with problems quickly arising upon disruption of this barrier. For example, leakage via damaged vascular barriers can cause oedema, a telling feature of sepsis (Goldenberg et al., 2011). In healthy ECs, the expression of VE-cadherin is critical for prevention of vascular leakage and leukocyte emigration. However, movement of VE-cadherin from the endothelial cell membrane to the cell interior leads to gaps between cells, increasing vessel permeability (Lee and Slutsky, 2010).

*In vitro* models of infective endocarditis (inflammation of the endothelial lining inside the heart) have allowed the effects of bacterial binding to human aortic endothelial cells (HAoECs) to be characterised at the protein level. *S. aureus, E. coli* and SARS-CoV-2 can all cause internalisation of HAoEC VE-cadherin leading to increased endothelium permeability and cell apoptosis (McDonnell et al., 2016, McHale, 2018, Nader et al., 2021). The integrin αvβ3 has been identified as a key binding protein for these interactions, with *S. aureus* clumping factor A protein able to bind αvβ3 using fibrinogen as a bridging molecule (McDonnell et al., 2016). Expression of αvβ3 is significantly increased when ECs are exposed to TNF-α, as they would be during the inflammatory response to the bacteria, further increasing bacterial binding. Similar findings have been shown in *E. coli,* for which OmpA is the key

protein that adheres to αvβ3 (McHale et al., 2018), and SARS-CoV-2, which likely binds αvβ3 via its spike RGD motif (Nader et al., 2021, Nader and Kerrigan, 2022).

The interaction of pathogens with ECs affects vessel homeostasis in multiple ways: the binding to EC receptors can activate the cells, leading to secretion of granules and cytokines, and it can also cause apoptosis of the cells, leading to gaps in the endothelium and vessel leakage (Kerrigan et al., 2019). Both of these results can cause platelet aggregation and secretion (or indeed enhance platelet activation already triggered by pathogen-platelet interactions). For example, secretion of EC Weibel-Palade bodies results in VWF deposits on the cell surface, engaging platelets and leading to thrombus formation. Furthermore, EC apoptosis and cell-cell detachment leads to exposure of the subendothelial matrix, where components such as collagen, fibronectin and tissue factor also trigger platelet aggregation and thrombus formation/stabilisation.

### 4.1.2 Pathogen-platelet interactions under flow conditions

In the previous chapter, platelet aggregation was measured with stirring at 1200 rpm, but this does not mimic the shear stress forces found in the blood vessels. Levels of shear stress have been shown to affect platelet bacterial interactions: for example, at shear rates of <500 $s^{-1}$, platelets do not interact with *S. aureus,* but at >800$s^{-1}$ aggregates form rapidly (Kerrigan et al., 2008). In the case of *S. oralis*, single platelets are able to adhere to the immobilised bacteria at shear rates of 50$s^{-1}$, with the number of platelets interacting increasing at shear rates increase. At higher shear rates (200$s^{-1}$ and 800$s^{-1}$), platelet microaggregates are able to form (Tilley et al., 2013).

### 4.1.3 Chapter aims

Taking into account the impact shown above of ECs and flow conditions, the aim of this chapter was to explore the platelet-*Salmonella* interactions observed in chapter 3 under more physiologically relevant conditions, to:

a) Identify whether *Salmonella* can interact with ECs, and explore possible plasma and/or bacterial components involved in the interaction
b) Investigate platelet interactions with *Salmonella* under venous and arterial flow conditions
c) Investigate platelet interactions with *Salmonella*-primed ECs under flow conditions

This work was carried out on a 3.5 month placement in the lab of Prof Steve Kerrigan at the Royal College of Surgeons in Ireland. It was funded through a grant from Boehringer Ingelheim supported by the University of Birmingham.

## 4.2 Results

### 4.2.1 Investigating the interactions between *Salmonella* and endothelial cells

#### 4.2.1.1 Plasma increases binding between endothelial cells and *Salmonella*

Many pathogens are known to interact with the endothelium upon systemic infection, including *Bartonella* species, *Candida albicans* and *S. aureus* (Obino and Duménil, 2019, McDonnell et al., 2016). In the Kerrigan lab, work focusses on bacterial-EC interactions relevant to infective endocarditis, using human aortic endothelial cells (HAoECs). To assess whether interactions occur between STm and HAoECs a binding assay was carried out. Briefly, this involved plating bacteria, adding static HAoECs on top, leaving to adhere, and washing off unbound cells. Remaining bound HAoECs were then lysed and a colorimetric substrate used to measure relative EC levels.

As shown in Figure 4.1A, *S. aureus,* (chosen as a positive control due to being well characterised and commonly used by the Kerrigan lab) binds well to the tissue culture plates used in the lab protocol. However, STm SL1344 failed to bind well to these plates, with the majority of bacteria washing off. To solve this issue, the assay was attempted using different types of plate. Nunc Maxisorp plates were chosen for use going forward as they provided a surface to which the STm SL1344 bound to a comparable level to *S. aureus* (Figure 4.1A).

Previous work from the Kerrigan lab using sheared HAoECs showed binding between *S. aureus* and HAoECs is increased when the HAoECs are treated with TNF-α and platelet poor plasma (PPP) (McDonnell et al., 2016). As seen in Figure 4.1B, STm SL1344 binds to the HAoECs, but binding levels are not increased upon treating the HAoECs with TNF-α. However, the presence of PPP led to a significant increase in binding, with almost double the amount of HAoECs attaching to the STm. To assess which components of plasma were important in mediating the increase, assays were carried out using physiological levels of fibrinogen or pooled human IgG in place of plasma. Both were able to cause binding to a similar level as the whole plasma (Figure 4.1C). However, it must be noted that

fibrinogen preparations can be contaminated with IgG (S.W. Kerrigan, 2022 personal communication, 21 October) making it difficult to assess whether the result seen for fibrinogen is due to fibrinogen itself, or unwanted IgG present in the product.

#### 4.2.1.2 Binding between *Salmonella* and endothelial cells remains consistent between lab and clinical strains and is unaffected by Omp knock-outs

With the knowledge that plasma increases binding between STm SL1344 and HAoECs, the assay was used to investigate the binding of further *Salmonella* strains. As used in chapter 3, the lab attenuated 'grand-daughter' strain of SL1344, SL3261, was tested, along with the invasive clinical isolate D23580. A further clinical isolate, a *Salmonella* Enteritidis strain (D24964) was also tested. There were no significant differences in binding between the four strains (Figure 4.2A).

In the case of *E. coli*, knocking-out the outer membrane protein A (OmpA) significantly reduced the ability of the bacteria to bind to HAoECs (McHale et al., 2018). To assess whether this was true of STm-HAoEC interactions, the available SL1344 Omp knock-out strains, OmpA, OmpD and OmpR, were used. OmpA has roles in protecting from host-induced stress, therefore aiding the virulence of *Salmonella* (Chowdhury et al., 2022), OmpD is the most abundant STm porin (Ipinza et al., 2014), and OmpR is involved in the regulation of the type III secretion system (Lee et al., 2000) and acid tolerance (Bang et al., 2000). None of the knock-outs showed any significant difference in binding compared to the wild type STm SL1344 (Figure 4.2B).

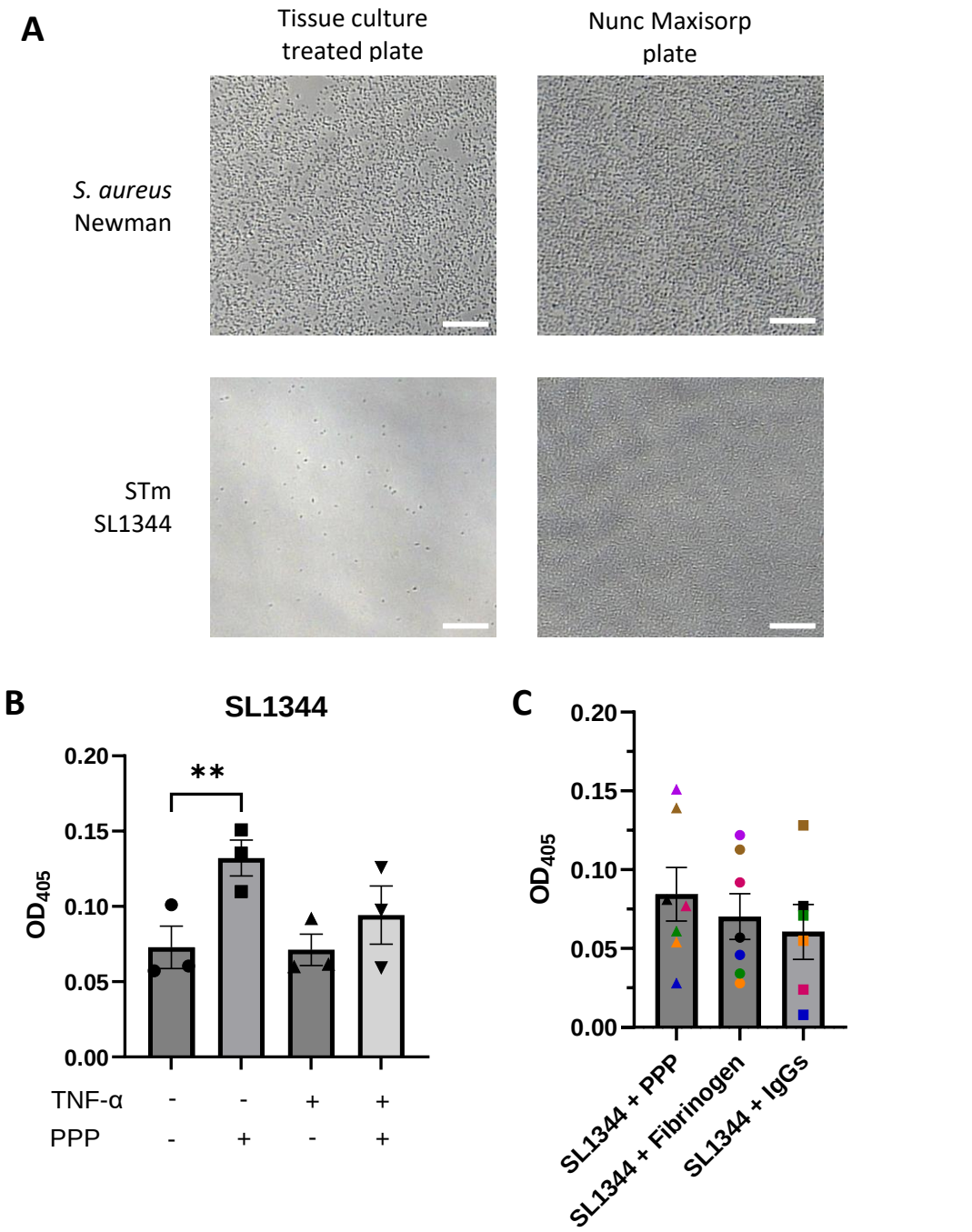


**Figure 4.1: Plasma increases binding between endothelial cells and *Salmonella*** A) Optimisation of binding assay. 1 x $10^7$ CFU *S. aureus* or 1 x $10^8$ CFU STm SL1344 were added per well. Bacteria were incubated at 37°C for 2 hours to adhere to plate, before 3x PBS washes. Images were taken after PBS washes to assess bacterial binding. Scale bar = 40µm. n =1. B) 1 x $10^8$ STm SL1344/well were seeded and incubated at 37°C for 2 hours to adhere, with an additional 30 minute incubation with PPP where indicated. Where indicated, endothelial cells were incubated with 10 ng/µl TNF-α for 4 hours at 37°C. 2.5x$10^4$ endothelial cells/well were added to the bacterial wells and incubated for 2 hours to allow adherence. Unbound cells were washed off, pNPP lysis buffer was added and incubated for 2 hours, before plate was read at 405nm as a measure of relative levels of endothelial cells bound to the bacteria. C) As B, with bacteria either incubated for 30 minutes with PPP, 4mg/ml fibrinogen or 0.1mg/ml pooled human IgG. n ≥ 6. Colours show different biological repeats (each average of 3 technical repeats) Bar = mean ± SEM (each point is average of 3 technical repeats). ** = $p < 0.005$, one-way repeated measures ANOVA with Dunnett's multiple comparisons test.

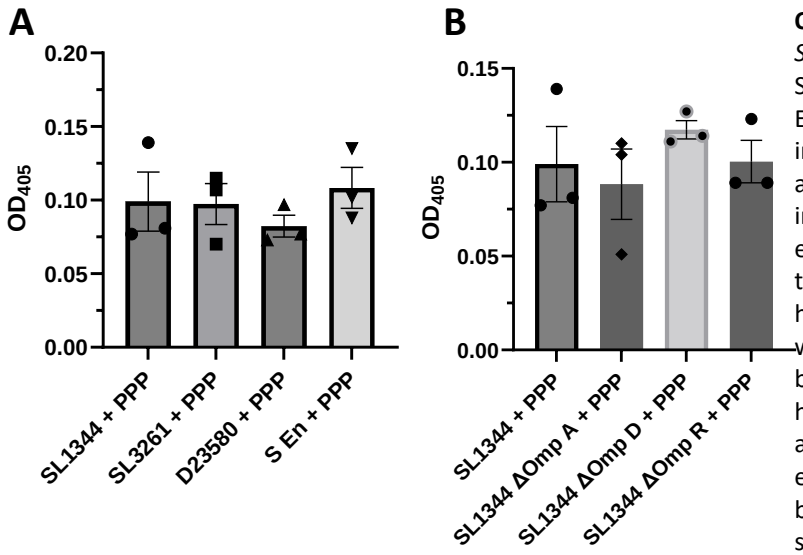


**Figure 4.2: Binding between *Salmonella* and endothelial cells remains consistent between lab and clinical strains and is unaffected by Omp knock outs.** A) ~1 x $10^8$ *Salmonella* (STm strains = SL1344, SL3261 and D23580; S En = *Salmonella* Enteritidis D24954) were seeded and incubated at 37°C for 2 hours to adhere, followed by 30 minutes incubation with PPP. 2.5x$10^4$ endothelial cells/well were added to the bacterial wells and incubated for 2 hours to allow adherence. After washing off unbound cells, pNPP lysis buffer was added and incubated for 2 hours, before plate was read at 405nm as a measure of relative levels of endothelial cells bound to the bacteria. B) As A, with all bacterial strains different Omp knock-outs of SL1344. n = 3. Bars = mean, ± SEM (each point is average of 3 technical repeats).

### 4.2.1.3 *Salmonella* infection causes breakdown in endothelial cell junctions

When culturing HAoECs, cells can be sheared to mimic the physiological conditions of blood vessels (McDonnell et al., 2016). Staining for adherens protein VE-cadherin highlights the different characteristics HAoECs exhibit when grown statically or under shear stress at 10 dyn/cm$^2$ for 24 hours. Statically grown HAoECs appear in random orientations, with a lack of VE-cadherin expression (Figure 4.3Ai), whereas sheared HAoECs align in the direction of flow, elongate, and upregulate their VE-cadherin expression (Figure 4.3Aii,iii). These characteristics allow the endothelium to form a continuous barrier, vital for normal blood vessel function.

Upon infection, the endothelial barrier can be damaged. For example, infecting HAoECs with multiplicity of infection (MOI) 400 *S. aureus* for 24 hours leads to reduced VE-cadherin staining, an increase in cell detachment and increase in permeability (McDonnell et al., 2016). The same was also reported when infecting with SARS-CoV-2 (MOI 0.4) (Nader et al., 2021, Nader and Kerrigan, 2022).

To test whether STm could induce similar effects, HAoECs were pre-treated with PPP, followed by MOI 10 or MOI 40 for 2 hours. At MOI 10, breakdown of the endothelial barrier can be seen, with gaps appearing between the cells, and the loss of the clear elongated cell morphology (Figure 4.3Bii). At MOI 40, as well as gaps, reduced expression of VE-cadherin at the cell periphery can be observed (Figure 4.3Biii).

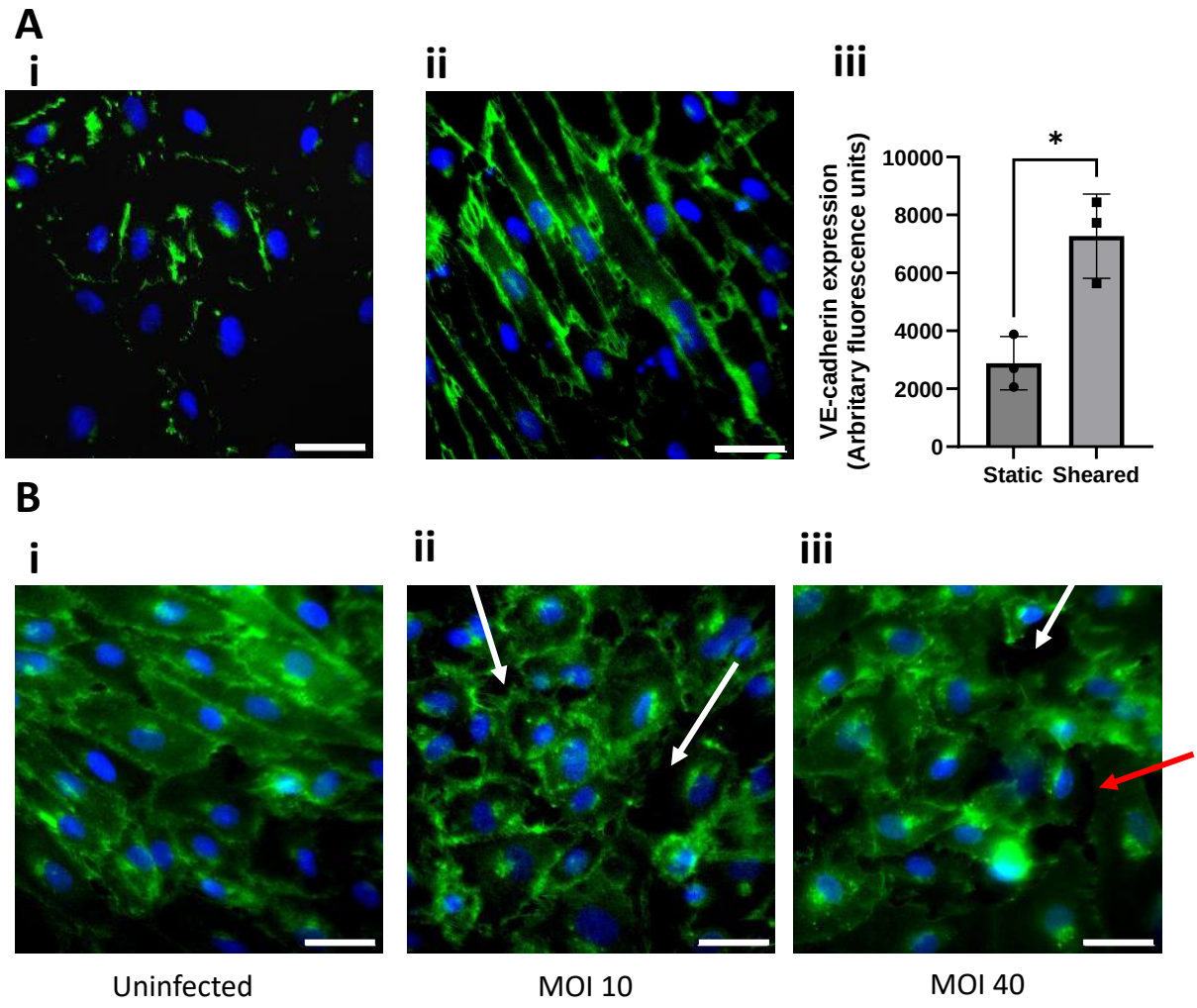


**Figure 4.3: *Salmonella* infection causes breakdown in endothelial cell junctions.** Immunofluorescence of human aortic endothelial cells (HAoECs) stained for VE-cadherin (green) and DNA (blue). Ai) Staining of static HAoECs. Aii) Staining of HAoECs sheared at 10 dyn/cm$^2$ for 24 hours. Aiii) Quantification of VE-cadherin staining carried out in Image J. t-test carried out, * = $p < 0.05$. Bi) HAoECs sheared at 10 dyn/cm$^2$ for 24 hours then treated with PPP for 30 minutes. Bii) As per i, with HAoECs incubated with multiplicity of infection (MOI) 10 of STm SL1344 for 2 hours prior to staining. Biii) As per ii, with MOI 40. Scale bars = 40µm. White arrows show gaps appearing between the ECs. Red arrow shows lack of VE-cadherin staining at cell periphery. Representative images from n = 3.

### 4.2.2 Investigating platelet adhesion to *Salmonella* under physiological flow conditions

#### 4.2.2.1 Optimising assay conditions for whole blood flow over *Salmonella*

To assess the binding of platelets to STm under flow conditions, Ibidi chambers were coated with STm, and blood containing $DiOC_6$ stained platelets was flowed across at a shear rate of $275s^{-1}$, representing venous shear. However, despite using the same concentration of $DiOC_6$ for platelet staining as in previously published assays with *S. aureus* (Kerrigan et al., 2008) and *S. oralis* (Tilley et al., 2013), it was unclear whether the staining seen in preliminary tests was platelet-specific. To test this, $DiOC_6$ in PBS was flowed over STm SL1344, which showed ~50% of the STm were taking up the dye (Figure 4.4A), rendering it unsuitable for use as a platelet stain.

Instead, the fluorescent probe Near Infrared BF2-azadipyrromethene (NIR-AZA) was used to stain the platelets. This dye non-specifically binds to plasma membrane and cytosol (Fitzpatrick et al., 2022), and once taken up is prevented from crossing back out over membranes due to its poly(ethylene-glycol) group. Figure 4.4B shows whole blood containing NIR-AZA stained platelets flowed over STm SL1344, and it is clear that with this dye the STm remain unstained, so NIR-AZA was used to stain platelets for all future assays.

It is worth noting that the work in Figure 4.4 was being carried out in parallel to that of section 4.2.1.1 (Figure 4.1A), optimising the plate surfaces for the binding of STm SL1344. Similarly to the static assay, the Ibidi chambers used initially were tissue culture treated, which STm SL1344 did not bind well to, hence the sparse bacterial coverage in Figure 4.4. For future experiments with STm, uncoated Ibidi chambers were used, which provided improved bacterial coverage.

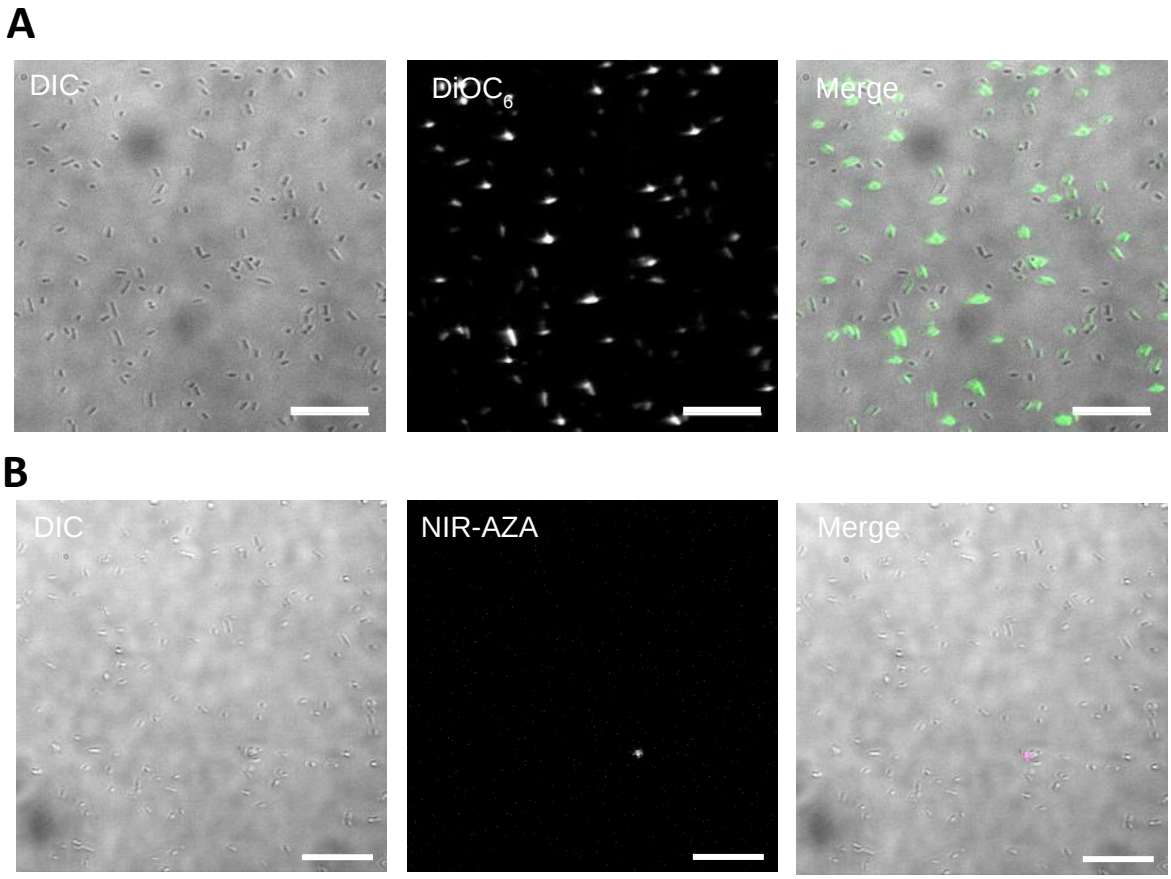


**Figure 4.4: Optimising assay conditions for whole blood flow over *Salmonella.*** A) ~5 x $10^6$ CFU STm SL1344 were used to coat IbiTreat µ-slide chamber. PBS with 1µM $DiOC_6$ was flowed over at $275s^{-1}$ for 1 minute before washing with PBS and imaging. B) As A, but this time whole blood stained with 5µM NIR-AZA was flowed over STm. Scale bars = 20µm. n = 1.

#### 4.2.2.2 Platelets adhere to immobilised *Salmonella* under venous shear

With the plastic surface for STm adhesion and the platelet stain issues resolved, assays were carried out flowing platelet-stained whole blood over STm at venous shear. Platelets did not adhere to the BSA-blocked control surface (Figure 4.5A), but did adhere to STm SL1344 (Figure 4.5B), with the number of platelets interacting increasing as time went on (Figure 4.5C). By 200-300s, microaggregates had begun to form (Figure 4.5B). Interestingly, it was observed that platelets were able to roll along the STm surface, before either adhering, or being carried out through the flow system. This is demonstrated in Figure 4.5D, where the yellow circle highlights well-adhered platelets, and the red circle highlights a slow rolling platelet that appears in the field of view, rolls and then disappears from the field of view over the course of 50 s.

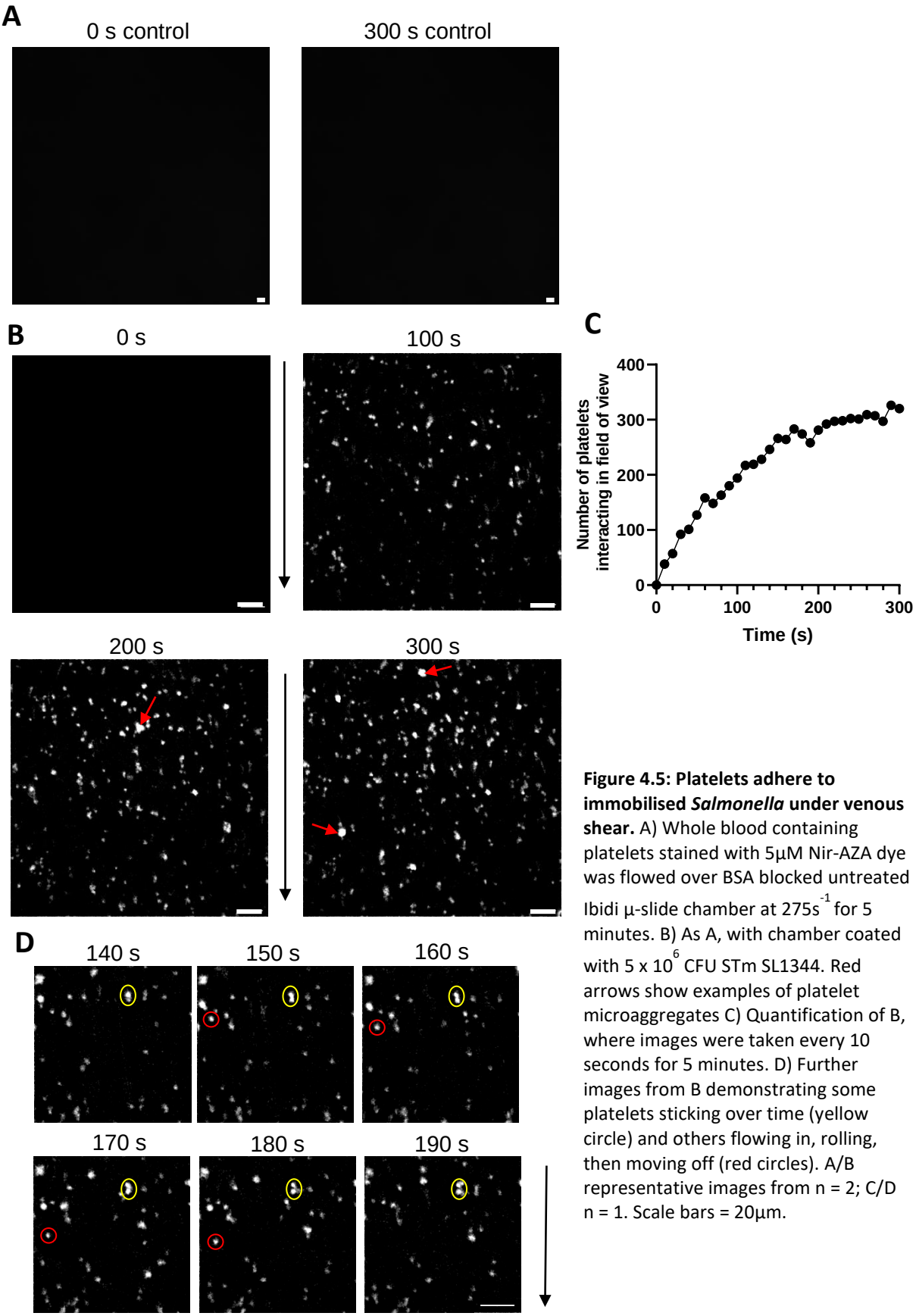


**Figure 4.5: Platelets adhere to immobilised *Salmonella* under venous shear.** A) Whole blood containing platelets stained with 5µM Nir-AZA dye was flowed over BSA blocked untreated Ibidi µ-slide chamber at $275s^{-1}$ for 5 minutes. B) As A, with chamber coated with $5 \times 10^6$ CFU STm SL1344. Red arrows show examples of platelet microaggregates C) Quantification of B, where images were taken every 10 seconds for 5 minutes. D) Further images from B demonstrating some platelets sticking over time (yellow circle) and others flowing in, rolling, then moving off (red circles). A/B representative images from n = 2; C/D n = 1. Scale bars = 20µm.

#### 4.2.2.3 Unidentified cells adhere to immobilised *Salmonella* under venous shear

Whilst carrying out the experiments in section 4.2.2.2, it was noted that cells other than platelets were binding to the STm. Figure 4.6A shows the cells whilst PBS was being run through the system (to allow easier distinction between cells that are adhered and cells that are flowing over the top). In order to identify these cells, the PBS was spiked with DAPI. The adhered cells did not stain with DAPI, perhaps suggesting they are red blood cells. Figure 4.6B shows the unidentified cells without shear forces being exerted. Measuring these cells gives an average diameter of approximately 6.9µM, in keeping with the diameter of red blood cells (Hoffbrand and Steensma, 2019).

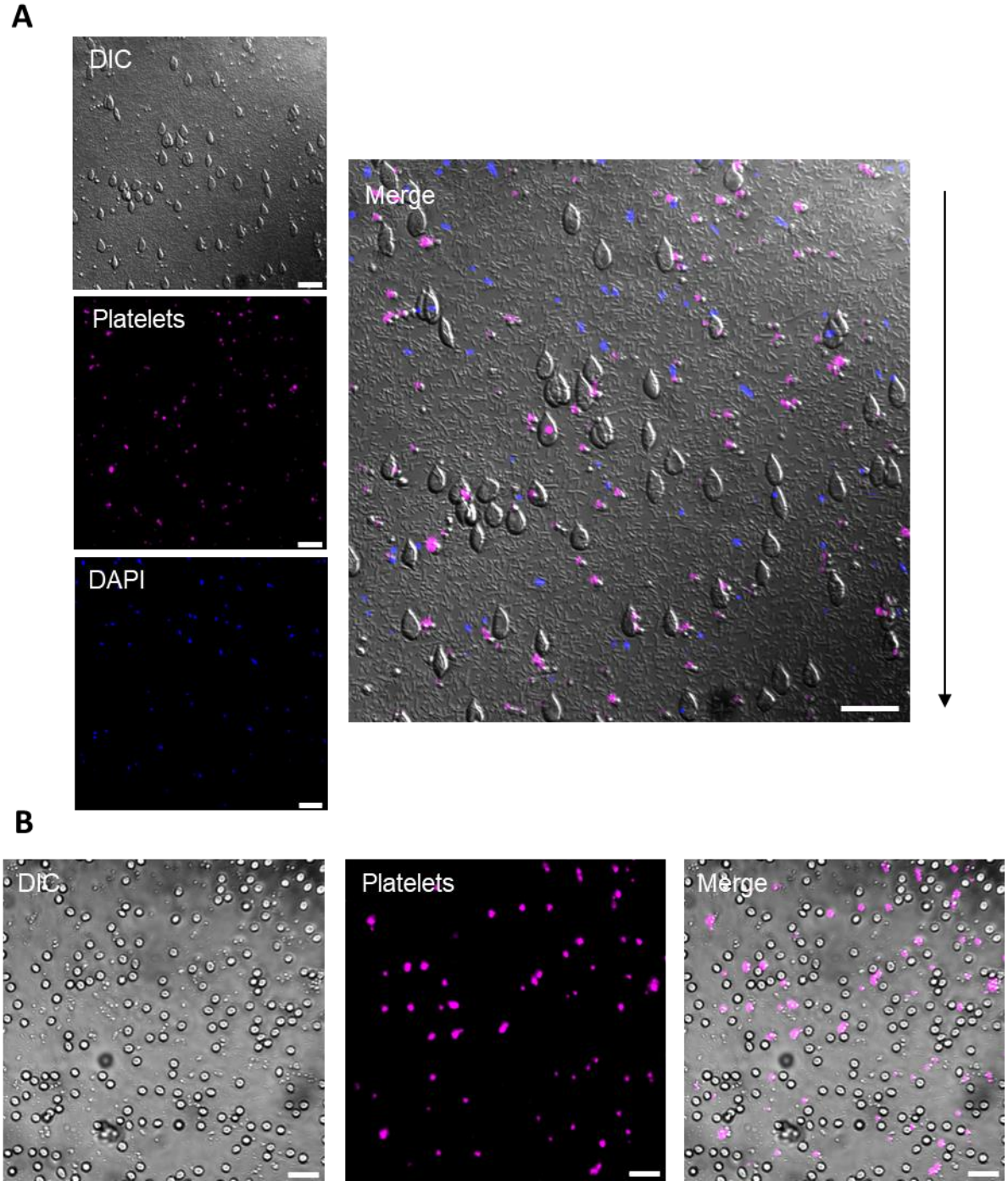


**Figure 4.6: Unidentified cells adhere to immobilised *Salmonella* under venous shear**. A) Untreated Ibidi µ-slide chambers were coated with 5 x $10^6$ CFU STm SL1344. Whole blood containing platelets stained with 5µM NIR-AZA was flowed over at $275s^{-1}$ for 5 minutes. PBS spiked with DAPI stain was flowed through to wash, and images taken whilst PBS flow was continuing for clarity as to which cells were bound. B) As per A, with images taken after PBS wash, with no flow force. Scale bars = 20µm. Images are representative from n = 2.

### 4.2.3 Investigating platelet adhesion to *Salmonella* primed endothelial cells under flow

#### 4.2.3.1 Platelets adhere to *Salmonella* primed endothelial cells at venous shear

Sections 4.2.1.1 and 4.2.2.2 have shown that in static experiments, STm can interact with HAoECs, and under flow platelets can interact with STm. The next experiments were designed to investigate the next step in complexity, assessing the three components in the same system.

Preliminary experiments used the platelet-stained whole blood spiked with mCherry labelled STm SL1344, but little platelet activation was seen. Instead, the approach taken was to prime the HAoECs with STm*,* by flowing STm in PBS over the cells for 2-3 minutes. Any unbound STm was then washed away, before whole blood was flowed through, washed, and imaged.

As shown in Figure 4.7 (top two panels), at venous shear rates, when the HAoECs are not primed with STm*,* few platelets adhere to them. Flowing through mCherry labelled STm confirms visually the results in Figure 4.1, showing binding interactions between HAoECs and STm (Figure 4.7, bottom two panels, *Salmonella*). After this priming with STm*,* when whole blood is flowed through, platelet adhesion increases, with many single platelets seen adhering to the HAoECs (Figure 4.7, bottom two panels). Some microaggregates have formed, as indicated by the white arrows in the figure. Therefore, not only can STm bind to HAoECs under venous shear, the results of this interaction are able to cause platelet activation, leading to microaggregate formation on the HAoECs.

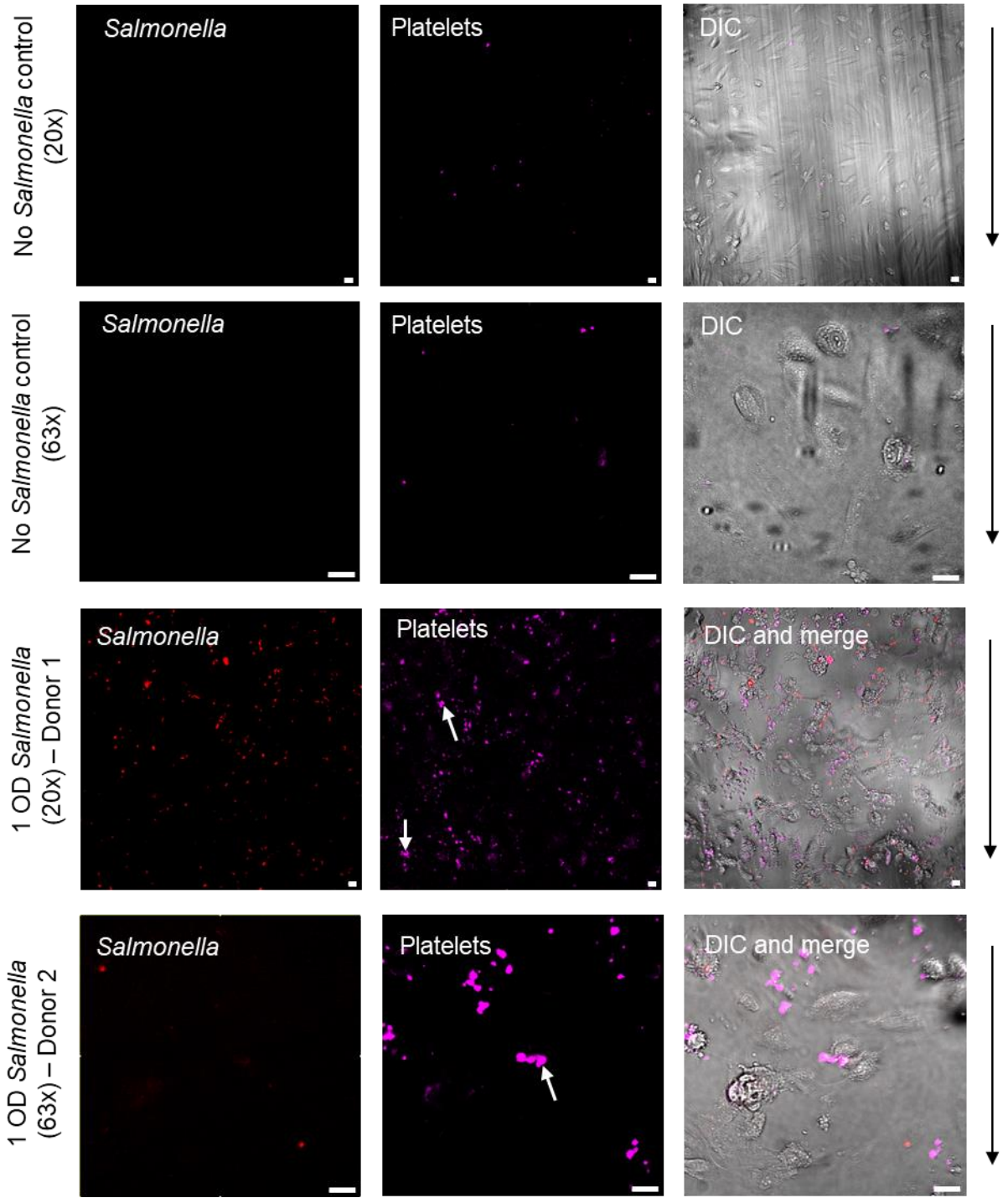


**Figure 4.7: Platelets adhere to *Salmonella* primed human aortic endothelial cells at venous shear.** IbiTreat µ-slides were coated with 80,000 sheared HAoECs per channel. Where indicated, 1 OD (1 x $10^8$ CFU/ml) STm mCherry SL1344 was flowed across HAoECs at $275s^{-1}$. After washing out unbound bacteria, whole blood containing platelets stained with 3.3µM NIR-AZA was flowed over at $275s^{-1}$ for 5 minutes. Unbound cells were washed using PBS and images taken. Scale bars = 20µm. Images representative of n = 3.

#### 4.2.3.2 Platelets adhere to *Salmonella* primed endothelial cells at arterial shear

To test whether interactions were different at higher shear rates, the same experiment was performed with blood flowed at a shear rate of $800s^{-1}$, representative of arterial shear. Similarly to the observations at venous shear, without STm priming, few platelets were able to firmly adhere to the HAoECs (Figure 4.8, top two panels). Interestingly, at the higher shear rate, less of the STm remain adhered to the HAoECs (Figure 4.8, bottom two panels, *Salmonella*), with most washing out, suggesting the binding strength between the two was not strong enough to withstand the higher shear forces. Platelets were still able to bind to the HAoECs, but tended to be arranged in vertical lines aligned with the direction of flow (Figure 4.8, bottom two panels). While these results show differences at venous and arterial rates of flow, the results cannot be directly compared as the arterial flow assay was carried out for three minutes compared to five minutes for venous flow due to the greater amount of blood required.

#### 4.2.3.3 Platelets adhere at sites distal to bacteria at both venous and arterial shear

The 63x images shown in Figure 4.7 and 4.8 show that the platelets are adhering to the HAoECs at sites distal to bound STm at both arterial and venous rates of shear, rather than to the bacteria themselves (Figure 4.9). This is an interesting finding, as chapter 3 shows that STm is able to cause platelet aggregation due to indirect interactions, and Figure 4.5 shows platelets binding to STm under flow, but here we observe the platelets appear to preferentially bind to the primed HAoECs compared to the STm. The images also reveal possible areas of improvement for the assay, with examples of unstained platelets highlighted in white circles, and an example of an unadhered and/or possibly apoptotic HAoEC circled in blue (Figure 4.9). Solutions to these problems are explored in the Discussion.

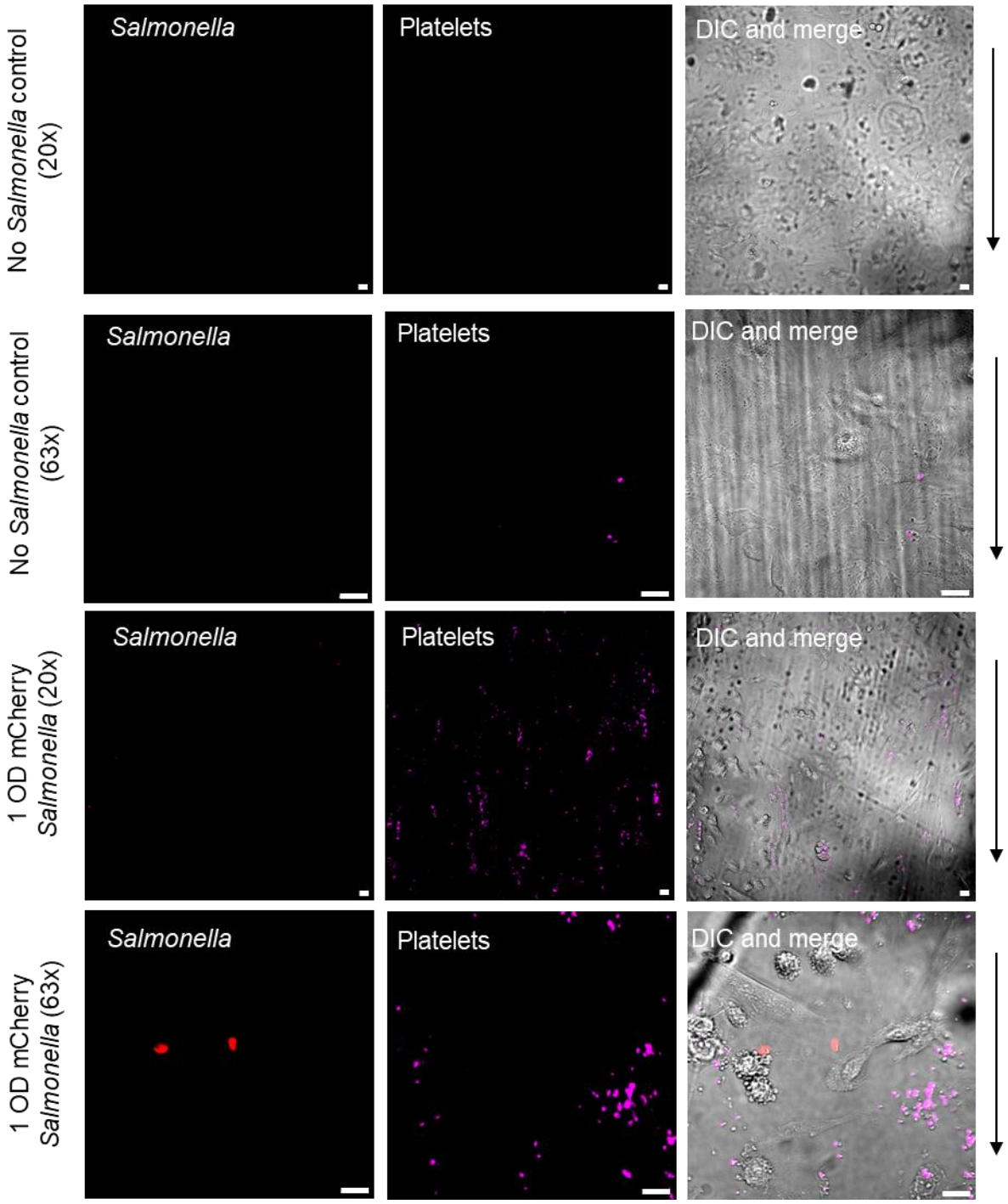


**Figure 4.8: Platelets adhere to *Salmonella* primed human aortic endothelial cells at arterial shear.** IbiTreat µ-slides were coated with 80,000 sheared HAoECs per channel. Where indicated, 1 OD (1 x $10^8$ CFU/ml) STm mCherry SL1344 was flowed across HAoECs at $275s^{-1}$. After washing out unbound bacteria, whole blood containing platelets stained with 3.3µM NIR-AZA was flowed over at $800s^{-1}$ for 3 minutes. Unbound cells were washed using PBS and images taken. Scale bars = 20µm. Images representative of n = 2.

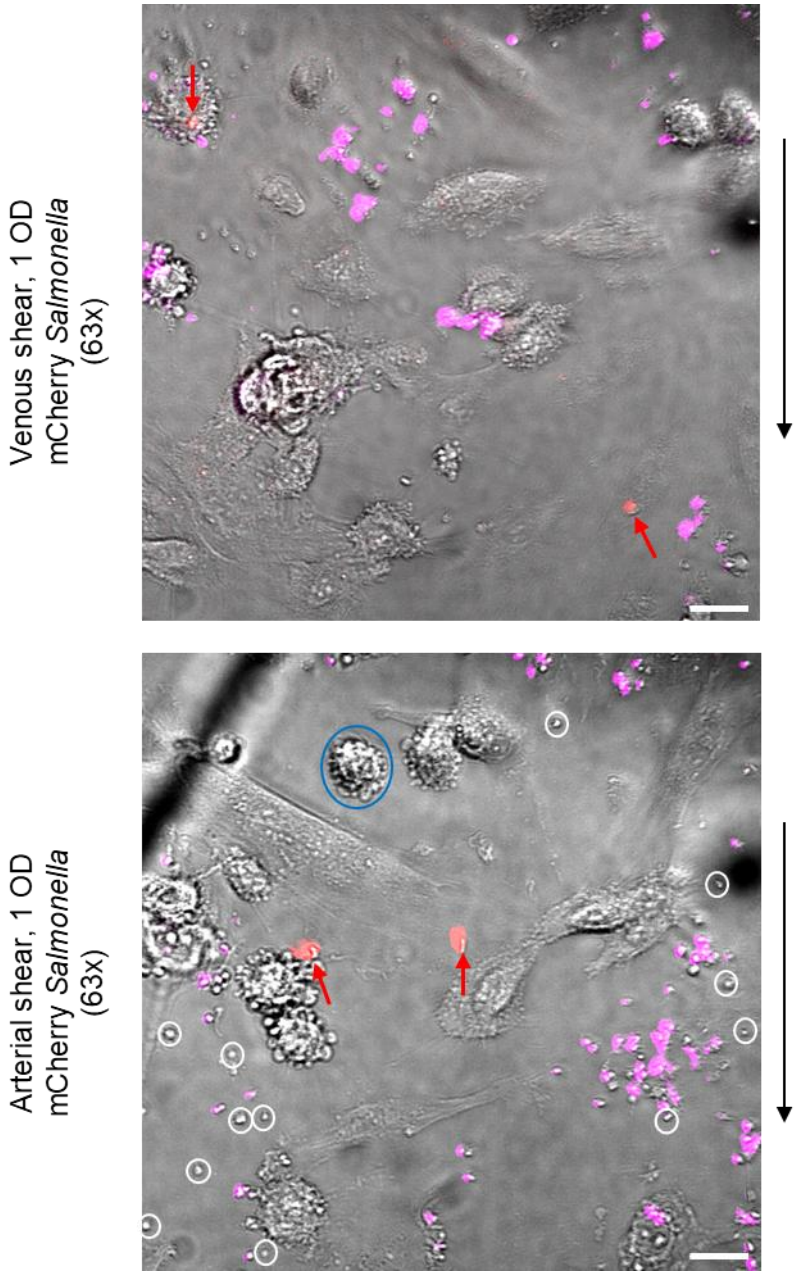


**Figure 4.9: Platelets adhere at sites distal to bacteria at both venous and arterial shear.** Enlarged images from Figures 4.7 and 4.8. Briefly, 1 x $10^8$ CFU/ml STm mCherry SL1344 was flowed across HAoECs at 275$s^{-1}$ then washed. Whole blood containing stained platelets was then flowed through at either 275$s^{-1}$ (venous) or 800$s^{-1}$ (arterial) shear. Red arrows show mCherry labelled STm SL1344. Magenta = platelets. White circles show possible unstained platelets. Blue circle shows example of unbound and/or dead HAoEC. Scale bars = 20µm. Images representative of n = 2.

## 4.3 Discussion

The results in this chapter show that *Salmonella* Typhimurium can bind to HAoECs, and lead to loss of VE-cadherin staining and cell-cell detachment of the endothelial layer. Under flow conditions, platelets can roll along STm and adhere, leading to microaggregate formation. When assessing STm, ECs and platelets in combination, platelets are able to adhere to STm primed ECs at both venous and arterial shear, and appear to do so at sites distal to bacterial binding.

The first aim in this chapter was to identify whether STm interacts with HAoECs. The assay used confirmed binding interactions between STm and ECs, and showed that the addition of plasma to the system increases the binding between the two. The components responsible for this increase appear to be IgG and potentially fibrinogen, although it is difficult to assess the contribution of fibrinogen as the preparations can be contaminated with IgG (Brennan et al., 2009, Pietrocola et al., 2005, Arman et al., 2014). To rectify this, experiments using fibrinogen depleted of any IgG using a protein A column could be carried out.

Whilst this assay was used to assess relative binding, other binding assays allow quantification of the bacterial binding to HAoECs. As shown in McDonnell et al (2016) and McHale et al (2018), by coating the plate with HAoECs then adding SYBR Green-I labelled bacteria, quantification is enabled. This was attempted with STm SL1344, but STm was unable to be successfully labelled with SYBR Green-I. As a possible solution, mCherry labelled STm was obtained, but unfortunately, the excitation/detection system on the plate reader was not strong enough to identify the signal from the fluorescent label. However, as seen from Figure 4.7, the mCherry signal can clearly be detected by microscopy, so future work could involve measurement via microscopy instead of using a plate reader. There was insufficient time during my secondment in the Kerrigan lab to investigate this further.

The assay proposed above has the further advantage of using sheared HAoECs, which are more physiologically representative than static cells. As well as the stark differences in cell morphology (as

can be seen in Figure 4.3Ai,ii), static and sheared ECs have different gene expression profiles - proteins such as ion channels, GPCRs and integrins are upregulated in sheared ECs over static ECs (Chen et al., 2001, García-Cardeña et al., 2001, McCormick et al., 2001). These differences are accentuated further upon stimulation of sheared cells with the pro-inflammatory cytokine TNF-α, with additional gene expression changes induced (Chiu et al, 2005), and the level of certain TNF receptors and associated factors being increased under shear (Chu and Peters, 2008). When assessing *S. aureus* binding to HAoECs, over twice the number of bacteria bound TNF-α and PPP treated sheared HAoECs than static HAoECs (McHale, 2018). The binding assay carried out in this chapter used static HAoECs, and binding to STm SL1344 did not increase upon addition of TNF-α. It would be of interest to see whether this result differed with the use of sheared cells, and whether the use of sheared cells affected binding of the Omp knock-out strains, especially that of OmpA. *E. coli* Omp A binds to sheared HAoECs via the αVβ3 integrin (McHale et al., 2018), and shares 95% sequence identity with STm SL1344 OmpA (as measured using Cluster Omega with sequences A0A718QEA6_SALTS and A0A085P3U1_ECOLX). In bovine aortic ECs, although shear stress did not increase the total amount of αvβ3, it did appear to increase the amount of high affinity αvβ3 (Tzima et al., 2001), which could potentially increase bacterial binding to the WT SL1344.

The immunofluorescence assay showed that upon incubation with STm, gaps start to appear between HAoECs, and the expression of VE-cadherin decreases at the cell periphery. MOI 10 and MOI 40 were used as a starting point, but it would be of worth to see how much lower the MOI could be taken whilst still causing endothelial damage. A study of the blood cultures of 158 iNTS cases in Malawi showed that the viable *Salmonella* load in blood was 1 CFU/ml (IQR 0.33-5.33 CFU/ml) (Gordon et al., 2010), so reducing the MOI used in the assay would perhaps provide more physiologically relevant results. Having said that, the demonstration in this thesis that STm can bind to HAoECs raises the interesting question as to how relevant blood culture results are for measuring the amount of bacteria found in the vessels. There could potentially be much higher amounts of bacteria in the blood vessels, which

are unable to be detected via blood culture as they are already bound to the ECs. As well as reducing the MOI used in the assay, one could increase the time the HAoECs are incubated with STm. In studies looking at *S. aureus* and SARS-CoV-2 (McDonnell et al., 2016, Nader et al., 2021), 24 hour incubations were carried out rather than the 2 hour incubation used in this thesis. These studies also assessed the impact of infection on the permeability of the endothelium, as well as measuring levels of apoptosis in the ECs, all of which could be carried out to help characterise the responses occurring to STm.

Investigating the effects of venous shear on platelet adherence to STm revealed platelets can roll along STm and adhere, with the formation of microaggregates. Interestingly, in studies on other bacteria, the level of shear stress impacts how platelets interact with the bacteria. Platelets do not interact with *S. aureus* at low shear rates, but do at high shear (Kerrigan et al., 2008), whereas the opposite response is seen when flowing platelets over *S. gordonii* (Kerrigan et al., 2007) or *S. sanguinis* (Plummer et al., 2005). Platelets interact with *S. oralis* at all shear rates, with increased platelet deposition as the shear rate increases. Therefore, further studies on whether the rate of shear has different effects on platelet interactions with STm would be useful. Amongst these studies, to further characterise the interactions occurring under flow, addition of various inhibitors could reveal details of the interactions taking place between platelets and STm. For example, platelet rolling on *S. oralis* was shown to be mediated by GP1bα – the use of anti-GP1bα blocking antibodies in the STm assay could reveal if the same mechanism is occurring. Furthermore, it would be interesting to take the findings from chapter 3 to see whether the mechanisms occurring in the aggregation set-up correspond with the mechanisms under shear – for example whether use of Fab IV.3 inhibits binding, and whether addition of anti-*Salmonella* antibody causes an increased amount of platelet microaggregates.

The flow experiments also revealed another cell adhering to the STm as well as platelets. The cells did not stain for DAPI, suggesting they do not have a nucleus and are therefore red blood cells. Their size and morphology also fit this theory. Haematoxylin and eosin staining would confirm this. There are

studies that show STm can cause human red blood cell agglutination, which would strengthen the argument that the unidentified cells are red blood cells. Miyake et al (1998) showed that the agglutination was likely due to an amino acid sequence contained in OmpF and OmpC that binds human blood type trisaccharide antigens. An alternative explanation is that *Salmonella* Typhimurium type 1 fimbriae can cause haemagglutination by binding to mannose on the red blood cell surface (Zeiner et al., 2012).

The third aim of this chapter was to investigate platelet interactions with STm primed HAoECs under flow conditions. These experiments showed that platelets adhere to HAoECs, singly under arterial shear, but with microaggregates forming at venous shear. The images in Figure 4.9 reveal some improvements could be made to the assay. Firstly, there appear to be many unstained platelets. For these assays the concentration of NIR-AZA dye was reduced from 5µM to 3.3µM to conserve supply – this appears to have had a larger impact on the ability to stain all the platelets than expected. The HAoECs also do not look particularly healthy – the method used here involved shearing the cells for 24 hours, then harvesting them on the day of the experiment and letting them adhere to the Ibidi chamber for 4 hours prior to use in the flow assay. However, this means the continuous layers that would have formed under shear will have been disrupted, leaving the cells to adhere randomly. It can be seen from the differential interference contrast (DIC) images that the cells do not look to be uniformly organised, with many gaps between them, and multiple cells looking to have not adhered well to the chamber surface. In future experiments, HAoECs should be seeded into the chambers, and then sheared directly in the chambers for 24 hours, as done in McHale (2018).

Thinking further about ECs, the cell characteristics differ between the venous and arterial systems, with arterial ECs tending to be narrower and more elongated than venous ECs, and adhesion molecules preferentially expressed on venous ECs over arterial ECs (Simionescu and Antohe, 2006). It would be interesting to investigate whether shearing the HAoECs at different rates affected the results seen.

Furthermore, the use of different types of EC could affect the results seen. One could argue that the use of HAoECs for studying STm interactions is not ideal, given infectious endocarditis due to STm is very rare (involved in an estimated 1.6% of iNTS cases (Marchello et al., 2022)). In the STm mouse model, thrombus formation is seen in certain vascular beds – particularly those of the spleen and liver, rather than the heart. In the heart, the endothelium forms a continuous layer, in contrast to the spleen and liver, in which the endothelium is discontinuous, meaning there are pores between the cells, to allow for particle exchange (Feletou, 2011). Given the basal lamina can be either present or absent in those gaps between the cells, this could have vastly different impacts on platelet deposition upon priming with STm.

In the assays carried out in this thesis, venous shear experiments were able to be carried out for five minutes, but due to the blood volumes involved, arterial shear experiments were only carried out for 3 minutes. To allow better comparisons to be drawn between the effects of the two different shear rates, the use of the smaller 0.1 Ibidi chambers would use almost 1000x less blood, allowing testing of more conditions per donor, and the scope to test higher shear rates.

As mentioned for the flow assay looking at platelet-STm interactions, following the results shown in chapter 3, it would be interesting to see whether the addition of anti-*Salmonella* antibody to the blood caused increased platelet adhesion, and whether the inhibition of FcγRIIA had any effect. Interestingly, the platelets appear to be binding the primed HAoECs, rather than the bound STm. We know from Figure 4.5 that platelets can bind to STm under flow, but further work would be needed to establish whether the platelets are being solely activated by the primed ECs, or whether they are activated by flowing over the bound bacteria which then enhances their likelihood of binding to the ECs. Whilst platelets start to bind to STm within 100s in Figure 4.5, in the aggregometry assays in chapter 3 the median lag time for STm SL1344 to cause platelet aggregation was eight minutes. Although the effects

of shear will affect this length of time, it would be interesting to run the assays for longer than five minutes to see whether a 'second-wave' of platelet activation occurs.

A further interesting point would be to try and encompass the conditions STm would encounter when trying to replicate in the bloodstream. For all assays presented, STm was grown under static conditions overnight before two hours incubation at 200 rpm. However, one study has shown that the invasive STm D23580 strain becomes more pathogenic when grown at physiological shear rates (Yang et al., 2016). It is unknown whether this would impact on the levels of platelet activation.

In conclusion, there are many factors to take into account when trying to model interactions between platelets, STm and ECs *in vitro*. This chapter started to explore the relationships between the three during a 3.5 month placement at the Royal College of Surgeons in Ireland, and provides scope for future experiments of differing levels of complexity. Whilst there are still many questions to be answered, it is promising to be able to show that platelets interact with STm under flow conditions, that STm can bind to HAoECs leading to damage to the endothelial barrier, and that platelets adhere to HAoECs that have been exposed to STm.

# CHAPTER 5: THE ROLE OF ANTIBODIES IN COMPLEMENT RESPONSES TO SARS-CoV-2

## 5.1 Introduction

During the early months of the SARS-CoV-2 pandemic, the novel nature of the virus meant there was limited knowledge of how to treat those that became severely ill. Therefore, attention turned to what could be learnt from previous coronavirus outbreaks.

### 5.1.1 Complement in SARS and MERS

Prior to the COVID-19 pandemic, there had been two other major coronavirus outbreaks in the 21st century: those of severe acute respiratory syndrome coronavirus (SARS-CoV) and middle eastern respiratory virus (MERS). The complement pathway has been implicated in the pathogenesis of both of these coronaviruses (Gralinski et al., 2018, Jiang et al., 2018).

In a SARS-CoV mouse model, complement components including C3, C4b and Factor B (FB) were detected in the lungs of wild-type mice from day 1 of infection. In the same model in C3 knock-out (KO) mice, significantly better outcomes were observed, with reduced weight loss and respiratory dysfunction, reduced neutrophil and monocyte lung infiltration, as well as lower cytokine and chemokine levels in both sera and lung tissue. Overall, the C3 KO mice had reduced lung pathology compared to wild-type, C4 KO or FB KO mice. With C4 KO mice unable to signal through the classical and lectin pathway, and FB KO mice unable to signal through the alternative pathway, and protection only being seen KO mice of the downstream component C3, this suggested multiple arms of the complement pathway were contributing to SARS-CoV pathology (Gralinski et al., 2018).

In a MERS mouse model, serum C5a levels were found to be significantly increased post-infection, and C5b-9 deposition was found on lung tissue. Treating the mice with an anti-C5a receptor (C5aR) antibody reduced systemic and local inflammatory responses, led to less tissue damage in the lungs

and spleen as well as limiting viral replication. However, overall survival in the mice was not significantly improved (Jiang et al., 2018).

Multiple studies have investigated the potential role of the lectin pathway in SARS-CoV, with differing results. Whilst some studies have shown mannose-binding lectin (MBL) does not bind to SARS-CoV spike protein (Leth-Larsen et al., 2007), and no association of SARS-CoV susceptibility with MBL genotype (Yuan et al., 2005), not all studies observe the same (Zhou et al., 2010, Ip et al., 2005). Therefore, while there appears to be agreement that complement could be playing a role in SARS and MERS pathogenesis, the molecular mechanisms and specific complement pathways involved are controversial.

### 5.1.2 Complement in SARS-CoV-2

Although SARS-CoV-2 is distinct from SARS-CoV and MERS, it still shares approximately 79% and 50% sequence identity respectively with them (Lu et al., 2020). There are some similarities in pathogenesis between these coronaviruses making findings from SARS-CoV and MERS helpful in identifying how to deal with the novel SARS-CoV-2 pathogen. Within these, was a focus on the role of complement activation in COVID-19 patients. A flurry of reviews and commentaries suggesting the importance of complement in COVID-19 pathology were published in response to the desperate need for new treatments (Noris et al., 2020, Risitano et al., 2020, Campbell and Kahwash, 2020). These viewpoints were gradually backed up by evidence from patient studies (Magro et al., 2020, Macor et al., 2021, Ma et al., 2021, Cugno et al., 2021, Holter et al., 2020, Satyam et al., 2021, Boussier et al., 2022, Detsika et al., 2022, Devalaraja-Narashimha et al., 2023).

Autopsy studies involving small numbers of patients performed in the early months of the pandemic showed deposits of complement in the lungs, with MASP-2, C4d and C5b-9 deposits found in the alveolar septum capillaries, the latter two components often colocalising with spike protein (S) (Magro et al., 2020). Systemically, many studies started to show increased levels of complement in the blood,

with consistently higher levels of C5a found in COVID-19 patients (Marcos-Jiménez et al., 2020, Marcos-Jimenez et al., 2021, Carvelli et al., 2020), and higher levels of sC5b-9 and C4d in those with respiratory failure (Holter et al., 2020). C4d, sC5b-9 and C5a were also shown to correlate with antiviral antibodies rather than viral load - significant correlations between all three complement factors and IgM against nucleoprotein (N) were observed, as well as between C4d to IgG against S receptor binding domain and N (Holter et al., 2020). Further papers confirmed these earlier studies, showing complement deposits in the lungs, kidneys and liver (Macor et al., 2021, Niederreiter et al., 2022, Satyam et al., 2021), and increased systemic blood levels of complement, with higher levels of blood complement markers linked to worse outcomes (Meroni et al., 2023, Ma et al., 2021, Henry et al., 2021, Gauchel et al., 2022, Georg et al., 2022, Detsika et al., 2022, Devalaraja-Narashimha et al., 2023, Cheng et al., 2021, Cugno et al., 2021, Leatherdale et al., 2022, Sinkovits et al., 2021).

### 5.1.3 Specific complement pathways in COVID-19

With complement so clearly indicated in severe COVID-19, the focus switched to elucidating the mechanisms behind this complement activation, including which of the three complement pathways were causing such high levels of complement to be present, with the hope of further understanding guiding clinical studies and treatment.

#### 5.1.3.1 The classical complement pathway in COVID-19

With the three complement pathways converging at the terminal pathway (see section 1.4), and the classical and lectin pathways sharing C3 convertase structure, supporting evidence of classical pathway involvement *in vivo* has to be found through identifying binding of C1q, C1r and/or C1s, the initiating molecules of the pathway. Autopsy studies have shown C1q deposition in various tissues including the lungs, liver and kidneys (Macor et al., 2021, Satyam et al., 2021). This has been confirmed systemically, with increased classical pathway activity seen in COVID-19 patients (Leatherdale et al., 2022, Hurler et

al., 2022, Defendi et al., 2021, Siggins et al., 2023, Boussier et al., 2022, Georg et al., 2022, Jarlhelt et al., 2021).

#### 5.1.3.2 The lectin complement pathway in COVID-19

Involvement of the lectin pathway was first suggested in March 2020 in a pre-print from Gao *et al.*, since fully published in 2022 . They showed *in vitro* that N protein from SARS-CoV, MERS and SARS-CoV-2 is capable of directly binding to MASP-2, a critical early component of the lectin pathway. This interaction was confirmed and further developed by Ali et al. (2021) who showed binding of MBL to both spike and nucleoprotein from SARS-CoV-2, as well as direct binding of MASP-2 to the SARS-CoV-2 nucleoprotein.

*In vivo*, the role of the lectin pathway has caused similar controversy to that which it did in SARS-CoV, with contrasting views being published. Some studies have argued that the lectin pathway is hyperactivated in severe COVID-19, with lower levels of MBL or MASP-2 measured in blood suggestive of component consumption (Defendi et al., 2021, Gotz et al., 2022), backed up by higher MBL2 and MASP-2 RNA levels found in moderate and severe COVID-19 patients (Boussier et al., 2022). On the other hand, despite correlation between lectin pathway marker MASP-1/C1-INH and disease severity (Hurler et al., 2023, Hurler et al., 2022), with no association between disease outcome/severity and genetic variation in MBL2 (Hurler et al., 2023), one group concluded the lectin pathway was playing only a minor role due to overall lack of consistency between lectin pathway components and disease outcome.

#### 5.1.3.3 The alternative complement pathway in COVID-19

The alternative pathway has also been indicated in the pathogenesis of COVID-19, with Yu et al. (2020) suggesting spike but not nucleoprotein could directly activate the alternative pathway. Many studies have followed, linking higher levels of blood Factor B, Factor Ba and Factor D and lower levels of

properdin with worse outcomes (Ma et al., 2021, Leatherdale et al., 2022, Siggins et al., 2023, Boussier et al., 2022).

### 5.1.4 The use of complement inhibitors in COVID-19

With complement levels so high in severe disease, and a lack of treatment options for the novel virus, the use of complement inhibitors was explored by some groups as a possible treatment option. An *in vivo* study using an acute lung injury mouse model with human C5aR1 knock-in, the C5aR1 blocking monoclonal antibody avdoralimab reduced immune cell infiltration and damage in the lungs (Carvelli et al., 2020).

This was followed by studies on very small (<5) numbers of patients using complement inhibitors. Multiple groups showed their patients recovered from severe COVID-19 when inhibiting C5, either with eculizumab (Diurno et al., 2020) or newer C5 blocking monoclonal antibodies (Zelek et al., 2020). Other groups utilised the C3 inhibitor peptide AMY-101 (Mastaglio et al., 2020, Skendros et al., 2022), showing this to give favourable broader immune responses in terms of NET reduction to eculizumab (Mastellos et al., 2020). Unfortunately, due to the rapid and pressing nature of COVID-19 research, these studies are lacking in control groups and/or adequate patient numbers to make any firm conclusions about complement inhibitor efficacy as a treatment. However, they did provide a basis for further clinical trials. A phase three randomised controlled trial (RCT) of ravulizumab, an anti-C5 mAb, in severe COVID-19 patients was stopped early due to futility (NCT04369469). Another phase three RCT using the anti-C5aR mAb avdoralimab completed, but found the drug to have no significant clinical benefit (Carvelli et al., 2022). So far the only clinical trial to report positive results is a phase three RCT using vilobelimab, an anti-C5a mAb, with an increase in survival of mechanically ventilated patients given the drug at day 28 (Vlaar et al., 2022). However, this is not without controversy, with doubts being raised over the way the multi-centre trial was analysed (Kalil and Proschan, 2022), and the

significance in survival being lost by day 60. Details of further ongoing clinical trials are summarized in Zelek and Harrison (2023).

### 5.1.5 Chapter aims

When this project began in 2020, multiple studies had shown complement levels to be raised in the blood of those with severe COVID-19 (Carvelli et al., 2020, Lam et al., 2020, Holter et al., 2020, Marcos-Jiménez et al., 2020), and it had been shown the lectin pathway could be activated by N protein (Gao et al., 2020). Whether SARS-CoV-2 could specifically activate the classical pathway was unknown. Following on from the successful development of a SARS-CoV-2 anti-IgGAM ELISA by the Clinical Immunology Service, the Cunningham lab and The Binding Site (Cook et al., 2021, Faustini et al., 2020, Faustini et al., 2021), we wanted to further develop the ELISA for application to the complement system.

We wanted to investigate the potential mechanisms of complement involvement in immune responses to SARS-CoV-2, and decipher whether anti-SARS-CoV-2 antibodies were able to activate the classical pathway, with a particular focus on the role of the antibody in this process. Therefore, the aims of this chapter were to:

a) Identify whether antibodies against SARS-CoV-2 spike and nucleoprotein can lead to the activation of the classical complement pathway
b) Identify whether antibodies from convalescent individuals with either mild or severe COVID-19 have different complement activation capabilities
c) Identify whether antibodies from vaccinated individuals activate complement in a similar or different manner to those with natural infection
d) Identify whether antibody titres relate to the levels of complement activation

The results of this work were published in Frontiers in Immunology, and the paper is presented here as part of an alternative format thesis. Author contributions are detailed at the end of the paper, but

in summary, Edith Marcial-Juarez led on development of the complement assay in collaboration with me. All experiments presented in the paper were performed by me, and I carried out all the data analysis. I wrote the paper in conjunction with Adam Cunningham. All other authors provided key reagents, samples or provided supervisory support.

# SARS-CoV-2 Spike- and Nucleoprotein-Specific Antibodies Induced After Vaccination or Infection Promote Classical Complement Activation

Frontiers in Immunology

Article number: 13:838780

# SARS-CoV-2 spike- and nucleoprotein-specific antibodies induced after vaccination or infection promote classical complement activation

**Rachel E Lamerton[1,2†], Edith Marcial-Juarez[1†], Sian E Faustini[1], Marisol Perez-Toledo[1], Margaret Goodall[1], Siân E Jossi[1], Maddy L Newby[3], Iain Chapple[4], Thomas Dietrich[4], Tonny Veenith[5], Adrian M Shields[1], Lorraine Harper[6], Ian R Henderson[7], Julie Rayes[2], David C Wraith[1], Steve P Watson[2], Max Crispin[3], Mark T Drayson[1], Alex G Richter[1], Adam F Cunningham[1*]**

†These authors contributed equally to this manuscript

[1] Institute of Immunology and Immunotherapy, University of Birmingham, Birmingham, UK
[2] Institute of Cardiovascular Sciences, University of Birmingham, Birmingham, UK
[3] School of Biological Sciences, University of Southampton, Southampton, UK
[4]Periodontal Research Group, School of Dentistry, Institute of Clinical Sciences, University of Birmingham, and Birmingham Community Healthcare NHS Trust, Birmingham, UK
[5] Department of Critical Care Medicine, University Hospitals Birmingham NHS Trust, Birmingham, UK
[6] Institute of Applied Health Research, University of Birmingham, Birmingham, UK
[7] Institute for Molecular Bioscience, University of Queensland, St Lucia, QLD, Australia

*** Correspondence:**

Corresponding Author

A.F.Cunningham@bham.ac.uk

**Keywords: Complement, COVID-19, SARS-CoV-2, vaccine, antibodies**

## Abstract

Antibodies specific for the spike glycoprotein (S) and nucleocapsid (N) SARS-CoV-2 proteins are typically present during severe COVID-19, and induced to S after vaccination. The binding of viral antigens by antibody can initiate the classical complement pathway. Since complement could play pathological or protective roles at distinct times during SARS-CoV-2 infection we determined levels of antibody-dependent complement activation along the complement cascade. Here, we used an ELISA assay to assess complement protein binding (C1q) and the deposition of C4b, C3b, and C5b to S and N antigens in the presence of antibodies to SARS-CoV-2 from different test groups: non-infected, single

and double vaccinees, non-hospitalised convalescent (NHC) COVID-19 patients and convalescent hospitalised (ITU-CONV) COVID-19 patients. C1q binding correlates strongly with antibody responses, especially IgG1 levels. However, detection of downstream complement components, C4b, C3b and C5b shows some variability associated with the subject group from whom the sera were obtained. In the ITU-CONV, detection of C3b-C5b to S was observed consistently, but this was not the case in the NHC group. This is in contrast to responses to N, where median levels of complement deposition did not differ between the NHC and ITU-CONV groups. Moreover, for S but not N, downstream complement components were only detected in sera with higher IgG1 levels. Therefore, the classical pathway is activated by antibodies to multiple SARS-CoV-2 antigens, but the downstream effects of this activation may differ depending the disease status of the subject and on the specific antigen targeted.

## Introduction

Infection with SARS-CoV-2, the causative agent of COVID-19, results in a spectrum of clinical presentations ranging from asymptomatic infections to severe disease and death. Although some factors that can predict risk of severe disease are known, such as obesity or age, it is clear that other host factors, including immune status, also contribute (Docherty et al., 2020, Petrilli et al., 2020, Shields et al., 2021b). Thus, it is likely that COVID-19 represents a collection of syndromes, caused by one pathogen, where disease severity is influenced by host and pathogen factors.

Two antigens that are common targets of the immune response to SARS-CoV-2 are the spike (S) glycoprotein, which is essential for both binding and entry into host cells, and the nucleocapsid (N) protein, involved in packaging the genomic material (Walls et al., 2020). Antibodies to these antigens are induced after infection, and antibodies to S glycoprotein can be protective (Shields et al., 2021a, Lumley et al., 2021, Hanrath et al., 2021). Indeed, the S glycoprotein is the sole SARS-CoV-2 viral antigen targeted by all current licensed vaccines (Darby and Hiscox, 2021). After natural infection of non-vaccinated individuals, although the appearance of antibodies to both of these antigens can occur

early in mild disease, the presence of such antibodies is usually well-established at times severe disease develops. This means that substantial levels of viral antigen may still be present within the host for these antibodies to bind (To et al., 2020). In contrast, in most vaccinated individuals who have not previously been infected, high levels of antibodies to S are present when they subsequently encounter the pathogen. This means that there can be circumstances when: i) there are concomitant high-levels of antibodies to S and N as well as relatively high-levels of antigen (antibodies induced during infection) and ii) high-levels of antibodies to S and relatively low-levels of antigen (infection of vaccinated, previously naïve individuals).

After antigen binding by antibody, complement activation can occur through the classical pathway (Dunkelberger and Song, 2010). This cascade requires C1q binding to antibody and the generation of a C3 convertase derived in part from C4, through the production of C4b. This results in the cleavage of C3 and C5, with C3b and C5b forming a complex proximal to the site of antibody binding. The activation of the complement cascade may have positive or negative effects for the host associated with the timing of its activation and possibly the different pathways involved (Carvelli et al., 2020, Holter et al., 2020, Ng and Powell, 2021, Kurtovic and Beeson, 2021, Ma et al., 2021).

To improve our understanding of the relationship between SARS-CoV-2-specific antibodies and complement activation, we developed a solid phase C1q-binding assay and C4b, C3b and C5b complement deposition assays using S and N proteins from the SARS-CoV-2 Wuhan strain. These studies identified differences in antibody-associated complement activation that were associated with the stage of infection in the host.

## Methods

### Ethics and patient samples

Sera were obtained from distinct groups of subjects from well-validated cohorts that are described below (Shields et al., 2021a, Shields et al., 2021b). Group 1: Non-vaccinated individuals without any reported COVID infection (NEG). Sera were obtained from subjects in May 2020, prior to widespread PCR testing and before the introduction of vaccines against SARS-CoV-2 infection. Sera were screened using a clinically validated, CE marked, ELISA assay that measures the IgG, IgA and IgM (IgGAM) response to the S glycoprotein (Cook et al., 2021, Faustini et al., 2021) (manufactured by The Binding Site (TBS; product code: MK654), Birmingham). This assay, described below in the section on detecting antibodies to S and N, has been clinically validated and reported to have a sensitivity of 98.6% (95% CI, 92.6-100.0%) and a specificity of 98.3% (95% CI, 96.4-99.4%)(Cook et al., 2021). Group 2: Individuals without evidence of infection (as determined by an absence of anti-N antibodies), vaccinated 28-35 days previously with BNT162b2 vaccine (VACC). Group 3: Individuals without evidence of infection (as determined by an absence of anti-N antibodies) who had received their second dose of BNT162b2 vaccine at least 28 days previously (DOUBLE VACC). Group 4: These sera were obtained in May 2020 from a cohort of healthcare workers from the University Hospitals Birmingham Foundation Trust, who had previously self-isolated a minimum of 28 days previously because they experienced symptoms suggestive of COVID-19, and had not been hospitalized for any of these symptoms. In May 2020 widespread PCR testing was not available, and thus most of these samples were not from individuals with prior confirmed PCR tests. Since the only predefined exclusion criteria was participation in existing SARS-CoV-2 vaccine trial or current COVID-19 symptomatology and the time was prior to the introduction of vaccines, anti-S antibodies could be used as a reliable surrogate of previous infection. Anti-S IgGAM were determined as described above using the clinically validated anti-S glycoprotein ELISA described above (non-hospitalised convalescents, NHC). Group 5: Non-vaccinated convalescent,

PCR confirmed SARS-CoV-2 infection patients who required ITU treatment, samples taken a minimum of 4 months after ITU discharge (ITU-CONV).

Ethical approval for obtaining samples for groups 1 -4 was provided by the London – Camden and Kings Cross Research Ethics Committee reference 20/HRA/1817. Ethical approval for obtaining samples for group 5 was provided by the North West ethics committee, Preston CIA UPH IRAS approval reference REC 20\NW\0240.

**Antigens used in this study**

To generate the spike glycoprotein used in this study, HEK293F cells were transiently transfected with a pα-H plasmid containing the near full-length sequence for the Wuhan SARS-CoV-2 spike (GenBank: MN908947). The spike glycoprotein used here contains 1208 amino acids and includes all the S1 and most of the S2 domain (Hsieh et al., 2020, Chawla et al., 2021). The protein has been modified so that there are an additional four prolines present in addition to the two which are normally expressed (2P) to stabilize recombinant spike (Hsieh et al., 2020). The 6 prolines are present at positions 817, 892, 899, 942, 986 and 987 (Hsieh et al., 2020). This so-called HexaPro spike glycoprotein expresses as a metastable recombinant SARS-CoV-2 prefusion ectodomain. Extensive comparisons between the native, 2P and HexaPro spike glycoproteins demonstrate that they have comparable native-like protein architecture, have similar antigenic properties including the induction of neutralizing antibodies (Seephetdee et al., 2021, McMillan et al., 2021, Walls et al., 2021) and have similar glycosylation profiles (Hsieh et al., 2020, Watanabe et al., 2020, Allen et al., 2021, Chawla et al., 2021).

The HEK293F cells were cultured in Freestyle 293 Expression medium (Fisher Scientific) and maintained at a density of 0.2 x $10^6$ cells/mL at 37°C, 8% $CO_2$ and 125 rpm shaking. Prior to transfection, two solutions of 25 mL Opti-MEM (Fisher Scientific) medium were prepared. The expression plasmid encoding SARS-CoV-2 HexaPro was added to the first solution to give a final concentration of 310 μg/L. To the other solution, 1 mg/mL pH7 polyethylenimine (PEI) max reagent was added to generate a ratio

of 3:1 PEI max:plasmid DNA. Both solutions were combined and incubated at room temperature for 30 minutes. Cells were transfected at a density of 1 x $10^6$ cells/mL and incubated for 7 days at 37°C, 8% $CO_2$ and 125 rpm shaking. Cells were centrifuged at 3041g for 30 minutes at 4°C and supernatant was applied to a 500 mL Stericup-HV sterile vacuum filtration system (Merck) with a pore size of 0.22 µm. Purification of HexaPro S protein was undertaken using an ÄKTA Pure system (Cytiva). A 5 mL HisTrap Excel column (Cytiva) charged with Ni(II) was equilibrated using 10 column volumes (CV) of wash buffer (50 mM $Na_2PO_4$, 300 mM NaCl, pH 7). Supernatant was then loaded onto the column at a flow rate of 5 mL/min and washed with 10 CV of washing buffer containing 50 mM imidazole. Protein was eluted from the column in 3 CV of elution buffer (300 mM imidazole in washing buffer) and buffer exchanged to phosphate buffered saline (PBS) and concentrated using a Vivaspin column (MWCO 100 kDa) (Cytiva).

The nickel purified eluate was concentrated to 1 mL in PBS and injected into a Superdex 200 pg 16/600 column (Cytiva) to further purify trimeric S protein using size exclusion chromatography (SEC). The column was washed with PBS at 1 mL/min for 2 hours where fractions corresponding to the correct peak on the size exclusion chromatogram were collected and concentrated to ~1 mL as above.

Nucleocapsid was generated as a recombinant protein from *E. coli* by the Protein Expression Facility at the University of Birmingham (Faustini et al., 2021).

**Detection of antibodies specific to S and N**

Antibody ELISAs were carried out as previously described (Faustini et al., 2021), with 50 µl per dilution used. In brief, 96 well high-binding plates (Corning) were coated with 0.1 µg S or N protein in PBS and incubated overnight at 4°C. PBS-0.1% Tween 20 was used to wash plates 3 times, and between all subsequent steps. Plates were blocked with 2% (w/v) BSA in PBS-0.1% (v/v) Tween 20 for 1 hr at room temperature (RT). Serum was diluted 1:40 and incubated for 1 hr at RT. HRP-conjugated anti-human secondary antibodies were added for 1 hr at RT. For combined anti-IgG, IgA and IgM (IgGAM) the

antibodies came in a combined pre-diluted form from The Binding Site (EACONJ654). The individual constituent HRP-labelled secondary antibodies used in this are polyclonal rabbit anti-human IgG (1:16,000), polyclonal rabbit anti-human IgA (1:2000) and polyclonal rabbit anti-human IgM (1:8000). Individual immunoglobulin isotypes were detected using HRP-conjugated monoclonal antibodies: mouse anti-human IgM (clone AF6, 1:2000), mouse anti-human IgG1 (clone MG6.41, 1:3000), mouse anti-human IgG3 (clone MG5.161, 1:1000). All monoclonal antibodies were produced at the University of Birmingham. Plates were developed for up to 20 minutes using 100 µl TMB Core (Bio-Rad) and the reaction was stopped with 50µl 0.2M $H_2SO_4$. Optical density (OD) was read at 450 nm using a SpectraMax ABS Plus plate reader.

**Solid phase C1q-binding assay**

Plates were coated as above. Plates were washed three times with PBS-0.1% Tween 20 – this wash step was carried out between all subsequent steps. Blocking was carried out for 1 hr at RT with 2% BSA in PBS-0.1% Tween 20. Test serum was heat inactivated at 56°C for 30 minutes, before being diluted 1 in 5 with 2% BSA supplemented with 5 mM calcium chloride and 5 mM magnesium chloride. 50 µl was added to the antigen-coated plate and incubated for 1hr at 37°C. After washing, 50 µl COVID negative normal human serum (same source used throughout all assays, containing no detectable S or N specific antibodies as measured by IgGAM ELISA) at a dilution of 1:40 (in 2% BSA plus 5 mM calcium chloride and 5 mM magnesium chloride) was added to each well for 1hr at RT. 100µl of rabbit anti-C1q FITC antibody (Invitrogen PA5-16601) at a 1:200 dilution in PBS-0.1% Tween 20 was added and incubated at 37°C for 1 hr. HRP conjugated swine anti-rabbit (Dako P0399) at a 1:2000 dilution was then incubated for 1 hr. The assay was amplified using the Perkin Elmer ELAST amplification kit as per manufacturer's instructions, with an optimised dilution of streptavidin, 1:800, incubated for 20 minutes. Plates were developed using 100 µl TMB Core (Bio-Rad) for 10 minutes, before being stopped with 50 µl 0.2M$H_2SO_4$. OD was measured as described above.

**C4b, C3b and C5b complement deposition assay**

Microtiter plates were coated and washed as described above and blocked with Starting Block (ThermoFisher) for 10 min. Test serum was heat inactivated at 56°C for 30 minutes, before being diluted 1 in 5 with Starting Block supplemented with 5 mM calcium chloride and 5 mM magnesium chloride. 50 µl was added to the antigen-coated plate and incubated for 1hr at 37°C. After washing, 50 µl COVID negative normal human serum (same source used throughout all assays, containing no detectable S or N specific antibodies as measured by IgGAM ELISA) at a dilution of 1:40 (in 2% Starting Block plus 5 mM calcium chloride and 5 mM magnesium chloride) was added to each well for 1 hr at 37°C. The following anti-human monoclonal complement antibodies (100ul, diluted in PBS-0.1% Tween 20) were added and incubated at 37°C for 1 hr: mouse anti-C4b, 1:22,500 (Invitrogen, LF-MA0198); mouse anti-C3b, 1:10,000 (Invitrogen MA1-70053); mouse anti-C5b, 1:10,000 (Invitrogen DIA 011-01-02). HRP conjugated goat anti-mouse at a 1:4000 (Southern Biotech 1010-05) was then incubated at RT for 1 h. Plates were developed and read as described above.

**Statistics**

Statistical analysis was carried out using GraphPad Prism 9.0. Kruskal-Wallis followed by Dunn's post-hoc test for multiple groups was used to calculate p values. Statistical significance was accepted at $P<0.05$. Spearman correlation was carried out on the appropriate data sets.

## Results

### Anti-S, but not anti-N antibody responses differ between NHC and ITU-CONV patients

Total IgGAM antibody responses to trimeric S and N were assessed in five different groups: individuals without any reported COVID-19 infection (NEG); post first BNT162b2 vaccine, infection-naïve individuals (VACC); post second BNT162b2 vaccine, infection-naïve individuals (DOUBLE VACC); convalescing non-hospitalised patients (NHC) and convalescing patients who had been hospitalised and required ITU treatment (ITU-CONV). The VACC, DOUBLE VACC, NHC, ITU-CONV groups all had significantly higher anti-S glycoprotein IgGAM responses than the NEG group (Figure 5.1A), whereas IgGAM levels against N in the two convalescent groups were higher than the NEG, VACC and DOUBLE VACC groups (Figure 5.1B). There were no significant differences in the anti-N responses between the NEG group and the VACC and DOUBLE VACC groups, consistent with individuals within these groups not having had prior SARS-CoV-2 infections. Similar results were observed when specific IgG1 responses, an IgG isotype efficient at fixing complement, were assessed (Figure 5.1C). No differences in anti-S IgGAM and IgG1 antibody responses were observed between the VACC and patient groups. Anti-S IgGAM and IgG1 responses were higher in the ITU-CONV group compared to the NHC group, but no differences were observed for anti-N responses in these two groups (Figure 5.1D). Modest IgM and IgG3 responses to S and N were detected in some individuals (Supplementary Figures 5.1A,B and Supplementary Table 1).

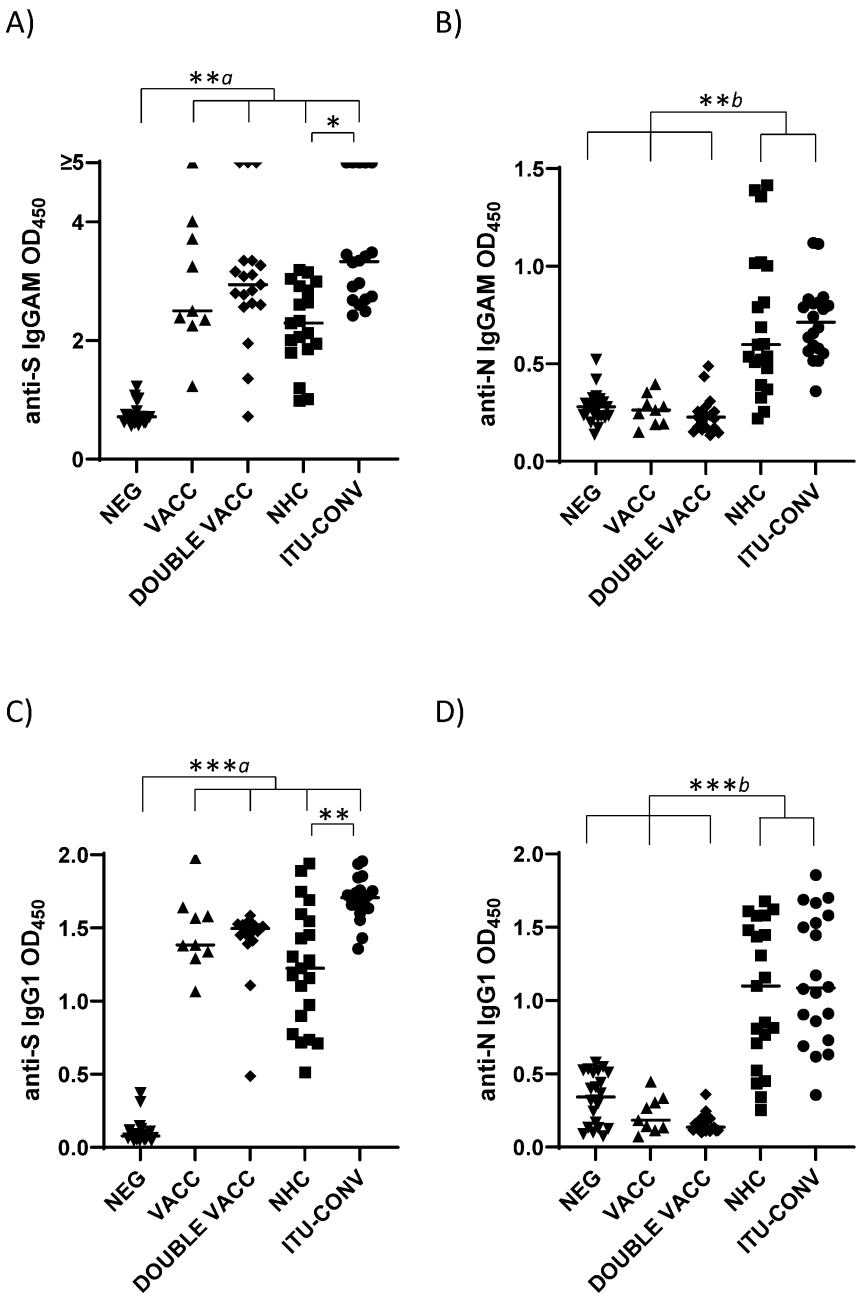


**Figure 5.1 Anti-S, but not anti-N antibody responses differ between NHC and ITU-CONV patients.** Using an ELISA against 0.1ug S (a, c) or N (b,d) with HRP-conjugated IgGAM or IgG1 secondary antibodies, GAM and IgG1 levels were assessed in the following subject groups: COVID-19 negatives (NEG, n ≥20), COVID-19 naïve one month post first BNT162b2 vaccine (VACC, n = 9), COVID-19 naïve one month post second BNT162b2 vaccine (DOUBLE VACC, n = 19), COVID-19 positive non-hospitalised convalescents (NHC, n ≥ 19) and COVID-19 positive convalescents who required ITU treatment (ITU-CONV, n ≥ 18) Kruskal-Wallis with Dunn's multiple comparisons test was used to test significance. a indicates that the four groups bracketed (VACC, DOUBLE VACC, NHC and ITU-CONV) were individually significantly different to the NEG group; b indicates that NHC and ITU-CONV are independently significantly different to NEG, VACC and DOUBLE VACC. *** $p < 0.001$, ** $p < 0.01$, * $p < 0.05$. Bars represent median values for each group.

**C1q binding *in vitro* correlates with levels of S- and N-specific IgGAM and IgG1 antibodies**

To determine if the complement protein C1q can bind to SARS-CoV-2-specific immunoglobulins *in vitro* we developed a solid phase C1q-binding assay. In these antigen-specific assays, the test serum from COVID-19 patients or vaccinees is heat-inactivated and standardisation of complement is provided by using sera from non-infected, non-vaccinated subjects. Results from this assay showed that C1q binding mirrored IgG1 levels for both S and N antigens, with the lowest signals for S seen in the NEG group (Figure 5.2A), and for N in the NEG, VACC and DOUBLE VACC groups (Figure 5.2B). The lack of C1q binding detected for N when sera from the VACC and DOUBLE VACC groups were tested is expected and consistent with a lack of prior infection by SARS-CoV-2 in these groups (Figure 5.2B), and we have included these two groups in our downstream analyses of the response to N for their value as control groups. No difference in C1q binding was observed between sera from the two convalescent groups (Figures 5.2A,B). Plotting IgG1 responses against C1q responses shows a positive correlation between the amount of IgG1 antibody and the amount of C1q binding detected (Figure 5.2C,D). Therefore, C1q binding reflects the serological response to both antigens.

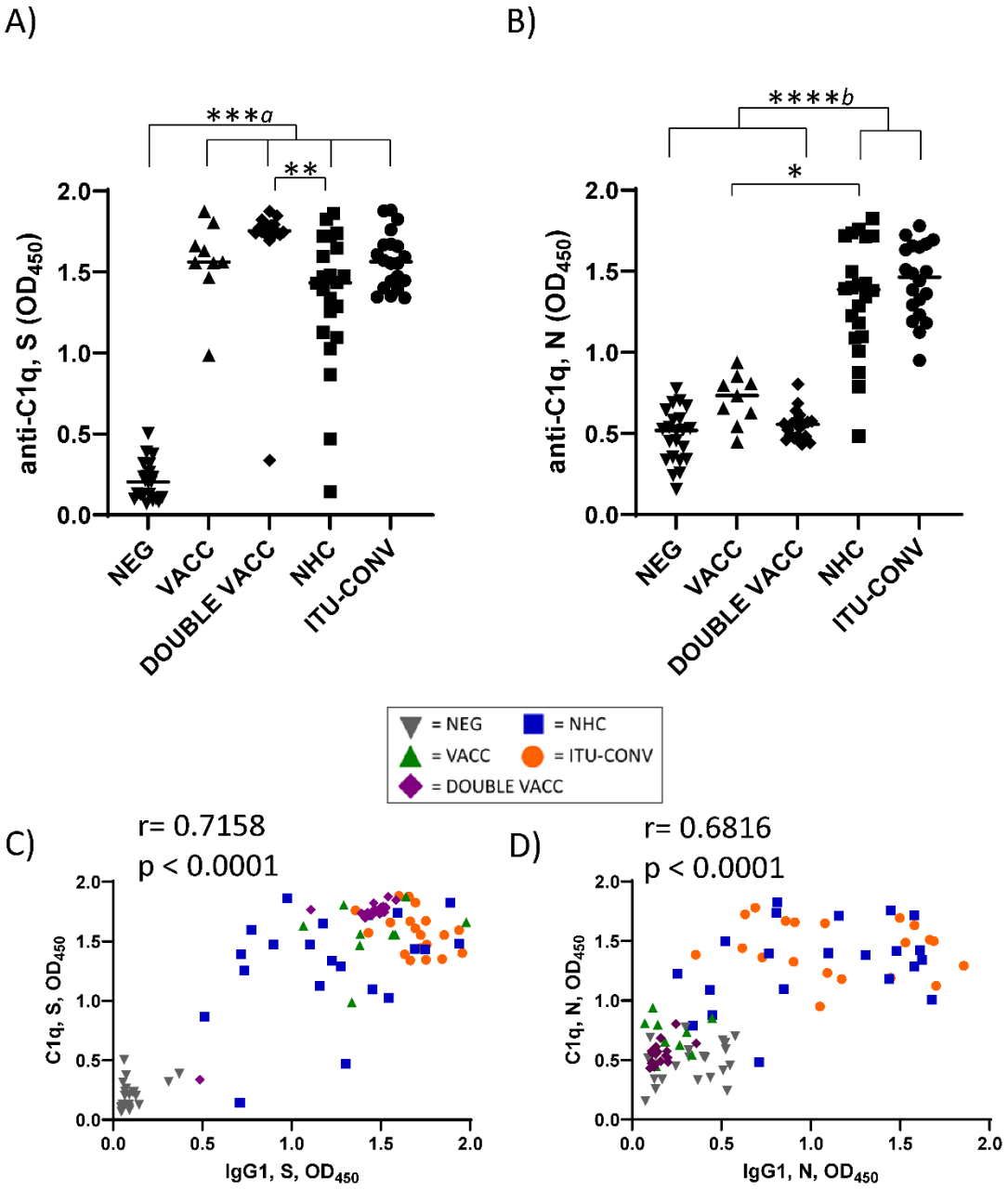


**Figure 5.2: C1q binding to S and N correlates with IgG1 responses.** Using an ELISA against 0.1ug S (a) or N (b) with an anti-C1q secondary antibody, followed by an HRP-conjugated tertiary, and the ELAST amplification kit, C1q binding was measured. Correlations of IgG1 OD and C1q OD against S (c) and N (d). NEG, n= 22. VACC, n =9. DOUBLE VACC n = 19. NHC, n ≥ 21. ITU-CONV n = 20. Kruskal-Wallis with Dunn's multiple comparisons test was used. a indicates that the four groups bracketed were individually significantly different to the NEG group; b indicates that NHC and ITU-CONV are independently significantly different to NEG and DOUBLE VACC. ** p < 0.01, * p <0.05. Bars represent median values for each group. Correlations were determined using the Spearman's rank correlation test (r and p values presented).

**Deposition of C4b, C3b and C5b varies dependent upon antigen tested and subject group**

To determine whether C1q binding reflected downstream activation of the complement cascade, we examined whether complement breakdown products could be detected. Deposition of C4b, a major component of the classical pathway C3 convertase, and the effector molecules C3b and C5b were assessed. In the absence of S or N-specific antibodies, C4b, C3b and C5b breakdown products were not detected, but they were detected in the presence of specific antibodies, indicating involvement of the classical complement pathway (Figure 5.3). When S was used as the assay antigen, the highest median levels of C4b, C3b and C5b deposition detected were in the DOUBLE VACC and ITU-CONV groups (Figure 5.3A), whereas the VACC and NHC groups showed similar lower levels of downstream activation. The median levels of C4b, C3b and C5b deposition detected when N was used as the assay antigen were similar between the NHC and ITU-CONV groups (Figure 5.3B). In contrast, for the NEG, VACC and DOUBLE VACC groups, where anti-N antibody responses and C1q binding were not detected, there was no downstream activation of the complement cascade. Therefore, in this assay differences in complement activation by antibody can be detected dependent upon what patient group and antigen were examined.

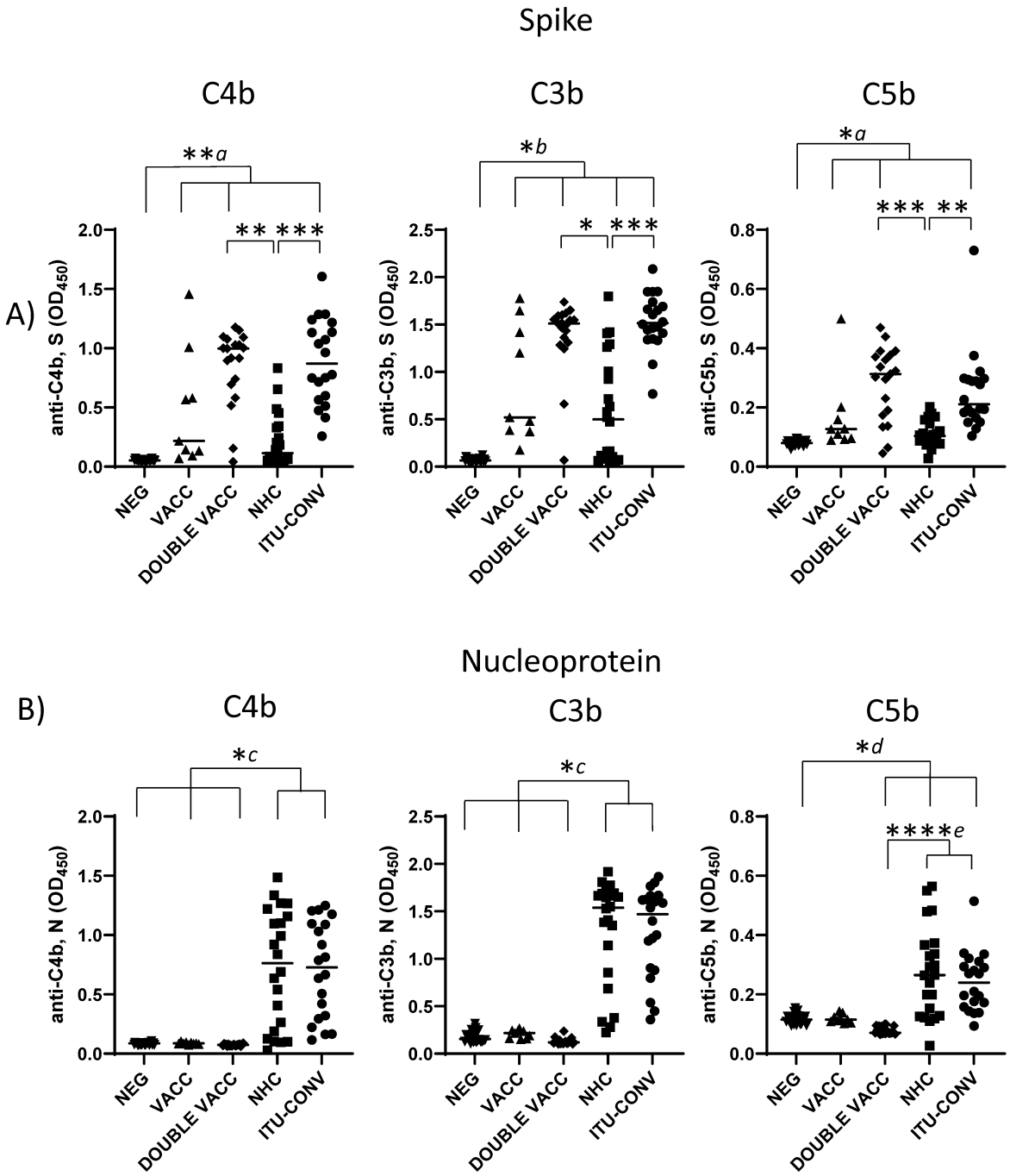


**Figure 5.3: C4b, C3b and C5b show antigen and subject status-dependent variability**. Using an ELISA against 0.1ug S (a) or N (b) with either anti-C4b, C3b or C5b secondary antibody, followed by an HRP-conjugated tertiary, downstream complement binding was measured. NEG, n= 22. VACC, n =9. DOUBLE VACC, n = 19. NHC, n = 22. ITU-CONV n = 20. Kruskal-Wallis with Dunn's multiple comparisons test was used. a and b indicate that the groups bracketed were individually significantly different to the NEG group; c indicates that NHC and ITU-CONV are independently significantly different to NEG, VACC and DOUBLE VACC; d indicates that DOUBLE VACC, NHC and ITU-CONV are all significantly different to NEG; e indicates that NHC and ITU-CONV are both significantly different to DOUBLE VACC. **** $p < 0.0001$, *** $p < 0.001$, ** $p < 0.01$, * $p < 0.05$. Bars represent median values for each group.

**Downstream complement activation associates with threshold IgG1 responses**

In contrast to the linear association between anti-S IgG1 and C1q detection, there was a non-linear association between IgG1 and C4b, where C4b was only detectable beyond a threshold level of IgG1. A correlation between C4b and IgG1 to N was also observed, as was a threshold response, although the threshold response was less clear for N than for S (Figure 5.4A). Similar threshold responses for IgG1 to S and N were also observed if C3b or C5b were plotted against IgG1 (Supplementary Figures 5.2A,B). When correlations were performed for C1q vs C4b (Figure 5.4B), C4b vs C3b (Figure 5.4C) and C3b vs C5b (Figure 5.4D) for both antigens, then clear correlations were observed. This suggests that in this assay threshold levels of IgG1 are needed to activate downstream complement components for S and N.

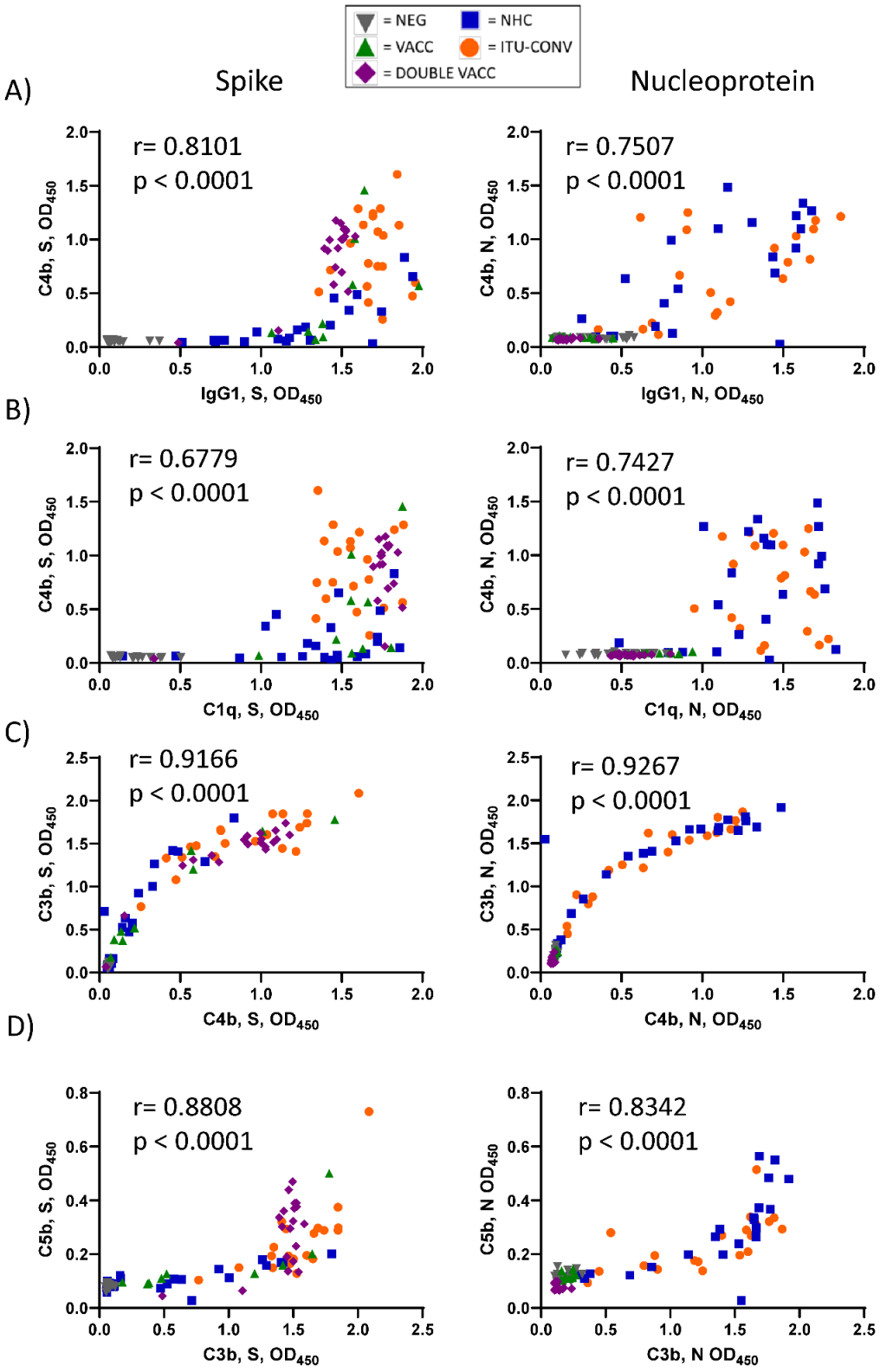


**Figure 5.4: C4b responses demonstrate a threshold response to IgG1 levels against S but not N.** All further downstream complement components correlate linearly. Correlations of data obtained in Figures 5.1c and 5.1d, Figure 5.2a and 5.2b and Figures 5.3a and 5.3b were plotted. XY pairs, n ≥ 91. Correlations were determined using the Spearman's rank correlation test (r and p values presented).

**IgG1 correlates with complement activation in sera with the lowest IgM levels detected**

IgM is the most efficient antibody isotype for fixing and activating complement (Keyt et al., 2020) yet most sera tested had only low levels of anti-S or anti-N IgM (Supplementary Figure 5.1A). This was expected due to the convalescent nature of our infected groups, and the minimum one month period after vaccination that sera were obtained from our vaccinated groups. This suggested IgG1 or IgG3 might compensate for IgM when IgM is not present at high levels. Therefore, we examined the level of complement fixation (C1q binding) and activation (C3b deposition) associated with antigen-specific IgM and how this correlated with antigen-specific IgG1 and IgG3 levels (Figure 5.5 and Supplementary Figure 5.3). To do this the IgM to S or N was correlated with C1q and C3b. There were modest correlations between IgM against S and C1q and C3b ($r = 0.4613$, $p < 0.0001$ and $r = 0.4753$, $p < 0.0001$ respectively; Figure 5.5A,C). To N protein, no correlation was identified, although only a few sera had elevated levels of IgM (IgM vs C1q, $r = 0.1661$, $p = 0.1155$ and IgM vs C3b $r = 0.09955$, $p = 0.3478$; Figure 5.5B,D) and if the 2 vaccinated groups (lacking anti-N responses) were excluded from the analysis for N, then the correlation became stronger (IgM vs C1q, $r = 0.3019$. $p = 0.0162$; IgM vs C3b, $r = 0.03509$, $p = 0.0048$). These results are consistent with IgM being able to activate complement when present, but not always being present at sufficiently high levels to do so. C1q binding and C3b deposition was detected for many sera in which IgM responses to S or N were low. We hypothesized that sera which exhibited the lowest IgM responses, but which could still fix and activate complement had higher levels of IgG1 or IgG3. We therefore divided the sera with the lower IgM levels into 2 groups, one group in which we detected the highest C1q or C3b levels (termed $IgM^{lo}C1q^{hi}$ and $IgM^{lo}C3b^{hi}$ respectively) and another group where we detected the lowest C1q and C3b levels (termed $IgM^{lo}C1q^{lo}$ and $IgM^{lo}C3b^{lo}$ respectively). The C1q or C3b response was then plotted against the IgG1 or IgG3 response. In the $IgM^{lo}C1q^{hi}$ and $IgM^{lo}C3b^{hi}$ groups higher levels of IgG1 were detected than in the $IgM^{lo}C1q^{lo}$ and $IgM^{lo}C3b^{lo}$ groups (Figure 5.5A-D and Supplementary Figure 5.3), and this difference was observed for both S and N. IgG3 levels were also higher in the $IgM^{lo}C1q^{hi}$ and $IgM^{lo}C3b^{hi}$ groups

than in the $IgM^{lo}C1q^{lo}$ and $IgM^{lo}C3b^{lo}$ groups (Figure 5.5A-D and Supplementary Figure 5.3). Therefore, complement fixation and activation is observed in the presence of IgG1 or IgG3 when IgM levels are low.

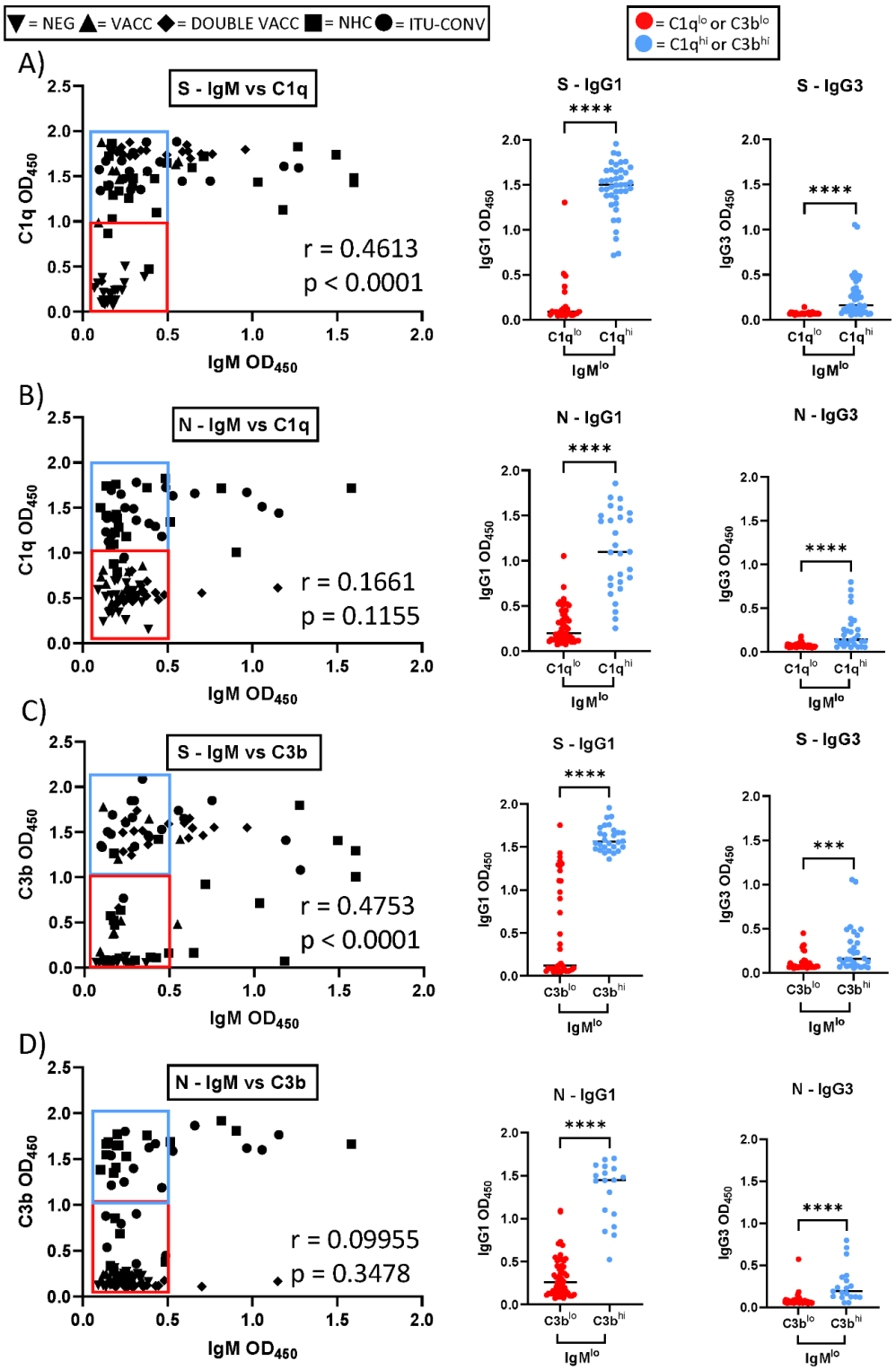


**Figure 5.5: Complement activation by sera with low levels of IgM to S and N**. (a) Left hand panel shows the IgM levels plotted against levels of C1q for S (left hand panel; results for 91 sera presented from NEG, VACC, DOUBLE VACC, NHC and ITU-CONV donors). The IgG1 levels for sera presented in the blue box ($IgM^{lo}C1q^{hi}$) or red box ($IgM^{lo}C1q^{lo}$) are shown in the central graph and for IgG3 in the right hand graph (n ≥ 18 for each group). Each coloured dot represents one sera from the corresponding coloured box. (b) As for a, but the anti-N response is presented. (c) and (d), as for (a) and (b) respectively but with the results for C3b binding shown rather than C1q. Correlations were determined using the Spearman's rank correlation test (r and p values presented). Mann-Whitney was used to test significance in the IgG1 and IgG3 column graphs, where **** $p < 0.0001$ and *** $p < 0.001$. Bars represent median values for each group.

## Discussion

Here we show (i) that antibodies to S and N can activate the classical complement cascade and (ii) the level of activation of the cascade detected vary dependent upon the subject group examined and the antigen used in the test. Therefore, antibodies to two different antigens within the same pathogen can activate the complement cascade *in vitro*, albeit at levels that depend on the severity of COVID-19. In the presence of specific antibodies to both S and N, similar levels of C1q binding were observed and the greatest variability was detected downstream of C1q binding. In contrast, in the NEG, VACC and DOUBLE VACC groups, where antibodies to N were not detected, activation of the complement cascade was not detected.

In this study, antibody needed to bind antigen in order to detect complement activation. Although threshold IgG1 levels were associated with activation of the complement cascade, the spread in the complement responses observed to spike and nucleoprotein did show some differences (e.g. Figure 3). Such observations may reflect the assay or other factors such as how antibodies themselves interact with these antigens or intrinsic differences in the antigens themselves. For instance, S is a trimeric protein and the approximately 420 kDa trimer is substantially larger than N, which is approximately 46 kDa. This difference may influence how IgG binds to the antigen and affects complement activation. Moreover, the trimeric structure of S means identical epitopes can be juxtaposed to one another in a highly defined manner (Hsieh et al., 2020, Bangaru et al., 2020, Wrapp et al., 2020) enabling multiple Fab to bind their target epitopes and promoting cross-linking of antigen. Other factors may also contribute to this process, such as which epitopes are targeted within the S protein. For instance, large-scale changes in the glycosylation pattern of S proteins has a surprisingly limited impact on the level of antibody binding by patient sera as determined by ELISA (Chawla et al., 2021). One interpretation of this is that there are only a limited number of antibody sites available on each S glycoprotein for antibodies to bind, presumably in part because of a combination of relatively few (proteinaceous)

epitopes targeted and the steric effects of antibodies themselves. This is similar to what we have observed for epitope recognition by antibodies targeting cell surface proteins on the surface of *Salmonella enterica* serovar Typhimurium (Domínguez-Medina et al., 2020). Moreover, studies examining antibody responses to the S glycoprotein of the Omicron variant in sera from vaccinated individuals suggest that amino acid changes in the relatively hypoglycosylated RBD (Watanabe et al., 2020, Grant et al., 2020, Wu et al., 2022) region can have dramatic effects on antibody binding (Faustini et al., 2022) and so may be more likely to affect the level of complement activation. Other factors that may influence complement activation include how antigen is distributed on the surface of the virus (for S) and elsewhere in the host after natural infection. In the context of this assay, technical factors such as how antigen binds to the plate may influence the results observed. Furthermore, the trimeric vs monomeric nature of the antigens tested, the maintenance of native conformation, and the level of antigen denaturing may all influence the results observed using these assays. This highlights the need to develop multiple approaches to study antibody-antigen interactions *in vivo* to contextualise the *in vitro* results presented here.

IgM is the most efficient antibody isotype for activating the complement cascade (Keyt et al., 2020). Nevertheless, as seen in many studies, the sera used in this study from individuals' convalescent post-vaccination or infection, had modest or background levels of antigen-specific IgM detected. Those $IgM^{lo}$ sera that could bind complement had higher IgG1/3 levels than those $IgM^{lo}$ sera that could not activate the complement cascade. Therefore, the results from this study are possibly most relevant for understanding the relationship between IgG isotypes and complement activation, whereas the more pronounced complement-fixing properties of IgM may modulate the strengths of the responses observed. It is likely that in the presence of high levels of IgM, such as during the acute phase of a primary infection, there would be enhanced levels of complement activation. Nevertheless, the activation of the complement cascade in the absence of IgM may be possible and important for the pathophysiology of disease in other scenarios, as well as in the convalescent subjects we have

presented here. For instance, many children with severe complications from COVID-19 (Multisystem Inflammatory Syndrome in Children (MIS-C)/paediatric inflammatory multisystem syndrome temporally associated with SARS-CoV-2 infection (PIMS-TS)) present with disease at times when they have low/negligible levels of IgM, yet high levels of IgG, especially IgG1 and IgG3 (Perez-Toledo et al., 2021). This correlates with a strong signature associated with complement activation (Syrimi et al., 2021). Collectively, this likely means that IgM can play important roles in activating the complement cascade, but that it is not essential.

The results from these studies lead to further hypotheses to test. For instance, it is known that ITU subjects can have greater activation of the complement cascade (Carvelli et al., 2020, Holter et al., 2020), and this could be compounding their disease. Indeed, targeting both C3 and C5 within the complement cascade as a way to treat COVID-19 shows promise (Annane et al., 2020, Zelek et al., 2020, Mastellos et al., 2020, Vlaar et al., 2020). The availability of assays such as those described here will help increase understanding of how these inhibitors act to interfere with the complement cascade in the presence of antibody to different SARS-CoV-2 proteins. Alternatively, since all these subjects survived severe COVID-19 infections it could be hypothesised that the activation of complement is associated with a beneficial outcome. As we did not have sera from individuals who died this is not testable here. One caveat in this argument is that exogenous sources of complement in the form of sera from non-infected individuals were used in these studies and that patients own sera may differ in potency, or polymorphisms in complement components themselves could influence the consequences of complement activation (Ramlall et al., 2020, Delanghe et al., 2021). This was not assessed here as the focus was on antibody-mediated activation of complement where we have attempted to standardize the amount of complement available, particularly for the downstream complement components. Additionally, these studies were performed using sera from patients who were infected or immunized weeks previously and the antibodies present may not reflect the antibodies present at the time of infection. Certainly, it could be expected that the affinity of the antibodies would increase

over time. One striking feature was the variability in the anti-C4b/C3b response detected in the VACC group. It is unclear why this is the case, but it could simply be that there is variability within the wider population in the ability to activate complement downstream. Ultimately, the results generated by these assays are trying to recapitulate the complexity of the complement cascade *in vivo*, which is considerably more complex than what is observed or testable *in vitro*. For these reasons, it is important to interpret the outcomes from these assays as the starting point for further investigations. For instance, in these assays potential inhibition of activation is not attempted. Neither is the separation of competition for epitopes between antibody isotypes that are associated with greater complement-activating potential (e.g. IgM or IgG1) than others (e.g. IgA), or controlling for the absolute levels of each isotype present. Nevertheless, the differences observed may be indicative of differences that can occur in the patients in different tissues or organs or at different stages of infection.

The complement cascade has been reported to be activated through multiple pathways after SARS-CoV-2 infection (Ali et al., 2021, Jarlhelt et al., 2021, Medjeral-Thomas et al., 2021, Yu et al., 2020). Amongst these, the engagement of the classical pathway is distinct to the non-antibody-dependent pathways due to the potential multiple roles antibody can play during the course of infection. If induced whilst an infection is ongoing, then the activation of the complement cascade by antibody could worsen disease, particularly as antibody responses become detectable concomitant with risk of severe disease. This could happen either through enhanced inflammation (Jarlhelt et al., 2021), such as observed during acute respiratory distress syndrome, or through enhancing the complications of thrombosis and coagulopathy after infection (Magro et al., 2020, Skendros et al., 2020). Moreover, antibodies are induced to multiple SARS-CoV-2 antigens and as we show, antibodies to S and N proteins have the capacity to activate complement *in vitro*. At the sites where complement is activated during primary infection, there could be additional increases in the anaphylatoxins C3a, C4a and C5a, as has been reported (Carvelli et al., 2020, Lipcsey et al., 2021, Ma et al., 2021, Holter et al., 2020). These could augment local inflammation through promoting the recruitment of more neutrophils and

monocytes leading to tissue damage and worsen disease in patients. In addition, in humans challenged with influenza virus increased levels of C3a and C5a were detected in the upper respiratory tract (Bjornson et al., 1990), intriguingly most often during the recovery phase rather than the acute infection phase, presumably concomitant with when antibody responses are established. Other effects of complement activation may include the destruction of host cells due to the formation of MAC and the activation of the coagulation cascade and effects on the vasculature (Lo et al., 2020, Ramlall et al., 2020, Lipcsey et al., 2021, Martínez-Salazar et al., 2022).

Balancing this, positive roles for antibody-mediated complement activation have also been proposed during active infection and vaccination (Kurtovic and Beeson, 2021). Potentially, the most valuable contribution antibody-mediated complement activation could make to protection is in vaccinated individuals or in those recovered from prior infection. In such individuals, the level of antigen present is likely to be low when antibody encounters its target antigen. This binding of antigen by pre-existing antibody will still result in immune cell recruitment and activation, helping to prevent the wider dissemination of the virus, but the overall magnitude of these sequelae will be lower. This reduced level of inflammation compared to what is observed when antibody is induced during infection could result in reduced levels of immunopathology. Therefore, antibody-mediated activation of complement in this context may be more beneficial for the host because it is contributing to control of infection when the pathogen burden is relatively low and less likely to provoke severe inflammatory responses.

The site of pathogen encounter is likely to influence the type of antibody present, the amount of complement and the outcomes from complement activation. At mucosal surfaces there is an enrichment of anti-pathogen IgA as well as the presence of IgG: IgA is less efficient at activating complement than IgM, IgG1 and IgG3 (Woof and Russell, 2011, Daha et al., 2011). In saliva, which is often used as a proxy for mucosal responses, both IgA and IgG to SARS-CoV-2 are readily detectable after infection (Cervia et al., 2021, Costantini et al., 2022), but this is less so after vaccination alone

(Azzi et al., 2022). In contrast, IgM is typically not a major component of the antibody repertoire detected in saliva (Klingler et al., 2021). Although there are significant levels of complement in the upper and lower respiratory tract (Bolger et al., 2007, Varsano et al., 2000), the relative predominance of IgA may mean there is less activation of the complement cascade even between the upper and lower respiratory tracts. Limiting any inflammation or immunopathology associated with complement activation may be beneficial for maintaining barrier integrity. Nevertheless, significant levels of complement and its breakdown components are found in the respiratory tract after many different infections (Mateu-Borrás et al., 2022, Wells et al., 2014, Satyam et al., 2021). This means that complement can be activated in the respiratory tract and so in some circumstances may have negative impacts on the host.

In summary, we have identified activation of the classical complement pathway after vaccination against COVID-19, or after COVID-19 infection. Future studies will help us further understand how complement is activated in the presence of antibodies and how this may contribute to protection and harm in those who encounter this pathogen.

**Author Contributions**

Conceptualization: EMJ, AS, LH, IH, JR, DW, MC, MD, AR, AC. Methodology: RL, EMJ, MPT, SJ. Investigation: RL. Data analysis: RL. Resources: SF, MG, MN, IC, TD, TV, AS, AR. Supervision: SW, AC. Writing – original draft: RL, AC. All authors reviewed and edited the final manuscript.

# *Supplementary Material*

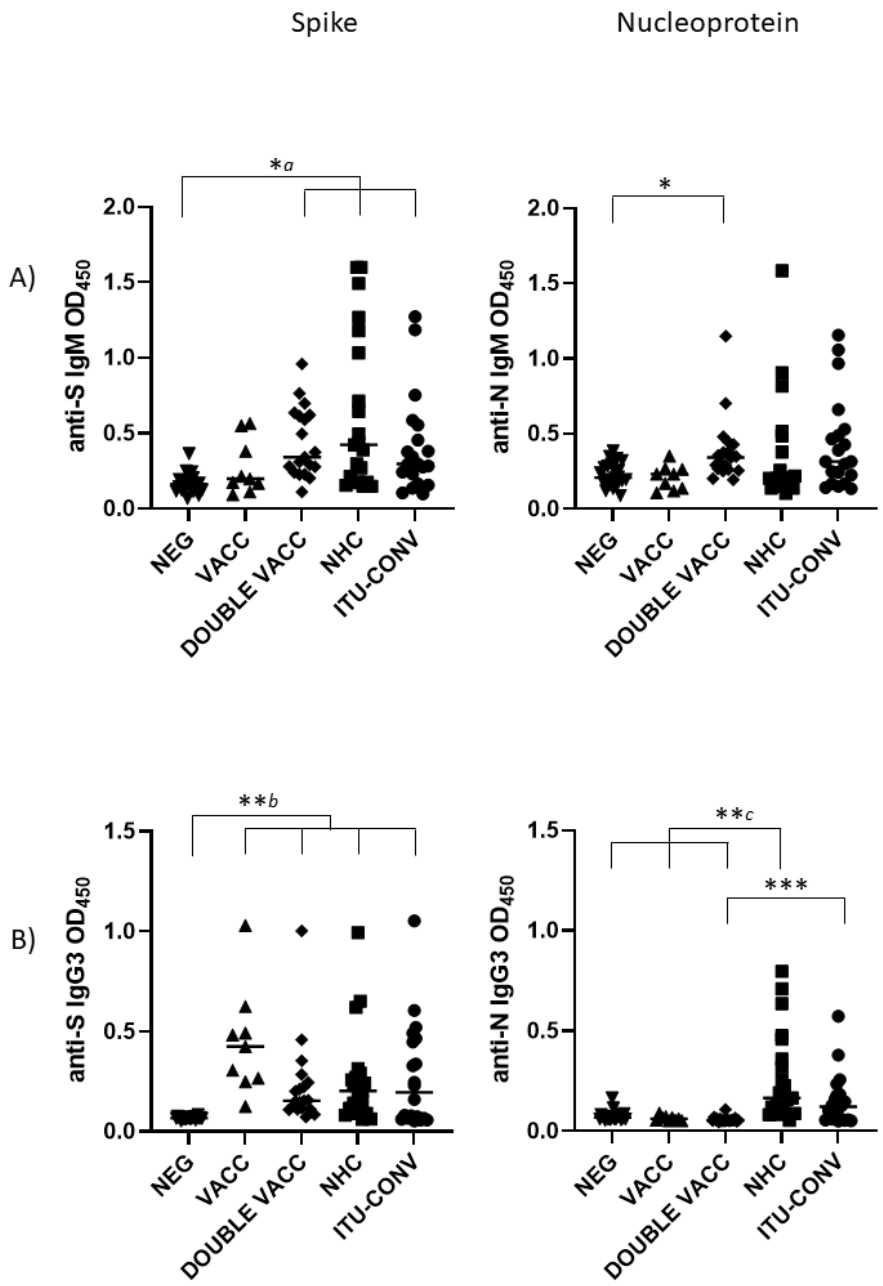


**Supplementary Figure 5.1: Anti-S and N IgM and IgG3 responses in sera from different groups after infection or vaccination.** Serological responses were assessed by ELISA using HRP labelled a) anti-IgM and b) IgG3 against 0.1ug purified S or N. Kruskal-Wallis with Dunn's multiple comparisons test was used to test significance. a and b indicate that the groups bracketed were individually significantly different to the NEG group; c indicates that NEG, VACC and DOUBLE VACC are independently significantly different to NHC. *** $p < 0.001$, ** $p < 0.01$, $p < 0.05$. Bars represent median values for each group. NEG, n = 22. VACC, n = 9. DOUBLE VACC, n = 19. NHC, n = 21. ITU-CONV, n = 20.

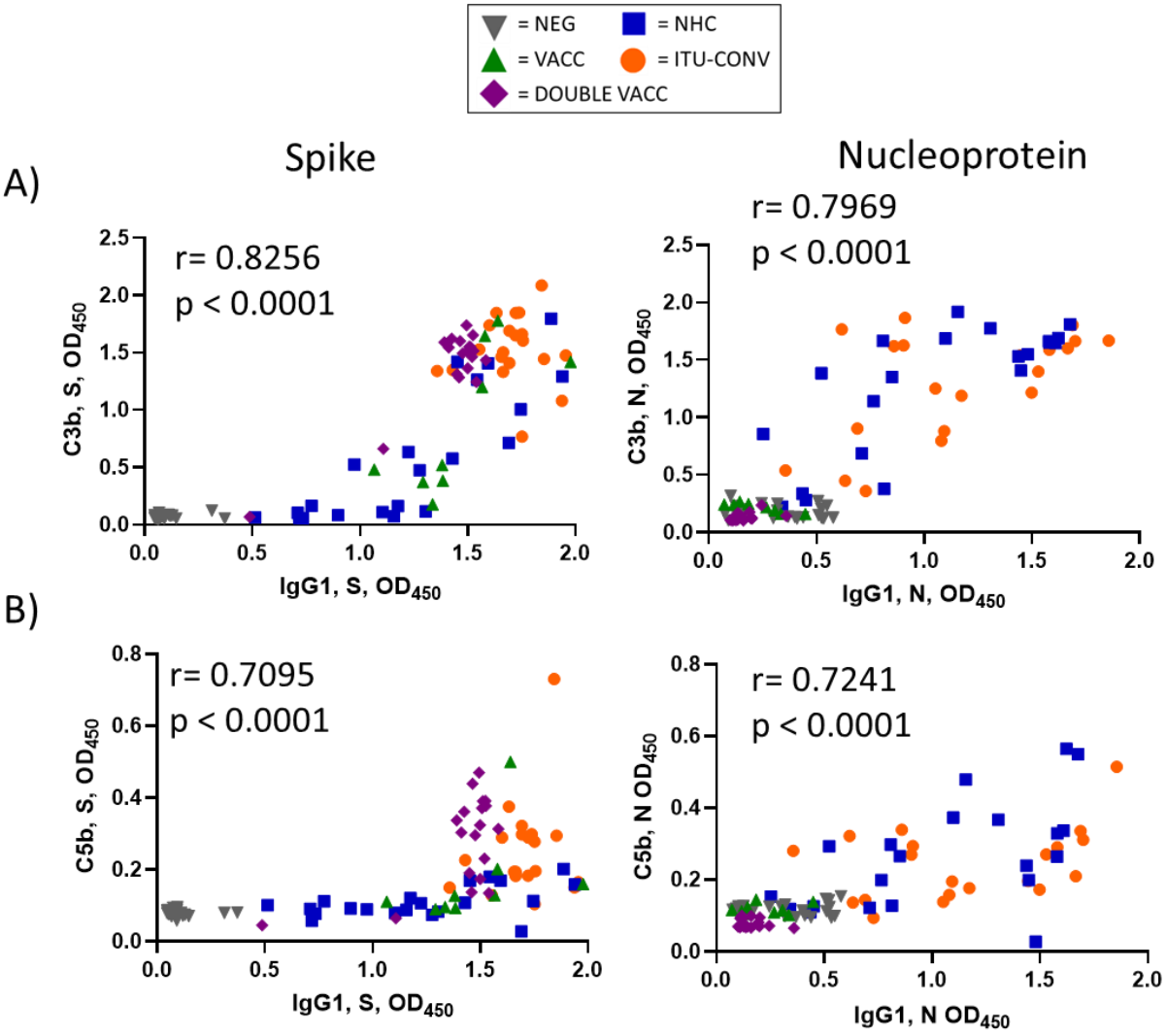


**Supplementary Figure 5.2: Correlations between (A) IgG1 and C3b or (B) IgG1 and C5b for S and N.** Correlations of data obtained in Figs 1c and 1d, and Figs 3a and 3b were plotted. XY pairs, n = 91. Spearman correlation was used to assign r and p values.

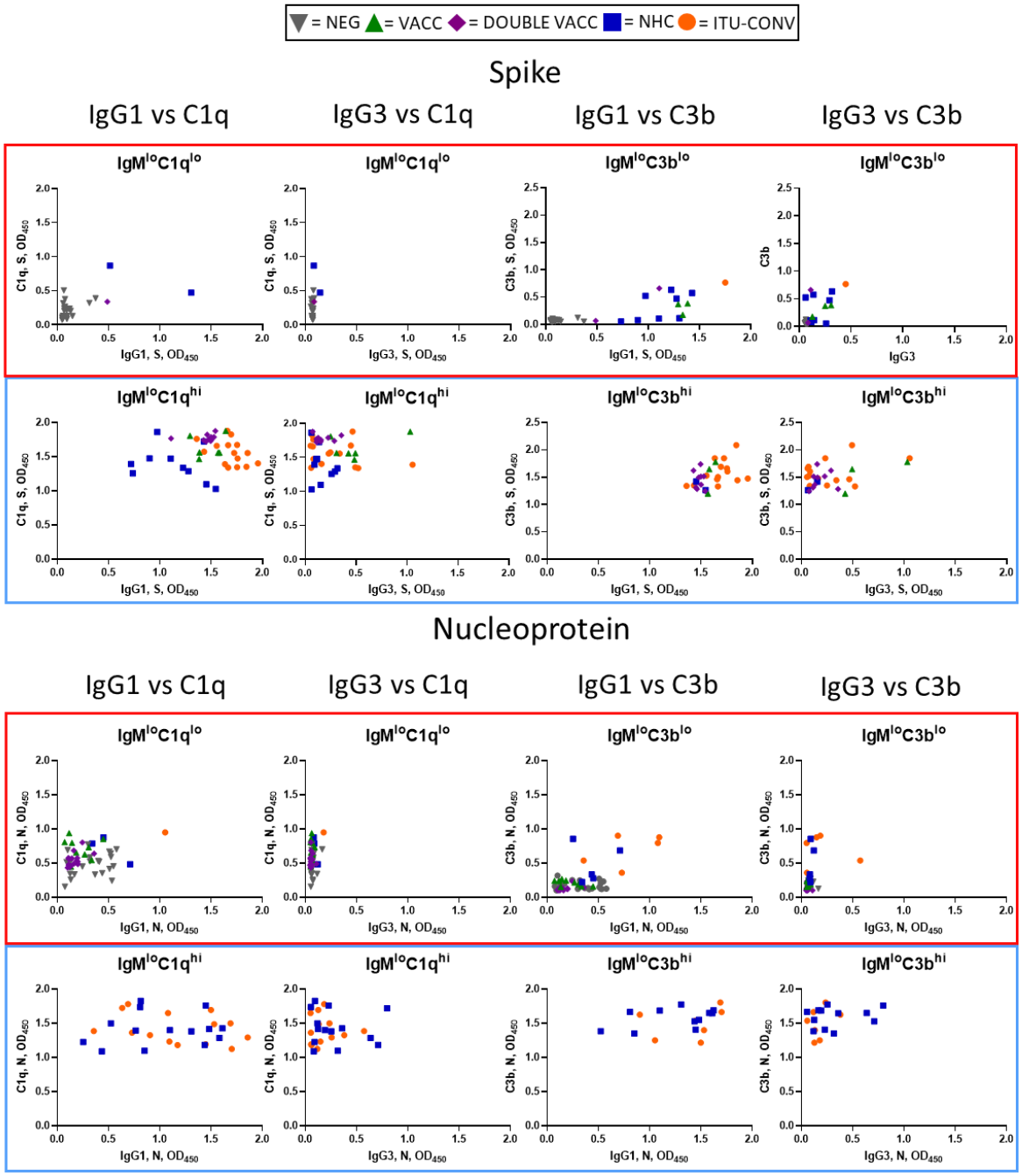


**Supplementary Figure 5.3: Results of comparisons between IgG1 or IgG3 and C1q and C3b from sera with low levels of IgM to S and N.** Scatter graphs showing IgG1 vs C1q, IgG3 vs C1q, IgG1 vs C3b or IgG3 vs C3b for the sera contained in the blue or red boxes shown in Figure 5.

| | NEG | VACC | DOUBLE VACC | NHC | ITU-CONV |
|---|---|---|---|---|---|
| S IgGAM | 0.72 | 2.50 | 2.95 | 2.28 | 3.32 |
| N IgGAM | 0.28 | 0.26 | 0.22 | 0.60 | 0.72 |
| S IgG1 | 0.07 | 1.38 | 1.49 | 1.22 | 1.71 |
| N IgG1 | 0.34 | 0.18 | 0.14 | 1.10 | 1.09 |
| S IgM | 0.16 | 0.20 | 0.33 | 0.42 | 0.30 |
| N IgM | 0.20 | 0.23 | 0.34 | 0.20 | 0.31 |
| S IgG3 | 0.07 | 0.42 | 0.15 | 0.20 | 0.19 |
| N IgG3 | 0.07 | 0.06 | 0.05 | 0.16 | 0.12 |

**Supplementary Table 1: Summary table of median antibody optical density values against S and N in different patient groups.** Median values obtained from data in Figure 1 and Supplementary Figure 1. n ≥ 18 for all groups.

END OF PAPER

## 5.2 Discussion

Our paper confirms that both spike and nucleoprotein can activate the classical complement pathway *in vitro*. In this short discussion, in addition to the one in the paper, I aim to show how our work fits in with literature published during/after our submission, and what this might mean more broadly in terms of classical pathway activation in COVID-19.

One study published while we were finalising our manuscript mirrors what we find with deposition of C3, C4 and C5b-9 *in vitro*, as well as positive correlations of these with IgG levels. However this study was limited to assessing responses to S protein using convalescent samples (Jarlhelt et al., 2021). A further study looking at maternal transfer of SARS-CoV-2 antibodies in mice has also showed C1q deposition on S protein, with this positively correlating with IgG level (Agostinis et al., 2023). Furthermore, other studies have shown deposition of C1q on various cells and tissues in COVID-19 patients, including brain endothelial cells and platelets (Lee et al., 2022), blood monocytes (Lage et al., 2022) , kidneys (Jamaly et al., 2021), cardiac macrophages (Weckbach et al., 2022) as well as the lung, skin and liver deposition shown early on in the pandemic (Magro et al., 2020, Macor et al., 2021).

Despite consistencies between the studies above, there are studies whose findings differ. For instance, despite Magro et al. (2020) showing co-localisation of C4d and C5b-9 with spike protein in the lungs, another group failed to replicate this in their study. Niederreiter et al. (2022) did not see a significant increase in C1q deposition in their COVID-19 lung autopsy tissue compared to controls, and could only identify spike protein in 22% of lung samples. Many of the complement deposits and spike protein colocalization shown in Magro et al were in the microvasculature, which Niederreiter were unable to study due to poor tissue quality, which could perhaps explain the discrepancies between these studies. Furthermore, 19/38 of the Niederreiter cohort had an illness duration of ≤10 days, so even where spike protein was present in the lung tissues, the short duration of illness could mean a lack of anti-spike antibody for the C1q to bind to.

It is important to state that not all of the studies mentioned above looked for co-localisation of SARS-CoV-2 proteins, while some looked, but could not find evidence of SARS-CoV-2 presence in their tissues (eg. brain (Lee et al., 2022) and heart biopsy (Weckbach et al., 2022), although another study found SARS-CoV-2 can be found in the heart, but infected cells were very rare, with a median of 1 infected cell/$cm^2$ (Bearse et al., 2021)). Therefore, although our paper shows classical pathway activation can take place in response to SARS-CoV-2 proteins, it is worth remembering that not all papers reporting C1q deposition *in vivo* have shown whether this is related to COVID antigen-antibody complexes, or is a more generic, secondary inflammatory response.

One study that demonstrates this secondary complement upregulation is that by Zhang et al. (2023), focussing on the vasculature. They used conditioned media from SARS-CoV-2 infected (or mock infected) hACE2-A549 epithelial cells and investigated the effects of this media on human lung microvascular endothelial cells (HLMVECs). The HLMVECs cultured in the conditioned media from infected epithelial cells media (compared to the mock infected cell conditioned media) for 24 hours had upregulated levels of C3, C3aR1, FB and C1QA mRNA and protein (Zhang et al., 2023), demonstrating secondary complement upregulation due to the local proinflammatory environment, rather than SARS-CoV-2 proteins themselves.

Whilst the liver is believed to be the main organ that synthesises circulating complement, production of complement is not restricted to this organ (Kolev et al., 2014, Lubbers et al., 2017). C1q (along with C1r/s, C4, C3 and C5) can be produced by numerous immune cells, including monocytes, macrophages and dendritic cells (Lubbers et al., 2017), as well as endothelial cells (Morgan and Gasque, 1997). This production can be triggered by local inflammation, with many cytokines, such as IFN-γ and IL-1, known to stimulate complement synthesis (Falus et al., 1990, Zhou et al., 2001). Therefore, although some of the studies mentioned above show an increase in C1q, it is difficult to distinguish *in vivo* between increased production of components, and actual initiation and further downstream activity of the

complement pathway in these locations, without staining for multiple components at once. Whilst our paper has shown that classical complement activation is very much possible where SARS-CoV-2 proteins reside, clearly other mechanisms related to the general inflammatory nature of COVID-19 will be involved where SARS-CoV-2 proteins are not found (or found very sparsely), such as in the brain and heart (Lee et al., 2022, Weckbach et al., 2022).

For example, classical pathway activation could be taking place via non-SARS-CoV-2 antibodies, such as natural antibodies or autoantibodies. Many autoantibodies have been linked with COVID-19, (reviewed in detail in (Damoiseaux et al., 2022)) varying from angiotensin-II (vasoconstricting peptide) (Briquez et al., 2022) to E-selectin (cell adhesion molecule expressed on endothelial cells) (Juanes-Velasco et al., 2022), to cytokines such as IL-1β, IFN-γ, IL-21 and GM-CSF (Wang et al., 2021, Manry et al., 2022). With all these examples present in the blood vessels, they could potentially be activating the classical pathway in sites distal to the actual SARS-CoV-2 infection, rather than SARS-CoV-2 itself.

In conclusion, our results show that classical complement pathway activation by SARS-CoV-2 spike and nucleoprotein in the presence of specific antibodies is possible, and that antibodies from non-hospitalised convalescent patients differ in their ability to activate downstream complement compared to ICU-convalescent patients. The downstream complement responses of double vaccinees are of similar levels to that of ICU-convalescent patients against spike protein, with these groups depositing the highest levels of C3b, C4b and C5b on spike protein out of the cohorts tested. Our work is consistent with subsequently published work, although one must be mindful with autopsy and blood measurements that look at C1q alone that deposition may not always be directly linked to SARS-CoV-2 proteins as shown in our study, but could be due to binding to C reactive protein for example, or increased expression due to the local proinflammatory environment. These considerations further add to the complexities of determining the mechanistic intricacies of COVID-19.

# CHAPTER 6: FINAL DISCUSSION

In this thesis, inflammatory host responses to the pathogens *Salmonella* Typhimurium and SARS-CoV-2 have been investigated. A wide variation in host platelet responses were seen to STm strains, which is likely due to the levels of antibodies that recognise *Salmonella* in the donor plasma. In a physiological blood flow system, STm was able to bind to endothelial cells, with platelets binding to these primed ECs. Looking at SARS-CoV-2, both spike and nucleoprotein are able to activate the classical complement pathway, with the strength of downstream complement activation differing across different convalescent and vaccinated patient groups. In this final discussion, I aim to bring together the work done in my three chapters, focussing on platelets, endothelial cells, and complement, and how this triad of components could be involved in severe host-responses to pathogens.

## 6.1 Mechanisms behind donor variation in platelets to *Salmonella*

In chapter 3, I show that donor variation in platelet responses to STm is likely due to differing levels of *Salmonella*-binding antibodies present in the plasma. My proposed mechanism behind this is shown diagrammatically in Figure 6.1. In a donor who has little *Salmonella*-binding antibody, the chances of the antibody coming into contact with a *Salmonella* molecule are low, as are the chances of this complex binding to platelet FcγRIIA. However, if these interactions do occur, due to the low level of antibody on the *Salmonella* molecule, and the low affinity of the Fc domain for FcγRIIA, the platelet FcγRIIA receptor is unable to be cross-linked/clustered, so platelet activation does not occur (Figure 6.1, top panel). In a donor who has a higher level of *Salmonella*-binding antibodies, there is an increased probability of antibody-*Salmonella* complexes forming, and of these interacting with platelet FcγRIIA. In this case, the higher level of antibody bound to *Salmonella* is able to cross-link FcγRIIA and cause the receptors to cluster. This triggers downstream signalling leading to platelet activation, and ultimately platelet aggregation (Figure 6.1, bottom panel).

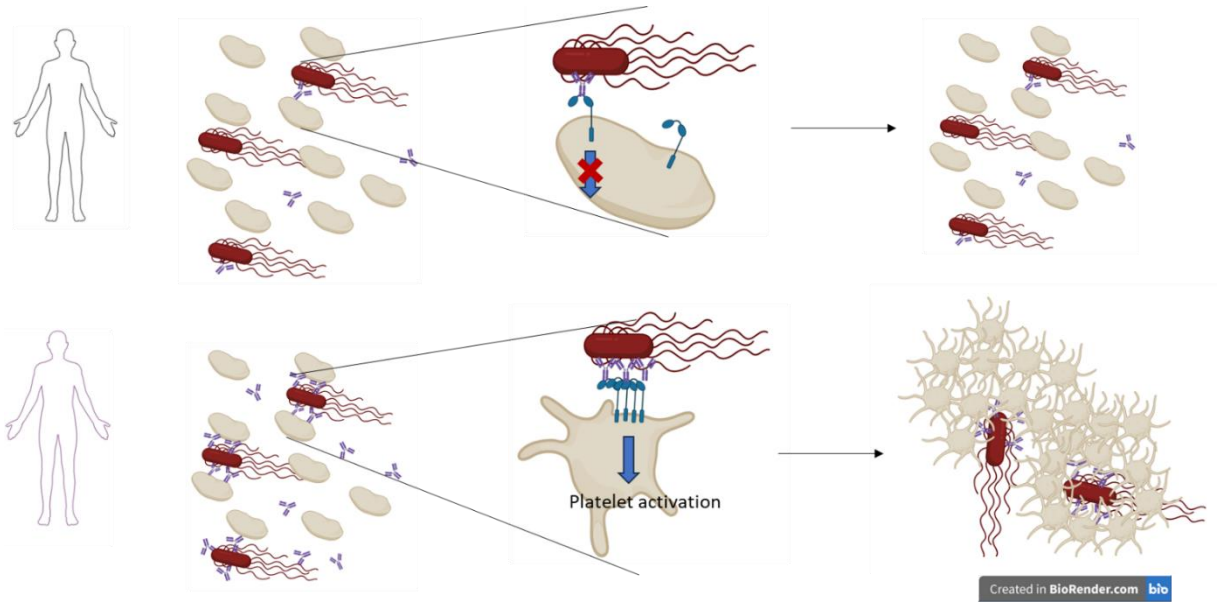


**Figure 6.1: Diagram of hypothesised mechanism for donor variation in platelet responses to *Salmonella*.** Briefly, in the top panel, the donor has few *Salmonella*-binding antibodies, so any antibody-antigen complexes binding to platelets are unable to cause FcγRIIA clustering, therefore the platelet is not activated. In the bottom panel, the donor has many anti-*Salmonella* antibodies, so the antigen-antibody complexes are able to induce FcγRIIA clustering, leading to downstream signalling and platelet activation. Positive feedback mechanisms then cause further platelet aggregation.

Given antibodies signal via FcγRIIA, an interesting point to raise here are the findings of the *Salmonella* mouse model. Platelet activation in response to *Salmonella* infection takes place in these mice, leading to thrombus formation in the liver and spleen, but the mechanisms must be different, as mouse platelets do not express FcγRIIA, so therefore cannot activate platelets via the mechanism proposed here for humans. This is perhaps one potential explanation as to why human platelet aggregation *in vitro* can take place in the space of minutes, yet *in vivo* in the mouse takes one and seven days for the spleen and liver respectively. The CLEC-2/podoplanin axis has been shown to be important in mice for thrombus formation in response to *Salmonella.* Whether this is the case in humans is currently unknown, but given the findings of this thesis, one could hypothesise this pathway would likely play a lesser role in humans compared to mice, especially as CLEC-2 expression on mouse platelets is over 10 times greater than on human platelets (Gitz et al., 2014, Zeiler et al., 2014).

Only IgG levels were measured in this thesis as human platelets do not have any other antibody receptors. However, *in vivo*, or in whole blood, other antibody isotypes could be important. For

instance, IgM is the most efficient antibody at engaging the complement system. As discussed in introduction section 1.5.6, platelets have the complement receptor C1q, albeit expressed at a low level (Burkhart et al., 2012), and may express C3R upon activation (Martel et al., 2011). Therefore, there is the potential for IgM levels to influence platelet aggregation via these. Of course, this would require further research, and the confirmation that complement is indeed capable of causing platelet activation upon binding to platelet complement receptors, but this would be something worth exploring.

With the link between IgG levels and aggregation demonstrated in this thesis, it could be suggested that development of a drug targeting FcγRIIA would be worthy of more research. FcγRIIA however is also expressed on monocytes, macrophages, neutrophils, eosinophils, basophils, mast cells and some T cell populations, where it has roles in stimulating phagocytosis, granulocyte release and even perhaps enhancement of T cell proliferation (Anania et al., 2019). Therefore, any drug aiming to block the interaction between IgG-*Salmonella* complexes with the aim of reducing platelet activation/thrombus formation, would also affect the broader immune response, which could have many undesired effects.

One thing to note is that the concentration of bacteria required in this thesis to induce platelet responses is very high. The STm strains were regularly used at a final concentration of ~3.3 x $10^8$ CFU/ml, in contrast to the average blood culture result of iNTS patients of 1 CFU/ml (Gordon et al., 2010). Whilst blood culture findings could be an underestimate due to the potential of *Salmonella* binding to the endothelium, the concentrations in blood are still not going to reach those used in this thesis. However, it is not uncommon for bacterial-platelet interaction studies to use high concentrations of bacteria, with the amounts of *Salmonella* used here in the same order of magnitude as many other bacterial-platelet interaction studies (Ford et al., 1996, Arman et al., 2014, Corcoran et al., 2007, Keane et al., 2010b, Kerrigan et al., 2002). One must also bear in mind that the high concentration of bacteria used are allowing platelet aggregation to take place very quickly, within 30

minutes. In comparison, in the mouse model, thrombi occur after 1 and 7 days in the spleen and liver respectively. Duration of illness in humans with iNTS has limited study data (Marchello et al., 2022) but tends to be in the order of weeks. Therefore, whilst the experiments are not physiological in this way, with high concentrations of bacteria allowing an artificially fast response, they still provide a useful setting in which to elucidate the potential mechanisms involved at the molecular level.

## 6.2 Complement and COVID-19

Whilst our paper showed the SARS-CoV-2 proteins S and N are capable of activating the classical complement pathway *in vitro*, and many studies have shown increased levels of both blood complement and complement deposits in patients with severe COVID-19 (Boussier et al., 2022, Defendi et al., 2021, Holter et al., 2020, Lage et al., 2022, Ma et al., 2021, Macor et al., 2021), it is still unclear as to whether the complement system is playing a positive role, helping to clear SARS-CoV-2, or whether its dysregulation is causing more harm than good by damaging the host. This proves to be a very difficult question to answer, and as seen for platelet responses to *Salmonella* in chapter 3, could be variable between individuals. Defendi et al. (2021) studied complement activation markers of 74 hospitalised COVID patients, clustering them based on these markers. Interestingly, the cluster of patients with the highest levels of alternative and lectin complement pathway markers had the worst outcomes, with the highest proportion of patients requiring oxygen treatment, ICU treatment, or dying. This has been confirmed in other studies by assessing RNA levels of markers (Boussier et al., 2022), and in another study that looked at alternative pathway markers only (Siggins et al., 2023). In contrast, the cluster with the highest classical complement pathway markers had the lowest mortality, and low requirements for oxygen or ICU treatment. However, one study found severe disease in their cohorts was marked by higher levels of classical pathway activation (Devalaraja-Narashimha et al., 2023), with a further group linking C1q, C1r (classical pathway) and Factor D (alternative pathway) to fatal outcomes (Georg et al., 2022). Interestingly, this group also showed that higher levels of Factor I (which inhibits classical and lectin pathways) led to better outcomes (Georg et al., 2022).

As well as these contrasting studies obtaining different results, the issue of whether complement activation is a helpful or harmful response is further complicated in Defendi et al. (2021) by the other two patient clusters. Both clusters had normal levels of all complement markers, yet half (and therefore split into one cluster) of the patients had severe disease, whilst the other half had low levels of ICU treatment and mortality, highlighting that other factors aside from complement are involved in severe disease. There still remains much research to be done to establish which complement pathways are helpful in clearing SARS-CoV-2, and whether this is true for all patients, and at what point the complement response switches from helpful to harmful.

One perspective that seems to have been sidelined is the impact of complement regulatory proteins. A large number of complement studies have focused on the complement system from the perspective of complement activation markers, but if damaging host responses were occurring due to complement dysregulation, perhaps investigating abnormalities or polymorphisms in regulatory proteins such as Factor H, Factor I and decay accelerating factor would be of use. This indeed has been done, but to a much lesser extent than studies on the actual complement activation itself. Ramlall et al. (2020) showed genetic defects in Factor H and decay accelerating factor associated with COVID-19 disease severity. The Factor H missense variant has also been implicated in severe COVID-19 by Asteris et al. (2022) and Gavriilaki et al. (2021). Whilst this variant appears to be linked to severe COVID-19, it does not appear to extrapolate to patient mortality, with Tsiftsoglou et al. (2023) finding no differences in Factor H SNPs between survivors and non-survivors.

Whilst it is still debated which complement pathways play a role in increased disease severity, and at which stage of the disease timeline these responses occur, one part of the COVID-19 pathology that can be agreed upon is the link to endothelial dysfunction and coagulation.

## 6.3 The endothelium, complement and platelets in COVID-19

In severe COVID-19 Georg et al. (2022) showed that the inflammatory environment caused by the complement system promotes differentiation of T-cells to the highly cytotoxic CD16+ phenotype, which promote microvascular EC injury. The complement system has also been linked with EC activation markers in other studies, both *in vitro* and *in vivo. In vitro*, using human microvascular cells and serum from COVID-19 patients, Aiello et al. (2022) showed that C5a leads to exocytosis of VWF and P-selectin on ECs, which then leads to significant platelet aggregation. Increased VWF and P-selectin expression on ECs was confirmed by a separate group (Perico et al., 2023), who used a blood flow model to show the spike protein S1 subunit was able to cause this, which then led to platelet aggregation on the EC surface. Investigating further, they found that treating the ECs with a complement source prior to whole blood perfusion increased the area of platelet aggregate formation by 10 times, as well as increasing the levels of VWF deposition. Increased levels of VWF and C3 deposits after spike S1 injection were also seen in a humanised ACE2 transgenic mouse model (Perico et al., 2023). These studies fit with patient studies that have shown sC5b-9 levels correlate with VWF levels, both of which parallel with disease severity (Cugno et al., 2021) and in observation of complement deposits on ECs in the lungs, kidney and liver of COVID-19 autopsy patients (Macor et al., 2021).

These studies lead me to hypothesise the triad of endothelial cell damage, complement activation and platelet aggregation are all possibly potentiating each other, exacerbating dysfunction and leading to severe disease, as will be discussed below.

## 6.4 Parallels between iNTS and COVID-19

It is at this point one can take a step back and assess the parallels between iNTS and COVID-19. In terms of clinical presentation, both diseases reach their maximum severity after 7-10 days of infection, something which could be key to the mechanisms of host damage caused by these pathogens. Both iNTS and SARS-CoV-2 are able to cause EC damage, as shown in Chapter 4 and in Nader et al. (2021).

This EC damage has the ability to lead on to platelet adhesion and activation, causing thrombosis in both diseases. Both are also able to activate the complement system. For COVID this has been discussed above, but STm is also capable of activating complement. Salmonella LPS components are able to activate different aspects of the complement system – O-antigen can cause alternative pathway activation, and lipid A is able to activate the classical pathway (Krukonis and Thomson, 2020). Whilst this is usually helpful to the human immune system, allowing clearance of the bacteria, *Salmonella* has evolved ways to evade clearance by the complement system, with very long O-antigen repeats (as seen in STm) shown to provide resistance to serum complement killing (Krukonis and Thomson, 2020). In terms of platelet aggregation, whilst this thesis has shown that STm can activate platelets in aggregometry testing, this is not the case for SARS-CoV-2 (Puhm et al., 2022, Kusudo et al., 2023). Clearly in COVID-19, despite this lack of direct platelet activation, microthrombi are still able to form, likely due to the damaged and activated endothelial cells.

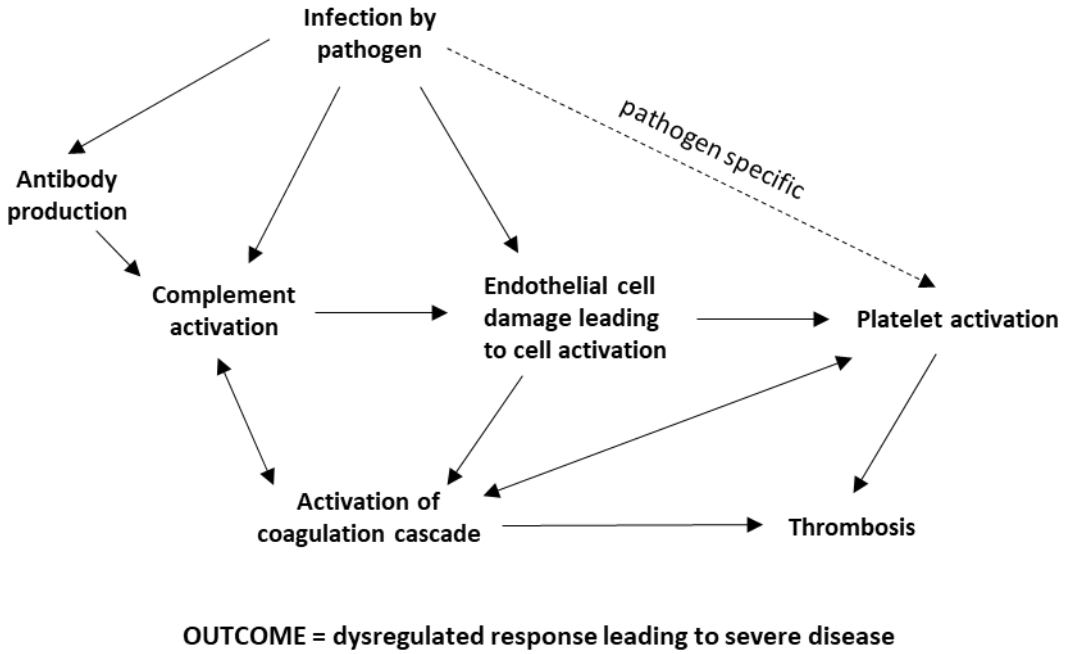


**Figure 6.2: Possible interactions between pathogens, endothelial cells, complement and platelets, leading to dysregulation of immune response and severe disease in the host**. Interactions shown occur in both invasive *Salmonella* Typhimurium infections and SARS-CoV-2 infection. Platelet activation is pathogen specific – *Salmonella* Typhimurium is able to activate platelets but SARS-CoV-2 is not.

Figure 6.2 summarises these possible interactions between pathogens, the endothelium, complement, and platelets, as well as the coagulation cascade. Both COVID-19 and STm are able to induce endothelial damage, which can trigger the coagulation cascade and lead to thrombus formation. STm is also able to act on platelets, leading to thrombus formation via antibody-STm complexes. In parallel to this, both STm and COVID-19 are able to activate the complement pathway, leading to release of proinflammatory mediators. This can lead to further endothelial cell damage and/or activation, as shown in COVID-19, providing a positive feedback loop (Aiello et al., 2022, Perico et al., 2023, Zhang et al., 2023) – further research is needed to establish whether this can occur in iNTS. Cross-talk between the complement pathways and the coagulation cascade can take place, as reviewed in Pryzdial et al. (2022), which could provide further positive feedback loops. Given the complexity of interactions between pathogens, ECs, complement and platelets, and how activation of one area can lead to activation of another, with positive feedback loops forming, it becomes understandable how dysregulated host immune responses are able spiral out of control. Clearly due to the complexity of the pathways involved, much more research is needed before this hypothesis could be confirmed or denied, and further complexities are introduced when considering the role of neutrophils and NETs, along with other immune cells. Due to the complex interactions between components, studying dysregulated host responses as a whole is very difficult. An advantage of mouse models is that they allow experiments looking at the bigger picture and interactions between different components of the vasculature. Although there are similarities between mouse models and humans, it must also be taken into account that mice have many differences compared to humans, especially in terms of platelets and immune responses (Mestas and Hughes, 2004), causing difficulties in extrapolating these results to humans. This is where *in vitro* models are needed, however, it is currently still very difficult to model all the aspects potentially involved in dysregulated host responses to pathogens *in vitro*. Research into developing more advanced blood flow models *in vitro* is progressing (Mangin et al., 2021, Dellaquila et al., 2021), but there is still a way to go until the complex interactions between platelets, endothelial

cells, complement, and other immune cells such as neutrophils can be studied in tandem *in vitro* helping us unravel the complexities of inflammatory dysregulation in response to pathogens.

## 6.5 Future work

Whilst there is clearly a vast amount of research to be done to untangle the complex mechanisms behind host immune and inflammatory dysfunction in iNTS and COVID-19, work continuing from the experiments carried out in this thesis could include:

- The use of super-resolution microscopy to investigate the relationship between FcγRIIA clustering and platelet activation, and whether clustering levels differ between *Salmonella* Typhimurium responders and non-responders
- Investigating how *Salmonella* affects other immune cells under flow conditions:
    - Does NET formation occur?
    - Can complement activate other immune cells upon activation by *Salmonella?*
    - Further investigations on whether changing the anti-coagulant used causes different platelet responses in aggregometry and under flow, especially regarding a potential role for the complement pathway.
- Use of the blood flow model to identify similarities and differences between the effects of *Salmonella* Typhimurium and SARS-CoV-2 on endothelial cells and platelets
- With VWF deposits having a key role in COVID-19 pathogenesis, does VWF also play a role in the *Salmonella* flow model?
- With sickle cell anaemia being a risk factor for iNTS (Lim et al., 2018), aggregometry and/or flow experiments on these patients to see whether a higher degree of platelet activation is shown, and whether other mechanisms are involved in these patients (with sickle cell blood being a safer alternative to the more obvious HIV connection)

- Further experiments on the structural components of STm that cause aggregation and/or binding to endothelial cells using strains with common membrane proteins knocked-out to try and elucidate why the three strains used in chapter 3 give different aggregation responses
- Investigating antibody levels and related complement activation from samples of those that died of COVID-19 to see whether levels differed compared to those that survived
- Characterisation of the *Salmonella* Typhimurium donor complement responses to using the complement ELISA. Do these results correlate with the platelet activation levels seen?

## 6.6 Conclusions

To conclude, this thesis has demonstrated that *Salmonella* Typhimurium strains are able to cause platelet activation via indirect binding to the platelet FcγRIIA receptor through IgG antibodies. The donor variation in platelet responses is likely caused by the differing amounts of antibody able to bind *Salmonella* that donors have. A possible reason behind the responses varying by STm strain could be differences in O-antigen chain length, which appear to play a role in enhancing aggregation responses. Moving from a platelet aggregometry system to a physiological whole blood flow system confirmed that STm can bind to endothelial cells, and that platelets are able to adhere to STm primed ECs.

Whilst this thesis has shown STm can cause thromboinflammatory host responses, SARS-CoV-2 can also lead to these responses. To aid the global research effort into this pathogen, we showed that the SARS-CoV-2 spike and nucleoproteins are able to induce the classical complement pathway once antibody is present in the blood, and that these downstream complement responses differ between non-hospitalised convalescent patients and those that required ITU treatment.

## References


AGOSTINIS, C., TOFFOLI, M., BALDUIT, A., MANGOGNA, A., YASMIN, H., RAGAZZON, C., PEGORARO, S., CAMPISCIANO, G., STABILE, G., ZITO, G., KISHORE, U., COMAR, M., SCRIMIN, F., BULLA, R. & RICCI, G. 2023. Anti-Spike Antibodies Present in the Milk of SARS-CoV-2 Vaccinated Mothers Are Complement-Activating. *International Journal of Molecular Sciences,* 24.

AIELLO, S., GASTOLDI, S., GALBUSERA, M., RUGGENENTI, P., PORTALUPI, V., ROTA, S., RUBIS, N., LIGUORI, L., CONTI, S., TIRONI, M., GAMBA, S., SANTARSIERO, D., BENIGNI, A., REMUZZI, G. & NORIS, M. 2022. C5a and C5aR1 are key drivers of microvascular platelet aggregation in clinical entities spanning from aHUS to COVID-19. *Blood Advances,* 6**,** 866-881.

ALI, R. A., WUESCHER, L. M. & WORTH, R. G. 2015. Platelets: essential components of the immune system. *Current Trends in Immunology,* 16**,** 65-78.

ALI, Y. M., FERRARI, M., LYNCH, N. J., YASEEN, S., DUDLER, T., GRAGEROV, S., DEMOPULOS, G., HEENEY, J. L. & SCHWAEBLE, W. J. 2021. Lectin pathway mediates complement activation by SARS-CoV-2 proteins. *Frontiers in Immunology,* 12**,** 714511.

ALKARITHI, G., DUVAL, C., SHI, Y., MACRAE, F. L. & ARIENS, R. A. S. 2021. Thrombus Structural Composition in Cardiovascular Disease. *Arteriosclerosis, Thrombosis, and Vascular Biology,* 41**,** 2370-2383.

ALKHAMIS, T. M., BEISSINGER, R. L. & CHEDIAK, J. R. 1988. Red blood cell effect on platelet adhesion and aggregation in low-stress shear flow. *Transactions of the American Society for Artificial Internal Organs,* 34**,** 868-873.

ALLEN, J. D., CHAWLA, H., SAMSUDIN, F., ZUZIC, L., SHIVGAN, A. T., WATANABE, Y., HE, W.-T., CALLAGHAN, S., SONG, G., YONG, P., BROUWER, P. J. M., SONG, Y., CAI, Y., DUYVESTEYN, H. M. E., MALINAUSKAS, T., KINT, J., PINO, P., WURM, M. J., FRANK, M., CHEN, B., STUART, D. I., SANDERS, R. W., ANDRABI, R., BURTON, D. R., LI, S., BOND, P. J. & CRISPIN, M. 2021. Site-specific steric control of SARS-CoV-2 spike glycosylation. *Biochemistry,* 60**,** 2153-2169.

ANANIA, J. C., CHENOWETH, A. M., WINES, B. D. & HOGARTH, P. M. 2019. The Human FcgammaRII (CD32) Family of Leukocyte FcR in Health and Disease. *Frontiers in Immunology,* 10**,** 464.

ANDERSSON, M. I., ARANCIBIA-CARCAMO, C. V., AUCKLAND, K., BAILLIE, J. K., BARNES, E., BENEKE, T., BIBI, S., BROOKS, T., CARROLL, M., CROOK, D., DINGLE, K., DOLD, C., DOWNS, L. O., DUNN, L., EYRE, D. W., GILBERT JARAMILLO, J., HARVALA, H., HOOSDALLY, S., IJAZ, S., JAMES, T., JAMES, W., JEFFERY, K., JUSTICE, A., KLENERMAN, P., KNIGHT, J. C., KNIGHT, M., LIU, X., LUMLEY, S. F., MATTHEWS, P. C., MCNAUGHTON, A. L., MENTZER, A. J., MONGKOLSAPAYA, J., OAKLEY, S., OLIVEIRA, M. S., PETO, T., PLOEG, R. J., RATCLIFF, J., ROBBINS, M. J., ROBERTS, D. J., RUDKIN, J., RUSSELL, R. A., SCREATON, G., SEMPLE, M. G., SKELLY, D., SIMMONDS, P., STOESSER, N., TURTLE, L., WAREING, S. & ZAMBON, M. 2020. SARS-CoV-2 RNA detected in blood products from patients with COVID-19 is not associated with infectious virus. *Wellcome Open Research,* 5**,** 181.

ANNANE, D., HEMING, N., GRIMALDI-BENSOUDA, L., FRÉMEAUX-BACCHI, V., VIGAN, M., ROUX, A.-L., MARCHAL, A., MICHELON, H., ROTTMAN, M. & MOINE, P. 2020. Eculizumab as an emergency treatment for adult patients with severe COVID-19 in the intensive care unit: A proof-of-concept study. *EClinicalMedicine,* 28**,** 100590.

ANTCZAK, A. J., VIETH, J. A., SINGH, N. & WORTH, R. G. 2011. Internalization of IgG-coated targets results in activation and secretion of soluble CD40 ligand and RANTES by human platelets. *Clinical and Vaccine Immunology,* 18**,** 210-6.

AOYAMA, T., INO, Y., OZEKI, M., ODA, M., SATO, T., KOSHIYAMA, Y., SUZUKI, S. & FUJITA, M. 1984. Pharmacological studies of FUT-175, nafamstat mesilate. I. Inhibition of protease activity in in vitro and in vivo experiments. *The Japanese Journal of Pharmacology,* 35**,** 203-27.

ARMAN, M. & KRAUEL, K. 2015. Human platelet IgG Fc receptor FcgammaRIIA in immunity and thrombosis. *Journal of Thrombosis and Haemostasis,* 13**,** 893-908.

ARMAN, M., KRAUEL, K., TILLEY, D. O., WEBER, C., COX, D., GREINACHER, A., KERRIGAN, S. W. & WATSON, S. P. 2014. Amplification of bacteria-induced platelet activation is triggered by FcgammaRIIA, integrin alphaIIbbeta3, and platelet factor 4. *Blood,* 123**,** 3166-74.

ASSINGER, A. 2014. Platelets and infection - an emerging role of platelets in viral infection. *Frontiers in Immunology,* 5**,** 649.

ASSINGER, A., LAKY, M., SCHABBAUER, G., HIRSCHL, A. M., BUCHBERGER, E., BINDER, B. R. & VOLF, I. 2011. Efficient phagocytosis of periodontopathogens by neutrophils requires plasma factors, platelets and TLR2. *Journal of Thrombosis and Haemostasis,* 9**,** 799-809.

ASTERIS, P. G., GAVRIILAKI, E., TOULOUMENIDOU, T., KORAVOU, E. E., KOUTRA, M., PAPAYANNI, P. G., POULERES, A., KARALI, V., LEMONIS, M. E., MAMOU, A., SKENTOU, A. D., PAPALEXANDRI, A., VARELAS, C., CHATZOPOULOU, F., CHATZIDIMITRIOU, M., CHATZIDIMITRIOU, D., VELENI, A., RAPTI, E., KIOUMIS, I., KAIMAKAMIS, E., BITZANI, M., BOUMPAS, D., TSANTES, A., SOTIROPOULOS, D., PAPADOPOULOU, A., KALANTZIS, I. G., VALLIANATOU, L. A., ARMAGHANI, D. J., CAVALERI, L., GANDOMI, A. H., HAJIHASSANI, M., HASANIPANAH, M., KOOPIALIPOOR, M., LOURENÇO, P. B., SAMUI, P., ZHOU, J., SAKELLARI, I., VALSAMI, S., POLITOU, M., KOKORIS, S. & ANAGNOSTOPOULOS, A. 2022. Genetic prediction of ICU hospitalization and mortality in COVID-19 patients using artificial neural networks. *Journal of Cellular and Molecular Medicine,* 26**,** 1445-1455.

AURSNES, I. & VIKHOLM, V. 1984. On a possible interaction between ADP and mechanical stimulation in platelet activation. *Thrombosis and Haemostasis,* 51**,** 54-56.

AZZI, L., DALLA GASPERINA, D., VERONESI, G., SHALLAK, M., IETTO, G., IOVINO, D., BAJ, A., GIANFAGNA, F., MAURINO, V., FOCOSI, D., MAGGI, F., FERRARIO, M. M., DENTALI, F., CARCANO, G., TAGLIABUE, A., MAFFIOLI, L. S., ACCOLLA, R. S. & FORLANI, G. 2022. Mucosal immune response in BNT162b2 COVID-19 vaccine recipients. *eBioMedicine,* 75**,** 103788.

BANG, I. S., KIM, B. H., FOSTER, J. W. & PARK, Y. K. 2000. OmpR Regulates the Stationary-Phase Acid Tolerance Response of *Salmonella enterica* Serovar Typhimurium. *Journal of Bacteriology,* 182**,** 2245-2252.

BANGARU, S., OZOROWSKI, G., TURNER, H. L., ANTANASIJEVIC, A., HUANG, D., WANG, X., TORRES, J. L., DIEDRICH, J. K., TIAN, J.-H., PORTNOFF, A. D., PATEL, N., MASSARE, M. J., YATES, J. R., 3RD, NEMAZEE, D., PAULSON, J. C., GLENN, G., SMITH, G. & WARD, A. B. 2020. Structural analysis of full-length SARS-CoV-2 spike protein from an advanced vaccine candidate. *Science,* 370**,** 1089-1094.

BAZZONI, G. & DEJANA, E. 2004. Endothelial cell-to-cell junctions: molecular organization and role in vascular homeostasis. *Physiological Reviews,* 84**,** 869-901.

BEARSE, M., HUNG, Y. P., KRAUSON, A. J., BONANNO, L., BOYRAZ, B., HARRIS, C. K., HELLAND, T. L., HILBURN, C. F., HUTCHISON, B., JOBBAGY, S., MARSHALL, M. S., SHEPHERD, D. J., VILLALBA, J. A., DELFINO, I., MENDEZ-PENA, J., CHEBIB, I., NEWTON-CHEH, C. & STONE, J. R. 2021. Factors associated with myocardial SARS-CoV-2 infection, myocarditis, and cardiac inflammation in patients with COVID-19. *Modern Pathology,* 34**,** 1345-1357.

BEEBE, D. P., SCHREIBER, R. D. & COOPER, N. R. 1983. Neutralization of influenza virus by normal human sera: mechanisms involving antibody and complement. *The Journal of Immunology,* 130**,** 1317-1322.

BENNETT, J. S. 2005. Structure and function of the platelet integrin alphaIIbbeta3. *Journal of Clinical Investigation,* 115**,** 3363-9.

BERISTAIN-COVARRUBIAS, N., PEREZ-TOLEDO, M., FLORES-LANGARICA, A., ZUIDSCHERWOUDE, M., HITCHCOCK, J. R., CHANNELL, W. M., KING, L. D. W., THOMAS, M. R., HENDERSON, I. R., RAYES, J., WATSON, S. P. & CUNNINGHAM, A. F. 2019a. Salmonella-induced thrombi in mice develop asynchronously in the spleen and liver and are not effective bacterial traps. *Blood,* 133**,** 600-604.

BERISTAIN-COVARRUBIAS, N., PEREZ-TOLEDO, M., THOMAS, M. R., HENDERSON, I. R., WATSON, S. P. & CUNNINGHAM, A. F. 2019b. Understanding Infection-Induced Thrombosis: Lessons Learned From Animal Models. *Frontiers in Immunology,* 10.

BJORNSON, A. B., MELLENCAMP, M. A. & SCHIFF, G. M. 1990. Complement is activated in the upper respiratory tract during influenza virus infection. *American Review of Respiratory Disease,* 143**,** 1062-1066.

BOLGER, M. S., ROSS, D. S., JIANG, H., FRANK, M. M., GHIO, A. J., SCHWARTZ, D. A. & WRIGHT, J. R. 2007. Complement levels and activity in the normal and LPS-injured lung. *American Journal of Physiology-Lung Cellular and Molecular Physiology,* 292**,** L748-L759.

BOUSSIER, J., YATIM, N., MARCHAL, A., HADJADJ, J., CHARBIT, B., EL SISSY, C., CARLIER, N., PENE, F., MOUTHON, L., THARAUX, P. L., BERGERON, A., SMADJA, D. M., RIEUX-LAUCAT, F., DUFFY, D., KERNEIS, S., FREMEAUX-BACCHI, V. & TERRIER, B. 2022. Severe COVID-19 is associated with hyperactivation of the alternative complement pathway. *Journal of Allergy and Clinical Immunology,* 149**,** 550-556 e2.

BRENNAN, M. P., LOUGHMAN, A., DEVOCELLE, M., ARASU, S., CHUBB, A. J., FOSTER, T. J. & COX, D. 2009. Elucidating the role of Staphylococcus epidermidis serine-aspartate repeat protein G in platelet activation. *Journal of Thrombosis and Haemostasis,* 7**,** 1364-72.

BRENNER, F. W., VILLAR, R. G., ANGULO, F. J., TAUXE, R. & SWAMINATHAN, B. 2000. *Salmonella* nomenclature. *Journal of Clinical Microbiology,* 38**,** 2465-2467.

BREWER, J. W., RANDALL, T. D., PARKHOUSE, R. M. E. & CORLEY, R. B. 1994. IgM hexamers? *Immunology Today,* 15**,** 165-168.

BRINKMANN, V., REICHARD, U., GOOSMANN, C., FAULER, B., UHLEMANN, Y., WEISS, D. S., WEINRAUCH, Y. & ZYCHLINSKY, A. 2004. Neutrophil Extracellular Traps Kill Bacteria. *Science,* 303**,** 1532-1535.

BRIQUEZ, P. S., ROUHANI, S. J., YU, J., PYZER, A. R., TRUJILLO, J., DUGAN, H. L., STAMPER, C. T., CHANGROB, S., SPERLING, A. I., WILSON, P. C., GAJEWSKI, T. F., HUBBELL, J. A. & SWARTZ, M. A. 2022. Severe COVID-19 induces autoantibodies against angiotensin II that correlate with blood pressure dysregulation and disease severity. *Science Advances,* 8**,** eabn3777.

BRUHNS, P., IANNASCOLI, B., ENGLAND, P., MANCARDI, D. A., FERNANDEZ, N., JORIEUX, S. & DAERON, M. 2009. Specificity and affinity of human Fcgamma receptors and their polymorphic variants for human IgG subclasses. *Blood,* 113**,** 3716-25.

BUCHMANN, K. 2014. Evolution of Innate Immunity: Clues from Invertebrates via Fish to Mammals. *Frontiers in Immunology,* 5.

BUKA, R. J., MONTAGUE, S. J., MORAN, L. A., MARTIN, E. M., SLATER, A., WATSON, S. P. & NICOLSON, P. L. R. 2024. PF4 activates the c-Mpl-Jak2 pathway in platelets. *Blood,* 143**,** 64-69.

BURKHART, J. M., VAUDEL, M., GAMBARYAN, S., RADAU, S., WALTER, U., MARTENS, L., GEIGER, J., SICKMANN, A. & ZAHEDI, R. P. 2012. The first comprehensive and quantitative analysis of human platelet protein composition allows the comparative analysis of structural and functional pathways. *Blood,* 120**,** e73-82.

BYRNE, M. F., KERRIGAN, S. W., CORCORAN, P. A., ATHERTON, J. C., MURRAY, F. E., FITZGERALD, D. J. & COX, D. M. 2003. Helicobacter pylori binds von Willebrand factor and interacts with GPIb to induce platelet aggregation. *Gastroenterology,* 124**,** 1846-54.

CAMPBELL, C. M. & KAHWASH, R. 2020. Will complement inhibition be the new target in treating COVID-19 related systemic thrombosis *Circulation,* 141**,** 1739-1741.

CAREY, J., BUCHSTEIN, S. & SHAH, S. 2001. Septic deep vein thrombosis due to Salmonella johannesburg. *J Infect,* 42**,** 79-80.

CARVELLI, J., DEMARIA, O., VÉLY, F., BATISTA, L., BENMANSOUR, N. C., FARES, J., CARPENTIER, S., THIBULT, M.-L., MOREL, A., REMARK, R., ANDRÉ, P., REPRESA, A., PIPEROGLOU, C., MIRANDA, L. A., BARON, W., BELAID, N., CAILLET, C., CARAGUEL, F., CARRETTE, B., CARRETTE, F., CHANUC, F., COURTOIS, R., FENIS, A., GIORDANO, M., GIRARD-MADOUX, M., GIRAUDON-PAOLI, M., GOURDIN, N., GRONDIN, G., GUILLOT, F., HABIF, G., JAUBERT, S., LOPEZ, J., LE VAN, M., LOVERA, N., MANSUY, M., BONNET, E., SANSALONI, A., REBOUL, A., MITRY, E., NEKKAR-CONSTANT, C., PÉRI, V., RICAUT, P., SIMON, L., VALLIER, J.-B., VÉTIZOU, M., ZERBIB, R., CORDIER, P. Y., LE DAULT, E., GUERVILLY, C., SIMEONE, P., GAINNIER, M., MOREL, Y., EBBO, M., SCHLEINITZ, N., VIVIER, E., UGOLINI, S., ETIENNOT, M., GALLUSO, J., LYONNET, L., FOREL, J.-M., PAPAZIAN, L., VELLY, L., ANDRÉ, B., BRIANTAIS, A., FAUCHER, B., JEAN, E., SEGUIER, J., VEIT, V., HARLÉ, J.-R., PASTORINO, B., DELTEIL, C., DANIEL, L., BOUDSOCQ, J.-P., CLERC, A., DELMOND, E., VIDAL, P.-O., SAVINI, H., COUTARD, B., THE EXPLORE, C.-I. P. H. G. & THE EXPLORE, C.-M. I. G. 2020. Association of COVID-19 inflammation with activation of the C5a–C5aR1 axis. *Nature,* 588**,** 146.

CARVELLI, J., MEZIANI, F., DELLAMONICA, J., CORDIER, P. Y., ALLARDET-SERVENT, J., FRAISSE, M., VELLY, L., BARBAR, S. D., LEHINGUE, S., GUERVILLY, C., DESGROUAS, M., CAMOU, F., PIPEROGLOU, C., VELY, F., DEMARIA, O., KARAKUNNEL, J., FARES, J., BATISTA, L., ROTOLO, F., VIOTTI, J., BOYER-CHAMMARD, A., LACOMBE, K., LE DAULT, E., CARLES, M., SCHLEINITZ, N., VIVIER, E. & GROUP,

F. C. E. S. 2022. Avdoralimab (Anti-C5aR1 mAb) Versus Placebo in Patients With Severe COVID-19: Results From a Randomized Controlled Trial (FOR COVID Elimination [FORCE]). *Critical Care Medicine,* 50**,** 1788-1798.

CATTANEO, M., CERLETTI, C., HARRISON, P., HAYWARD, C. P., KENNY, D., NUGENT, D., NURDEN, P., RAO, A. K., SCHMAIER, A. H., WATSON, S. P., LUSSANA, F., PUGLIANO, M. T. & MICHELSON, A. D. 2013. Recommendations for the Standardization of Light Transmission Aggregometry: A Consensus of the Working Party from the Platelet Physiology Subcommittee of SSC/ISTH. *Journal of Thrombosis and Haemostasis,* 11**,** 1183–1189.

CATTANEO, M., LECCHI, A., ZIGHETTI, M. L. & LUSSANA, F. 2007. Platelet aggregation studies: autologous platelet-poor plasma inhibits platelet aggregation when added to platelet-rich plasma to normalize platelet count. *Haematologica,* 92**,** 694-697.

CAUGHMAN, G. B., BOACKLE, R. J. & VESELY, J. 1982. A postulated mechanism for heparin's potentiation of C1 inhibitor function. *Molecular Immunology,* 19**,** 287-95.

CERVIA, C., NILSSON, J., ZURBUCHEN, Y., VALAPERTI, A., SCHREINER, J., WOLFENSBERGER, A., RAEBER, M. E., ADAMO, S., WEIGANG, S., EMMENEGGER, M., HASLER, S., BOSSHARD, P. P., DE CECCO, E., BÄCHLI, E., RUDIGER, A., STÜSSI-HELBLING, M., HUBER, L. C., ZINKERNAGEL, A. S., SCHAER, D. J., AGUZZI, A., KOCHS, G., HELD, U., PROBST-MÜLLER, E., RAMPINI, S. K. & BOYMAN, O. 2021. Systemic and mucosal antibody responses specific to SARS-CoV-2 during mild versus severe COVID-19. *Journal of Allergy and Clinical Immunology,* 147**,** 545-557.e9.

CHAWLA, H., JOSSI, S. E., FAUSTINI, S. E., SAMSUDIN, F., ALLEN, J. D., WATANABE, Y., NEWBY, M. L., MARCIAL-JUÁREZ, E., LAMERTON, R. E., MCLELLAN, J. S., BOND, P. J., RICHTER, A. G., CUNNINGHAM, A. F. & CRISPIN, M. 2021. Glycosylation and serological reactivity of an expression-enhanced SARS-CoV-2 viral spike mimetic. *Journal of Molecular Biology***,** 167332.

CHEN, B. P., LI, Y.-S., ZHAO, Y., CHEN, K.-D., LI, S., LAO, J., YUAN, S., SHYY, J. Y.-J. & CHIEN, S. 2001. DNA microarray analysis of gene expression in endothelial cells in response to 24-h shear stress. *Physiological genomics,* 7**,** 55-63.

CHEN, Y., YUAN, Y. & LI, W. 2018. Sorting machineries: how platelet-dense granules differ from alpha-granules. *Bioscience Reports,* 38**,** BSR20180458.

CHENG, W., HORNUNG, R., XU, K., YANG, C. H. & LI, J. 2021. Complement C3 identified as a unique risk factor for disease severity among young COVID-19 patients in Wuhan, China. *Scientific Reports,* 11**,** 7857.

CHOWDHURY, A. R., SAH, S., VARSHNEY, U. & CHAKRAVORTTY, D. 2022. Salmonella Typhimurium outer membrane protein A (OmpA) renders protection from nitrosative stress of macrophages by maintaining the stability of bacterial outer membrane. *Plos Pathogens,* 18**,** e1010708.

CHU, T. J. & PETERS, D. G. 2008. Serial analysis of the vascular endothelial transcriptome under static and shear stress conditions. *Physiological Genomics,* 34**,** 185-192.

COENEN, D. M., MASTENBROEK, T. G. & COSEMANS, J. M. E. M. 2017. Platelet interaction with activated endothelium: mechanistic insights from microfluidics. *Blood,* 130**,** 2819-2828.

COLLINS, J., VAN PIJKEREN, J.-P., SVENSSON, L., CLAESSON, M. J., STURME, M., LI, Y., COONEY, J. C., VAN SINDEREN, D., WALKER, A. W., PARKHILL, J., SHANNON, O. & O'TOOLE, P. W. 2012. Fibrinogen-binding and platelet-aggregation activities of a Lactobacillus salivarius septicaemia isolate are mediated by a novel fibrinogen-binding protein. *Molecular Microbiology,* 85**,** 862-877.

COOK, A. M., FAUSTINI, S. E., WILLIAMS, L. J., CUNNINGHAM, A. F., DRAYSON, M. T., SHIELDS, A. M., KAY, D., TAYLOR, L., PLANT, T., HUISSOON, A., WALLIS, G., BECK, S., JOSSI, S. E., PEREZ-TOLEDO, M., NEWBY, M. L., ALLEN, J. D., CRISPIN, M., HARDING, S. & RICHTER, A. G. 2021. Validation of a combined ELISA to detect IgG, IgA and IgM antibody responses to SARS-CoV-2 in mild or moderate non-hospitalised patients. *Journal of Immunological Methods,* 494**,** 7.

CORCORAN, P. A., ATHERTON, J. C., KERRIGAN, S. W., WADSTROM, T., MURRAY, F. E., PEEK, R. M., FITZGERALD, D. J., COX, D. M. & BYRNE, M. F. 2007. The effect of different strains of H pylori on platelet aggregation. *Canadian Journal of Gastroenterology and Hepatology,* 21**,** 367-370.

COSTA, R., ALBEROLA, J., OLEA, B., GOZALBO-ROVIRA, R., GIMENEZ, E., CUEVAS-FERRANDO, E., TORRES, I., ALBERT, E., CARBONELL, N., FERRERES, J., SANCHEZ, G., RODRIGUEZ-DIAZ, J., BLASCO, M. L. & NAVARRO, D. 2022. Combined kinetic analysis of SARS-CoV-2 RNAemia, N-antigenemia and virus-specific antibodies in critically ill adult COVID-19 patients. *Scientific Reports,* 12**,** 8273.

COSTANTINI, V. P., NGUYEN, K., LYSKI, Z., NOVOSAD, S., BARDOSSY, A. C., LYONS, A. K., GABLE, P., KUTTY, P. K., LUTGRING, J. D., BRUNTON, A., THORNBURG, N. J., BROWN, A. C., MCDONALD, L. C., MESSER, W. & VINJÉ, J. 2022. Development and validation of an enzyme immunoassay for detection and quantification of SARS-CoV-2 salivary IgA and IgG. *Journal of Immunology,* 208**,** 1500-1508.

COX, D., KERRIGAN, S. W. & WATSON, S. P. 2011. Platelets and the innate immune system: mechanisms of bacterial-induced platelet activation. *Journal of Thrombosis and Haemostasis,* 9**,** 1097-1107.

CUGNO, M., MERONI, P. L., GUALTIEROTTI, R., GRIFFINI, S., GROVETTI, E., TORRI, A., LONATI, P., GROSSI, C., BORGHI, M. O., NOVEMBRINO, C., BOSCOLO, M., UCEDA RENTERIA, S. C., VALENTI, L., LAMORTE, G., MANUNTA, M., PRATI, D., PESENTI, A., BLASI, F., COSTANTINO, G., GORI, A., BANDERA, A., TEDESCO, F. & PEYVANDI, F. 2021. Complement activation and endothelial perturbation parallel COVID-19 severity and activity. *Journal of Autoimmunity,* 116**,** 102560.

CUMMINS, D., FISHER-HOCH, S. P., WALSHE, K. J., MACKIE, I. J., MCCORMICK, J. B., BENNETT, D., PEREZ, G., FARRAR, B. & MACHIN, S. J. 1989. A plasma inhibitor of platelet aggregation in patients with Lassa fever. *British Journal of Haematology,* 72**,** 543-8.

CUMMINS, D., MOLINAS, F. C., LERER, G., MAIZTEGUI, J. I., FAINT, R. & MACHIN, S. J. 1990. A plasma inhibitor of platelet aggregation in patients with Argentine hemorrhagic fever. *American Journal of Tropical Medicine and Hygiene,* 42**,** 470-5.

DAHA, N. A., BANDA, N. K., ROOS, A., BEURSKENS, F. J., BAKKER, J. M., DAHA, M. R. & TROUW, L. A. 2011. Complement activation by (auto-) antibodies. *Molecular Immunology,* 48**,** 1656-1665.

DALBY, T., STRID, M. A., BEYER, N. H., BLOM, J., MOLBAK, K. & KROGFELT, K. A. 2005. Rapid decay of Salmonella flagella antibodies during human gastroenteritis: a follow up study. *Journal of Microbiological Methods,* 62**,** 233-43.

DALY, H. C., SAMPEDRO, G., BON, C., WU, D., ISMAIL, G., CAHILL, R. A. & O'SHEA, D. F. 2017. BF(2)-azadipyrromethene NIR-emissive fluorophores with research and clinical potential. *European Journal of Medicinal Chemistry,* 135**,** 392-400.

DAMOISEAUX, J., DOTAN, A., FRITZLER, M. J., BOGDANOS, D. P., MERONI, P. L., ROGGENBUCK, D., GOLDMAN, M., LANDEGREN, N., BASTARD, P., SHOENFELD, Y. & CONRAD, K. 2022. Autoantibodies and SARS-CoV2 infection: The spectrum from association to clinical implication: Report of the 15th Dresden Symposium on Autoantibodies. *Autoimmunity Reviews,* 21**,** 103012.

DARBY, A. C. & HISCOX, J. A. 2021. COVID-19: variants and vaccination. *BMJ-British Medical Journal,* 372**,** 2.

DEFENDI, F., LEROY, C., EPAULARD, O., CLAVARINO, G., VILOTITCH, A., LE MARECHAL, M., JACOB, M. C., RASKOVALOVA, T., PERNOLLET, M., LE GOUELLEC, A., BOSSON, J. L., POIGNARD, P., ROUSTIT, M., THIELENS, N., DUMESTRE-PERARD, C. & CESBRON, J. Y. 2021. Complement Alternative and Mannose-Binding Lectin Pathway Activation Is Associated With COVID-19 Mortality. *Frontiers in Immunology,* 12**,** 742446.

DEJANA, E. 2004. Endothelial cell-cell junctions: happy together. *Nature Reviews Molecular Cell Biology,* 5**,** 261-70.

DEL CONDE, I., CRUZ, M. A., ZHANG, H., LOPEZ, J. A. & AFSHAR-KHARGHAN, V. 2005. Platelet activation leads to activation and propagation of the complement system. *Journal of Experimental Medicine,* 201**,** 871-9.

DELANGHE, J. R., DE BUYZERE, M. L. & SPEECKAERT, M. M. 2021. Genetic polymorphisms in the host and COVID-19 infection. *In:* REZAEI, N. (ed.) *Coronavirus Disease - COVID-19.* Cham: Springer International Publishing.

DELLAQUILA, A., LE BAO, C., LETOURNEUR, D. & SIMON-YARZA, T. 2021. In Vitro Strategies to Vascularize 3D Physiologically Relevant Models. *Advanced Science,* 8**,** 2100798.

DENOMME, G. A. 2012. Platelet and leukocyte FcY receptors in heparin-induced thrombocytopeania. *In:* WARKENTIN, T. E. & GREINACHER, A. (eds.) *Heparin-Induced Throbocytopenia.* 5 ed. Boca Raton: Taylor and Francis Group.

DES PREZ, R. M., STECKLEY, S., STROUD, R. M. & HAWIGER, J. 1980. Interaction of Histoplasma capsulatum with Human Platelets. *The Journal of Infectious Diseases,* 142**,** 32-39.

DESSIE, Z. G. & ZEWOTIR, T. 2021. Mortality-related risk factors of COVID-19: a systematic review and meta-analysis of 42 studies and 423,117 patients. *BMC Infectious Diseases,* 21**,** 855.

DETSIKA, M. G., DIAMANTI, E., AMPELAKIOTOU, K., JAHAJ, E., TSIPILIS, S., ATHANASIOU, N., DIMOPOULOU, I., ORFANOS, S. E., TSIROGIANNI, A. & KOTANIDOU, A. 2022. C3a and C5b-9 Differentially Predict COVID-19 Progression and Outcome. *Life* 12.

DEVALARAJA-NARASHIMHA, K., EHMANN, P. J., HUANG, C., RUAN, Q., WIPPERMAN, M. F., KAPLAN, T., LIU, C., AFOLAYAN, S., GLASS, D. J., MELLIS, S., YANCOPOULOS, G. D., HAMILTON, J. D., MACDONNELL, S., HAMON, S. C., BOYAPATI, A. & MORTON, L. 2023. Association of complement pathways with COVID-19 severity and outcomes. *Microbes and Infection,* 25**,** 105081.

DEVINE, D. V. & ROSSE, W. F. 1987. Regulation of the activity of platelet-bound C-3 convertase of the alternative pathway of complement by platelet Factor-H. *Proceedings of the National Academy of Sciences of the United States of America,* 84**,** 5873-5877.

DIEBOLDER, C. A., BEURSKENS, F. J., DE JONG, R. N., KONING, R. I., STRUMANE, K., LINDORFER, M. A., VOORHORST, M., UGURLAR, D., ROSATI, S., HECK, A. J. R., VAN DE WINKEL, J. G. J., WILSON, I. A., KOSTER, A. J., TAYLOR, R. P., SAPHIRE, E. O., BURTON, D. R., SCHUURMAN, J., GROS, P. & PARREN, P. 2014. Complement is activated by IgG hexamers assembled at the cell surface. *Science,* 343**,** 1260-1263.

DIURNO, F., NUMIS, F. G., PORTA, G., CIRILLO, F., MADDALUNO, S., RAGOZZINO, A., DE NEGRI, P., DI GENNARO, C., PAGANO, A., ALLEGORICO, E., BRESSY, L., BOSSO, G., FERRARA, A., SERRA, C., MONTISCI, A., D'AMICO, M., LO MORELLO, S. S., DI COSTANZO, G., TUCCI, A. G., MARCHETTI, P., DI VINCENZO, U., SORRENTINO, I., CASCIOTTA, A., FUSCO, M., BUONERBA, C., BERRETTA, M., CECCARELLI, M., NUNNARI, G., DIESSA, Y., CICALA, S. & FACCHINI, G. 2020. Eculizumab treatment in patients with COVID-19: preliminary results from real life ASL Napoli 2 Nord experience. *European Review for Medical and Pharmacological Sciences,* 24**,** 4040-4047.

DOCHERTY, A. B., HARRISON, E. M., GREEN, C. A., HARDWICK, H. E., PIUS, R., NORMAN, L., HOLDEN, K. A., READ, J. M., DONDELINGER, F., CARSON, G., MERSON, L., LEE, J., PLOTKIN, D., SIGFRID, L., HALPIN, S., JACKSON, C., GAMBLE, C., HORBY, P. W., NGUYEN-VAN-TAM, J. S., HO, A., RUSSELL, C. D., DUNNING, J., OPENSHAW, P. J., BAILLIE, J. K., SEMPLE, M. G. & INVESTIGATORS, I. C. 2020. Features of 20133 UK patients in hospital with covid-19 using the ISARIC WHO clinical characterisation protocol: prospective observational cohort study. *BMJ-British Medical Journal,* 369**,** 12.

DOMÍNGUEZ-MEDINA, C. C., PÉREZ-TOLEDO, M., SCHAGER, A. E., MARSHALL, J. L., COOK, C. N., BOBAT, S., HWANG, H., CHUN, B. J., LOGAN, E., BRYANT, J. A., CHANNELL, W. M., MORRIS, F. C., JOSSI, S. E., ALSHAYEA, A., ROSSITER, A. E., BARROW, P. A., HORSNELL, W. G., MACLENNAN, C. A., HENDERSON, I. R., LAKEY, J. H., GUMBART, J. C., LÓPEZ-MACÍAS, C., BAVRO, V. N. & CUNNINGHAM, A. F. 2020. Outer membrane protein size and LPS O-antigen define protective antibody targeting to the Salmonella surface. *Nature Communications,* 11**,** 851.

DUNKELBERGER, J. R. & SONG, W. C. 2010. Complement and its role in innate and adaptive immune responses. *Cell Research,* 20**,** 34-50.

DUTHIE, E. S. & LORENZ, L. L. 1952. Staphylococcal coagulase; mode of action and antigenicity. *Journal of General Microbiology,* 6**,** 95-107.

ENGELMANN, B. & MASSBERG, S. 2013. Thrombosis as an intravascular effector of innate immunity. *Nature Reviews Immunology,* 13**,** 34-45.

ERIKSSON, O., MOHLIN, C., NILSSON, B. & EKDAHL, K. N. 2019. The Human Platelet as an Innate Immune Cell: Interactions Between Activated Platelets and the Complement System. *Frontiers in Immunology,* 10**,** 1590.

FABREGA, A. & VILA, J. 2013. Salmonella enterica serovar Typhimurium skills to succeed in the host: virulence and regulation. *Clinical Microbiology Reviews,* 26**,** 308-41.

FALUS, A., ROKITA, H., WALCZ, E., BROZIK, E., HIDVEGI, T. & MERETEY, K. 1990. Hormonal regulation of complement biosyntehsis in human cell lines. *Molecular Immunology,* 27**,** 197-201.

FAUSTINI, S., SHIELDS, A., BANHAM, G., WALL, N., AL-TAEI, S., TANNER, C., AHMED, Z., EFSTATHIOU, E., TOWNSEND, N., GOODALL, M., PLANT, T., PEREZ-TOLEDO, M., JASIULEWICZ, A., PRICE, R., MCLAUGHLIN, J., FARNAN, J., MOORE, J., ROBERTSON, L., NESBIT, A., CURRY, G., BLACK, A., CUNNINGHAM, A., HARPER, L., MOORE, T., DRAYSON, M. & RICHTER, A. 2022. Cross reactivity of spike glycoprotein induced antibody against Delta and Omicron variants before and after third SARS-CoV-2 vaccine dose in healthy and immunocompromised individuals. *Journal of Infection,* 84**,** 579-613.

FAUSTINI, S. E., JOSSI, S. E., PEREZ-TOLEDO, M., SHIELDS, A., ALLEN, J. D., WATANABE, Y., NEWBY, M. L., COOK, A., WILLCOX, C. R., SALIM, M., GOODALL, M., HEANEY, J. L., MARCIAL-JUAREZ, E., MORLEY, G. L., TORLINSKA, B., WRAITH, D. C., VEENITH, T., HARDING, S., JOLLES, S., MARK, P. J., PLANT, T., HUISSOON, A., O'SHEA, M. K., WILLCOX, B. E., DRAYSON, M. T., CRISPIN, M., CUNNINGHAM, A. F. & RICHTER, A. G. 2020. Detection of antibodies to the SARS-CoV-2 spike glycoprotein in both serum and saliva enhances detection of infection. *medRxiv* 2020.06.16.20133025.

FAUSTINI, S. E., JOSSI, S. E., PEREZ-TOLEDO, M., SHIELDS, A. M., ALLEN, J. D., WATANABE, Y., NEWBY, M. L., COOK, A., WILLCOX, C. R., SALIM, M., GOODALL, M., HEANEY, J. L., MARCIAL-JUAREZ, E., MORLEY, G. L., TORLINSKA, B., WRAITH, D. C., VEENITH, T. V., HARDING, S., JOLLES, S., PONSFORD, M. J., PLANT, T., HUISSOON, A., O'SHEA, M. K., WILLCOX, B. E., DRAYSON, M. T., CRISPIN, M., CUNNINGHAM, A. F. & RICHTER, A. G. 2021. Development of a high-sensitivity ELISA detecting IgG, IgA and IgM antibodies to the SARS-CoV-2 spike glycoprotein in serum and saliva. *Immunology,* 164**,** 135-147.

FEASEY, N. A., DOUGAN, G., KINGSLEY, R. A., HEYDERMAN, R. S. & GORDON, M. A. 2012. Invasive non-typhoidal salmonella disease: an emerging and neglected tropical disease in Africa. *The Lancet,* 379**,** 2489-2499.

FELETOU, M. 2011. The Endothelium *Part 1: Multiple Functions of the Endothelial Cells - Focus on Endothelium-Derived Vasoactive Mediators.* San Rafael: Morgan and Claypool Life Sciences.

FERRANTE, A., BEARD, L. J. & FELDMAN, R. G. 1990. IgG subclass distribution of antibodies to bacterial and viral antigens. *The Pediatric Infectious Disease Journal,* 9**,** 516-524.

FIERER, J. & GUINEY, D. G. 2001. Diverse virulence traits underlying different clinical outcomes of Salmonella infection. *Journal of Clinical Investigation,* 107**,** 775-80.

FITZGERALD, J. R., LOUGHMAN, A., KEANE, F., BRENNAN, M., KNOBEL, M., HIGGINS, J., VISAI, L., SPEZIALE, P., COX, D. & FOSTER, T. J. 2006. Fibronectin-binding proteins of Staphylococcus aureus mediate activation of human platelets via fibrinogen and fibronectin bridges to integrin GPIIb/IIIa and IgG binding to the FcgammaRIIa receptor. *Molecular Microbiology,* 59**,** 212-30.

FITZPATRICK, G., NADER, D., WATKIN, R., MCCOY, C. E., CURLEY, G. F. & KERRIGAN, S. W. 2022. Human endothelial cell-derived exosomal microRNA-99a/b drives a sustained inflammatory response during sepsis by inhibiting mTOR expression. *Frontiers in Cellular and Infection Microbiology,* 12**,** 854126.

FLAJNIK, M. F. & KASAHARA, M. 2010. Origin and evolution of the adaptive immune system: genetic events and selective pressures. *Nature Reviews Genetics,* 11**,** 47-59.

FLINSENBERG, T. W. H., JANSSEN, W. J., HERCZENIK, E., BOROSS, P., NEDEREND, M., JONGENEEL, L. H., SCHOLMAN, R. C., BOELENS, J. J., MAAS, C., VAN GIJN, M. E., VAN MONTFRANS, J. M., LEUSEN, J. H. & BOES, M. 2014. A novel FcgammaRIIa Q27W gene variant is associated with common variable immune deficiency through defective FcgammaRIIa downstream signaling. *Clinical Immunology,* 155**,** 108-117.

FORD, I., DOUGLAS, C. W. I., COX, D., REES, D. G. C., HEATH, J. & PRESTON, F. E. 1997. The role of immunoglobulin G and fibrinogen in platelet aggregation by Streptococcus sanguis. *British Journal of Haematology,* 97**,** 737-746.

FORD, I., DOUGLAS, C. W. I., HEATH, J., REES, C. & PRESTON, F. E. 1996. Evidence for the involvement of complement in platelet aggregation by Strep sanguis NCTC 7863. *British Journal of Haematology,* 94**,** 729-739.

FORRESTER, L. J., CAMPBELL, B. J., BERG, J. N. & BARRETT, J. T. 1985. Aggregation of platelets by Fusobacterium necrophorum. *Journal of Clinical Microbiology,* 22**,** 245-9.

FORTHAL, D. N. 2014. Functions of Antibodies. *Microbiology Spectrum,* 2**,** 1-17.

GAL-MOR, O., BOYLE, E. C. & GRASSL, G. A. 2014. Same species, different diseases: how and why typhoidal and non-typhoidal Salmonella enterica serovars differ. *Frontiers in Microbiology,* 5**,** 391.

GAO, T., HU, M., ZHANG, X., LI, H., ZHU, L., LIU, H., DONG, Q., ZHANG, Z., WANG, Z., HU, Y., FU, Y., JIN, Y., LI, K., ZHAO, S., XIAO, Y., LUO, S., LI, L., ZHAO, L., LIU, J., ZHAO, H., LIU, Y., YANG, W., PENG, J., CHEN, X., LI, P., LIU, Y., XIE, Y., SONG, J., ZHANG, L., MA, Q., BIAN, X., CHEN, W., LIU, X., MAO, Q. & CAO, C. 2020. Highly pathogenic coronavirus N protein aggravates lung injury by MASP-2-mediated complement over-activation. *medRxiv***,** 2020.03.29.20041962.

GAO, T., ZHU, L., LIU, H., ZHANG, X., WANG, T., FU, Y., LI, H., DONG, Q., HU, Y., ZHANG, Z., JIN, J., LIU, Z., YANG, W., LIU, Y., JIN, Y., LI, K., XIAO, Y., LIU, J., ZHAO, H., LIU, Y., LI, P., SONG, J., ZHANG, L., GAO, Y., KANG, S., CHEN, S., MA, Q., BIAN, X., CHEN, W., LIU, X., MAO, Q. & CAO, C. 2022. Highly pathogenic coronavirus N protein aggravates inflammation by MASP-2-mediated lectin complement pathway overactivation. *Signal Transduction and Targeted Therapy,* 7**,** 318.

GARCÍA-CARDEÑA, G., COMANDER, J., ANDERSON, K. R., BLACKMAN, B. R. & GIMBRONE JR, M. A. 2001. Biomechanical activation of vascular endothelium as a determinant of its functional phenotype. *Proceedings of the National Academy of Sciences,* 98**,** 4478-4485.

GARCÍA-FERNÁNDEZ-BRAVO, I., GONZÁLEZ-MUNERA, A., ORDIERES-ORTEGA, L., RUIZ CHIRIBOGA, D. & GONZÁLEZ-LEYTE, M. 2019. Thrombosis of an infrarenal aortic aneurysm secondary to Salmonella enteritidis infection. *Revista de Gastroenterologia de Mexico (Engl Ed),* 84**,** 522-524.

GAUCHEL, N., RIEDER, M., KRAUEL, K., GOLLER, I., JESERICH, M., SALZER, U., VENHOFF, A. C., BALDUS, N., POLLMEIER, L., WIRTH, L., KERN, W., RIEG, S., BUSCH, H. J., HOFMANN, M., BODE, C., DUERSCHMIED, D., LOTHER, A. & HEGER, L. A. 2022. Complement system component dysregulation is a distinctive feature of COVID-19 disease: a prospective and comparative analysis of patients admitted to the emergency department for suspected COVID-19 disease. *Journal of Thrombosis and Thrombolysis,* 53**,** 788-797.

GAVRIATOPOULOU, M., KOROMPOKI, E., FOTIOU, D., NTANASIS-STATHOPOULOS, I., PSALTOPOULOU, T., KASTRITIS, E., TERPOS, E. & DIMOPOULOS, M. A. 2020. Organ-specific manifestations of COVID-19 infection. *Clinical and Experimental Medicine,* 20**,** 493-506.

GAVRIILAKI, E., ASTERIS, P. G., TOULOUMENIDOU, T., KORAVOU, E. E., KOUTRA, M., PAPAYANNI, P. G., KARALI, V., PAPALEXANDRI, A., VARELAS, C., CHATZOPOULOU, F., CHATZIDIMITRIOU, M., CHATZIDIMITRIOU, D., VELENI, A., GRIGORIADIS, S., RAPTI, E., CHLOROS, D., KIOUMIS, I., KAIMAKAMIS, E., BITZANI, M., BOUMPAS, D., TSANTES, A., SOTIROPOULOS, D., SAKELLARI, I., KALANTZIS, I. G., PARASTATIDIS, S. T., KOOPIALIPOOR, M., CAVALERI, L., ARMAGHANI, D. J., PAPADOPOULOU, A., BRODSKY, R. A., KOKORIS, S. & ANAGNOSTOPOULOS, A. 2021. Genetic justification of severe COVID-19 using a rigorous algorithm. *Clinical Immunology,* 226**,** 108726.

GEORG, P., ASTABURUAGA-GARCIA, R., BONAGURO, L., BRUMHARD, S., MICHALICK, L., LIPPERT, L. J., KOSTEVC, T., GABEL, C., SCHNEIDER, M., STREITZ, M., DEMICHEV, V., GEMUND, I., BARONE, M., TOBER-LAU, P., HELBIG, E. T., HILLUS, D., PETROV, L., STEIN, J., DEY, H. P., PACLIK, D., IWERT, C., MULLEDER, M., AULAKH, S. K., DJUDJAJ, S., BULOW, R. D., MEI, H. E., SCHULZ, A. R., THIEL, A., HIPPENSTIEL, S., SALIBA, A. E., EILS, R., LEHMANN, I., MALL, M. A., STRICKER, S., ROHMEL, J., CORMAN, V. M., BEULE, D., WYLER, E., LANDTHALER, M., OBERMAYER, B., VON STILLFRIED, S., BOOR, P., DEMIR, M., WESSELMANN, H., SUTTORP, N., UHRIG, A., MULLER-REDETZKY, H., NATTERMANN, J., KUEBLER, W. M., MEISEL, C., RALSER, M., SCHULTZE, J. L., ASCHENBRENNER, A. C., THIBEAULT, C., KURTH, F., SANDER, L. E., BLUTHGEN, N., SAWITZKI, B. & GROUP, P.-C.-S. 2022. Complement activation induces excessive T cell cytotoxicity in severe COVID-19. *Cell,* 185**,** 493-512 e25.

GHOSH, J. B. & SAMANTA, S. 1994. Venous thrombosis in enteric fever. *Indian Pediatrics,* 31**,** 230-1.

GHUMAN, H., SHEPHERD-ROBERTS, A., WATSON, S., ZUIDSCHERWOUDE, M., WATSON, S. P. & VOELZ, K. 2019. Mucor circinelloides induces platelet aggregation through integrin αIIbβ3 and FcγRIIA. *Platelets,* 30**,** 256-263.

GIACOMELLI, A., RIGHINI, E., MICHELI, V., PINOLI, P., BERNASCONI, A., RIZZO, A., ORENI, L., RIDOLFO, A. L., ANTINORI, S., CERI, S. & RIZZARDINI, G. 2023. SARS-CoV-2 viremia and COVID-19 mortality: A prospective observational study. *PLoS One,* 18**,** e0281052.

GIL-CRUZ, C., BOBAT, S., MARSHALL, J. L., KINGSLEY, R. A., ROSS, E. A., HENDERSON, I. R., LEYTON, D. L., COUGHLAN, R. E., KHAN, M., JENSEN, K. T., BUCKLEY, C. D., DOUGAN, G., MACLENNAN, I. C., LOPEZ-MACIAS, C. & CUNNINGHAM, A. F. 2009. The porin OmpD from nontyphoidal Salmonella is a key target for a protective B1b cell antibody response. *Proceedings of the National Academy of Sciences of the United States of America,* 106**,** 9803-8.

GITZ, E., POLLITT, A. Y., GITZ-FRANCOIS, J. J., ALSHEHRI, O., MORI, J., MONTAGUE, S., NASH, G. B., DOUGLAS, M. R., GARDINER, E. E., ANDREWS, R. K., BUCKLEY, C. D., HARRISON, P. & WATSON, S. P. 2014. CLEC-2 expression is maintained on activated platelets and on platelet microparticles. *Blood,* 124**,** 2262-2270.

GOLDENBERG, N. M., STEINBERG, B. E., SLUTSKY, A. S. & LEE, W. L. 2011. Broken barriers: A new take on sepsis pathogenesis. *Science Translational Medicine,* 3**,** 88ps25.

GORDON, M. A., KANKWATIRA, A. M. K., MWAFULIRWA, G., WALSH, A. L., HOPKINS, M. J., PARRY, C. M., FARAGHER, E. B., ZIJLSTRA, E. E., HEYDERMAN, R. S. & MOLYNEUX, M. E. 2010. Invasive Non-

typhoid Salmonellae Establish Systemic Intracellular Infection in HIV-Infected Adults: An Emerging Disease Pathogenesis. *Clinical Infectious Diseases,* 50**,** 953-962.

GOTZ, M. P., SKJOEDT, M. O., BAYARRI-OLMOS, R., HANSEN, C. B., PEREZ-ALOS, L., JARLHELT, I., BENFIELD, T., ROSBJERG, A. & GARRED, P. 2022. Lectin Pathway Enzyme MASP-2 and Downstream Complement Activation in COVID-19. *Journal of Innate Immunity***,** 1-14.

GRALINSKI, L. E., SHEAHAN, T. P., MORRISON, T. E., MENACHERY, V. D., JENSEN, K., LEIST, S. R., WHITMORE, A., HEISE, M. T. & BARIC, R. S. 2018. Complement Activation Contributes to Severe Acute Respiratory Syndrome Coronavirus Pathogenesis. *Mbio,* 9**,** 15.

GRANT, O. C., MONTGOMERY, D., ITO, K. & WOODS, R. J. 2020. Analysis of the SARS-CoV-2 spike protein glycan shield reveals implications for immune recognition. *Scientific Reports,* 10**,** 14991.

GREINACHER, A. & WARKENTIN, T. E. 2023. Platelet factor 4 triggers thrombo-inflammation by bridging innate and adaptive immunity. *International Journal of Laboratory Hematology,* 45 Suppl 2**,** 11-22.

GUDBRANDSDOTTIR, S., HASSELBALCH, H. C. & NIELSEN, C. H. 2013. Activated platelets enhance IL-10 secretion and reduce TNF-alpha secretion by monocytes. *Journal of Immunology,* 191**,** 4059-67.

GUO, L. & RONDINA, M. T. 2019. The Era of Thromboinflammation: Platelets Are Dynamic Sensors and Effector Cells During Infectious Diseases. *Frontiers in Immunology,* 10**,** 2204.

GUSHIKEN, F. C., HAN, H., LI, J., RUMBAUT, R. E. & AFSHAR-KHARGHAN, V. 2009. Abnormal platelet function in C3-deficient mice. *Journal of Thrombosis and Haemostasis,* 7**,** 865-70.

HAGMAN, K., HEDENSTIERNA, M., RUDLING, J., GILLE-JOHNSON, P., HAMMAS, B., GRABBE, M., JAKOBSSON, J., DILLNER, J. & URSING, J. 2022. Duration of SARS-CoV-2 viremia and its correlation to mortality and inflammatory parameters in patients hospitalized for COVID-19: a cohort study. *Diagnostic Microbiology and Infectious Disease,* 102**,** 115595.

HAKIM, T. S., SUGIMORI, K., CAMPORESI, E. M. & ANDERSON, G. 1996. Half-life of nitric oxide in aqueous solutions with and without haemoglobin. *Physiological Measurement,* 17**,** 267-77.

HAMAD, O. A., EKDAHL, K. N., NILSSON, P. H., ANDERSSON, J., MAGOTTI, P., LAMBRIS, J. D. & NILSSON, B. 2008. Complement activation triggered by chondroitin sulfate released by thrombin receptor-activated platelets. *Journal of Thrombosis and Haemostasis,* 6**,** 1413-21.

HANNACHI, N., OGE-GANAYE, E., BAUDOIN, J. P., FONTANINI, A., BERNOT, D., HABIB, G. & CAMOIN-JAU, L. 2020. Antiplatelet Agents Have a Distinct Efficacy on Platelet Aggregation Induced by Infectious Bacteria. *Frontiers in Pharmacology,* 11**,** 863.

HANRATH, A. T., PAYNE, B. A. I., DUNCAN, C. J. A. & NEWCASTLE HOSP, H. C. W. T. G. 2021. Prior SARS-CoV-2 infection is associated with protection against symptomatic reinfection. *Journal of Infection,* 82**,** E29-E30.

HEIJNEN, H. & VAN DER SLUIJS, P. 2015. Platelet secretory behaviour: as diverse as the granules ... or not? *Journal of Thrombosis and Haemostasis,* 13**,** 2141-51.

HENRY, B. M., SZERGYUK, I., DE OLIVEIRA, M. H. S., LIPPI, G., BENOIT, J. L., VIKSE, J. & BENOIT, S. W. 2021. Complement levels at admission as a reflection of coronavirus disease 2019 (COVID-19) severity state. *Journal of Medical Virology,* 93**,** 5515-5522.

HINGRAT, Q. L., VISSEAUX, B., LAOUENAN, C., TUBIANA, S., BOUADMA, L., YAZDANPANAH, Y., DUVAL, X., BURDET, C., ICHOU, H., DAMOND, F., BERTINE, M., BENMALEK, N., CHOQUET, C., TIMSIT, J. F., GHOSN, J., CHARPENTIER, C., DESCAMPS, D., HOUHOU-FIDOUH, N., FRENCH COVID COHORT MANAGEMENT COMMITTEE, C.-C. S. G., MEMBERS OF THE FRENCH, C. C. S. G., MEMBER OF THE CO, V. C. S. G. P. I., STEERING, C., CO, V. C. C. C., COORDINATION, STATISTICAL, A., VIROLOGICAL, L., BIOLOGICAL, C., PARTNERS, SPONSOR & GENETIC 2020. Detection of SARS-CoV-2 N-antigen in blood during acute COVID-19 provides a sensitive new marker and new testing alternatives. *Clinical Microbiology and Infection,* 27**,** 789 e1-5.

HITCHCOCK, J. R., COOK, C. N., BOBAT, S., ROSS, E. A., FLORES-LANGARICA, A., LOWE, K. L., KHAN, M., DOMINGUEZ-MEDINA, C. C., LAX, S., CARVALHO-GASPAR, M., HUBSCHER, S., RAINGER, G. E., COBBOLD, M., BUCKLEY, C. D., MITCHELL, T. J., MITCHELL, A., JONES, N. D., VAN ROOIJEN, N., KIRCHHOFER, D., HENDERSON, I. R., ADAMS, D. H., WATSON, S. P. & CUNNINGHAM, A. F. 2015. Inflammation drives thrombosis after Salmonella infection via CLEC-2 on platelets. *Journal of Clinical Investigation,* 125**,** 4429-4446.

HOFFBRAND, A. V. & STEENSMA, D. P. 2019. *Hoffbrand's essential haematology,* Hoboken, John Wiley and Sons, Inc.

HOISETH, S. K. & STOCKER, B. A. D. 1981. Aromatic-dependent Salmonella Typhimurium are non-virulent and effective as live vaccines. *Nature,* 291**,** 238-239.

HOLTER, J. C., PISCHKE, S. E., DE BOER, E., LIND, A., JENUM, S., HOLTEN, A. R., TONBY, K., BARRATT-DUE, A., SOKOLOVA, M., SCHJALM, C., CHABAN, V., KOLDERUP, A., TRAN, T., TOLLEFSRUD GJØLBERG, T., SKEIE, L. G., HESSTVEDT, L., ORMÅSEN, V., FEVANG, B., AUSTAD, C., MÜLLER, K. E., FLADEBY, C., HOLBERG-PETERSEN, M., HALVORSEN, B., MÜLLER, F., AUKRUST, P., DUDMAN, S., UELAND, T., ANDERSEN, J. T., LUND-JOHANSEN, F., HEGGELUND, L., DYRHOL-RIISE, A. M. & MOLLNES, T. E. 2020. Systemic complement activation is associated with respiratory failure in COVID-19 hospitalized patients. *Proceedings of the National Academy of Sciences of the United States of America,* 117**,** 25018-25025.

HSIEH, C. L., GOLDSMITH, J. A., SCHAUB, J. M., DIVENERE, A. M., KUO, H. C., JAVANMARDI, K., LE, K. C., WRAPP, D., LEE, A. G., LIU, Y. T., CHOU, C. W., BYRNE, P. O., HJORTH, C. K., JOHNSON, N. V., LUDES-MEYERS, J., NGUYEN, A. W., PARK, J., WANG, N. S., AMENGOR, D., LAVINDER, J. J., IPPOLITO, G. C., MAYNARD, J. A., FINKELSTEIN, I. J. & MCLELLAN, J. S. 2020. Structure-based design of prefusion-stabilized SARS-CoV-2 spikes. *Science,* 369**,** 1501.

HURLER, L., SZILAGYI, A., MESCIA, F., BERGAMASCHI, L., MEZO, B., SINKOVITS, G., RETI, M., MULLER, V., IVANYI, Z., GAL, J., GOPCSA, L., REMENYI, P., SZATHMARY, B., LAKATOS, B., SZLAVIK, J., BOBEK, I., PROHASZKA, Z. Z., FORHECZ, Z., CSUKA, D., KAJDACSI, E., CERVENAK, L., KISZEL, P., MASSZI, T., VALYI-NAGY, I., WURZNER, R., CAMBRIDGE INSTITUTE OF THERAPEUTIC, I., INFECTIOUS DISEASE-NATIONAL INSTITUTE OF HEALTH RESEARCH, C. B. C., LYONS, P. A., TOONEN, E. J. M. & PROHASZKA, Z. 2023. Complement lectin pathway activation is associated with COVID-19 disease severity, independent of MBL2 genotype subgroups. *Frontiers in Immunology,* 14**,** 1162171.

HURLER, L., TOONEN, E. J. M., KAJDACSI, E., VAN BREE, B., BRANDWIJK, R., DE BRUIN, W., LYONS, P. A., BERGAMASCHI, L., CAMBRIDGE INSTITUTE OF THERAPEUTIC, I., INFECTIOUS DISEASE-NATIONAL INSTITUTE OF HEALTH RESEARCH, C. B. C., SINKOVITS, G., CERVENAK, L., WURZNER, R. & PROHASZKA, Z. 2022. Distinction of early complement classical and lectin pathway activation via quantification of C1s/C1-INH and MASP-1/C1-INH complexes using novel ELISAs. *Frontiers in Immunology,* 13**,** 1039765.

HURSTING, M. J., PAI, P. J., MCCRACKEN, J. E., HWANG, F., SUVARNA, S., LOKHNYGINA, Y., BANDARENKO, N. & AREPALLY, G. M. 2010. Platelet factor 4/heparin antibodies in blood bank donors. *American Journal of Clinical Pathology,* 134**,** 774-80.

IBA, T., LEVY, J. H., CONNORS, J. M., WARKENTIN, T. E., THACHIL, J. & LEVI, M. 2020. The unique characteristics of COVID-19 coagulopathy. *Critical Care,* 24**,** 360.

IP, W. K. E., CHAN, K. H., LAW, H. K. W., TSO, G. H. W., KONG, E. K. P., WONG, W. H. S., TO, Y. F., YUNG, R. W. H., CHOW, E. Y., AU, K. L., CHAN, E. Y. T., LIM, W., JENSENIUS, J. C., TURNER, M. W., PEIRIS, J. S. M. & LAU, Y. L. 2005. Mannose-binding lectin in severe acute respiratory syndrome coronavirus infection. *Journal of Infectious Diseases,* 191**,** 1697-1704.

IPINZA, F., COLLAO, B., MONSALVA, D., BUSTAMANTE, V. H., LURASCHI, R., ALEGRÍA-ARCOS, M., ALMONACID, D. E., AGUAYO, D., CALDERÓN, I. L., GIL, F., SANTIVIAGO, C. A., MORALES, E. H., CALVA, E. & SAAVEDRA, C. P. 2014. Participation of the Salmonella OmpD porin in the infection of RAW264.7 macrophages and BALB/c mice. *PLoS One,* 9**,** e111062.

JACOBS, J. L., BAIN, W., NAQVI, A., STAINES, B., CASTANHA, P. M. S., YANG, H., BOLTZ, V. F., BARRATT-BOYES, S., MARQUES, E. T. A., MITCHELL, S. L., METHE, B., OLONISAKIN, T. F., HAIDAR, G., BURKE, T. W., PETZOLD, E., DENNY, T., WOODS, C. W., MCVERRY, B. J., LEE, J. S., WATKINS, S. C., ST CROIX, C. M., MORRIS, A., KEARNEY, M. F., LADINSKY, M. S., BJORKMAN, P. J., KITSIOS, G. D. & MELLORS, J. W. 2022. Severe Acute Respiratory Syndrome Coronavirus 2 Viremia Is Associated With Coronavirus Disease 2019 Severity and Predicts Clinical Outcomes. *Clinical Infectious Diseases,* 74**,** 1525-1533.

JAHN, K., KOHLER, T. P., SWIATEK, L. S., WIEBE, S. & HAMMERSCHMIDT, S. 2022. Platelets, Bacterial Adhesins and the Pneumococcus. *Cells,* 11**,** 1121.

JAMALY, S., TSOKOS, M. G., BHARGAVA, R., BROOK, O. R., HECHT, J. L., ABDI, R., MOULTON, V. R., SATYAM, A. & TSOKOS, G. C. 2021. Complement activation and increased expression of Syk, mucin-1 and CaMK4 in kidneys of patients with COVID-19. *Clinical Immunology,* 229**,** 108795.

JANEWAY, C. A., TRAVERS, P., WALPORT, M. & SCHLOMCHIK, M. J. 2001a. The complement system and innate immunity. *Immunobiology.* 5th ed. New York: Garland Science.

JANEWAY, C. A., TRAVERS, P., WALPORT, M. & SCHLOMCHIK, M. J. 2001b. The distribution and functions of immunoglobulin isotypes. *Immunobiology.* 5th ed. New York: Garland Science.

JANSEN, A. J. G., SPAAN, T., LOW, H. Z., DI IORIO, D., VAN DEN BRAND, J., TIEKE, M., BARENDRECHT, A., ROHN, K., VAN AMERONGEN, G., STITTELAAR, K., BAUMGARTNER, W., OSTERHAUS, A., KUIKEN, T., BOONS, G. J., HUSKENS, J., BOES, M., MAAS, C. & VAN DER VRIES, E. 2020. Influenza-induced thrombocytopenia is dependent on the subtype and sialoglycan receptor and increases with virus pathogenicity. *Blood Advances,* 4**,** 2967-2978.

JARHULT, J. D., HULTSTROM, M., BERGQVIST, A., FRITHIOF, R. & LIPCSEY, M. 2021. The impact of viremia on organ failure, biomarkers and mortality in a Swedish cohort of critically ill COVID-19 patients. *Scientific Reports,* 11**,** 7163.

JARLHELT, I., NIELSEN, S. K., JAHN, C. X. H., HANSEN, C. B., PÉREZ-ALÓS, L., ROSBJERG, A., BAYARRI-OLMOS, R., SKJOEDT, M.-O. & GARRED, P. 2021. SARS-CoV-2 antibodies mediate complement and cellular driven inflammation. *Frontiers in Immunology,* 12.

JARVIK, T., SMILLIE, C., GROISMAN, E. A. & OCHMAN, H. 2010. Short-term signatures of evolutionary change in the Salmonella enterica serovar typhimurium 14028 genome. *Journal of Bacteriology,* 192**,** 560-7.

JERJES-SANCHEZ, C. 2004. Venous and arterial thrombosis: a continuous spectrum of the same disease? *European Heart Journal,* 26**,** 3-4.

JIANG, Y., ZHAO, G., SONG, N., LI, P., CHEN, Y., GUO, Y., LI, J., DU, L., JIANG, S., GUO, R., SUN, S. & ZHOU, Y. 2018. Blockade of the C5a-C5aR axis alleviates lung damage in hDPP4-transgenic mice infected with MERS-CoV. *Emerging Microbes and Infections,* 7**,** 77.

JOHNSON, J. B., CAPRARO, G. A. & PARKS, G. D. 2008. Differential mechanisms of complement-mediated neutralization of the closely related paramyxoviruses simian virus 5 and mumps virus. *Virology,* 376**,** 112-23.

JUANES-VELASCO, P., LANDEIRA-VINUELA, A., GARCIA-VAQUERO, M. L., LECREVISSE, Q., HERRERO, R., FERRUELO, A., GONGORA, R., CORRALES, F., RIVAS, J. L., LORENTE, J. A., HERNANDEZ, A. P. & FUENTES, M. 2022. SARS-CoV-2 Infection Triggers Auto-Immune Response in ARDS. *Frontiers in Immunology,* 13**,** 732197.

KAEUFFER, C., LE HYARIC, C., FABACHER, T., MOOTIEN, J., DERVIEUX, B., RUCH, Y., HUGEROT, A., ZHU, Y. J., POINTURIER, V., CLERE-JEHL, R., GREIGERT, V., KASSEGNE, L., LEFEBVRE, N., GALLAIS, F., MEYER, N., HANSMANN, Y., HINSCHBERGER, O. & DANION, F. 2020. Clinical characteristics and risk factors associated with severe COVID-19: prospective analysis of 1,045 hospitalised cases in North-Eastern France, March 2020. *Eurosurveillance,* 25.

KALIL, A. C. & PROSCHAN, M. 2022. Complement C5a inhibition: a new form of COVID-19 treatment for mechanically ventilated patients? *The Lancet Respiratory Medicine,* 10**,** 1103-1104.

KARAS, S. P., ROSSE, W. F. & KURLANDER, R. J. 1982. Characterization of the IgG-Fc receptor on human platelets. *Blood,* 60**,** 1277-1282.

KEANE, C., PETERSEN, H., REYNOLDS, K., NEWMAN, D. K., COX, D., JENKINSON, H. F., NEWMAN, P. J. & KERRIGAN, S. W. 2010a. Mechanism of outside-in {alpha}IIb{beta}3-mediated activation of human platelets by the colonizing Bacterium, Streptococcus gordonii. *Arteriosclerosis, Thrombosis, and Vascular Biology,* 30**,** 2408-15.

KEANE, C., TILLEY, D., CUNNINGHAM, A., SMOLENSKI, A., KADIOGLU, A., COX, D., JENKINSON, H. F. & KERRIGAN, S. W. 2010b. Invasive Streptococcus pneumoniae trigger platelet activation via Toll-like receptor 2. *Journal of Thrombosis and Haemostasis,* 8**,** 2757-65.

KERRIGAN, S. W. 2015. Platelet Interactions with Bacteria. *In:* KERRIGAN, S. W. & MORAN, N. (eds.) *The Non-Thrombotic Role of Platelets in Health and Disease.* Rijeka: IntechOpen.

KERRIGAN, S. W., CLARKE, N., LOUGHMAN, A., MEADE, G., FOSTER, T. J. & COX, D. 2008. Molecular Basis for Staphylococcus aureus–Mediated Platelet Aggregate Formation Under Arterial Shear In Vitro. *Arteriosclerosis, Thrombosis, and Vascular Biology,* 28**,** 335-340.

KERRIGAN, S. W., DEVINE, T., FITZPATRICK, G., THACHIL, J. & COX, D. 2019. Early Host Interactions That Drive the Dysregulated Response in Sepsis. *Frontiers in Immunology,* 10**,** 1748.

KERRIGAN, S. W., DOUGLAS, I., WRAY, A., HEATH, J., BYRNE, M. F., FITZGERALD, D. & COX, D. 2002. A role for glycoprotein Ib in Streptococcus sanguis–induced platelet aggregation. *Blood,* 100**,** 509-516.

KERRIGAN, S. W., JAKUBOVICS, N. S., KEANE, C., MAGUIRE, P., WYNNE, K., JENKINSON, H. F. & COX, D. 2007. Role of Streptococcus gordonii surface proteins SspA/SspB and Hsa in platelet function. *Infection and Immunity,* 75**,** 5740-7.

KEYT, B. A., BALIGA, R., SINCLAIR, A. M., CARROLL, S. F. & PETERSON, M. S. 2020. Structure, Function, and Therapeutic Use of IgM Antibodies. *Antibodies,* 9**,** 53.

KINGSLEY, R. A., MSEFULA, C. L., THOMSON, N. R., KARIUKI, S., HOLT, K. E., GORDON, M. A., HARRIS, D., CLARKE, L., WHITEHEAD, S., SANGAL, V., MARSH, K., ACHTMAN, M., MOLYNEUX, M. E., CORMICAN, M., PARKHILL, J., MACLENNAN, C. A., HEYDERMAN, R. S. & DOUGAN, G. 2009. Epidemic multiple drug resistant Salmonella Typhimurium causing invasive disease in sub-Saharan Africa have a distinct genotype. *Genome Research,* 19**,** 2279-87.

KLINGLER, J., LAMBERT, G. S., ITRI, V., LIU, S., BANDRES, J. C., ENYINDAH-ASONYE, G., LIU, X., SIMON, V., GLEASON, C. R., KLEINER, G., CHIU, H.-P., HUNG, C.-T., KOWDLE, S., AMANAT, F., LEE, B., ZOLLA-PAZNER, S., UPADHYAY, C. & HIOE, C. E. 2021. Detection of Antibody Responses Against SARS-CoV-2 in Plasma and Saliva From Vaccinated and Infected Individuals. *Frontiers in Immunology,* 12**,** 759688.

KLOK, F. A., KRUIP, M. J. H. A., VAN DER MEER, N. J. M., ARBOUS, M. S., GOMMERS, D. A. M. P. J., KANT, K. M., KAPTEIN, F. H. J., VAN PAASSEN, J., STALS, M. A. M., HUISMAN, M. V. & ENDEMAN, H. 2020. Incidence of thrombotic complications in critically ill ICU patients with COVID-19. *Thrombosis Research,* 191**,** 145-147.

KNIGHT, R., WALKER, V., IP, S., COOPER, J. A., BOLTON, T., KEENE, S., DENHOLM, R., AKBARI, A., ABBASIZANJANI, H., TORABI, F., OMIGIE, E., HOLLINGS, S., NORTH, T.-L., TOMS, R., JIANG, X., ANGELANTONIO, E. D., DENAXAS, S., THYGESEN, J. H., TOMLINSON, C., BRAY, B., SMITH, C. J., BARBER, M., KHUNTI, K., DAVEY SMITH, G., CHATURVEDI, N., SUDLOW, C., WHITELEY, W. N., WOOD, A. M., STERNE, J. A. C. & NULL, N. 2022. Association of COVID-19 With Major Arterial and Venous Thrombotic Diseases: A Population-Wide Cohort Study of 48 Million Adults in England and Wales. *Circulation,* 146**,** 892-906.

KOESSLER, J., NIKLAUS, M., WEBER, K., KOESSLER, A., KUHN, S., BOECK, M. & KOBSAR, A. 2019. The Role of Human Platelet Preparation for Toll-Like Receptors 2 and 4 Related Platelet Responsiveness. *TH Open,* 3**,** e94-e102.

KOLEV, M., LE FRIEC, G. & KEMPER, C. 2014. Complement--tapping into new sites and effector systems. *Nature Reviews Immunology,* 14**,** 811-20.

KRAUEL, K., POTSCHKE, C., WEBER, C., KESSLER, W., FURLL, B., ITTERMANN, T., MAIER, S., HAMMERSCHMIDT, S., BROKER, B. M. & GREINACHER, A. 2011. Platelet factor 4 binds to bacteria, [corrected] inducing antibodies cross-reacting with the major antigen in heparin-induced thrombocytopenia. *Blood,* 117**,** 1370-8.

KRAUEL, K., WEBER, C., BRANDT, S., ZAHRINGER, U., MAMAT, U., GREINACHER, A. & HAMMERSCHMIDT, S. 2012. Platelet factor 4 binding to lipid A of Gram-negative bacteria exposes PF4/heparin-like epitopes. *Blood,* 120**,** 3345-52.

KREIMANN, M., BRANDT, S., KRAUEL, K., BLOCK, S., HELM, C. A., WEITSCHIES, W., GREINACHER, A. & DELCEA, M. 2014. Binding of anti-platelet factor 4/heparin antibodies depends on the thermodynamics of conformational changes in platelet factor 4. *Blood,* 124**,** 2442-9.

KRUGER-GENGE, A., BLOCKI, A., FRANKE, R. P. & JUNG, F. 2019. Vascular Endothelial Cell Biology: An Update. *International Journal of Molecular Sciences,* 20**,** 4411.

KRUKONIS, E. S. & THOMSON, J. J. 2020. Complement evasion mechanisms of the systemic pathogens Yersiniae and Salmonellae. *FEBS Letters,* 594**,** 2598-2620.

KUEHN, M. J. & KESTY, N. C. 2005. Bacterial outer membrane vesicles and the host-pathogen interaction. *Genes Dev,* 19**,** 2645-55.

KURTOVIC, L. & BEESON, J. G. 2021. Complement factors in COVID-19 therapeutics and vaccines. *Trends in Immunology,* 42**,** 94-103.

KUSHNER, A., WEST, W. P., SUHEB, M. Z. K. & PILLARISETTY, L. S. 2022. *Virchow Triad* [Online]. Treasure Island (FL): StatPearls Publishing. Available: https://www.ncbi.nlm.nih.gov/books/NBK539697/ [Accessed 16/11/2023 2023].

KUSUDO, E., MURATA, Y., KAWAMOTO, S. & EGI, M. 2023. Variant-derived SARS-CoV-2 spike protein does not directly cause platelet activation or hypercoagulability. *Clinical and Experimental Medicine,* 23**,** 3701-3708.

LAGE, S. L., ROCCO, J. M., LAIDLAW, E., RUPERT, A., GALINDO, F., KELLOGG, A., KUMAR, P., POON, R., WORTMANN, G. W., LISCO, A., MANION, M. & SERETI, I. 2022. Activation of Complement Components on Circulating Blood Monocytes From COVID-19 Patients. *Frontiers in Immunology,* 13**,** 815833.

LAINE, O., JOUTSI-KORHONEN, L., LASSILA, R., KOSKI, T., HUHTALA, H., VAHERI, A., MÄKELÄ, S. & MUSTONEN, J. 2015. Hantavirus infection-induced thrombocytopenia triggers increased production but associates with impaired aggregation of platelets except for collagen. *Thrombosis Research,* 136**,** 1126-32.

LAM, L. K. M., MURPHY, S. J., KURI-CERVANTES, L., WEISMAN, A. R., ITTNER, C. A. G., REILLY, J. P., PAMPENA, M. B., BETTS, M. R., WHERRY, E. J., SONG, W.-C., LAMBRIS, J. D., CINES, D. B., MEYER, N. J. & MANGALMURTI, N. S. 2020. Erythrocytes Reveal Complement Activation in Patients with COVID-19. *medRxiv***,** 2020.05.20.20104398.

LAMERTON, R. E., MARCIAL-JUAREZ, E., FAUSTINI, S. E., PEREZ-TOLEDO, M., GOODALL, M., JOSSI, S. E., NEWBY, M. L., CHAPPLE, I., DIETRICH, T., VEENITH, T., SHIELDS, A. M., HARPER, L., HENDERSON, I. R., RAYES, J., WRAITH, D. C., WATSON, S. P., CRISPIN, M., DRAYSON, M. T., RICHTER, A. G. &

CUNNINGHAM, A. F. 2022. SARS-CoV-2 Spike- and Nucleoprotein-Specific Antibodies Induced After Vaccination or Infection Promote Classical Complement Activation. *Frontiers in Immunology,* 13**,** 838780.

LANDSEM, A., EMBLEM, A., LAU, C., CHRISTIANSEN, D., GEROGIANNI, A., KARLSEN, B. O., MOLLNES, T. E., NILSSON, P. H. & BREKKE, O. L. 2022. Complement C3b contributes to Escherichia coli-induced platelet aggregation in human whole blood. *Frontiers in Immunology,* 13**,** 1020712.

LEATHERDALE, A., STUKAS, S., LEI, V., WEST, H. E., CAMPBELL, C. J., HOILAND, R. L., COOPER, J., WELLINGTON, C. L., SEKHON, M. S., PRYZDIAL, E. L. G. & CONWAY, E. M. 2022. Persistently elevated complement alternative pathway biomarkers in COVID-19 correlate with hypoxemia and predict in-hospital mortality. *Medical Microbiology and Immunology,* 211**,** 37-48.

LEE, A. K., DETWEILER, C. S. & FALKOW, S. 2000. OmpR regulates the two-component system SsrA-ssrB in Salmonella pathogenicity island 2. *Journal of Bacteriology,* 182**,** 771-81.

LEE, M. H., PERL, D. P., STEINER, J., PASTERNACK, N., LI, W., MARIC, D., SAFAVI, F., HORKAYNE-SZAKALY, I., JONES, R., STRAM, M. N., MONCUR, J. T., HEFTI, M., FOLKERTH, R. D. & NATH, A. 2022. Neurovascular injury with complement activation and inflammation in COVID-19. *Brain,* 145**,** 2555-2568.

LEE, W. L. & SLUTSKY, A. S. 2010. Sepsis and endothelial permeablity. *New England Journal of Medicine,* 363**,** 689-691.

LETH-LARSEN, R., ZHONG, F., CHOW, V. T. K., HOLMSKOV, U. & LU, J. H. 2007. The SARS coronavirus spike glycoprotein is selectively recognized by lung surfactant protein D and activates macrophages. *Immunobiology,* 212**,** 201-211.

LEVI, M. & TEN CATE, H. 1999. Disseminated Intravascular Coagulation. *New England Journal of Medicine,* 341**,** 586-592.

LEVI, M. & VAN DER POLL, T. 2015. Coagulation in Patients with Severe Sepsis. *Seminars in Thrombosis and Hemostasis,* 41**,** 9-15.

LEVI, M. & VAN DER POLL, T. 2017. Coagulation and sepsis. *Thrombosis Research,* 149**,** 38-44.

LI, J., HUANG, D. Q., ZOU, B., YANG, H., HUI, W. Z., RUI, F., YEE, N. T. S., LIU, C., NERURKAR, S. N., KAI, J. C. Y., TENG, M. L. P., LI, X., ZENG, H., BORGHI, J. A., HENRY, L., CHEUNG, R. & NGUYEN, M. H. 2021a. Epidemiology of COVID-19: A systematic review and meta-analysis of clinical characteristics, risk factors, and outcomes. *Journal of Medical Virology,* 93**,** 1449-1458.

LI, X., IWAI, T., NAKAMURA, H., INOUE, Y., CHEN, Y., UMEDA, M. & SUZUKI, H. 2008. An ultrastructural study of Porphyromonas gingivalis-induced platelet aggregation. *Thrombosis Research,* 122**,** 810-9.

LI, Y., SCHNEIDER, A. M., MEHTA, A., SADE-FELDMAN, M., KAYS, K. R., GENTILI, M., CHARLAND, N. C., GONYE, A. L., GUSHTEROVA, I., KHANNA, H. K., LASALLE, T. J., LAVIN-PARSONS, K. M., LILLEY, B. M., LODENSTEIN, C. L., MANAKONGTREECHEEP, K., MARGOLIN, J. D., MCKAIG, B. N., PARRY, B. A., ROJAS-LOPEZ, M., RUSSO, B. C., SHARMA, N., TANTIVIT, J., THOMAS, M. F., REGAN, J., FLYNN, J. P., VILLANI, A. C., HACOHEN, N., GOLDBERG, M. B., FILBIN, M. R. & LI, J. Z. 2021b. SARS-CoV-

2 viremia is associated with distinct proteomic pathways and predicts COVID-19 outcomes. *Journal of Clinical Investigation,* 131**,** e148635.

LIM, S. H., METHÉ, B. A., KNOLL, B. M., MORRIS, A. & OBARO, S. K. 2018. Invasive non-typhoidal Salmonella in sickle cell disease in Africa: is increased gut permeability the missing link? *Journal of Translational Medicine,* 16**,** 239.

LIN, Y., HUANG, L., TU, Y., HUANG, B., ZHANG, S., CHEN, Y. & LI, W. 2022. Case report of Salmonella derby septicemia complicated with co-occurrence of disseminated intravascular coagulation and thrombotic microangiopathy. *BMC Infect Dis,* 22**,** 914.

LIPCSEY, M., PERSSON, B., ERIKSSON, O., BLOM, A. M., FROMELL, K., HULTSTRÖM, M., HUBER-LANG, M., EKDAHL, K. N., FRITHIOF, R. & NILSSON, B. 2021. The outcome of critically ill COVID-19 patients is linked to thromboinflammation dominated by the kallikrein/kinin system. *Frontiers in Immunology,* 12**,** 627579.

LITTMAN, R. J. 2009. The plague of Athens: epidemiology and paleopathology. *Mount Sinai Journal of Medicine,* 76**,** 456-67.

LO, M. W., KEMPER, C. & WOODRUFF, T. M. 2020. COVID-19: complement, coagulation, and collateral damage. *Journal of Immunology,* 205**,** 1488-1495.

LOPES-PACHECO, M., SILVA, P. L., CRUZ, F. F., BATTAGLINI, D., ROBBA, C., PELOSI, P., MORALES, M. M., CARUSO NEVES, C. & ROCCO, P. R. M. 2021. Pathogenesis of Multiple Organ Injury in COVID-19 and Potential Therapeutic Strategies. *Frontiers in Physiology,* 12**,** 593223.

LOPES PIRES, M. E., CLARKE, S. R., MARCONDES, S. & GIBBINS, J. M. 2017. Lipopolysaccharide potentiates platelet responses via toll-like receptor 4-stimulated Akt-Erk-PLA2 signalling. *PLoS One,* 12**,** e0186981.

LOUGHMAN, A., FITZGERALD, J. R., BRENNAN, M. P., HIGGINS, J., DOWNER, R., COX, D. & FOSTER, T. J. 2005. Roles for fibrinogen, immunoglobulin and complement in platelet activation promoted by Staphylococcus aureus clumping factor A. *Molecular Microbiology,* 57**,** 804-818.

LU, R. J., ZHAO, X., LI, J., NIU, P. H., YANG, B., WU, H. L., WANG, W. L., SONG, H., HUANG, B. Y., ZHU, N., BI, Y. H., MA, X. J., ZHAN, F. X., WANG, L., HU, T., ZHOU, H., HU, Z. H., ZHOU, W. M., ZHAO, L., CHEN, J., MENG, Y., WANG, J., LIN, Y., YUAN, J. Y., XIE, Z. H., MA, J. M., LIU, W. J., WANG, D. Y., XU, W. B., HOLMES, E. C., GAO, G. F., WU, G. Z., CHEN, W. J., SHI, W. F. & TAN, W. J. 2020. Genomic characterisation and epidemiology of 2019 novel coronavirus: implications for virus origins and receptor binding. *Lancet,* 395**,** 565-574.

LUBBERS, R., VAN ESSEN, M. F., VAN KOOTEN, C. & TROUW, L. A. 2017. Production of complement components by cells of the immune system. *Clinical and Experimental Immunology,* 188**,** 183-194.

LUMLEY, S. F., O'DONNELL, D., STOESSER, N. E., MATTHEWS, P. C., HOWARTH, A., HATCH, S. B., MARSDEN, B. D., COX, S., JAMES, T., WARREN, F., PECK, L. J., RITTER, T. G., DE TOLEDO, Z., WARREN, L., AXTEN, D., CORNALL, R. J., JONES, E. Y., STUART, D. I., SCREATON, G., EBNER, D., HOOSDALLY, S., CHAND, M., CROOK, D. W., O'DONNELL, A. M., CONLON, C. P., POUWELS, K. B., WALKER, A. S., PETO, T. E. A., HOPKINS, S., WALKER, T. M., JEFFERY, K., EYRE, D. W. & OXFORD

UNIV HOSP STAFF TESTING, G. 2021. Antibody status and incidence of SARS-CoV-2 infection in health care workers. *New England Journal of Medicine,* 384**,** 533-540.

MA, L., SAHU, S. K., CANO, M., KUPPUSWAMY, V., BAJWA, J., MCPHATTER, J., PINE, A., MEIZLISH, M. L., GOSHUA, G., CHANG, C. H., ZHANG, H., PRICE, C., BAHEL, P., RINDER, H., LEI, T., DAY, A., REYNOLDS, D., WU, X., SCHRIEFER, R., RAUSEO, A. M., GOSS, C. W., O'HALLORAN, J. A., PRESTI, R. M., KIM, A. H., GELMAN, A. E., DELA CRUZ, C. S., LEE, A. I., MUDD, P. A., CHUN, H. J., ATKINSON, J. P. & KULKARNI, H. S. 2021. Increased complement activation is a distinctive feature of severe SARS-CoV-2 infection. *Science Immunology,* 6**,** eabh2259.

MACLENNAN, C. A., GILCHRIST, J. J., GORDON, M. A., CUNNINGHAM, A. F., COBBOLD, M., GOODALL, M., KINGSLEY, R. A., VAN OOSTERHOUT, J. J., MSEFULA, C. L., MANDALA, W. L., LEYTON, D. L., MARSHALL, J. L., GONDWE, E. N., BOBAT, S., LOPEZ-MACIAS, C., DOFFINGER, R., HENDERSON, I. R., ZIJLSTRA, E. E., DOUGAN, G., DRAYSON, M. T., MACLENNAN, I. C. & MOLYNEUX, M. E. 2010. Dysregulated humoral immunity to nontyphoidal Salmonella in HIV-infected African adults. *Science,* 328**,** 508-12.

MACOR, P., DURIGUTTO, P., MANGOGNA, A., BUSSANI, R., DE MASO, L., D'ERRICO, S., ZANON, M., POZZI, N., MERONI, P. L. & TEDESCO, F. 2021. Multiple-Organ Complement Deposition on Vascular Endothelium in COVID-19 Patients. *Biomedicines,* 9**,** 1003.

MAGRO, C., MULVEY, J. J., BERLIN, D., NUOVO, G., SALVATORE, S., HARP, J., BAXTER-STOLTZFUS, A. & LAURENCE, J. 2020. Complement associated microvascular injury and thrombosis in the pathogenesis of severe COVID-19 infection: A report of five cases. *Translational Research,* 220**,** 1-13.

MANGIN, P. H., NEEVES, K. B., LAM, W. A., COSEMANS, J. M. E. M., KORIN, N., KERRIGAN, S. W. & PANTELEEV, M. A. 2021. In vitro flow-based assay: From simple toward more sophisticated models for mimicking hemostasis and thrombosis. *Journal of Thrombosis and Haemostasis,* 19**,** 582-587.

MANI, H., LUXEMBOURG, B., KLÄFFLING, C., ERBE, M. & LINDHOFF-LAST, E. 2005. Use of native or platelet count adjusted platelet rich plasma for platelet aggregation measurements. *Journal of Clinical Pathology,* 58**,** 747-50.

MANRY, J., BASTARD, P., GERVAIS, A., LE VOYER, T., ROSAIN, J., PHILIPPOT, Q., MICHAILIDIS, E., HOFFMANN, H. H., ETO, S., GARCIA-PRAT, M., BIZIEN, L., PARRA-MARTÍNEZ, A., YANG, R., HALJASMÄGI, L., MIGAUD, M., SÄREKANNU, K., MASLOVSKAJA, J., DE PROST, N., TANDJAOUI-LAMBIOTTE, Y., LUYT, C. E., AMADOR-BORRERO, B., GAUDET, A., POISSY, J., MOREL, P., RICHARD, P., COGNASSE, F., TROYA, J., TROUILLET-ASSANT, S., BELOT, A., SAKER, K., GARÇON, P., RIVIÈRE, J. G., LAGIER, J. C., GENTILE, S., ROSEN, L. B., SHAW, E., MORIO, T., TANAKA, J., DALMAU, D., THARAUX, P. L., SENE, D., STEPANIAN, A., MÉGARBANE, B., TRIANTAFYLLIA, V., FEKKAR, A., HEATH, J. R., FRANCO, J. L., ANAYA, J. M., SOLÉ-VIOLÁN, J., IMBERTI, L., BIONDI, A., BONFANTI, P., CASTAGNOLI, R., DELMONTE, O. M., ZHANG, Y., SNOW, A. L., HOLLAND, S. M., BIGGS, C. M., MONCADA-VÉLEZ, M., ARIAS, A. A., LORENZO, L., BOUCHERIT, S., ANGLICHEAU, D., PLANAS, A. M., HAERYNCK, F., DUVLIS, S., OZCELIK, T., KELES, S., BOUSFIHA, A. A., EL BAKKOURI, J., RAMIREZ-SANTANA, C., PAUL, S., PAN-HAMMARSTRÖM, Q., HAMMARSTRÖM, L., DUPONT, A., KUROLAP, A., METZ, C. N., AIUTI, A., CASARI, G., LAMPASONA, V., CICERI, F., BARREIROS, L. A., DOMINGUEZ-GARRIDO, E., VIDIGAL, M., ZATZ, M., VAN DE BEEK, D., SAHANIC, S., TANCEVSKI, I., STEPANOVSKYY, Y., BOYARCHUK, O., NUKUI, Y., TSUMURA, M., VIDAUR, L.,

TANGYE, S. G., BURREL, S., DUFFY, D., QUINTANA-MURCI, L., KLOCPERK, A., KANN, N. Y., SHCHERBINA, A., et al. 2022. The risk of COVID-19 death is much greater and age dependent with type I IFN autoantibodies. *Proceedings of the National Academy of Sciences of the United States of America,* 119**,** e2200413119.

MARCHELLO, C. S., BIRKHOLD, M., CRUMP, J. A., MARTIN, L. B., ANSAH, M. O., BREGHI, G., CANALS, R., FIORINO, F., GORDON, M. A., KIM, J.-H., HAMALUBA, M., HANUMUNTHADU, B., JACOBS, J., KARIUKI, S., MALVOLTI, S., MANTEL, C., MARKS, F., MEDAGLINI, D., MOGASALE, V., MSEFULA, C. L., MUTHUMBI, E., NIYRENDA, T. S., ONSARE, R., OWUSU-DABO, E., PETTINI, E., RAMASAMY, M. N., SOURA, B. A., SPADAFINA, T. & TACK, B. 2022. Complications and mortality of non-typhoidal salmonella invasive disease: a global systematic review and meta-analysis. *The Lancet Infectious Diseases,* 22**,** 692-705.

MARCHELLO, C. S., FIORINO, F., PETTINI, E., CRUMP, J. A. & VACC-I, N. T. S. C. C. 2021. Incidence of non-typhoidal Salmonella invasive disease: A systematic review and meta-analysis. *Journal of Infection,* 83**,** 523-532.

MARCOS-JIMÉNEZ, A., SÁNCHEZ-ALONSO, S., ALCARAZ-SERNA, A., ESPARCIA, L., LÓPEZ-SANZ, C., SAMPEDRO-NÚÑEZ, M., MATEU-ALBERO, T., SÁNCHEZ-CERRILLO, I., MARTÍNEZ-FLETA, P., GABRIE, L., DEL CAMPO GUEROLA, L., LÓPEZ-TRASCASA, M., MARTÍN-GAYO, E., CALZADA, M., CASTAÑEDA, S., DE LA FUENTE, H., GONZÁLEZ-ÁLVARO, I., SÁNCHEZ-MADRID, F., MUÑOZ-CALLEJA, C. & ALFRANCA, A. 2020. Deregulated cellular circuits driving immunoglobulins and complement consumption associate with the severity of COVID-19. *medRxiv*.

MARCOS-JIMENEZ, A., SANCHEZ-ALONSO, S., ALCARAZ-SERNA, A., ESPARCIA, L., LOPEZ-SANZ, C., SAMPEDRO-NUNEZ, M., MATEU-ALBERO, T., SANCHEZ-CERRILLO, I., MARTINEZ-FLETA, P., GABRIE, L., DEL CAMPO GUEROLA, L., RODRIGUEZ-FRADE, J. M., CASASNOVAS, J. M., REYBURN, H. T., VALES-GOMEZ, M., LOPEZ-TRASCASA, M., MARTIN-GAYO, E., CALZADA, M. J., CASTANEDA, S., DE LA FUENTE, H., GONZALEZ-ALVARO, I., SANCHEZ-MADRID, F., MUNOZ-CALLEJA, C. & ALFRANCA, A. 2021. Deregulated cellular circuits driving immunoglobulins and complement consumption associate with the severity of COVID-19 patients. *European Journal of Immunology,* 51**,** 634-647.

MARSHALL, J. S., WARRINGTON, R., WATSON, W. & KIM, H. L. 2018. An introduction to immunology and immunopathology. *Allergy, Asthma and Clinical Immunology,* 14**,** 49.

MARTEL, C., COINTE, S., MAURICE, P., MATAR, S., GHITESCU, M., THEROUX, P. & BONNEFOY, A. 2011. Requirements for membrane attack complex formation and anaphylatoxins binding to collagen-activated platelets. *PLoS One,* 6**,** e18812.

MARTÍNEZ-SALAZAR, B., HOLWERDA, M., STÜDLE, C., PIRAGYTE, I., MERCADER, N., ENGELHARDT, B., RIEBEN, R. & DÖRING, Y. 2022. COVID-19 and the vasculature: current aspects and long-term consequences. *Frontiers in Cell and Developmental Biology,* 10**,** 824851.

MASTAGLIO, S., RUGGERI, A., RISITANO, A. M., ANGELILLO, P., YANCOPOULOU, D., MASTELLOS, D. C., HUBER-LANG, M., PIEMONTESE, S., ASSANELLI, A., GARLANDA, C., LAMBRIS, J. D. & CICERI, F. 2020. The first case of COVID-19 treated with the complement C3 inhibitor AMY-101. *Clinical Immunology,* 215**,** 108450.

MASTELLOS, D. C., PIRES DA SILVA, B. G. P., FONSECA, B. A. L., FONSECA, N. P., AUXILIADORA-MARTINS, M., MASTAGLIO, S., RUGGERI, A., SIRONI, M., RADERMACHER, P., CHRYSANTHOPOULOU, A., SKENDROS, P., RITIS, K., MANFRA, I., IACOBELLI, S., HUBER-LANG, M., NILSSON, B., YANCOPOULOU, D., CONNOLLY, E. S., GARLANDA, C., CICERI, F., RISITANO, A. M., CALADO, R. T. & LAMBRIS, J. D. 2020. Complement C3 vs C5 inhibition in severe COVID-19: Early clinical findings reveal differential biological efficacy. *Clinical Immunology,* 220**,** 108598.

MATEU-BORRÁS, M., GONZÁLEZ-ALSINA, A., DOMÉNECH-SÁNCHEZ, A., QUEROL-GARCÍA, J., FERNÁNDEZ, F. J., VEGA, M. C. & ALBERTÍ, S. 2022. Pseudomonas aeruginosa adaptation in cystic fibrosis patients increases C5a levels and promotes neutrophil recruitment. *Virulence,* 13**,** 215-224.

MATSUMOTO, M. L. 2022. Molecular Mechanisms of Multimeric Assembly of IgM and IgA. *Annu Rev Immunol,* 40**,** 221-247.

MAYNARD, D. M., HEIJNEN, H. F. G., HORNE, M. K., WHITE, J. G. & GAHL, W. A. 2007. Proteomic analysis of platelet alpha granules using mass spectrometry. *Journal of Thrombosis and Haemostasis,* 5**,** 1945-1955.

MCCORMICK, S. M., ESKIN, S. G., MCINTIRE, L. V., TENG, C. L., LU, C.-M., RUSSELL, C. G. & CHITTUR, K. K. 2001. DNA microarray reveals changes in gene expression of shear stressed human umbilical vein endothelial cells. *Proceedings of the National Academy of Sciences,* 98**,** 8955-8960.

MCDONNELL, C. J., GARCIARENA, C. D., WATKIN, R. L., MCHALE, T. M., MCLOUGHLIN, A., CLAES, J., VERHAMME, P., CUMMINS, P. M. & KERRIGAN, S. W. 2016. Inhibition of major integrin alphaV beta3 reduces Staphylococcus aureus attachment to sheared human endothelial cells. *Journal of Thrombosis and Haemostasis,* 14**,** 2536-2547.

MCHALE, T. M. 2018. *Inhibition of endothelial integrin αvβ3 Prevents Bacterial and Neutrophil - Induced Vascular Damage in an Experimental Model of Infection.* PhD, Royal College of Surgeons in Ireland.

MCHALE, T. M., GARCIARENA, C. D., FAGAN, R. P., SMITH, S. G. J., MARTIN-LOCHES, I., CURLEY, G. F., FITZPATRICK, F. & KERRIGAN, S. W. 2018. Inhibition of Vascular Endothelial Cell Leak Following Escherichia coli Attachment in an Experimental Model of Sepsis. *Critical Care Medicine,* 46**,** e805-e810.

MCMILLAN, C. L. D., CHOO, J. J. Y., IDRIS, A., SUPRAMANIAM, A., MODHIRAN, N., AMARILLA, A. A., ISAACS, A., CHEUNG, S. T. M., LIANG, B., BIELEFELDT-OHMANN, H., AZUAR, A., ACHARYA, D., KELLY, G., FERNANDO, G. J. P., LANDSBERG, M. J., KHROMYKH, A. A., WATTERSON, D., YOUNG, P. R., MCMILLAN, N. A. J. & MULLER, D. A. 2021. Complete protection by a single dose skin patch delivered SARS-CoV-2 spike vaccine. *bioRxiv***,** 2021.05.30.446357.

MEDJERAL-THOMAS, N. R., TROLDBORG, A., HANSEN, A. G., GISBY, J., CLARKE, C. L., PRENDECKI, M., MCADOO, S. P., SANDHU, E., LIGHTSTONE, L., THOMAS, D. C., WILLICOMBE, M., BOTTO, M., PETERS, J. E., PICKERING, M. C. & THIEL, S. 2021. Plasma lectin pathway complement proteins in patients with COVID-19 and renal disease. *Frontiers in Immunology,* 12**,** 11.

MENG, R., WU, J., HARPER, D. C., WANG, Y., KOWALSKA, M. A., ABRAMS, C. S., BRASS, L. F., PONCZ, M., STALKER, T. J. & MARKS, M. S. 2015. Defective release of α granule and lysosome contents from platelets in mouse Hermansky-Pudlak syndrome models. *Blood,* 125**,** 1623-32.

MERONI, P. L., CROCI, S., LONATI, P. A., PREGNOLATO, F., SPAGGIARI, L., BESUTTI, G., BONACINI, M., FERRIGNO, I., ROSSI, A., HETLAND, G., HOLLAN, I., CUGNO, M., TEDESCO, F., BORGHI, M. O. & SALVARANI, C. 2023. Complement activation predicts negative outcomes in COVID-19: The experience from Northen Italian patients. *Autoimmunity Reviews,* 22**,** 103232.

MESTAS, J. & HUGHES, C. C. W. 2004. Of Mice and Not Men: Differences between Mouse and Human Immunology. *The Journal of Immunology,* 172**,** 2731-2738.

MIAJLOVIC, H., LOUGHMAN, A., BRENNAN, M., COX, D. & FOSTER, T. J. 2007. Both complement- and fibrinogen-dependent mechanisms contribute to platelet aggregation mediated by Staphylococcus aureus clumping factor B. *Infection and Immunity,* 75**,** 3335-43.

MICHIELS, C. 2003. Endothelial cell functions. *Journal of Cellular Physiology,* 196**,** 430-43.

MIYAKE, M., ZHAO, L., EZAKI, T., HIROSE, K., KHAN, A. Q., KAWAMURA, Y., SHIMA, R., KAMIJO, M., MASUZAWA, T. & YANAGIHARA, Y. 1998. Vi deficient and nonfimbriated mutants of Salmonella typhi agglutinate human blood type antigens and are hyperinvasive. *FEMS Microbiology Letters,* 161**,** 75-82.

MORENS, D. M., DASZAK, P., MARKEL, H. & TAUBENBERGER, J. K. 2020. Pandemic COVID-19 Joins History's Pandemic Legion. *mBio,* 11**,** 10.1128/mbio.00812-20.

MORGAN, B. P. 1989. Complement membrane attack on nucleated cells, resistance, recovery and non-lethal effects. *Biochemical Journal,* 264**,** 1-14.

MORGAN, B. P. 1990. *Complement: Clinical aspects and relevance to disease,* London, Academic Press Limited.

MORGAN, B. P. & GASQUE, P. 1997. Extrahepatic complement biosynthesis where, when and why. *Clinical and Experimental Immunology,* 107**,** 1-7.

MORIARTY, R. D., COX, A., MCCALL, M., SMITH, S. G. J. & COX, D. 2016. Escherichia coli induces platelet aggregation in an Fc gamma RIIa-dependent manner. *Journal of Thrombosis and Haemostasis,* 14**,** 797-806.

MORIKIS, D., ASSA-MUNT, N., SAHU, A. & LAMBRIS, J. D. 1998. Solution structure of Compstatin, a potent complement inhibitor. *Protein Science,* 7**,** 619-27.

MORPETH, S. C., RAMADHANI, H. O. & CRUMP, J. A. 2009. Invasive non-Typhi Salmonella disease in Africa. *Clin Infect Dis,* 49**,** 606-11.

MSEMBURI, W., KARLINSKY, A., KNUTSON, V., ALESHIN-GUENDEL, S., CHATTERJI, S. & WAKEFIELD, J. 2023. The WHO estimates of excess mortality associated with the COVID-19 pandemic. *Nature,* 613**,** 130-137.

MURPHY, K., TRAVERS, P. & WALPORT, M. 2008. *Janeway's Immunobiology,* Abingdon, Garland Science.

MYHRE, P. L., PREBENSEN, C., JONASSEN, C. M., BERDAL, J. E. & OMLAND, T. 2021. SARS-CoV-2 Viremia is Associated With Inflammatory, But Not Cardiovascular Biomarkers, in Patients Hospitalized for COVID-19. *Journal of the American Heart Association,* 10**,** e019756.

NADER, D., FLETCHER, N., CURLEY, G. F. & KERRIGAN, S. W. 2021. SARS-CoV-2 uses major endothelial integrin alphavbeta3 to cause vascular dysregulation in-vitro during COVID-19. *PLoS One,* 16**,** e0253347.

NADER, D. & KERRIGAN, S. W. 2022. Molecular Cross-Talk between Integrins and Cadherins Leads to a Loss of Vascular Barrier Integrity during SARS-CoV-2 Infection. *Viruses,* 14.

NAGELKERKE, S. Q., SCHMIDT, D. E., DE HAAS, M. & KUIJPERS, T. W. 2019. Genetic Variation in Low-To-Medium-Affinity Fcgamma Receptors: Functional Consequences, Disease Associations, and Opportunities for Personalized Medicine. *Frontiers in Immunology,* 10**,** 2237.

NAITO, M., SAKAI, E., SHI, Y., IDEGUCHI, H., SHOJI, M., OHARA, N., YAMAMOTO, K. & NAKAYAMA, K. 2006. Porphyromonas gingivalis-induced platelet aggregation in plasma depends on Hgp44 adhesin but not Rgp proteinase. *Molecular Microbiology,* 59**,** 152-67.

NG, N. & POWELL, C. A. 2021. Targeting the complement cascade in the pathophysiology of COVID-19 disease. *Journal of Clinical Medicine,* 10**,** 13.

NGUYEN, T., GHEBREHIWET, B. & PEERSCHKE, E. I. B. 2000. *Staphylococcus aureus* Protein A Recognises Platelet gC1qR/p33: a Novel Mechanism for Staphylococcal Interations with Platelets. *Infection and Immunity,* 68**,** 2061-2068.

NIEDERREITER, J., ECK, C., RIES, T., HARTMANN, A., MARKL, B., BUTTNER-HEROLD, M., AMANN, K. & DANIEL, C. 2022. Complement Activation via the Lectin and Alternative Pathway in Patients With Severe COVID-19. *Frontiers in Immunology,* 13**,** 835156.

NORIS, M., BENIGNI, A. & REMUZZI, G. 2020. The case of complement activation in COVID-19 multiorgan impact. *Kidney International,* 98**,** 314-322.

O'BRIEN, L., KERRIGAN, S. W., KAW, G., HOGAN, M., PENADÉS, J., LITT, D., FITZGERALD, D. J., FOSTER, T. J. & COX, D. 2002. Multiple mechanisms for the activation of human platelet aggregation by Staphylococcus aureus: roles for the clumping factors ClfA and ClfB, the serine-aspartate repeat protein SdrE and protein A. *Molecular Microbiology,* 44**,** 1033-44.

OBINO, D. & DUMÉNIL, G. 2019. The Many Faces of Bacterium-Endothelium Interactions during Systemic Infections. *Microbiology Spectrum,* 7**,** 10.1128/microbiolspec.bai-0010-2019.

OGATA, A. F., MALEY, A. M., WU, C., GILBOA, T., NORMAN, M., LAZAROVITS, R., MAO, C. P., NEWTON, G., CHANG, M., NGUYEN, K., KAMKAEW, M., ZHU, Q., GIBSON, T. E., RYAN, E. T., CHARLES, R. C., MARASCO, W. A. & WALT, D. R. 2020. Ultra-Sensitive Serial Profiling of SARS-CoV-2 Antigens and Antibodies in Plasma to Understand Disease Progression in COVID-19 Patients with Severe Disease. *Clinical Chemistry,* 66**,** 1562-1572.

OKAMOTO, K., TAMURA, T. & SAWATSUBASHI, Y. 2016. Sepsis and disseminated intravascular coagulation. *Journal of Intensive Care,* 4**,** 23.

OMAR, A. H., SHIBATA, H., YASUNAMI, M., YAMAZAKI, A., OFORI, M. F., AKANMORI, B. D., SHUAIBU, M. N., KIKUCHI, M. & HIRAYAMA, K. 2012. The rs150311303 polymorphism in FcgammaRIIa enhances IgG binding capacity. *Scandinavian Journal of Immunology,* 76**,** 167-74.

PALANKAR, R. & GREINACHER, A. 2019. Challenging the concept of immunothrombosis. *Blood,* 133**,** 508-509.

PAMPOLINA, C. & MCNICOL, A. 2005. Streptococcus sanguis-induced platelet activation involves two waves of tyrosine phosphorylation mediated by FcgammaRIIA and alphaIIbbeta3. *Thrombosis and Haemostasis,* 93**,** 932-9.

PEERSCHKE, E. I. & GHEBREHIWET, B. 1997. C1q augments platelet activation in response to aggregated Ig. *The Journal of Immunology,* 159**,** 5594-5598.

PEERSCHKE, E. I. B., MURPHY, T. K. & GHEBREHIWET, B. 2003. Activation-dependent surface expression of gC1qR/p33 on human blood platelets. *Thrombosis and Haemostasis,* 89**,** 331-9.

PEREZ-TOLEDO, M., FAUSTINI, S. E., JOSSI, S. E., SHIELDS, A. M., MARCIAL-JUAREZ, E., KANTHIMATHINATHAN, H. K., ALLEN, J. D., WATANABE, Y., GOODALL, M., WILLCOX, B. E., WILLCOX, C. R., SALIM, M., WRAITH, D. C., VEENITH, T. V., SYRIMI, E., DRAYSON, M. T., JYOTHISH, D., AL-ABADI, E., CHIKERMANE, A., WELCH, S. B., MASILAMANI, K., HACKETT, S., CRISPIN, M., SCHOLEFIELD, B. R., CUNNINGHAM, A. F. & RICHTER, A. G. 2021. SARS-CoV-2-specific IgG1/IgG3 but not IgM in children with pediatric inflammatory multi-system syndrome. *Pediatric Allergy and Immunology,* 32**,** 1125-1129.

PERICO, L., MORIGI, M., PEZZOTTA, A., LOCATELLI, M., IMBERTI, B., CORNA, D., CERULLO, D., BENIGNI, A. & REMUZZI, G. 2023. SARS-CoV-2 spike protein induces lung endothelial cell dysfunction and thrombo-inflammation depending on the C3a/C3a receptor signalling. *Scientific Reports,* 13**,** 11392.

PETERSSON, F., KILSGARD, O., SHANNON, O. & LOOD, R. 2018. Platelet activation and aggregation by the opportunistic pathogen Cutibacterium (Propionibacterium) acnes. *PLoS One,* 13**,** e0192051.

PETRILLI, C. M., JONES, S. A., YANG, J., RAJAGOPALAN, H., O'DONNELL, L., CHERNYAK, Y., TOBIN, K. A., CERFOLIO, R. J., FRANCOIS, F. & HORWITZ, L. I. 2020. Factors associated with hospital admission and critical illness among 5279 people with coronavirus disease 2019 in New York City: prospective cohort study. *BMJ-British Medical Journal,* 369**,** 15.

PIETROCOLA, G., SCHUBERT, A., VISAI, L., TORTI, M., FITZGERALD, J. R., FOSTER, T. J., REINSCHEID, D. J. & SPEZIALE, P. 2005. FbsA, a fibrinogen-binding protein from Streptococcus agalactiae, mediates platelet aggregation. *Blood,* 105**,** 1052-9.

PLUMMER, C., WU, H., KERRIGAN, S. W., MEADE, G., COX, D. & IAN DOUGLAS, C. W. 2005. A serine-rich glycoprotein of Streptococcus sanguis mediates adhesion to platelets via GPIb. *British Journal of Haematology,* 129**,** 101-109.

POLLEY, M. J. & NACHMAN, R. L. 1983. Human platelet activation by C3a and C3a des-arg. *Journal of Experimental Medicine,* 158**,** 603-615.

PRAKASH, P. S., NOMELLINI, V. & KAPLAN, L. J. 2016. Lower Extremity Salmonella Abscess with Vascular Thrombosis and Wall Destruction. *Surgical Infections Case Reports,* 1**,** 79-81.

PRYZDIAL, E. L. G., LEATHERDALE, A. & CONWAY, E. M. 2022. Coagulation and complement: Key innate defense participants in a seamless web. *Frontiers in Immunology,* 13**,** 918775.

PUHM, F., ALLAEYS, I., LACASSE, E., DUBUC, I., GALIPEAU, Y., ZAID, Y., KHALKI, L., BELLEANNÉE, C., DUROCHER, Y., BRISSON, A. R., WOLBERG, A. S., LANGLOIS, M. A., FLAMAND, L. & BOILARD, E. 2022. Platelet activation by SARS-CoV-2 implicates the release of active tissue factor by infected cells. *Blood Advances,* 6**,** 3593-3605.

QIAO, J., AL-TAMIMI, M., BAKER, R. I., ANDREWS, R. K. & GARDINER, E. E. 2015. The platelet Fc receptor, FcγRIIa. *Immunological Reviews,* 268**,** 241-52.

RAMLALL, V., THANGARAJ, P. M., MEYDAN, C., FOOX, J., BUTLER, D., KIM, J., MAY, B., DE FREITAS, J. K., GLICKSBERG, B. S., MASON, C. E., TATONETTI, N. P. & SHAPIRA, S. D. 2020. Immune complement and coagulation dysfunction in adverse outcomes of SARS-CoV-2 infection. *Nature Medicine,* 26**,** 1609-1615.

RAZAKANDRAINIBE, R., COMBES, V., GRAU, G. E. & JAMBOU, R. 2013. Crossing the wall: The opening of endothelial cell junctions during infectious diseases. *The International Journal of Biochemistry & Cell Biology,* 45**,** 1165-1173.

RISITANO, A. M., MASTELLOS, D. C., HUBER-LANG, M., YANCOPOULOU, D., GARLANDA, C., CICERI, F. & LAMBRIS, J. D. 2020. Complement as a target in COVID-19? *Nature Reviews Immunology,* 20**,** 343-344.

RISPENS, T. & HUIJBERS, M. G. 2023. The unique properties of IgG4 and its roles in health and disease. *Nat Rev Immunol,* 23**,** 763-778.

ROSENFELD, S. I., RYAN, D. H., LOONEY, R. J., ANDERSON, C. L., ABRAHAM, G. N. & LEDDY, J. P. 1987. Human Fc gamma receptors: stable inter-donor variation in quantitative expression on platelets correlates with functional responses. *The Journal of Immunology,* 138**,** 2869-2873.

ROSS, G. D. 1986. *Immunobiology of the complement system,* London, Academic Press.

RUDD, K. E., JOHNSON, S. C., AGESA, K. M., SHACKELFORD, K. A., TSOI, D., KIEVLAN, D. R., COLOMBARA, D. V., IKUTA, K. S., KISSOON, N., FINFER, S., FLEISCHMANN-STRUZEK, C., MACHADO, F. R., REINHART, K. K., ROWAN, K., SEYMOUR, C. W., WATSON, R. S., WEST, T. E., MARINHO, F., HAY, S. I., LOZANO, R., LOPEZ, A. D., ANGUS, D. C., MURRAY, C. J. L. & NAGHAVI, M. 2020. Global, regional, and national sepsis incidence and mortality, 1990-2017: analysis for the Global Burden of Disease Study. *Lancet,* 395**,** 200-211.

SAA, P., FINK, R. V., BAKKOUR, S., JIN, J., SIMMONS, G., MUENCH, M. O., DAWAR, H., DI GERMANIO, C., HUI, A. J., WRIGHT, D. J., KRYSZTOF, D. E., KLEINMAN, S. H., CHEUNG, A., NESTER, T., KESSLER, D. A., TOWNSEND, R. L., SPENCER, B. R., KAMEL, H., VANNOY, J. M., DAVE, H., BUSCH, M. P., STRAMER, S. L., STONE, M., JACKMAN, R. P., NORRIS, P. J., EPIDEMIOLOGY, N. R. & DONOR EVALUATION STUDY, I. V. P. 2022. Frequent detection but lack of infectivity of SARS-CoV-2 RNA in presymptomatic, infected blood donor plasma. *Journal of Clinical Investigation,* 132**,** e159876.

SAGGU, G., CORTES, C., EMCH, H. N., RAMIREZ, G., WORTH, R. G. & FERREIRA, V. P. 2013. Identification of a novel mode of complement activation on stimulated platelets mediated by properdin and C3(H2O). *Journal of Immunology,* 190**,** 6457-67.

SAINI, R., JESRANI, G., GUPTA, M., GUPTA, S. & CHHABRA, A. 2021. Salmonella paratyphi-induced splenic vein thrombosis: A case report on infrequent cause of acute abdomen. *Turk J Emerg Med,* 21**,** 210-213.

SAMEER, A. S. & NISSAR, S. 2021. Toll-Like Receptors (TLRs): Structure, Functions, Signaling, and Role of Their Polymorphisms in Colorectal Cancer Susceptibility. *BioMed Research International,* 2021**,** 1157023.

SATHE, A. & CUSICK, J. K. 2022. Biochemistry, Immunoglobulin M. Treasure Island (FL): StatPearls Publishing.

SATYAM, A., TSOKOS, M. G., BROOK, O. R., HECHT, J. L., MOULTON, V. R. & TSOKOS, G. C. 2021. Activation of classical and alternative complement pathways in the pathogenesis of lung injury in COVID-19. *Clinical Immunology,* 226**,** 108716.

SCHMITT, A., GUICHARD, J., MASSÉ, J.-M., DEBILI, N. & CRAMER, E. M. 2001. Of mice and men: Comparison of the ultrastructure of megakaryocytes and platelets. *Experimental Hematology,* 29**,** 1295-1302.

SCHROTTMAIER, W. C., SCHMUCKENSCHLAGER, A., PIRABE, A. & ASSINGER, A. 2022. Platelets in Viral Infections - Brave Soldiers or Trojan Horses. *Frontiers in Immunology,* 13**,** 856713.

SCRIDON, A. 2022. Platelets and Their Role in Hemostasis and Thrombosis-From Physiology to Pathophysiology and Therapeutic Implications. *International Journal of Molecular Sciences,* 23**,** 12772.

SEEPHETDEE, C., BUASRI, N., BHUKHAI, K., SRISANGA, K., MANOPWISEDJAROEN, S., LERTJINTANAKIT, S., PHUEAKPHUD, N., PAKIRANAY, C., KANGWANRANGSAN, N., SRICHATRAPIMUK, S., KIRDLARP, S., SUNGKANUPARPH, S., CHUTIPONGTANATE, S., THITITHANYANONT, A., HONGENG, S. & WONGTRAKOONGATE, P. 2021. Mice immunized with the vaccine candidate HexaPro spike produce neutralizing antibodies against SARS-CoV-2. *Vaccines,* 9**,** 498.

SENDER, R., FUCHS, S. & MILO, R. 2016. Revised Estimates for the Number of Human and Bacteria Cells in the Body. *PLoS Biol,* 14**,** e1002533.

SHANNON, O., HERTZÉN, E., NORRBY-TEGLUND, A., MÖRGELIN, M., SJÖBRING, U. & BJÖRCK, L. 2007. Severe streptococcal infection is associated with M protein-induced platelet activation and thrombus formation. *Molecular Microbiology,* 65**,** 1147-57.

SHANNON, O., MÖRGELIN, M. & RASMUSSEN, M. 2010. Platelet Activation and Biofilm Formation by *Aerococcus urinae*, an Endocarditis-Causing Pathogen. *Infection and Immunity,* 78**,** 4268-4275.

SHIELDS, A. M., FAUSTINI, S. E., KRISTUNAS, C. A., COOK, A. M., BACKHOUSE, C., DUNBAR, L., EBANKS, D., EMMANUEL, B., CROUCH, E., KROGER, A., HIRSCHFELD, J., SHARMA, P., JAFFERY, R., NOWAK, S., GEE, S., DRAYSON, M. T., RICHTER, A. G., DIETRICH, T. & CHAPPLE, I. L. C. 2021a. COVID-19: Seroprevalence and vaccine responses in UK dental care professionals. *Journal of Dental Research,* 100**,** 1220-1227.

SHIELDS, A. M., FAUSTINI, S. E., PEREZ-TOLEDO, M., JOSSI, S., ALLEN, J. D., AL-TAEI, S., BACKHOUSE, C., DUNBAR, L. A., EBANKS, D., EMMANUEL, B., FANIYI, A. A., GARVEY, M., GRINBERGS, A., MCGINNELL, G., O'NEILL, J., WATANABE, Y., CRISPIN, M., WRAITH, D. C., CUNNINGHAM, A. F.,

DRAYSON, M. T. & RICHTER, A. G. 2021b. Serological responses to SARS-CoV-2 following non-hospitalised infection: clinical and ethnodemographic features associated with the magnitude of the antibody response. *BMJ Open Respiratory Research,* 8**,** e000872.

SIGGINS, M. K., DAVIES, K., FELLOWS, R., THWAITES, R. S., BAILLIE, J. K., SEMPLE, M. G., OPENSHAW, P. J. M., ZELEK, W. M., HARRIS, C. L., MORGAN, B. P. & INVESTIGATORS, I. C. 2023. Alternative pathway dysregulation in tissues drives sustained complement activation and predicts outcome across the disease course in COVID-19. *Immunology,* 168**,** 473-492.

SILHAVY, T. J., KAHNE, D. & WALKER, S. 2010. The bacterial cell envelope. *Cold Spring Harbour Perspectives in Biology,* 2**,** a000414.

SIMIONESCU, M. & ANTOHE, F. 2006. Functional Ultrastructure of the Vascular Endothelium: Changes in Various Pathologies. *In:* MONCADA, S. & HIGGS, A. (eds.) *The Vascular Endothelium I.* Berlin: Springer.

SIMS, P. J. & WIEDMER, T. 1995. Induction of cellular procoagulant activity by the membrane attack complex of complement. *Seminars in Cell Biology,* 6**,** 275-282.

SINKOVITS, G., MEZO, B., RETI, M., MULLER, V., IVANYI, Z., GAL, J., GOPCSA, L., REMENYI, P., SZATHMARY, B., LAKATOS, B., SZLAVIK, J., BOBEK, I., PROHASZKA, Z. Z., FORHECZ, Z., CSUKA, D., HURLER, L., KAJDACSI, E., CERVENAK, L., KISZEL, P., MASSZI, T., VALYI-NAGY, I. & PROHASZKA, Z. 2021. Complement Overactivation and Consumption Predicts In-Hospital Mortality in SARS-CoV-2 Infection. *Frontiers in Immunology,* 12**,** 663187.

SKENDROS, P., GERMANIDIS, G., MASTELLOS, D. C. A., C. GAVRIILIDIS, E., KALOPITAS, G., SAMAKIDOU, A., LIONTOS, A. C., A. NTINOPOULOU, M., KOGIAS, D., KARANIKA, I., SMYRLIS, A., CEPAITYTE, D., FOTIADOU, I., ZIOGA, N., MITROULIS, I., GATSELIS, N. K., PAPAGORAS, C., METALLIDIS, S., MILIONIS, H., DALEKOS, G. N., WILLEMS, L., PERSSON, B., MANIVEL, V. A., NILSSON, B., CONNOLLY, E. S., LACOBELLI, S., PAPADOPOULOS, V. C., R. T., HUBER-LANG, M., RISITANO, A. M. Y., D., RITIS, K. & LAMBRIS, J. D. 2022. Complement C3 inhibition in severe COVID-19 using compstatin AMY-101. *Science Advances,* 8**,** eabo2341.

SKENDROS, P., MITSIOS, A., CHRYSANTHOPOULOU, A., MASTELLOS, D. C., METALLIDIS, S., RAFAILIDIS, P., NTINOPOULOU, M., SERTARIDOU, E., TSIRONIDOU, V., TSIGALOU, C., TEKTONIDOU, M., KONSTANTINIDIS, T., PAPAGORAS, C., MITROULIS, I., GERMANIDIS, G., LAMBRIS, J. D. & RITIS, K. 2020. Complement and tissue factor-enriched neutrophil extracellular traps are key drivers in COVID-19 immunothrombosis. *Journal of Clinical Investigation,* 130**,** 6151-6157.

SKOGLUND, C., WETTERÖ, J., TENGVALL, P. & BENGTSSON, T. 2010. C1q induces a rapid up-regulation of P-selectin and modulates collagen- and collagen-related peptide-triggered activation in human platelets. *Immunobiology,* 215**,** 987-995.

SNYDERMAN, R. & PIKE, M. C. 1975. Interaction of complex polysaccharides with the complement system: effect of calcium depletion on terminal component consumption. *Infection and Immunity,* 11**,** 273-9.

SORMAN, A., ZHANG, L., DING, Z. & HEYMAN, B. 2014. How antibodies use complement to regulate antibody responses. *Molecular Immunology,* 61**,** 79-88.

SPETH, C., RAMBACH, G., WÜRZNER, R., LASS-FLÖRL, C., KOZARCANIN, H., HAMAD, O. A., NILSSON, B. & EKDAHL, K. N. 2015. Complement and platelets: Mutual interference in the immune network. *Molecular Immunology,* 67**,** 108-118.

STAESSENS, S., DENORME, F., FRANCOIS, O., DESENDER, L., DEWAELE, T., VANACKER, P., DECKMYN, H., VANHOORELBEKE, K., ANDERSSON, T. & DE MEYER, S. F. 2020. Structural analysis of ischemic stroke thrombi: histological indications for therapy resistance. *Haematologica,* 105**,** 498-507.

STANAWAY, J. D., PARISI, A., SARKAR, K., BLACKER, B. F., REINER, R. C., HAY, S. I., NIXON, M. R., DOLECEK, C., JAMES, S. L., MOKDAD, A. H., ABEBE, G., AHMADIAN, E., ALAHDAB, F., ALEMNEW, B. T. T., ALIPOUR, V., ALLAH BAKESHEI, F., ANIMUT, M. D., ANSARI, F., ARABLOO, J., ASFAW, E. T., BAGHERZADEH, M., BASSAT, Q., BELAYNEH, Y. M. M., CARVALHO, F., DARYANI, A., DEMEKE, F. M., DEMIS, A. B. B., DUBEY, M., DUKEN, E. E., DUNACHIE, S. J., EFTEKHARI, A., FERNANDES, E., FOULADI FARD, R., GEDEFAW, G. A., GETA, B., GIBNEY, K. B., HASANZADEH, A., HOANG, C. L., KASAEIAN, A., KHATER, A., KIDANEMARIAM, Z. T., LAKEW, A. M., MALEKZADEH, R., MELESE, A., MENGISTU, D. T., MESTROVIC, T., MIAZGOWSKI, B., MOHAMMAD, K. A., MOHAMMADIAN, M., MOHAMMADIAN-HAFSHEJANI, A., NGUYEN, C. T., NGUYEN, L. H., NGUYEN, S. H., NIRAYO, Y. L., OLAGUNJU, A. T., OLAGUNJU, T. O., POURJAFAR, H., QORBANI, M., RABIEE, M., RABIEE, N., RAFAY, A., REZAPOUR, A., SAMY, A. M., SEPANLOU, S. G., SHAIKH, M. A., SHARIF, M., SHIGEMATSU, M., TESSEMA, B., TRAN, B. X., ULLAH, I., YIMER, E. M., ZAIDI, Z., MURRAY, C. J. L. & CRUMP, J. A. 2019. The global burden of non-typhoidal salmonella invasive disease: a systematic analysis for the Global Burden of Disease Study 2017. *The Lancet Infectious Diseases,* 19**,** 1312-1324.

STEIN, S. R., RAMELLI, S. C., GRAZIOLI, A., CHUNG, J. Y., SINGH, M., YINDA, C. K., WINKLER, C. W., SUN, J., DICKEY, J. M., YLAYA, K., KO, S. H., PLATT, A. P., BURBELO, P. D., QUEZADO, M., PITTALUGA, S., PURCELL, M., MUNSTER, V. J., BELINKY, F., RAMOS-BENITEZ, M. J., BORITZ, E. A., LACH, I. A., HERR, D. L., RABIN, J., SAHARIA, K. K., MADATHIL, R. J., TABATABAI, A., SOHERWARDI, S., MCCURDY, M. T., CONSORTIUM, N. C.-A., PETERSON, K. E., COHEN, J. I., DE WIT, E., VANNELLA, K. M., HEWITT, S. M., KLEINER, D. E. & CHERTOW, D. S. 2022. SARS-CoV-2 infection and persistence in the human body and brain at autopsy. *Nature,* 612**,** 758-763.

STOCKDALE, L., NALWOGA, A., NASH, S., ELIAS, S., ASIKI, G., KUSEMERERWA, S., GILCHRIST, J. J., NEWTON, R. & MACLENNAN, C. A. 2019. Cross-sectional study of IgG antibody levels to invasive nontyphoidal Salmonella LPS O-antigen with age in Uganda. *Gates Open Research,* 3**,** 1501.

STRID, M. A., DALBY, T., MOLBAK, K. & KROGFELT, K. A. 2007. Kinetics of the human antibody response against Salmonella enterica Serovars Enteritidis and Typhimurium determined by lipopolysaccharide enzyme-linked immunosorbent assay. *Clinical and Vaccine Immunology,* 14**,** 741-7.

STRUTYNSKAYA, A. D., KARNAUSHKINA, M. A., TYURIN, I. E. & KOMAROVA, I. S. 2020. Salmonella sepsis in a patient with TLR4 gene polymorphisms. *Radiology Case Reports,* 15**,** 1545-1551.

SUBRAMANIAM, S., JURK, K., HOBOHM, L., JÄCKEL, S., SAFFARZADEH, M., SCHWIERCZEK, K., WENZEL, P., LANGER, F., REINHARDT, C. & RUF, W. 2017. Distinct contributions of complement factors to platelet activation and fibrin formation in venous thrombus development. *Blood,* 129**,** 2291-2302.

SULLAM, P. M., JARVIS, G. A. & VALONE, F. H. 1988. Role of immunoglobulin G in platelet aggregation by viridans group streptococci. *Infection and Immunity,* 56**,** 2907-11.

SUPPAMUTHARWYAM, M. & RADHAKRISHNAN, A. P. 2022. An Unusual Case of Deep Vein Thrombosis and Mycotic Aneurysms Secondary to <i>Salmonella</i> Bacteraemia. *Case Reports in Clinical Medicine,* 11**,** 37-47.

SVENSSON, L., BAUMGARTEN, M., MÖRGELIN, M. & SHANNON, O. 2014. Platelet Activation by Streptococcus pyogenes Leads to Entrapment in Platelet Aggregates, from Which Bacteria Subsequently Escape. *Infection and Immunity,* 82**,** 4307-4314.

SYRIMI, E., FENNELL, E., RICHTER, A., VRLJICAK, P., STARK, R., OTT, S., MURRAY, P. G., AL-ABADI, E., CHIKERMANE, A., DAWSON, P., HACKETT, S., JYOTHISH, D., KANTHIMATHINATHAN, H. K., MONAGHAN, S., NAGAKUMAR, P., SCHOLEFIELD, B. R., WELCH, S., KHAN, N., FAUSTINI, S., DAVIES, K., ZELEK, W. M., KEARNS, P. & TAYLOR, G. S. 2021. The immune landscape of SARS-CoV-2-associated Multisystem Inflammatory Syndrome in Children (MIS-C) from acute disease to recovery. *iScience,* 24**,** 103215.

TAKAMATSU, D., BENSING, B. A., CHENG, H., JARVIS, G. A., SIBOO, I. R., LÓPEZ, J. A., GRIFFISS, J. M. & SULLAM, P. M. 2005. Binding of the Streptococcus gordonii surface glycoproteins GspB and Hsa to specific carbohydrate structures on platelet membrane glycoprotein Ibalpha. *Molecular Microbiology,* 58**,** 380-92.

TANEDA, K., ADACHI, T., WATANABE, Y. & HANAJIMA, R. 2019. Cerebral Venous Thrombosis due to Nontyphoidal *Salmonella* Bacteremia. *Internal Medicine,* 58**,** 1943-1946.

TANG, Y. Q., YEAMAN, M. R. & SELSTED, M. E. 2002. Antimicrobial peptides from human platelets. *Infection and Immunity,* 70**,** 6524-33.

THOMAS, D. D., LIU, X., KANTROW, S. P. & LANCASTER, J. R., JR. 2001. The biological lifetime of nitric oxide: implications for the perivascular dynamics of NO and O2. *Proceedings of the National Academy of Sciences of the U S A,* 98**,** 355-60.

TILLEY, D. O. 2013. *Pathways to human platelet activation : convergence of streptococcus pneumoniae and streptococcus oralis at a universal actor, Fc gamma RIIA.* PhD, Royal College of Surgeons in Ireland.

TILLEY, D. O., ARMAN, M., SMOLENSKI, A., COX, D., O'DONNELL, J. S., DOUGLAS, C. W. I., WATSON, S. P. & KERRIGAN, S. W. 2013. Glycoprotein Ib alpha and Fc gamma RIIa play key roles in platelet activation by the colonizing bacterium, Streptococcus oralis. *Journal of Thrombosis and Haemostasis,* 11**,** 941-950.

TO, K. K. W., TSANG, O. T. Y., LEUNG, W. S., TAM, A. R., WU, T. C., LUNG, D. C., YIP, C. C. Y., CAI, J. P., CHAN, J. M. C., CHIK, T. S. H., LAU, D. P. L., CHOI, C. Y. C., CHEN, L. L., CHAN, W. M., CHAN, K. H., IP, J. D., NG, A. C. K., POON, R. W. S., LUO, C. T., CHENG, V. C. C., CHAN, J. F. W., HUNG, I. F. N., CHEN, Z. W., CHEN, H. L. & YUEN, K. Y. 2020. Temporal profiles of viral load in posterior oropharyngeal saliva samples and serum antibody responses during infection by SARS-CoV-2: an observational cohort study. *Lancet Infectious Diseases,* 20**,** 565-574.

TOMIYAMA, Y., KUNICKI, T. J., ZIPF, T. F., FORD, S. B. & ASTER, R. H. 1992. Response of Human Platelets to Activating Monoclonal Antibodies: Importance of FCγRII (CD32) Phenotype and Level of Expression. *Blood,* 80**,** 2261-2268.

TSIFTSOGLOU, S. A., GAVRIILAKI, E., TOULOUMENIDOU, T., KORAVOU, E.-E., KOUTRA, M., PAPAYANNI, P. G., KARALI, V., PAPALEXANDRI, A., VARELAS, C., CHATZOPOULOU, F., CHATZIDIMITRIOU, M., CHATZIDIMITRIOU, D., VELENI, A., RAPTI, E., KIOUMIS, I., KAIMAKAMIS, E., BITZANI, M., BOUMPAS, D. T., TSANTES, A., SOTIROPOULOS, D., PAPADOPOULOU, A., SAKELLARI, I., KOKORIS, S. & ANAGNOSTOPOULOS, A. 2023. Targeted genotyping of COVID-19 patients reveals a signature of complement C3 and factor B coding SNPs associated with severe infection. *Immunobiology,* 228**,** 152351.

TURVEY, S. E. & BROIDE, D. H. 2010. Innate immunity. *Journal of Allergy and Clinical Immunology,* 125**,** S24-32.

TZIMA, E., DEL POZO, M. A., SHATTIL, S. J., CHIEN, S. & SCHWARTZ, M. A. 2001. Activation of integrins in endothelial cells by fluid shear stress mediates Rho-dependent cytoskeletal alignment. *EMBO Journal,* 20**,** 4639-47.

ULKER, P., SATI, L., CELIK-OZENCI, C., MEISELMAN, H. J. & BASKURT, O. K. 2009. Mechanical stimulation of nitric oxide synthesizing mechanisms in erythrocytes. *Biorheology,* 46**,** 121-32.

ULKER, P., YARAS, N., YALCIN, O., CELIK-OZENCI, C., JOHNSON, P. C., MEISELMAN, H. J. & BASKURT, O. K. 2011. Shear stress activation of nitric oxide synthase and increased nitric oxide levels in human red blood cells. *Nitric Oxide,* 24**,** 184-91.

VALLANCE, P. & CHAN, N. 2001. Endothelial function and nitric oxide: clinical relevance. *Heart,* 85**,** 342.

VAN PUYVELDE, S., DE BLOCK, T., SRIDHAR, S., BAWN, M., KINGSLEY, R. A., INGELBEEN, B., BEALE, M. A., BARBÉ, B., JEON, H. J., MBUYI-KALONJI, L., PHOBA, M.-F., FALAY, D., MARTINY, D., VANDENBERG, O., AFFOLABI, D., RUTANGA, J. P., CEYSSENS, P.-J., MATTHEUS, W., CUYPERS, W. L., VAN DER SANDE, M. A. B., PARK, S. E., KARIUKI, S., OTIENO, K., LUSINGU, J. P. A., MBWANA, J. R., ADJEI, S., SARFO, A., AGYEI, S. O., ASANTE, K. P., OTIENO, W., OTIENO, L., TAHITA, M. C., LOMPO, P., HOFFMAN, I. F., MVALO, T., MSEFULA, C., HASSAN-HANGA, F., OBARO, S., MACKENZIE, G., DEBORGGRAEVE, S., FEASEY, N., MARKS, F., MACLENNAN, C. A., THOMSON, N. R., JACOBS, J., DOUGAN, G., KARIUKI, S. & LUNGUYA, O. 2023. A genomic appraisal of invasive Salmonella Typhimurium and associated antibiotic resistance in sub-Saharan Africa. *Nature Communications,* 14**,** 6392.

VAN STRIJP, J. A. G., VAN KESSEL, K. P. M., VAN DER TOL, M. E. & VERHOEF, J. 1989. Complement-mediated phagocytosis of herpes simplex virus by granulocytes. *Journal of Clinical Investigation,* 84**,** 107-112.

VANASSCHE, T., KAUSKOT, A., VERHAEGEN, J., PEETERMANS, W. E., VAN RYN, J., SCHNEEWIND, O., HOYLAERTS, M. F. & VERHAMME, P. 2012. Fibrin formation by staphylothrombin facilitates *Staphylococcus aureus* -induced platelet aggregation. *Thrombosis and Haemostasis,* 107**,** 1107-1121.

VARSANO, S., KAMINSKY, M., KAISER, M. & RASHKOVSKY, L. 2000. Generation of complement C3 and expression of cell membrane complement inhibitory proteins by human bronchial epithelium cell line. *Thorax,* 55**,** 364.

VERKERKE, H. P., DAMHORST, G. L., GRACIAA, D. S., MCLENDON, K., O'SICK, W., ROBICHAUX, C., CHEEDARLA, N., POTLAPALLI, S., WU, S. C., HARRINGTON, K. R. V., WEBSTER, A., KRAFT, C., ROSTAD, C. A., WAGGONER, J. J., GANDHI, N. R., GUARNER, J., AULD, S. C., NEISH, A., ROBACK, J. D., LAM, W. A., SHAH, N. S. & STOWELL, S. R. 2022. Nucleocapsid Antigenemia Is a Marker of Acute SARS-CoV-2 Infection. *Journal of Infectious Diseases,* 226**,** 1577-1587.

VERSCHOOR, A., NEUENHAHN, M., NAVARINI, A. A., GRAEF, P., PLAUMANN, A., SEIDLMEIER, A., NIESWANDT, B., MASSBERG, S., ZINKERNAGEL, R. M., HENGARTNER, H. & BUSCH, D. H. 2011. A platelet-mediated system for shuttling blood-borne bacteria to CD8alpha+ dendritic cells depends on glycoprotein GPIb and complement C3. *Nature Immunology,* 12**,** 1194-201.

VIDARSSON, G., DEKKERS, G. & RISPENS, T. 2014. IgG subclasses and allotypes: from structure to effector functions. *Frontiers in Immunology,* 5**,** 520.

VIGNE, P., BREITTMAYER, J. P. & FRELIN, C. 1998. Analysis of the influence of nucleotidases on the apparent activity of exogenous ATP and ADP at P2Y1 receptors. *British Journal of Pharmacology,* 125**,** 675-80.

VISENTIN, G. P., MOGHADDAM, M., BEERY, S. E., MCFARLAND, J. G. & ASTER, R. H. 2001. Heparin is not required for detection of antibodies associated with heparin-induced thrombocytopenia/thrombosis. *Journal of Laboratory and Clinical Medicine,* 138**,** 22-31.

VLAAR, A. P. J., DE BRUIN, S., BUSCH, M., TIMMERMANS, S. A. M. E. G., VAN ZEGGEREN, I. E., KONING, R., TER HORST, L., BULLE, E. B., VAN BAARLE, F. E. H. P., VAN DE POLL, M. C. G., KEMPER, E. M., VAN DER HORST, I. C. C., SCHULTZ, M. J., HORN, J., PAULUS, F., BOS, L. D., WIERSINGA, W. J., WITZENRATH, M., RUECKINGER, S., PILZ, K., BROUWER, M. C., GUO, R.-F., HEUNKS, L., VAN PAASSEN, P., RIEDEMANN, N. C. & VAN DE BEEK, D. 2020. Anti-C5a antibody IFX-1 (vilobelimab) treatment versus best supportive care for patients with severe COVID-19 (PANAMO): an exploratory, open-label, phase 2 randomised controlled trial. *The Lancet Rheumatology,* 2**,** e764-e773.

VLAAR, A. P. J., WITZENRATH, M., VAN PAASSEN, P., HEUNKS, L. M. A., MOURVILLIER, B., DE BRUIN, S., LIM, E. H. T., BROUWER, M. C., TUINMAN, P. R., SARAIVA, J. F. K., MARX, G., LOBO, S. M., BOLDO, R., SIMON-CAMPOS, J. A., CORNET, A. D., GREBENYUK, A., ENGELBRECHT, J. M., MUKANSI, M., JORENS, P. G., ZERBIB, R., RUCKINGER, S., PILZ, K., GUO, R., VAN DE BEEK, D., RIEDEMANN, N. C. & GROUP, P. S. 2022. Anti-C5a antibody (vilobelimab) therapy for critically ill, invasively mechanically ventilated patients with COVID-19 (PANAMO): a multicentre, double-blind, randomised, placebo-controlled, phase 3 trial. *Lancet Respiratory Medicine,* 10**,** 1137-1146.

WALLS, A. C., MIRANDA, M. C., SCHÄFER, A., PHAM, M. N., GREANEY, A., ARUNACHALAM, P. S., NAVARRO, M.-J., TORTORICI, M. A., ROGERS, K., O'CONNOR, M. A., SHIRREFF, L., FERRELL, D. E., BOWEN, J., BRUNETTE, N., KEPL, E., ZEPEDA, S. K., STARR, T., HSIEH, C.-L., FIALA, B., WRENN, S., PETTIE, D., SYDEMAN, C., SPROUSE, K. R., JOHNSON, M., BLACKSTONE, A., RAVICHANDRAN, R., OGOHARA, C., CARTER, L., TILLES, S. W., RAPPUOLI, R., LEIST, S. R., MARTINEZ, D. R., CLARK, M., TISCH, R., O'HAGAN, D. T., VAN DER MOST, R., VAN VOORHIS, W. C., CORTI, D., MCLELLAN, J. S., KLEANTHOUS, H., SHEAHAN, T. P., SMITH, K. D., FULLER, D. H., VILLINGER, F., BLOOM, J., PULENDRAN, B., BARIC, R. S., KING, N. P. & VEESLER, D. 2021. Elicitation of broadly protective sarbecovirus immunity by receptor-binding domain nanoparticle vaccines. *Cell,* 184**,** 5432-5447.e16.

WALLS, A. C., PARK, Y. J., TORTORICI, M. A., WALL, A., MCGUIRE, A. T. & VEESLER, D. 2020. Structure, function, and antigenicity of the SARS-CoV-2 spike glycoprotein. *Cell,* 181**,** 281-292.

WANG, E. Y., MAO, T., KLEIN, J., DAI, Y., HUCK, J. D., JAYCOX, J. R., LIU, F., ZHOU, T., ISRAELOW, B., WONG, P., COPPI, A., LUCAS, C., SILVA, J., OH, J. E., SONG, E., PEROTTI, E. S., ZHENG, N. S., FISCHER, S., CAMPBELL, M., FOURNIER, J. B., WYLLIE, A. L., VOGELS, C. B. F., OTT, I. M., KALINICH, C. C., PETRONE, M. E., WATKINS, A. E., YALE, I. T., DELA CRUZ, C., FARHADIAN, S. F., SCHULZ, W. L., MA, S., GRUBAUGH, N. D., KO, A. I., IWASAKI, A. & RING, A. M. 2021. Diverse functional autoantibodies in patients with COVID-19. *Nature,* 595**,** 283-288.

WANG, W., XU, Y., GAO, R., LU, R., HAN, K., WU, G. & TAN, W. 2020. Detection of SARS-CoV-2 in Different Types of Clinical Specimens. *Journal of the American Medical Association,* 323**,** 1843-1844.

WATANABE, Y., ALLEN JOEL, D., WRAPP, D., MCLELLAN JASON, S. & CRISPIN, M. 2020. Site-specific glycan analysis of the SARS-CoV-2 spike. *Science,* 369**,** 330-333.

WATSON, C. N., KERRIGAN, S. W., COX, D., HENDERSON, I. R., WATSON, S. P. & ARMAN, M. 2016. Human platelet activation by Escherichia coli: roles for FcgammaRIIA and integrin alphaIIbbeta3. *Platelets,* 27**,** 535-40.

WECKBACH, L. T., SCHWEIZER, L., KRAECHAN, A., BIEBER, S., ISHIKAWA-ANKERHOLD, H., HAUSLEITER, J., MASSBERG, S., STRAUB, T., KLINGEL, K., GRABMAIER, U., ZWIEBEL, M., MANN, M., SCHULZ, C. & GROUP, E. M. B. S. 2022. Association of Complement and MAPK Activation With SARS-CoV-2-Associated Myocardial Inflammation. *JAMA Cardiology,* 7**,** 286-297.

WELLS, T. J., WHITTERS, D., SEVASTSYANOVICH, Y. R., HEATH, J. N., PRAVIN, J., GOODALL, M., BROWNING, D. F., O'SHEA, M. K., CRANSTON, A., DE SOYZA, A., CUNNINGHAM, A. F., MACLENNAN, C. A., HENDERSON, I. R. & STOCKLEY, R. A. 2014. Increased severity of respiratory infections associated with elevated anti-LPS IgG2 which inhibits serum bactericidal killing. *Journal of Experimental Medicine,* 211**,** 1893-1904.

WHITE, D. O. & BROWN, L. E. 1999. Respiratory Viruses. *In:* GRANOFF, A. & WEBSTER, R. G. (eds.) *Encyclopedia of Virology.* Second ed.: Academic Press.

WHITE, J. G. 2006. Why human platelets fail to kill bacteria. *Platelets,* 17**,** 191-200.

WHO. 2020. *WHO announces COVID-19 outbreak a pandemic* [Online]. World Health Organization. Available: https://www.euro.who.int/en/health-topics/health-emergencies/coronavirus-covid-19/news/news/2020/3/who-announces-covid-19-outbreak-a-pandemic [Accessed 03/08/2020].

WICK, K. D., LELIGDOWICZ, A., WILLMORE, A., CARRILLO, S. A., GHALE, R., JAUREGUI, A., CHAK, S. S., NGUYEN, V., LEE, D., JONES, C., DEWAR, R., LANE, H. C., KANGELARIS, K. N., HENDRICKSON, C. M., LIU, K. D., SINHA, P., ERLE, D. J., LANGELIER, C. R., KRUMMELL, M. F., WOODRUFF, P. G., CALFEE, C. S., MATTHAY, M. A. & CONSORTIUM, C. 2022. Plasma SARS-CoV-2 nucleocapsid antigen levels are associated with progression to severe disease in hospitalized COVID-19. *Critical Care,* 26**,** 278.

WILLCOX, M. D. P., WEBB, B. C., THAKUR, A. & HARTY, D. W. S. 1998. Interactions between Candida species and platelets. *Journal of Medical Microbiology,* 47**,** 103-110.

WINGERT, A., PILLAY, J., GATES, M., GUITARD, S., RAHMAN, S., BECK, A., VANDERMEER, B. & HARTLING, L. 2021. Risk factors for severity of COVID-19: a rapid review to inform vaccine prioritisation in Canada. *BMJ Open,* 11**,** e044684.

WOLFF, M., HANDTKE, S., PALANKAR, R., WESCHE, J., KOHLER, T. P., KOHLER, C., GRUEL, Y., HAMMERSCHMIDT, S. & GREINACHER, A. 2020. Activated platelets kill Staphylococcus aureus, but not Streptococcus pneumoniae-The role of FcgammaRIIa and platelet factor 4/heparinantibodies. *Journal of Thrombosis and Haemostasis,* 18**,** 1459-1468.

WOOF, J. M. & RUSSELL, M. W. 2011. Structure and function relationships in IgA. *Mucosal Immunology,* 4**,** 590-597.

WORTH, R. G., CHIEN, C. D., CHIEN, P., REILLY, M. P., MCKENZIE, S. E. & SCHREIBER, A. D. 2006. Platelet FcgammaRIIA binds and internalizes IgG-containing complexes. *Experimental Hematology,* 34**,** 1490-5.

WORTHINGTON, R. E., CARROLL, R. C. & BOUCHEIX, C. 1990. Platelet activation by CD9 monoclonal antibodies is mediated by the FcYRII receptor. *British Journal of Haematology,* 74**,** 216-222.

WRAPP, D., WANG, N., CORBETT, K. S., GOLDSMITH, J. A., HSIEH, C.-L., ABIONA, O., GRAHAM, B. S. & MCLELLAN, J. S. 2020. Cryo-EM structure of the 2019-nCoV spike in the prefusion conformation. *Science,* 367**,** 1260-1263.

WRIGHT, A. & KANEGASAKI, S. 1971. Molecular aspects of lipopolysaccharides. *Physiological Reviews,* 51**,** 748-84.

WU, D., DALY, H. C., CONROY, E., LI, B., GALLAGHER, W. M., CAHILL, R. A. & O'SHEA, D. F. 2019. PEGylated BF(2)-Azadipyrromethene (NIR-AZA) fluorophores, for intraoperative imaging. *European Journal of Medicinal Chemistry,* 161**,** 343-353.

WU, L., ZHOU, L., MO, M., LIU, T., WU, C., GONG, C., LU, K., GONG, L., ZHU, W. & XU, Z. 2022. SARS-CoV-2 Omicron RBD shows weaker binding affinity than the currently dominant Delta variant to human ACE2. *Signal Transduction and Targeted Therapy,* 7**,** 8.

YAHIAOUI, R. Y., DEN HEIJER, C., D. J. , VAN BIJNEN, E., M. E., PAGET, W. J., PRINGLE, M., GOOSSENS, H., BRUGGEMAN, C. A., SCHELLEVIS, F. G., STOBBERINGH, E. E. & THE, A. S. T. 2016. Prevalence and antibiotic resistance of commensal Streptococcus pneumoniae in nine European countries. *Future Microbiology,* 11**,** 737-744.

YANG, J., BARRILA, J., ROLAND, K. L., KILBOURNE, J., OTT, C. M., FORSYTH, R. J. & NICKERSON, C. A. 2015. Characterization of the Invasive, Multidrug Resistant Non-typhoidal Salmonella Strain D23580 in a Murine Model of Infection. *PLoS Neglected Tropical Diseases,* 9**,** e0003839.

YANG, J., BARRILA, J., ROLAND, K. L., OTT, C. M. & NICKERSON, C. A. 2016. Physiological fluid shear alters the virulence potential of invasive multidrug-resistant non-typhoidal Salmonella Typhimurium D23580. *NPJ Microgravity,* 2**,** 16021.

YEAMAN, M. R. 2010. Platelets in defense against bacterial pathogens. *Celllar and Molecular Life Sciences,* 67**,** 525-44.

YEAMAN, M. R., YOUNT, N. Y., WARING, A. J., GANK, K. D., KUPFERWASSER, D., WIESE, R., BAYER, A. S. & WELCH, W. H. 2007. Modular determinants of antimicrobial activity in platelet factor-4 family kinocidins. *Biochimica et Biophysica Acta,* 1768**,** 609-19.

YU, J., YUAN, X., CHEN, H., CHATURVEDI, S., BRAUNSTEIN, E. M. & BRODSKY, R. A. 2020. Direct activation of the alternative complement pathway by SARS-CoV-2 spike proteins is blocked by factor D inhibition. *Blood,* 136**,** 2080-2089.

YUAN, F. F., TANNER, J., CHAN, P. K. S., BIFFIN, S., DYER, W. B., GECZY, A. F., TANG, J. W., HUI, D. S. C., SUNG, J. J. Y. & SULLIVAN, J. S. 2005. Influence of Fc gamma RIIA and MBL polymorphisms on severe acute respiratory syndrome. *Tissue Antigens,* 66**,** 291-296.

ZEILER, M., MOSER, M. & MANN, M. 2014. Copy number analysis of the murine platelet proteome spanning the complete abundance range. *Molecular and Cellular Proteomics,* 13**,** 3435-45.

ZEINER, S. A., DWYER, B. E. & CLEGG, S. 2012. FimA, FimF, and FimH are necessary for assembly of type 1 fimbriae on Salmonella enterica serovar Typhimurium. *Infection and Immunity,* 80**,** 3289-96.

ZELEK, W. M., COLE, J., PONSFORD, M. J., HARRISON, R. A., SCHROEDER, B. E., WEBB, N., JOLLES, S., FEGAN, C., MORGAN, M., WISE, M. P. & MORGAN, B. P. 2020. Complement inhibition with the C5 blocker LFG316 in severe COVID-19. *American Journal of Respiratory and Critical Care Medicine,* 202**,** 1304-1308.

ZELEK, W. M. & HARRISON, R. A. 2023. Complement and COVID-19: Three years on, what we know, what we don't know, and what we ought to know. *Immunobiology,* 228**,** 152393.

ZHANG, G., HAN, J., WELCH, E. J., YE, R. D., VOYNO-YASENETSKAYA, T. A., MALIK, A. B., DU, X. & LI, Z. 2009. Lipopolysaccharide stimulates platelet secretion and potentiates platelet aggregation via TLR4/MyD88 and the cGMP-dependent protein kinase pathway. *Journal of Immunology,* 182**,** 7997-8004.

ZHANG, H., GERASIMOVSKAYA, E., MCCARTHY, M. K., MAY, N. A., PRASAD, R. R., RIDDLE, S., MCKEON, B. A., KUMAR, S., LI, M., HU, C., FRID, M. G., MORRISON, T. E. & STENMARK, K. R. 2023. Local Complement Contributes to Pathogenic Activation of Lung Endothelial Cells in SARS-CoV-2 Infection. *American Journal of Respiratory Cell and Molecular Biology,* 69**,** 210-219.

ZHANG, W., LIU, W., LIN, J., JIN, J., ZHAO, K., ZHU, L., WANG, X., WANG, L., TANG, R., ZHU, Y., ZHOU, W., YOU, E., ZHANG, L., LIU, X., WU, J., CHEN, L., WANG, W., ZHANG, Q. & GAO, R. 2022. Highly Prevalent SARS-CoV-2 Antigenemia in COVID-19 Patients. *Infectcious Diseases and Immunity,* 2**,** 193-199.

ZHOU, W., MARSH, J. E. & SACKS, S. H. 2001. Intrarenal synthesis of complement. *Kidney International,* 59**,** 1227-35.

ZHOU, Y., XU, Z. & LIU, Z. 2022. Impact of Neutrophil Extracellular Traps on Thrombosis Formation: New Findings and Future Perspective. *Frontiers in Cellular and Infection Microbiology,* 12**,** 910908.

ZHOU, Y. C., LU, K., PFEFFERLE, S., BERTRAM, S., GLOWACKA, I., DROSTEN, C., POHLMANN, S. & SIMMONS, G. 2010. A Single Asparagine-Linked Glycosylation Site of the Severe Acute Respiratory Syndrome Coronavirus Spike Glycoprotein Facilitates Inhibition by Mannose-Binding Lectin through Multiple Mechanisms. *Journal of Virology,* 84**,** 8753-8764.